

Field Investigation of Moisture Buffering Potential of Gypsum Board in a Residential Setting
under Varying Operating Conditions in a Marine Climate

Shahrzad Pedram

A Thesis

In

The Graduate Program

of

Building Science / Building Engineering

Presented in Partial Fulfillment of the Requirements
for the Degree of Master of Applied Science/Building Engineering at
British Columbia Institute of Technology
Burnaby, British Columbia, Canada

April 2016

© Shahrzad Pedram, 2016

BRITISH COLUMBIA INSTITUTE OF TECHNOLOGY
Building Science Graduate program

This is to certify that the thesis prepared

By: Shahrzad Pedram

Entitled: Field Investigation of Moisture Buffering Potential of Gypsum Board in a Residential Setting under Varying Operating Conditions in a Marine Climate

and submitted in partial fulfillment of the requirements for the degree of

Master of Applied Science/Building Engineering

complies with the regulations of the Institute and meets the accepted standards with respect to originality and quality.

Signed by the final Examining Committee:



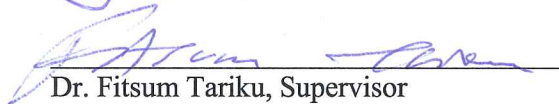
Dr. Rodrigo Mora, Chair



Mr. Greg Johnson, Examiner, external to program



Mr. John Lovatt, Examiner



Dr. Fitsum Tariku, Supervisor

Approved by


Graduate Program Director

ABSTRACT

Field Investigation of Moisture Buffering Potential of Gypsum Board in a Residential Setting under Varying Operating Conditions in a Marine Climate

By Shahrzad Pedram

Indoor relative humidity is of critical importance to maintain at acceptable and stable levels for building occupants' health and comfort, energy efficiency, and building envelope durability. The main factors that determine the indoor relative humidity levels in a building are ventilation rate and scheme, moisture sources and sinks, and moisture buffering effect of materials. As buildings enclosures are retrofitted for improvements in water shedding and energy performance, they are becoming more airtight. Such a retrofit measure without addressing increased ventilation needs will lead to significant building envelope and indoor air quality problems. In this thesis, this point is highlighted in a reference residential building, occupied by low-income, high occupancy residents.

This research aims to determine the effect of moisture buffering of unfinished gypsum board as a passive means to regulate indoor humidity in a field experiment setting. Two identical test buildings exposed to real climatic loads are used to evaluate the moisture buffering effect of gypsum board for different simulated occupant densities and ventilation strategies. The effect of passive and active indoor moisture management measures are compared between 8 test cases. Implications on indoor air quality and ventilation heat loss are also discussed.

The results show that moisture buffering is an effective means of passively regulating indoor relative humidity levels in Vancouver's marine climate, when coupled with adequate ventilation as recommended by ASHRAE, even under high moisture loading. When working in tandem with adequate ventilation, moisture buffering helps to regulate changes in relative humidity levels by

reducing humidity peaks. This in effect decreases dew point temperatures, and the likelihood of condensation and microbial growth.

4 ventilation schemes are provided as active measures to manage indoor moisture coupled with moisture buffering in the field experiment. The results show competing benefits when it comes to managing indoor air quality, indoor humidity, and minimizing ventilation heat loss. Time-controlled ventilation is effective at maintaining relative humidity at acceptable levels for thermal comfort. Time-controlled ventilation also provides considerable savings in ventilation heat losses of 20% in comparison to constant ventilation. However, CO₂ levels are exceeded beyond what is acceptable for good indoor air quality for 50% of the monitoring period. Conversely, demand-controlled ventilation schemes produce favourable indoor air quality based on CO₂ levels, while compromising indoor humidity levels.

ACKNOWLEDGEMENTS & DEDICATIONS

First, I am grateful for the financial support provided by the Canada Foundation for Innovation (CFI), Natural Sciences and Engineering Research Council of Canada (NSERC), Home Protection Office (HPO), Western Economic Diversification (WED) and the School of Construction and the Environment at the British Columbia Institute of Technology (BCIT) for making this research possible.

I would like to thank my advisor, Dr. Fitsum Tariku, for his support and guidance throughout my time at BCIT. This thesis would not have been completed without the technical support of BCIT Building Science department staff and summer students Doug Horn, Wendy Simpson, Timothy Lee, Justin Reiher, Jordan Ho, Jacob Mandy, William Lei, and Fargol Moshiri. I would also like to extend my gratitude to Elsa Ngudjiharto, Nima Khalkhali Shijini, Loveleen Atwal, and Lloyd Ramberg for both their moral support, and their help with the WBPRL facilities. I would also like to thank other BCIT staff and faculty for their sage guidance throughout the years, and for endowing me with invaluable knowledge in the field of building science.

I sincerely appreciate my colleagues and employers at RDH Building Engineering Ltd. for being so patient and accommodating while I spent time away from work to complete this thesis.

Last and not least, I owe my parents Sousan and Masoud Pedram, and my siblings Shahriar and Shirin the holidays, birthdays, and times I spent away from their company to pursue this endeavour. Thank you for being so supportive.

I dedicate this thesis to my late grandmother who I miss dearly.

TABLE OF CONTENTS

LIST OF TABLES	ix
LIST OF EQUATIONS	xi
LIST OF FIGURES	xii
1 INTRODUCTION	1
2 LITERATURE REVIEW.....	5
2.1 Indoor Humidity: Uncertainty in Occupants' Moisture Loads	5
2.2 Ventilation and Indoor Air Quality	8
2.2.1 Using CO ₂ as a Surrogate Measure of Indoor Air Quality	10
2.2.2 Indoor Humidity, Thermal Comfort, and Occupant Health	11
2.2.3 Mechanical Ventilation as a Means to Control Indoor Air Quality and Humidity	13
2.3 Moisture Buffering Properties, and Effects on Indoor Humidity	16
2.3.1 Significance of Moisture Buffering of Materials	17
2.3.2 Properties of Moisture Buffering Materials	18
2.3.3 Moisture Buffering, Thermal Comfort, and Mould Growth Potential	30
2.3.4 Moisture Buffering and Energy Efficiency.....	32
3 PROBLEM STATEMENT	36
4 RESEARCH APPROACH.....	38
4.1 Research Hypothesis & Objective	38
4.2 Research Scope	38
4.3 Research Methodology.....	38
4.4 Description of Reference Building	39
5 OVERVIEW OF FIELD TESTING FACILITIES	43
5.1 Construction	45
5.2 Buildings' Airtightness	47
5.3 HVAC System.....	48
5.3.1 Forced Airflow System.....	48
5.3.2 Air Handling Unit (AHU)	51
5.4 Occupant Simulators	52
5.4.1 Humidifiers	53
5.4.2 CO ₂ Dispensing System	55
6 EXPERIMENTAL SET-UP.....	59

6.1	Experiment Design Variables.....	60
6.2	Instrumentation & Calibration.....	65
6.2.1	RHT Sensors	65
6.2.2	CO ₂ Sensors	69
6.3	Determination of Interior Moisture and Carbon Dioxide Generation Profiles.....	72
6.3.1	Moisture Production Profiles.....	73
6.3.2	Carbon Dioxide Generation Profile.....	83
6.4	Implementation of Daily Profiles in Occupant Simulators	86
6.4.1	Implementation of Moisture Generation Profiles	86
6.4.2	Implementation of Carbon Dioxide Generation Profiles	93
6.5	Ventilation Scheme Algorithms	94
6.5.1	Constant Ventilation.....	95
6.5.2	Time-controlled Ventilation	96
6.5.3	RH-controlled Ventilation	98
6.5.4	CO ₂ -controlled Ventilation.....	99
7	EXPERIMENTAL RESULTS AND ANALYSIS	100
7.1	Data Processing.....	100
7.2	Passive Moisture Management Methods	105
7.2.1	Test Case 1 (Benchmark Test).....	105
7.2.2	Test Case 2	108
7.2.3	Test Case 3	109
7.2.4	Test Case 4	111
7.2.5	Analysis.....	112
7.3	Active Moisture Management Methods	124
7.3.1	Test Case 5	125
7.3.2	Test Case 6	128
7.3.3	Test Case 7	132
7.3.4	Test Case 8	135
7.3.5	Analysis.....	138
8	CONCLUSION.....	157
8.1	Concluding Remarks.....	157
8.2	Limitations and Improvements.....	159
8.3	Areas for Future Research.....	160

9	REFERENCES	162
10	PUBLICATIONS.....	168
11	APPENDICES	169
11.1	APPENDIX A.....	170
11.2	APPENDIX B	175
11.3	APPENDIX C	182

LIST OF TABLES

Table 1. Moisture production by occupants and their activities as defined by various sources	7
Table 2. Duration of Time (Equivalent Nights) That the Humidity, Temperature, Warm Respiratory Comfort, and Perceived Air Quality Are Unfavorable for Different Ventilation Rates (Simonson, et al. 2004)	30
Table 3. Airtightness of the test building facilities at the WBPRL.....	47
Table 4. Classifications of buildings' airtightness (ASHRAE, 2013).....	48
Table 5. List of Test Parameters for Test Cases 1 – 8	63
Table 6. Errors in readings from calibration of north and south building RHT sensors	69
Table 7. Selection of four <i>m</i> -profiles based on 50th and 95th percentile values for hour-9 and hour-20.....	78
Table 8. Four short-listed moisture production curves, and their total production per day	81
Table 9. Estimated CO ₂ generation rates of family of four.....	85
Table 10. Linear correlation fits from the nebulizer calibration tests and corresponding mean and standard deviation of characteristic misting rates.....	89
Table 11. Duty cycles of humidifiers based on pre-determined moisture generation profiles	91
Table 12. List of Test Parameters for Test Cases 1 – 4	105
Table 13. Comparison of indoor relative humidity (RH) between the control & test building for TC1	107
Table 14. Comparison of indoor relative humidity (RH) between the control & test building for TC2.....	109
Table 15. Comparison of indoor relative humidity (RH) between the control & test building for TC3	110
Table 16. Comparison of indoor relative humidity (RH) between the control & test building for TC4.....	112

Table 17. List of Test Parameters for Test Cases 5 – 8	125
Table 18. Comparison of indoor relative humidity, RH (%) and CO ₂ (ppm) between the control & test building for TC5 (TC2 shown in parentheses for comparison)	127
Table 19. Comparison of indoor relative humidity (RH) between the control & test building for TC6	130
Table 20. Comparison of indoor relative humidity (RH) between the control & test building for TC7	133
Table 21. Comparison of indoor relative humidity (RH) between the control & test building for TC8	137
Table 22. % of time CO ₂ levels exceed 1000 PPM threshold.....	145

LIST OF EQUATIONS

Equation 1. Ideal Moisture Buffering Value of materials as defined by NORDTEST (Rode, 2005)	21
Equation 2. Moisture effusivity.....	22
Equation 3. Practical Moisture Buffering Value of materials as defined by NORDTEST (Rode, 2005).....	22
Equation 4. Determination of absolute humidity.....	75
Equation 5. Determination of moisture production rate	75
Equation 6. Oxygen Consumption of Occupants (ASTM D6245, 2012)	83
Equation 7. Equilibrium Analysis (ASTM D6245, 2012)	95
Equation 8. Determination of relative humidity in control building (north) for test building (south) equivalent temperature	103
Equation 9. Determination of “% Difference” between RH values.....	107
Equation 10. Ventilation heat loss (J/s).....	146
Equation 11. Ventilation heat loss energy (J).....	153

LIST OF FIGURES

Figure 1. Percentage of dissatisfied visitors and occupants as a function of calculated steady-state ventilation rate for occupants (Berg-Munch et al 1986).....	10
Figure 2. Acceptable range of operative temperature and humidity to indoor spaces to meet 80% of occupants' satisfaction from ASHRAE Standard 55 (ASHRAE, 2010)	12
Figure 3. Comparison of simulated indoor CO ₂ levels with different mechanical ventilation systems for a single family residence in Vancouver, BC (Atwal & Mora, 2014). The acceptable threshold for indoor CO ₂ is 1000ppm (red line).	14
Figure 4. The effect of moisture buffering of interior wall finish material (plaster without paint) and non-moisture buffering material (aluminum) on indoor humidity levels (Kuenzel, et al. 2004). The buffering effect results in lower relative humidity peaks and higher relative humidity lows. 17	
Figure 5. Synergies between the moisture buffering capacity of a building is dependent on the building structure, outdoor climate, building use, and HVAC strategies (Hameury, 2006).....	19
Figure 6. Three levels of moisture buffering defined by NORDTEST (Rode, 2005)	20
Figure 7. Typical sorption isotherm of a hygroscopic material (Straube, 2006). This physical property affects moisture buffering in the hygroscopic region (highlighted in yellow).	21
Figure 8. An example of a hygroscopic material sample's mass variation measurements (due to moisture uptake) exposed to NORDTEST standard cyclic relative humidity excitations (Rode, 2005).....	23
Figure 9. Standard relative humidity maximum and minimum cycle for exposure of material samples to determine $MBV_{\text{practical}}$ per NORDTEST testing protocol (Rode, 2005)	23
Figure 10. $MBV_{\text{practical}}$ of common building materials as determined by Rode, et al. (2005)	24
Figure 11. $MBV_{\text{practical}}$ of common North American building materials as determined by Wu, et al. (2007).....	24

Figure 12. $MBV_{practical}$ of Scots pine with different coating systems: primer (1), plant-based oils (2–4), water-borne silicate coatings (5–6) waterborne acrylic-based coatings (7–8), and no coating (ref), (Hameury, 2007)	25
Figure 13. Classification of moisture buffering potential of materials based on $MBV_{practical}$ (Rode, 2005).....	26
Figure 14. The diminishing effect of increase in moisture buffering material surface area, on overall moisture buffering performance at room level (Mitamura, et al. 2004).....	27
Figure 15. Increase in ventilation decreases the moisture buffering effect in at room level as shown in Cases 1-1 (0 air changes per hour), Case 1-2 (1.5 air changes per hour), and Case 1-3 (10 air changes per hour)	28
Figure 16. The effect of moisture buffering and non-moisture buffering building enclosure materials on interior humidity conditions at room level (Svennberg, Lengsfeld, Harderup, & Holm, 2007).....	29
Figure 17. The mould growth risk assessment of a hygroscopic (hi) vs. non-hygroscopic (ref) interior finish clad test room for six different test cases (Ramos & de Freitas, 2008)	32
Figure 18. Total potential direct (a) heating and (b) and cooling energy savings when applying hygroscopic materials (Osanyintola & Simonson, 2006)	34
Figure 19. Rainscreen exterior wall assembly implemented during the building rehabilitation ...	40
Figure 20. Aerial photograph (a) and field photograph (b) of the Whole Building Performance Research Laboratory (WBPRL) at the British Columbia Institute of Technology (BCIT).....	44
Figure 21. Typical floor plan of test buildings at the WBPRL	46
Figure 22. Concrete floor and footing (left) and gypsum board ceiling (right) were isolated from interaction with indoor air moisture by installing polyethylene sheet	47
Figure 23. Schematic diagram of forced air system in the WBPRL mechanical system design (adapted from Tariku, et al. 2013).....	49

Figure 24. Locations of the diffuser on the ceiling (bottom left) and return vent on the partition wall (bottom right) and indicated on floor plan (top)	51
Figure 25. Schematic diagram of the of the Air Handling Unit.....	52
Figure 26. Occupant simulator equipped with control box, humidifiers, water reservoirs, pumps, CO ₂ release valve (not shown), and heat generating bulb (not shown)	53
Figure 27. Plexiglas humidifier Box	54
Figure 28. A humidifier connected to a control box, pump, and reservoir	54
Figure 29. Schematic of Carbon Dioxide Dispersion System	55
Figure 30. Photos of the components of CO ₂ dispensing system: CO ₂ tank and regulator (a), solenoid valve (b), laminar flow element with pressure tubes (c), and end of tube outlet suspended near ceiling (d)	56
Figure 31. A solenoid valve in its fully closed state (source: solenoid-valve-info.com)	57
Figure 32. Schematic diagram of field experiment set-up.....	59
Figure 33. Designation of the North (Control) and South (Test) buildings	61
Figure 34. Locations of 5 RHT sensors inside the test space: 3 sensors are located at mid-height, 1 sensor is below mid-height and 1 is above mid-height at the south-east quadrant.....	66
Figure 35. Temperature set-point, data from five RHT sensors in the north building, one RHT sensor in the south building, and climate chamber sensor used in calibration	67
Figure 36. Temperature set-point, data from four RHT sensors in the south building, and climate chamber sensor used in calibration	67
Figure 37. Relative humidity set-points, data from five RHT sensors in the north building, one RHT sensor in the south building, and climate chamber sensor used in calibration	68
Figure 38. Relative set-points, data from four RHT sensors in the south building, and climate chamber sensor used in calibration	68
Figure 39. CO ₂ Sensor can measure and record CO ₂ concentration	70

Figure 40. CO₂ data recorded over a duration of 4 days. The self-calibration function occurs on day 3 (denoted by arrow) to the north building’s sensor, thereby reducing the % difference between the two CO₂ sensor readings. 71

Figure 41. CO₂ data recorded in each building. The self-calibration function occurs in both buildings, resulting in % difference in CO₂ level readings of 0%. Readings for a separate CO₂ sensor by a difference manufacturer are also plotted for comparison. 72

Figure 42. Floor plan of Suite A 74

Figure 43. Daily indoor relative humidity profiles of ‘Suite A’ for December 1st to February 28th 76

Figure 44. Daily indoor moisture production profiles (*m*) of Suite A for December 1st to February 28th. Standard deviation or “spread” (σ) of data sets is indicated for ventilation “on” and “off” periods. 77

Figure 45. Normal distribution curve, cumulative distribution function, and linear probability correlation of *m* for hour-9 (a–c) and hour-20 (d–f) from 90 days of Suite A monitoring data 79

Figure 46. Four curves isolated amongst the data set in Figure 44, two representing typical or 50th percentile (red), and two representing high or 95th percentile (black) moisture production profiles 80

Figure 47. *m*-profiles obtained from Suite A scaled down 75% (a), and typical (based on Dec. 3) and high (based on Jan. 30) smoothed curves used as moisture production profiles in the field experiments to simulate the moisture generation of occupants and their activities (b)..... 82

Figure 48. Dependence of CO₂ Production per Person on the Level of Activity (ASHRAE 62.1, 2013)..... 84

Figure 49. Typical activities of a family of four throughout the day and their corresponding metabolic activity..... 85

Figure 50. Plot of cumulative loss of mass of water from humidifier box over time for each pair or individual nebulizer 87

Figure 51. Water Droplets Forming on the Interior Surfaces of Humidifier Box	88
Figure 52. Water level measured 2.5 cm above nebulizers	92
Figure 53. CO ₂ dispensing rate for the north building (a) and south building (b) based on 100% continuously on duty cycle, adjusted	94
Figure 54. Representation of ventilation algorithm for constant ventilation, test cases T1 to TC5	96
Figure 55. Representation of ventilation algorithm for time-controlled ventilation	97
Figure 56. Representation of ventilation algorithm for RH-controlled ventilation	98
Figure 57. Representation of ventilation algorithm for CO ₂ -controlled ventilation.....	99
Figure 58. RHT sensor readings from the control building (north) show relative humidity and temperature readings in each test room deviate within the % error of the sensor	101
Figure 59. RHT sensor readings from the test building (south) show relative humidity and temperature readings in each test room deviate within the % error of the sensor	101
Figure 60. Oscillation pattern seen in interior conditions of WBPRL buildings during field testing TC1 to TC4.....	102
Figure 61. (a) 5-minute indoor conditions, (b) after temperature correction for control building	104
Figure 62. The indoor temperature and relative humidity of the control building (red) and test building (blue) under TC1 – benchmarking case. Relative humidity peaks coincide with moisture loading peaks.	106
Figure 63. Maximum RH, minimum RH, RH amplitude and mean RH for Cycle 2	107
Figure 64. The indoor temperature and relative humidity of the control building (red) and test building (blue) under TC2 – normal occupancy and ventilation	108
Figure 65. The indoor temperature and relative humidity of the control building (red) and test building (blue) under TC3 – normal occupancy, under-ventilation.....	110
Figure 66. The indoor temperature and relative humidity of the control building (red) and test building (blue) under TC4 – high occupancy	112

Figure 67. RH amplitude (Max RH – Min RH) for Cycle 1 & 2 from test cases TC1, TC2, TC3, and TC4	113
Figure 68. % Difference in RH amplitudes between the control and test building from test cases TC1, TC2, TC3, and TC4	114
Figure 69. Minimum, maximum, and mean RH for Cycle 1 & 2 from test cases TC1, TC2, TC3, and TC4. The test building is shown in solid and the control building is shown in hatched. Optimal interior RH range is highlighted in blue.	115
Figure 70. Difference in minimum, maximum, and mean RH between the control and test building from test cases TC1, TC2, TC3, and TC4	116
Figure 77. The indoor and dew point temperatures of the control building (red) and test building (blue) under TC1 – bench marking test.....	118
Figure 78. The indoor and dew point temperatures of the control building (red) and test building (blue) under TC2.....	118
Figure 79. The indoor and dew point temperatures of the control building (red) and test building (blue) under TC3 – under-ventilation.....	119
Figure 80. The indoor and dew point temperatures of the control building (red) and test building (blue) under TC4 – high occupancy	119
Figure 71. Interior and exterior absolute humidity in the control building during test cases TC1 and TC2	120
Figure 72. Excess humidity (interior absolute humidity – exterior absolute humidity) in the control building during test cases TC1 and TC2	121
Figure 73. Excess humidity in the test building during test cases TC1 and TC2	122
Figure 74. Excess humidity in the test building during test cases TC2 and TC3	122
Figure 75. Excess humidity in the test building during test cases TC2 and TC4	123
Figure 81. % of time interior relative humidity levels exceed high thresholds for TC2, TC3, and TC4.....	124

Figure 82. The indoor relative humidity and ventilation rate of the control building (red) and test building (blue) under TC5 – constant ventilation.....	126
Figure 83. Outdoor vapour pressures for duration of 28 hours during TC2 and TC5	127
Figure 84. Indoor CO ₂ levels of the control building (red) and test building (blue) under TC5 – constant ventilation	128
Figure 85. The indoor relative humidity and ventilation rate of the control building (red) and test building (blue) under TC6 – time-controlled ventilation.....	129
Figure 86. Maximum RH, minimum RH, RH amplitude and mean RH in control building for Cycle 2.....	130
Figure 87. Indoor CO ₂ levels of the control building (red) and test building (blue) under TC6 – time-controlled ventilation	131
Figure 88. The indoor relative humidity and ventilation rate of the control building (red) and test building (blue) under TC7 – RH-controlled ventilation	133
Figure 89. Indoor CO ₂ levels of the control building measured (red) and simulated using HAMFitPlus model (dotted red), and test building (blue) under TC7 – RH-controlled ventilation	135
Figure 90. The indoor relative humidity and ventilation rate of the control building (red) and test building (blue) under TC8 – CO ₂ -controlled ventilation. Control building data is simulated using HAMFitPlus.....	136
Figure 91. Indoor CO ₂ levels of the test building under TC8 – CO ₂ -controlled ventilation	138
Figure 92. RH amplitude (Max RH – Min RH) for Cycle 1 & 2 from test cases TC5, TC6, TC7, and TC8	139
Figure 93. % Difference in RH amplitudes between the control and test building from test cases TC1, TC2, TC3, and TC4	140

Figure 94. Minimum, maximum, and mean RH for Cycle 1 & 2 from test cases TC5, TC6, TC7, and TC8. The test building is shown in solid and the control building is shown in hatched. Optimal interior RH range is highlighted in blue.	140
Figure 95. Difference in minimum, maximum, and mean RH between the control and test building from test cases TC5, TC6, TC7, and TC8	141
Figure 96. Outdoor CO ₂ Levels.....	143
Figure 97. Minimum, maximum, and mean CO ₂ for Cycle 1 & 2 from test cases TC5, TC6, TC7, and TC8. The test building is shown in solid and the control building is shown in hatched. Optimal interior RH range is highlighted in blue.	144
Figure 98. % Difference in minimum, maximum, and mean CO ₂ between the control and test building from test cases TC5, TC6, TC7, and TC8.....	145
Figure 99. Ventilation heat loss, indoor and outdoor temperatures for the control building (red) and test building (blue), and outdoor temperatures under TC5 – constant ventilation.....	147
Figure 100. Ventilation heat loss, and ventilation rate for the control building (red) and test building (blue) under TC5 – constant ventilation.....	148
Figure 101. Ventilation heat loss, indoor and outdoor temperatures for the control building (red) and test building (blue), and outdoor temperatures under TC6 – time-controlled ventilation	149
Figure 102. Ventilation heat loss, ventilation rate for the control building (red) and test building (blue) under TC6 – time-controlled ventilation.....	149
Figure 103. Ventilation heat loss, indoor and outdoor temperatures for the control building (red) and test building (blue), and outdoor temperature under TC7 – RH-controlled ventilation.....	150
Figure 104. Ventilation Heat Loss and ventilation rate for the control building (red) and test building (blue) under TC7 – RH-controlled ventilation	151
Figure 105. Ventilation heat loss, indoor and outdoor temperatures for the control building (red) and test building (blue), and outdoor temperature under TC8 – CO ₂ -controlled ventilation	152

Figure 106. Ventilation heat loss and ventilation rate for the control building (red) and test building (blue) under TC8 – CO₂-controlled ventilation 152

Figure 107. Area under each ventilation heat loss curve used for calculation of heat loss energy under TC5 to TC8..... 154

Figure 108. Total energy loss (heating and cooling) due to ventilation for a duration of 28 hours under test cases TC5 to TC8. Values indicated above each bar are energy loss in kilowatt-hours. 155

1 INTRODUCTION

Climate change, peak oil, sustainability, green energy, energy efficiency: these are some of the buzz words that have made their way from academic panels, scientific literature, and political roundtables, into mainstream media, corporate marketing, and family dinner tables. The consumer, the investor, the policy maker, and the researcher, all have varying motives for contributing to realm that surrounds these buzz words. Whether it is environmental conscientiousness, economic payback, being (or appearing as) a socially responsible world class citizen/ entity, the conversation around the future of the environment and quality of life on planet earth is bringing these pressing issues to the forefront of human development. However, these varying motives have also blurred the lines between fact and opinion, precedence and non-relevance, and even what is morally right or wrong. As individuals, professionals, and institutions, it is our prerogative to further the agendas that will allow future generations to be entitled to the same privileges as we are entitled to here and now.

In the building science community, it has been recognized that buildings, in all stages of their life-cycle, are one of the major contributors to greenhouse gas emissions. Most academic papers in the field arouse the interest of the reader beginning by stating this fact: The buildings sector is one of the biggest contributors to global greenhouse gas emissions. There are varying breakdowns, percentages, and ranks of emissions between different sectors depending on the source. In general, transportation, industry, and buildings sectors are recognized as the top emitters. What differentiates the buildings sectors is that it has the highest potential for delivering the most significant and cost-effective reduction in greenhouse gas emissions (UNEP, 2009).

There are already technologies, methods and rating systems established for targeting the energy efficiency and greenhouse gas emission reduction in both new construction and existing building stock. The intent of this thesis is not to delve into this but rather to cover considerations when it

comes to the energy efficiency and durability of buildings based on field investigations, especially when it comes to low-income and high occupancy residential settings.

Typically in new building construction, special attention is given to ensure airtightness of the building enclosure as an energy efficiency measure. A more airtight building enclosure is an energy efficiency measure in that it can reduce the heating energy required for replacing heat loss from air leakage through the building enclosure. Some jurisdictions such as the Washington State Energy Code require air leakage testing. In some cases compliance with a maximum air leakage rate may be required (Washington State Energy Code, 2012).

In the Lower Mainland of BC, many buildings have undergone rehabilitation to prevent water ingress and deterioration following widespread poorly constructed leaky condos from the 1980's and 1990's. In order to prevent future rainwater penetration from the exterior, the building enclosures are designed for better water shedding and watertightness. Rehabilitation of the building enclosure for preventing water ingress also presents opportunities to improve the airtightness. Building retrofits such as those extensively done in the Lower Mainland of British Columbia for water ingress prevention or elimination have resulted in significantly more airtight buildings. However, in many instances, the enclosures were made more airtight without consideration for the need to increase ventilation (Roppel, Lawton & Hubbs, 2007). Adequate ventilation is crucial especially when moisture production of occupants may exceed design moisture loading. Without adequate ventilation, tighter building enclosures will generally result in elevated humidity levels and higher humidity peaks, and increase the risk of condensation in the building enclosure and on cold surfaces such as window glazing.

Condensation can adversely affect the durability of a building. Chronic condensation and moisture accumulation leads to deterioration of the building enclosure and structural materials, such as softening of gypsum drywall, wood decay, corrosion of steel, peeling of paint finishes,

damage to moisture sensitive insulation, and growth of mould, mildew, and fungi which can be detrimental to health (HPO, 2006). With rehabilitation resulting in tighter building enclosures, sufficient ventilation measures are required to avoid building durability issues. Sufficient ventilation can be achieved by means of retrofitting mechanical systems such as installing exhaust fans where there are none existing, upgrading existing exhaust fans to a higher flow rate model, implementing make-up air supply systems or heat recovery ventilators. Physical constraints of the building or cost limitations may render mechanical ventilation retrofits infeasible, in which case opening windows or running exhaust fans more frequently or continuously are required to reduce indoor humidity. Opening windows and running ventilation fans more frequently may address condensation and durability issues, but since more heating energy is required for additional outdoor air intake, they are also measures that compromise energy efficiency.

The motivation for this thesis comes from a low-income housing reference building in Vancouver, BC with high indoor humidity and building durability issues brought on by air-tightening the building enclosure following rehabilitation. Implementation of new ventilation exhaust fans and operating schemes were not sufficient in addressing the building humidity and durability issues. Field experiments were designed to mimic the scenario of a suite in the low-income housing building and used to develop solutions to address the high indoor humidity problem, while also considering heat loss through ventilation and indoor air quality. The effect of moisture buffering of interior gypsum board as a passive means to reduce indoor humidity was investigated.

This thesis is structured as follow: Chapter 1 consists of this introduction. Chapter 2 covers literature relevant to the thesis topic including uncertainty in occupants' moisture loads, ventilation and indoor air quality, and the phenomenon of the moisture buffering of materials. Chapter 3 forms the problem statement. Chapter 4 outlines the research objective, hypothesis,

scope, and methodology, and leads into Chapters 5 and 6: overview of the testing facilities and experimental set-up for the field investigation. Chapter 7 presents the results obtained from the field experiments and analysis of the results. Finally, Chapter 8 provides concluding remarks, limitations and improvements, as well as areas for future research. References and appendices are provided at the end of the thesis.

2 LITERATURE REVIEW

The literature review for this research is based on the following focus areas:

- Indoor humidity: uncertainty in occupants' moisture loads;
- Ventilation and indoor air quality; and
- Moisture buffering properties, and effects on indoor humidity.

2.1 Indoor Humidity: Uncertainty in Occupants' Moisture Loads

High occupancy residences are characterized as those that have more number of occupants (typically adults) than typical for a certain square footage and number bedrooms in a unit, or as dictated by ASHRAE Standard 160 (2009). Low-income family housing residences are typically high occupancy. Due to financial limitations, these buildings may not be maintained as needed and durability may be compromised. Characteristics that are typical of high occupancy / low-income residences are high indoor humidity, poor indoor air quality, poor building maintenance, and poor building durability (National Council on Welfare, 2007). Moreover, the rate of moisture generation is increased with increasing number of occupants, thus occupant activities in high occupancy residences generate more moisture than in normal occupancy residences (TenWolde & Walker, 2001). This is due to moisture produced from activities such as more frequent showering, cleaning, laundry, and cooking. Additional factors such as line-drying clothes indoors, cooking predominantly by boiling, and not using spot ventilation (bathroom and kitchen hood ventilation) can also contribute to increased indoor humidity in high occupancy residences.

TenWolde and Walker (2001) laid the foundation for interior moisture design by developing ASHRAE Standard 160P. This standard defines models that determine moisture loading based on occupant density and ventilation rate (the Intermediate Model), or moisture loading based on outdoor conditions (the Simple Model). Simple moisture balance models which do not consider hygrothermal or moisture buffering effects of materials may suffice in predicting overall indoor

humidity averages over the long-term, for instance on a seasonal or yearly scale (Lu , 2003; Loudon, 1971; TenWolde & Walker, 2001), but not on a smaller time scale. However, models that do take hygrothermal capacities of materials into account such as Jone (1993), reasonably predict indoor states for short-term periods (e.g. hourly, daily, weekly). The role moisture buffering plays in affecting indoor moisture is on a smaller resolution in time scale than what moisture prediction models commonly use (Glass & TenWolde, 2009).

Tariku, et al. (2009) used five moisture prediction models to assess the risk of condensation on the corner of a wood-frame building enclosure, where it is coldest due to thermal bridging. The results are highly variable from no risk of condensation to high risk of condensation. This reiterates the fact that there is a need for better and more accurate moisture prediction models, because it can have important implications for design decisions.

Moisture production in houses depends on climate (external factors), type of ventilation and building enclosure (building factors) and number of occupants and the nature of their activities (internal factors), (Kalamees, Vinha, & Kurnitski, 2006). In this research, the first two factors are controlled, and the latter factor is a variable of interest.

There are numerous literatures on the moisture production of occupants due to their activities (Table 1). Unfortunately, in these literatures the rates of moisture production defined are not always consistent. For example, in one literature alone, the rate of moisture produced from cooking three meals for a family of four people varies between 0.8 to 3.0 kg per day (Kalamees, Vinha, & Kurnitski, 2006). Roppel, Brown & Lawton (2007) report the rate of moisture production for washing floors as 0.3 kg of moisture per day, whereas it is reported as a rate dependent on floor area by Christian (2009).

Table 1. Moisture production by occupants and their activities as defined by various sources

Literature*	Moisture Production Categories Defined	Average or Typical Rate			High or Maximum Rate		
		kg/hr	kg/d	Other	kg/hr	kg/d	Other
1	Moisture Sources (2 bedroom apartment)						
	People (3 occupants)	0.16	3.75	-	-	-	-
	Bath/shower	0.03	0.8	-	-	-	-
	Cooking (3 meals)	0.04	0.9	-	-	-	-
	Dish washing	0.02	0.5	-	-	-	-
	Plants	0.01	0.2	-	-	-	-
	Floor washing	0.01	0.3	-	-	-	-
	Total	0.27	6.5	-	-	-	-
2	Literature						
	IEA Annex XIV	0.34	8.2	-	-	-	-
	TenWolde and Walker (2001)	0.28	6.8	-	-	-	-
	Lawton (1998), top 50 percentile for mould (4.46 occupants)	0.85	20.4	-	-	-	-
	Lawton (1998), bottom 50 percentile for mould (4.26 occupants)	0.51	12.2	-	-	-	-
3	Literature						
	ASHRAE 160P, 1 bdrm	0.33	8.0	-	-	-	-
	ASHRAE 160P, 2 bdrm	0.50	12.0	-	-	-	-
	ASHRAE 160P, 3 bdrm	0.58	14.0	-	-	-	-
	ASHRAE 160P, additional bdrms	0.04	1.0	-	-	-	-
4	Daily Moisture Production of "Below-Average" Home						
	≤3 occupants	0.19	4.6	-	0.46	11.0	-
	>3 occupants	0.24	5.8	-	0.60	14.5	-
	All houses	0.21	5.1	-	0.53	12.7	-
	Daily Moisture Production of "Above-Average" Home						
	≤3 occupants	0.24	5.8	-	0.45	10.8	-
	>3 occupants	0.31	7.5	-	0.59	14.2	-
	All houses	0.28	6.8	-	0.53	12.8	-
	Moisture Production Rates from Literature						
	People	0.04	0.90	-	0.10	2.40	-
	Asleep	0.04	0.96	-	-	-	-
	Active	0.06	1.32	-	-	-	-
	light activity	0.03	0.72	-	0.06	1.44	-
	med activity	0.12	2.90	-	0.20	4.80	-
	hard word	0.20	4.80	-	0.30	7.20	-
	dog/cat	-	-	0.1 of adult weight	-	-	0.4 of adult weight
	Cooking (family of 4, electric / gas)	0.03	0.80	-	0.10	2.40	-
	Breakfast	0.01	0.17	-	0.01	0.27	-
	Lunch	0.01	0.25	-	0.01	0.32	-
	dinner	0.02	0.58	-	0.03	0.75	-
	3 meals	0.04	0.90	-	0.13	3.00	-
	Dishwashing (family of 4)	0.00	0.10	-	0.02	0.45	-
	House plants	0.02	0.40	-	0.03	0.80	-
	small	0.01	0.12	-	0.01	0.24	-
	med (fern)	0.01	0.17	-	0.02	0.36	-
	med (rubber)	0.02	0.50	-	-	-	-
	Shower (once)	0.01	0.19	-	0.02	0.40	-
5-minute	0.01	0.22	-	0.01	0.25	-	
Sauna (once)	1.28	n/a	-	-	-	-	
Clothes drying	0.04	1.00	-	0.15	3.50	-	
spin dried	0.00	0.05	-	0.01	0.20	-	
dripping wet	0.02	0.45	-	0.10	2.30	-	

Literature*	Moisture Production Categories Defined	Average or Typical Rate			High or Maximum Rate		
5	Moisture Production Rate for Different Occupant Activities						
	Metabolic (per person)	0.05	1.25	-	-	-	-
	light activity	0.03	0.72	-	0.06	1.44	-
	med activity	0.12	2.9	-	0.20	4.8	-
	hard work	0.20	4.8	-	0.30	7.2	-
	Bathing	0.01	0.22	-	0.01	0.25	-
	personal hygiene (per person)	0.03	0.6	-	-	-	-
	Kitchen (family of 4)	0.10	2.4	-	-	-	-
	gas range	0.10	2.35	-	-	-	-
	electric range	0.04	1	-	-	-	-
	Dishwashing (family of 4, 3 meals)	0.02	0.5	-	-	-	-
	breakfast	0.00	0.1	-	-	-	-
	Lunch	0.00	0.08	-	-	-	-
	dinner	0.01	0.32	-	-	-	-
	Plants	0.02	0.5	-	-	-	-
	Floor mopping	-	-	0.15 L/m ²	-	-	-
	Laundry	0.03	0.6	-	-	-	-
	Clothes drying - vented dryer	0.02	0.5	-	-	-	-
	Clothes drying - line	0.09	2.2	-	0.13	3	-
	Clothes drying - spin dried	-	-	0.01 L/kg laun- dry	-	-	0.04 L/kg laun- dry

* - The source of the literature can be cross referenced with numbers and citations below:

- 1 Roppel, Brown, & Lawton (2007)
- 2 Roppel, Lawton, & Brown (2009)
- 3 TenWolde & Walker (2001)
- 4 Kalamees, et al. (2006)
- 5 Christian (2009)

Uncertainty in moisture loading is not the only issue that can be detrimental to buildings and occupants' health due to higher than expected indoor humidity. Ventilation strategy can also dictate indoor moisture levels. The importance of ventilation and indoor air quality is further highlighted in the next section.

2.2 Ventilation and Indoor Air Quality

After studying the ventilation strategy in a newly retrofitted building with condensation issues, Roppel, Lawton & Hubbs (2007) found that adequate air supply was not provided to the suites. As a result, the relative humidity levels, carbon dioxide levels, and interior vapour pressure from monitoring were all found to be higher than acceptable standard levels. Adequate fresh air intake was getting to the pressurized corridors but not necessarily to the suites through door undercuts. As well, the principal mechanical exhausts were bathroom fans, which were very close to the

door undercuts, creating a short-circuit in the fresh air flow. The building retrofit which resulted in a more airtight building was undertaken without consideration for ventilation strategy, resulting in poor indoor air quality, high indoor moisture and consequent condensation and durability issues.

ASHRAE Standard 62.1 defines ventilation as the process of supplying air to or removing air from a space for the purpose of controlling air contaminant levels, humidity, or temperature within the space. Adequate ventilation design for acceptable indoor air quality goes back as far as the 1930's (Yaglou, Riley, & Coggins, 1936). In the 80's, Berg-Munch, Clausen & Fanger (1986) conducted studies on evaluating the adequate ventilation rate required to keep body odour in an auditorium occupied by more than 100 people at a minimum. Odour intensity levels were rated by visitors who were not acclimatized to the space, as acceptable or unacceptable on a six-point scale. The odour intensity ratings were then related to carbon dioxide (CO₂) concentration in the room for a given CO₂ production rate per person, and the corresponding steady-state ventilation rates were determined. Based on their findings, the steady-state ventilation rate required to keep less than 20% of visitors (non-acclimatized occupants) dissatisfied is 8 L/s or 17 CFM (Figure 1). The indoor air is deemed acceptable if less than 20% of the occupants exposed do not express dissatisfaction (ASHRAE 62.1, 2013). Based on this work, CO₂ is often used as a surrogate measure of indoor air quality.

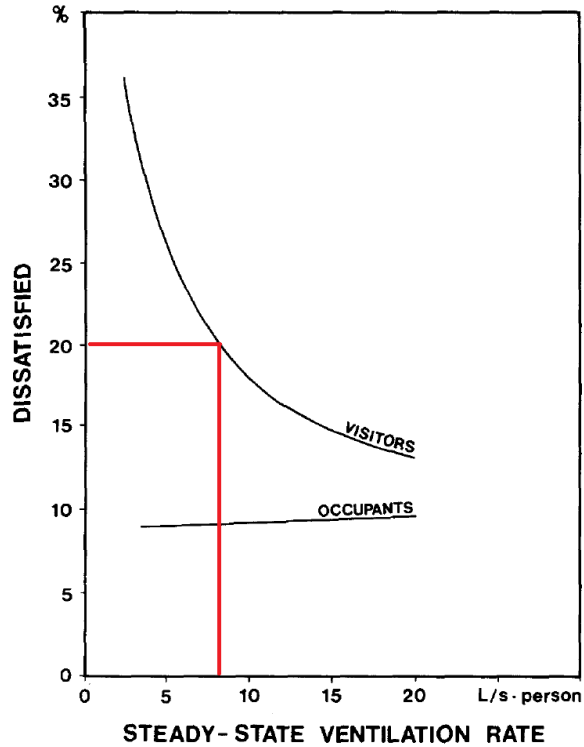


Figure 1. Percentage of dissatisfied visitors and occupants as a function of calculated steady-state ventilation rate for occupants (Berg-Munch et al 1986).

2.2.1 Using CO₂ as a Surrogate Measure of Indoor Air Quality

Using CO₂ as an indicator of indoor air quality is useful and simple; it can provide insight on the level of occupants' activity and breathing rate, the pattern of occupancy in a room, expected comfort levels of occupants based on body odour intensity, and adequacy of a ventilation system to dilute the space with outdoor air. There is a test standard, ASTM Standard D6245, dedicated to using CO₂ as an indicator to evaluate indoor air quality and space ventilation. However there are limitations to this method. Firstly, CO₂ is not an all-encompassing measure of indoor air quality. There are a plethora of contaminants in the air that can be detrimental to indoor air quality, such as combustion gases, tobacco smoke, radon, and volatile organic compounds (VOCs) from materials and chemicals to name a few. When possible, these contaminants can be reduced by source control, however in some cases such as household cleaning chemicals, they cannot be fully eliminated. As well, certain occupant activities that are high moisture emitting can be detrimental

to thermal comfort, and encourage microbial growth as they raise the humidity levels in a space, resulting in unhygienic conditions. These factors cannot be captured in CO₂ level measurements, despite their adverse effects on the indoor environment. Secondly, the relationship between ventilation rate per person and indoor CO₂ concentration are based on a set of assumptions. Some of these assumptions include the following:

- The correlation between body odour intensity and CO₂ concentration is based on studies with occupants of a certain age group, national geographic origin, diet, and hygienic habits (Berg-Munch, et al. 1986);
- The activity level and breathing rate of occupants are pre-defined;
- The CO₂ concentration indoors is in equilibrium with the outdoors;
- In order for equilibrium to occur, the ventilation rate must be constant (i.e. steady-state).

It is important to note, there are limitations to using CO₂ as a surrogate measure of indoor air quality, and that its assumptions must be applicable to the situation at hand. Moreover, CO₂ should be utilized in conjunction with other parameters, such as indoor humidity, to evaluate indoor air quality.

2.2.2 Indoor Humidity, Thermal Comfort, and Occupant Health

Indoor humidity is an important consideration as it dictates perceived indoor air quality and occupant thermal comfort. High indoor humidity can also create favourable conditions for mould and fungi growth, which can be detrimental to occupant health.

ASHRAE Standard 55 (2010) *Thermal Environmental Conditions for Human Occupancy* defines thermal comfort as the condition in which the mind expresses satisfaction with the thermal environment. Physiological and psychological variations from person to person make it difficult to satisfy all occupants in a space. Extensive empirical testing has been undertaken to statistically determine the indoor conditions in which at least 80% of occupants will perceive the indoor

environment as comfortable. To achieve 80% occupant acceptability of indoor conditions for most indoor spaces, ASHRAE recommends a high upper humidity ratio limit of 0.012 $\text{kg}_{\text{water}}/\text{kg}_{\text{dryair}}$ (or dew-point temperature of 16.8°C), which corresponds to 55% to 85% relative humidity for operative temperatures at 28°C and 19°C respectively (Figure 2).

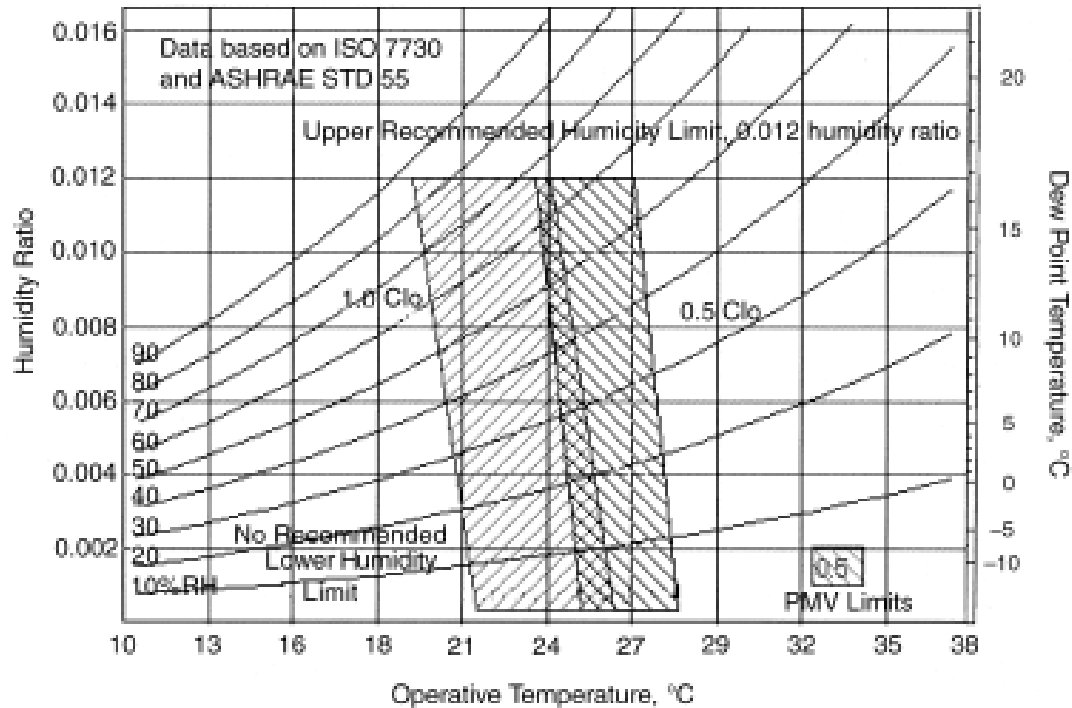


Figure 2. Acceptable range of operative temperature and humidity to indoor spaces to satisfy 80% of occupants from ASHRAE Standard 55 (ASHRAE, 2010)

Management of indoor humidity and maintaining occupants' comfort is important. For example, if indoor moisture exceeds the recommended levels and occupants are subjected to high space humidity in the cooling season, they may respond by lowering the thermostat setting in an attempt to achieve comfort. Lowering the thermostat in turn cools the interior space further, resulting in increased dew point temperatures along with the increased risk of condensation on supply air ducts, floors, and other building surfaces (Ouazia, Manning, Swinton, & Barhoun, 2008).

Moreover, relative humidity levels above 75% at room temperature (21°C) result in germination and growth of mould and fungi (Sedlbauer, 2002). Decrease in temperature and humidity levels to

an extent may cause mould fungi to become inactive after germination, but growth resumes when conditions become favourable again (Viitanen, et al. 2010). Moreover, dust mites grow and survive in relative humidity of 45% or greater, but undergo more rapid growth at higher relative humidities (Arlian, 1992). While average zone conditions may be within thresholds, localized conditions that favour microbial growth cyclically or consistently can sustain survival of mould, fungi, and allergens. This poses a health hazard to the building occupants, as well as a cause of damage to buildings (for example, wood rotting fungi in wood building structures). High indoor humidity may also cause the release of volatile organic compounds (VOCs) such as formaldehyde from building materials and furniture that may contain these chemicals, contributing to one of the major causative factors of sick building syndrome and building related illness (Hameury, 2006).

In general excess humidity in indoor spaces is undesirable and measures must be taken to manage it. Indoor humidity not only affects the perceived thermal comfort of occupants, but also the quality of the indoor air, and inherently the health of occupants.

2.2.3 Mechanical Ventilation as a Means to Control Indoor Air Quality and Humidity

Ventilation can be achieved by adding outdoor air to or removing indoor air from a space either passively (e.g. by openings windows) or actively (e.g. with mechanical systems). This can be achieved by a number of different methods and systems. This section will discuss mechanical ventilation as a means to control indoor air quality and humidity. Three examples of mechanical ventilation systems as defined by ASHRAE 62.1 (2013) are listed below:

- Continuous supply ventilation: air delivered continuously by a mechanical system to a space, composed of any combination of outdoor air, recirculated air, or transfer air.
- Continuous exhaust ventilation: air removed continuously from a space and discharged to outside the building by means of a mechanical system.

- **Balanced ventilation:** a mechanical system that uses a combination of removing indoor air and supplying outdoor, with or without heat recovery, to a space in tandem to achieve desired indoor air conditions.

In general, one mechanical ventilation system may out-perform another depending on the building construction, geometry, climate, and occupants' habits. Atwal & Mora (2014) undertake airflow simulation modeling to compare the performance of each of these systems on maintaining CO₂ levels below the acceptable threshold (1000 ppm) for a single-family residence in Vancouver, BC (Figure 3). They also compare the findings to the current ventilation system of the house, a forced-air heating system that supplies make up air for ventilation only when heating is required.

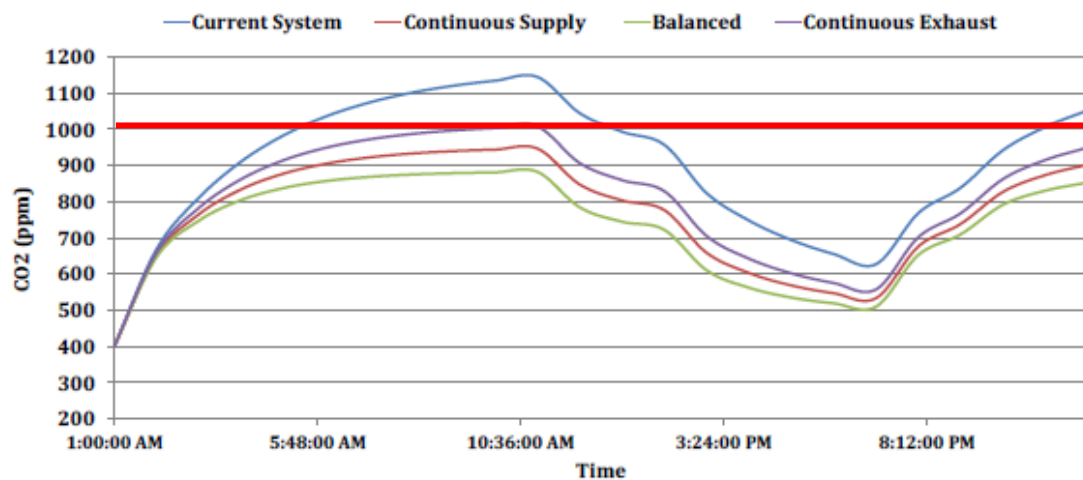


Figure 3. Comparison of simulated indoor CO₂ levels with different mechanical ventilation systems for a single family residence in Vancouver, BC (Atwal & Mora, 2014). The acceptable threshold for indoor CO₂ is 1000ppm (red line).

In general, a continuous supply, continuous exhaust, or balanced ventilation system may perform differently for the same building. In Figure 3, a balanced ventilation system is determined to be the best approach for this house. However, limitations such as costs to implement that system, excess building enclosure air leakage, and climate may not justify the implementation of the system (Atwal & Mora, 2014).

ASHRAE Standards 62.1 (2013) and 62.2 (2013) prescribe ventilation rate requirements to achieve acceptable indoor air quality in buildings, the basis of which is based on Equilibrium Analysis (Equilibrium Analysis will be further discussed in Section 6.5). The prescribed rates do not differentiate between different ventilation systems. Thus, any of the three ventilation systems (supply, exhaust, or balanced ventilation) may be designed to achieve the required ventilation rates. However, the suitability of each system based on costs, building construction, airtightness of the enclosure, and airflow paths must be considered.

The intent of ventilation is to promote good indoor air quality by displacing indoor air ridden with pollutants and odours and allowing outdoor air to replace displaced air. In cold climates, it also allows indoor moisture-laden air to be exhausted to the exterior and be replaced with dryer outdoor air. Ventilation of indoor air also allows for removal of excess indoor moisture and management of indoor humidity.

ASHRAE Standard 160 (2009) *Criteria for Moisture-Control Design Analysis in Buildings* has design provisions for continuous ventilation rates based on indoor and outdoor vapour pressures, outdoor temperatures, and design moisture generation rate of occupants to maintain the indoor environment within an acceptable relative humidity range. The upper and lower relative humidity threshold of indoor spaces is debated. In general, consensus is that interior relative humidity should not exceed 60% (70% at a building surface) to avoid mould growth and germination. The lower threshold is less concrete, however ASHRAE recommends that indoor relative humidity stay above 25% to avoid irritation of the respiratory mucus membrane and the eyes (Lstiburek, 2002).

Staying within this range is challenging for buildings located in marine climates such as the Pacific Northwest of the United States, and Southern West Coast of British Columbia. In these climates, outdoor air temperature is mild and the air is humid. Therefore ventilation alone may

not suffice in managing indoor moisture, especially if moisture generation of occupants exceeds the design moisture generation rate. In these climates, further passive measures such as the aid of moisture buffering materials, or active measures such as dehumidification may be required to manage indoor moisture.

2.3 Moisture Buffering Properties, and Effects on Indoor Humidity

Moisture buffering (also known as hygric inertia, hygroscopicity, or humidity buffering) is the phenomenon that allows hygroscopic materials to absorb moisture in the air when humidity levels rise, and release moisture back into the air when humidity levels falls (Figure 4). This effect can regulate indoor humidity levels, and allow acceptable range for thermal comfort, inhibition of microbial growth, and prevention of formation of condensation to be more easily maintained. The characteristics of moisture buffering have been studied on three levels: on a material level (Künzel, 1965; Künzel, 1968; Rode, 2005; Svennberg, 2006), system level (Kuenzel, et al. 2004; Hameury, 2006; Hameury, 2007; Wu, Fazio, & Kumaran, 2007; Yang, 2010), and room level (Mitamura, et al. 2004; Kalamees, et al. 2009; Li, Fazio, & Rao, 2010; Vereecken, Roels, & Janssen, 2011; Padfield & Jensen, 2011). There have also been studies on utilizing the phenomenon to achieve ventilation energy savings (Osanyintola & Simonson, 2006; Woloszyn & Rode, 2008; Woloszyn, et al. 2009).

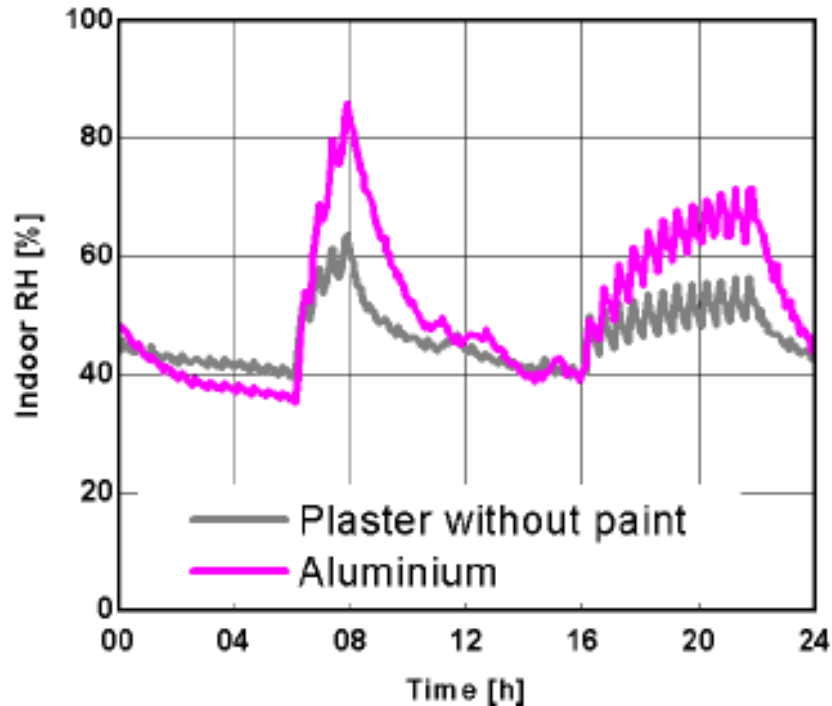


Figure 4. The effect of moisture buffering of interior wall finish material (plaster without paint) and non-moisture buffering material (aluminum) on indoor humidity levels (Kuenzel, et al. 2004). The buffering effect results in lower relative humidity peaks and higher relative humidity lows.

Moisture buffering can take effect on different time scales, affecting indoor moisture on an annual or seasonal level with variation in seasonal temperatures, or on a smaller scale at a diurnal or hourly time resolution.

2.3.1 Significance of Moisture Buffering of Materials

Healthy buildings have a balance between durability, good indoor air quality, energy efficiency, and aesthetics. With focus on only one measure in building design, other aspects of this balance may become compromised. Whole-building performance and design has been identified by designers and researchers as one of the approaches for optimizing all these pillars of building design.

Whole-building design involves the consideration of heat, air, and moisture (HAM) transfer and control in a building. Simulation tools and field studies have been utilized to implement whole-building design and optimization, understand hygrothermal performance of buildings, and

prolong the durability of buildings and building enclosures. One hygrothermal building simulation model, HAMFitPlus, takes into account the dynamic HAM interactions between the indoor environment, building enclosure, and mechanical systems (Tariku, 2008). One major consideration in HAMFitPlus is the effect of moisture buffering materials such as furniture and interior finishing materials on indoor moisture levels – that is, the hygroscopic properties of moisture buffering materials allow moisture in the indoor air to be absorbed at high humidity levels and desorbed (released back into the air) at low humidity levels.

Approximately one-third of moisture generated in a room may be absorbed by moisture buffering materials (El Diasty et al. 1992). Simulations have shown significant discrepancies in predicted interior humidity levels between models that take into account the moisture buffering effects, and others that do not (Woloszyn & Rode 2008). For example, in Tariku et al. (2011), it is found that when moisture buffering effect of the interior layer of the building enclosure is omitted from the HAMFitPlus model, interior relative humidity peaks are greatly overestimated.

2.3.2 Properties of Moisture Buffering Materials

Moisture buffering is not a new concept. Svennberg et al (2007) outline works done by German and Swedish researchers from the 1960's to 2000 on absorption-desorption behaviour of materials. Much work was done on this phenomenon during that time, which was referred to as “hygric inertia.” Experiments were also done on numerous materials (interior plasters and concrete, different species of wood, and textiles) in the form of absorption step-responses, desorption step-responses, or double sided step-responses (Künzel, 1965; Künzel 1968).

Hameury (2006) describes moisture buffering as the synergy between the building enclosure and the indoor environment. The moisture buffering capacity of a building is dependent on the building structure, outdoor climate, the building use, and HVAC (heating, ventilation and air-conditioning) strategy (Figure 5).

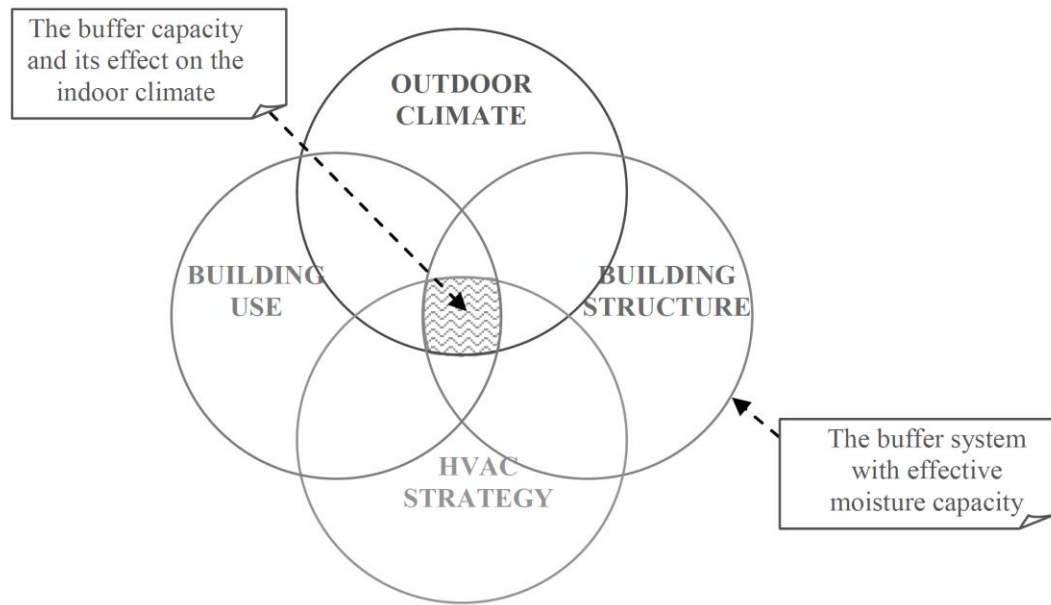


Figure 5. Synergies between the moisture buffering capacity of a building is dependent on the building structure, outdoor climate, building use, and HVAC strategies (Hameury, 2006)

The NORDTEST standard is the first attempt at quantifying the buffering ability of building materials on the indoor environment (Rode, 2005). It identifies the three levels of moisture buffering, and the properties that affect moisture buffering at each level (Figure 6). The three levels are identified as follows:

- Material level: On the material level the quantities are determined with negligible influence from the surrounding climate, e.g. boundary air layers.
- System level: material combinations where the simplest form of a material combination is a homogeneous material with the convective boundary air layer normally present in indoor environments. Systems may also comprise composite products.
- Room level: building and furnishing materials exposed to the indoor air as well as moisture loads, ventilation rate, indoor climate and other factors influencing the moisture buffering in the room.

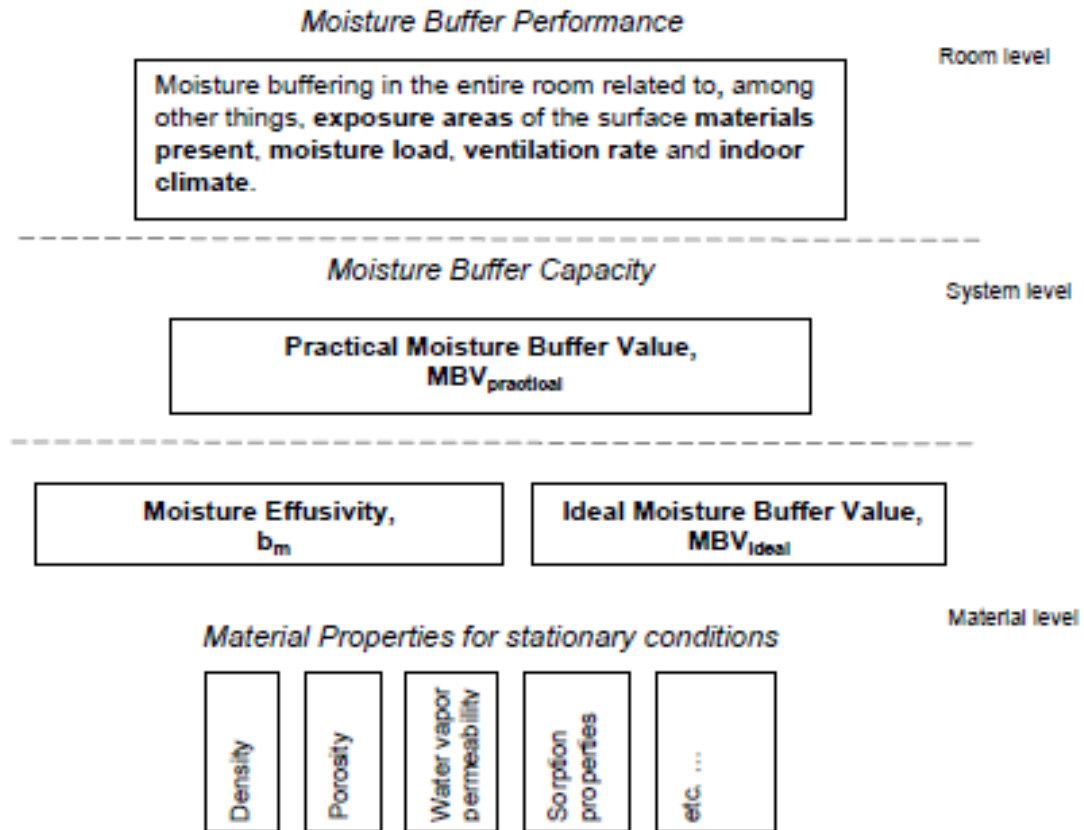


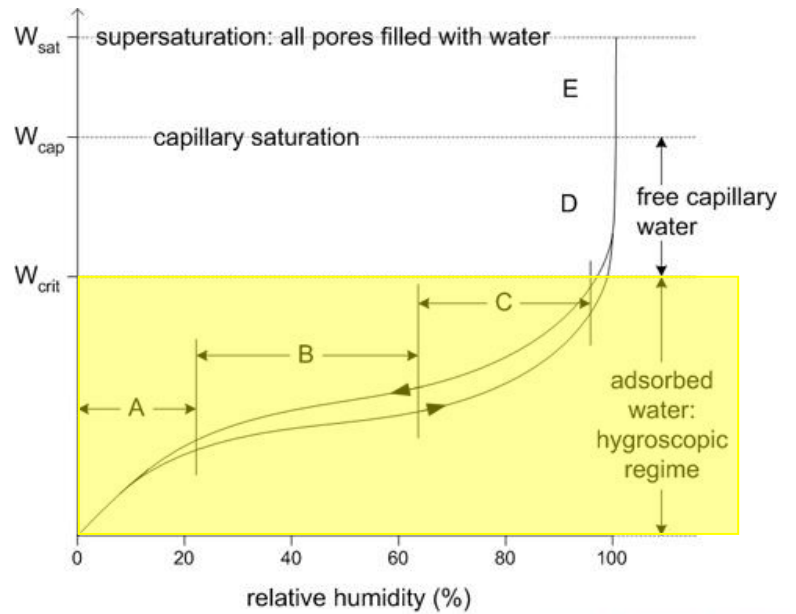
Figure 6. Three levels of moisture buffering defined by NORDTEST (Rode, 2005)

2.3.2.1 Moisture buffering at material level

Different models have been developed to determine and define moisture buffering mechanisms at a micro level, such as the moisture penetration depth model (Cunningham, 2003; Woloszyn & Rode, 2008); hygric capacitance model (Vereecken, et al. 2011); and moisture buffering value (MBV) model (Rode, 2005). In general what is common between all the models is that the material properties that govern moisture buffering mechanisms are the following:

- 1) Vapour permeability – governs how fast moisture is diffused into the material.
- 2) Sorption capacity – dictates the quantity of moisture that may be absorbed by the material at a given temperature, relative humidity, and moisture content, determined by the slope of its sorption isotherm (Figure 7).

- 3) Surface mass transfer – dictates the ease of mass transfer of water vapour particles from the air into the material at the boundary layer.



- A: Single-layer of adsorbed molecules
 B: Multiple layers of adsorbed molecules
 C: Interconnected layers (internal capillary condensation)
 D: Free water in Pores, capillary suction
 E: Supersaturated Regime

Figure 7. Typical sorption isotherm of a hygroscopic material (Straube, 2006). This physical property affects moisture buffering in the hygroscopic region (highlighted in yellow).

NORDTEST first quantified the moisture buffering of hygroscopic materials by defining the Ideal Moisture Buffering Value, MBV_{ideal} (Equation 1). The MBV_{ideal} is dependent on saturated vapour pressure of the surrounding air (p_s), the material moisture effusivity (b_m), and the time period during which the material is subjected to variations in relative humidity of surrounding air (t_p).

Equation 1. Ideal Moisture Buffering Value of materials as defined by NORDTEST (Rode, 2005)

$$MBV_{ideal} \approx 0.00568 \cdot p_s \cdot b_m \cdot \sqrt{t_p}$$

MBV_{ideal} = Ideal Moisture Buffering Value

p_s = saturated vapour pressure

b_m = moisture effusivity of material (defined by Equation 2)

t_p = time period of excitation

Moisture effusivity (Equation 2) is a function of vapour permeability, sorption capacity and saturated vapour pressure (which affects surface mass transfer).

Equation 2. Moisture effusivity

$$b_m = \sqrt{\frac{\delta_p \cdot \xi_v}{p_s}}$$

b_m = moisture effusivity of material

δ_p = vapour permeability [$\text{kg}\cdot\text{m}^{-1}\cdot\text{s}^{-1}\cdot\text{Pa}^{-1}$]

ξ_v = volumetric sorption capacity [$\text{kg}\cdot\text{m}^{-1}\cdot\text{s}^{-1}\cdot\text{Pa}^{-1}$]

p_s = saturated vapour pressure [Pa]

2.3.2.2 Moisture buffering at system level

$\text{MBV}_{\text{ideal}}$ defines the moisture buffering effect in theoretical terms. However, it is difficult to determine in practical terms. As a result, NORDTEST developed Practical Moisture Buffering Value, or $\text{MBV}_{\text{practical}}$, to allow the determination and quantification of moisture buffering of materials experimentally (Equation 3). The $\text{MBV}_{\text{practical}}$ is determined in an experimental set-up where a material sample is exposed to cyclic step-changes, in an environment with a maximum relative humidity (RH_{max}) and minimum relative humidity (RH_{min}) for 8 and 16 hours respectively, while the sample mass is measured quasi-continuously (Figure 8).

Equation 3. Practical Moisture Buffering Value of materials as defined by NORDTEST (Rode, 2005)

$$\text{MBV}_{\text{practical}} = \frac{m_{\text{max}} - m_{\text{min}}}{A \cdot (\text{RH}_{\text{max}} - \text{RH}_{\text{min}})}$$

$\text{MBV}_{\text{practical}}$ = Practical Moisture Buffering Value [$\text{g}\cdot\text{m}^{-2}\cdot\%\text{RH}^{-1}$]

m_{max} = maximum mass of material sample [g]

m_{min} = minimum mass of material sample [g]

A = surface area of material exposed to relative humidity variation cycle [m^2]

RH_{max} = maximum relative humidity material sample exposed to cyclically [%]

RH_{min} = minimum relative humidity material sample exposed to cyclically [%]

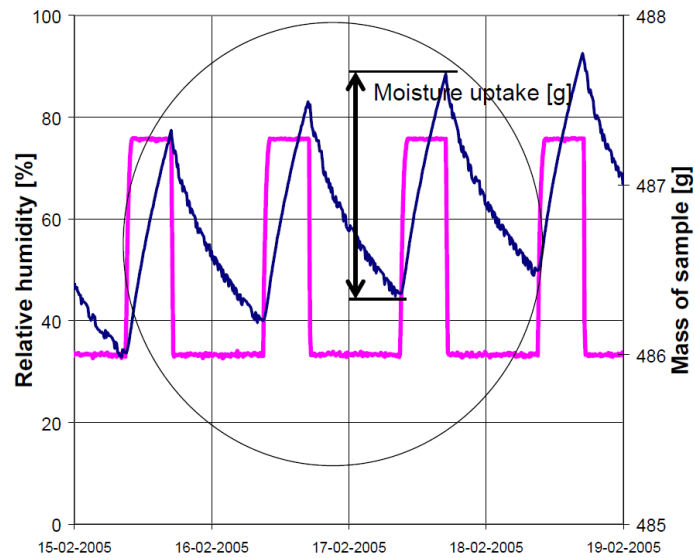


Figure 8. An example of a hygroscopic material sample’s mass variation measurements (due to moisture uptake) exposed to NORDTEST standard cyclic relative humidity excitations (Rode, 2005)

NORDTEST has developed a protocol for determining the $MBV_{\text{practical}}$ of materials and has standardized the relative humidity cycle variation time period, as well as RH_{max} and RH_{min} , which is depicted in Figure 9.

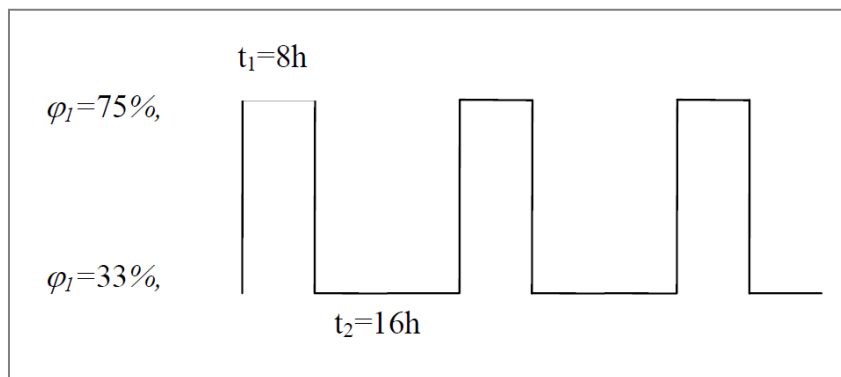


Figure 9. Standard relative humidity maximum and minimum cycle for exposure of material samples to determine $MBV_{\text{practical}}$ per NORDTEST testing protocol (Rode, 2005)

Using the NORDTEST protocol, $MBV_{\text{practical}}$ of common construction and building materials have been quantified (Figure 10 & Figure 11).

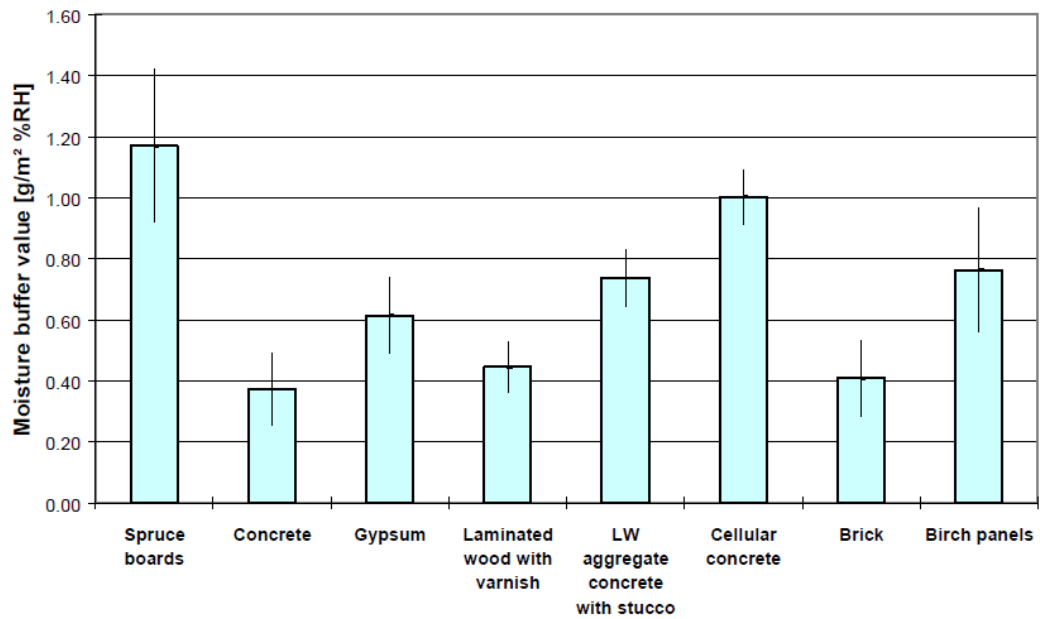


Figure 10. $MBV_{\text{practical}}$ of common building materials as determined by Rode, et al. (2005)

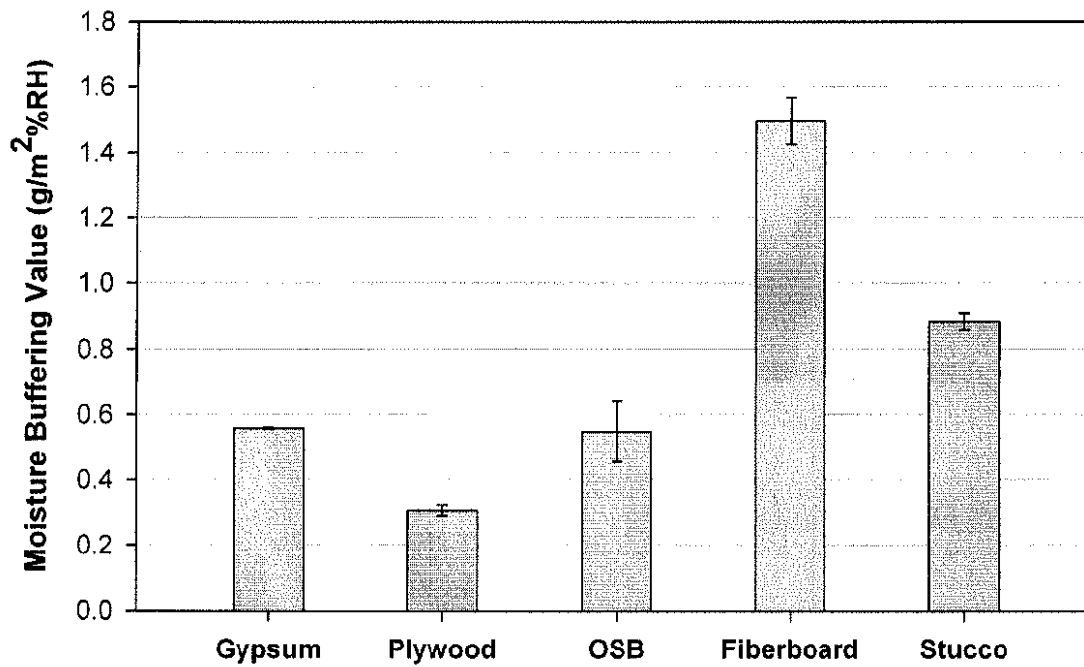


Figure 11. $MBV_{\text{practical}}$ of common North American building materials as determined by Wu, et al. (2007)

Coatings highly affect moisture buffering, as they affect the mass transfer coefficient of materials. Salonvaara, et al. (2004) found indoor relative humidity of a test room to be 40% higher at peak relative humidity for painted plaster walls than with standard plaster. Changes in sorption

capacity and vapour permeability were also evaluated. It was found that they still affect moisture buffering performance but are less sensitive. Hameury (2007) evaluates the effect of different coatings on Scots pine (Figure 12). The findings generally show that coatings decrease MBV and reduce moisture buffering capacity of Scots pine. However, it was found that waterborne alkali silicate coatings may potentially increase the MBV due to formation of micro cracks on the coating, and therefore an increase in surface area. Furthermore, using magnetic resonance imaging, it is confirmed that the penetration depth (i.e. mass transfer in the indoor air and the material surface boundary layer) is confined to a few millimeters deep from the surface of the material, when exposed to diurnal humidity excitations. The penetration depth of moisture decreases when low permeability coatings such as waterborne acrylic-based paints and primers are applied to wood.

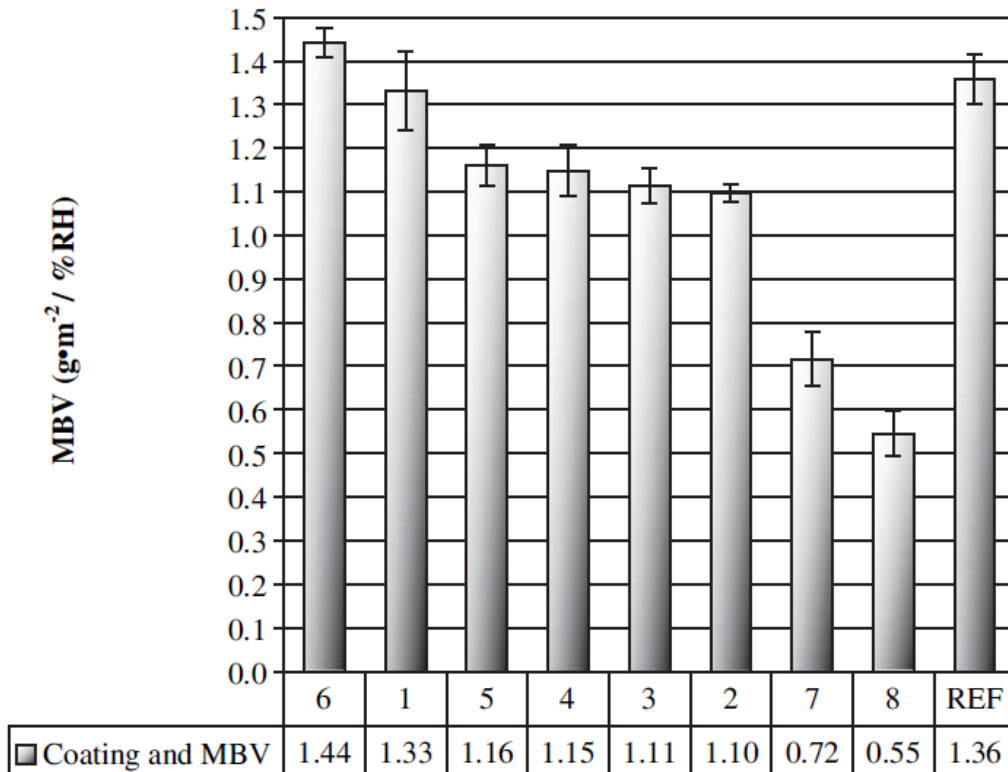


Figure 12. MBV_{practical} of Scots pine with different coating systems: primer (1), plant-based oils (2–4), waterborne silicate coatings (5–6) waterborne acrylic-based coatings (7–8), and no coating (ref), (Hameury, 2007)

NORDTEST goes as far as classifying the moisture buffering potential of materials based on their determined $MBV_{\text{practical}}$ (Figure 13). A material with good moisture buffering value is classified as one that can buffer the same magnitude of moisture flow rate as the minimum required ventilation air change. Generally it is very rare for common building materials to have a MBV value greater than $1.2 \text{ g/m}^2 \cdot \%RH$. With further research and innovation in material science, it may be possible to develop materials with significant moisture buffering potential that can buffer high volumes of moisture, and/ or have rapid response to changes in the indoor environment.

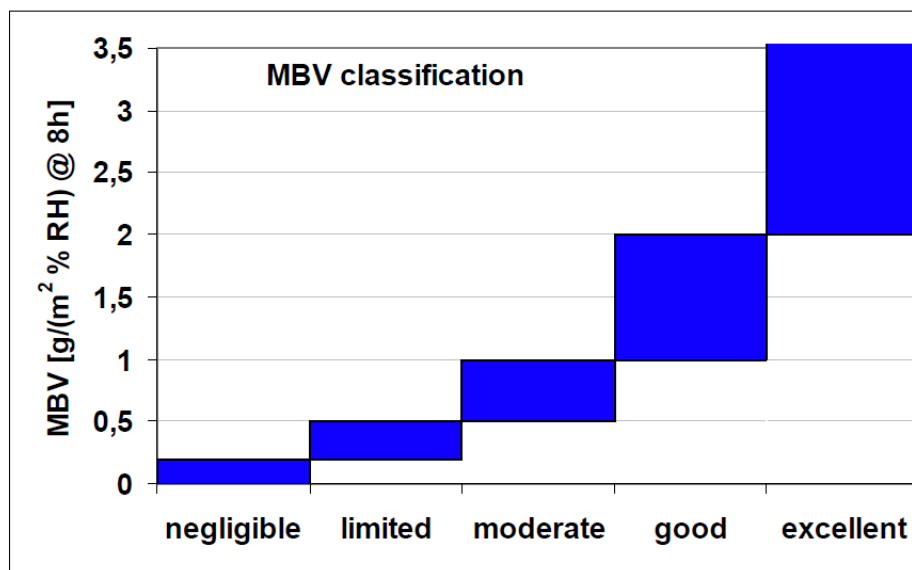


Figure 13. Classification of moisture buffering potential of materials based on $MBV_{\text{practical}}$ (Rode, 2005)

2.3.2.3 Moisture buffering at room level

Global factors such as ventilation rate in a zone, and material surface area also affect moisture buffering performance of materials. Increase in surface area has a diminishing returns effect on moisture buffering. It positively impacts moisture buffering performance up to an optimal point, after which increasing surface area only improves moisture buffering performance slightly (Salonvaara, et al. 2004; Mitamura, et al. 2004). This is demonstrated in Figure 14, which shows the diminishing effect of increase in moisture buffering material surface area, on overall moisture buffering performance at room level. S^7/S is absolute humidity change between the reference case

(moisture buffering surface area = 0 m²) and test case (moisture buffering surface area > 0 m²).

Volume rate is the ratio of the total moisture buffering surface area to volume of the room.

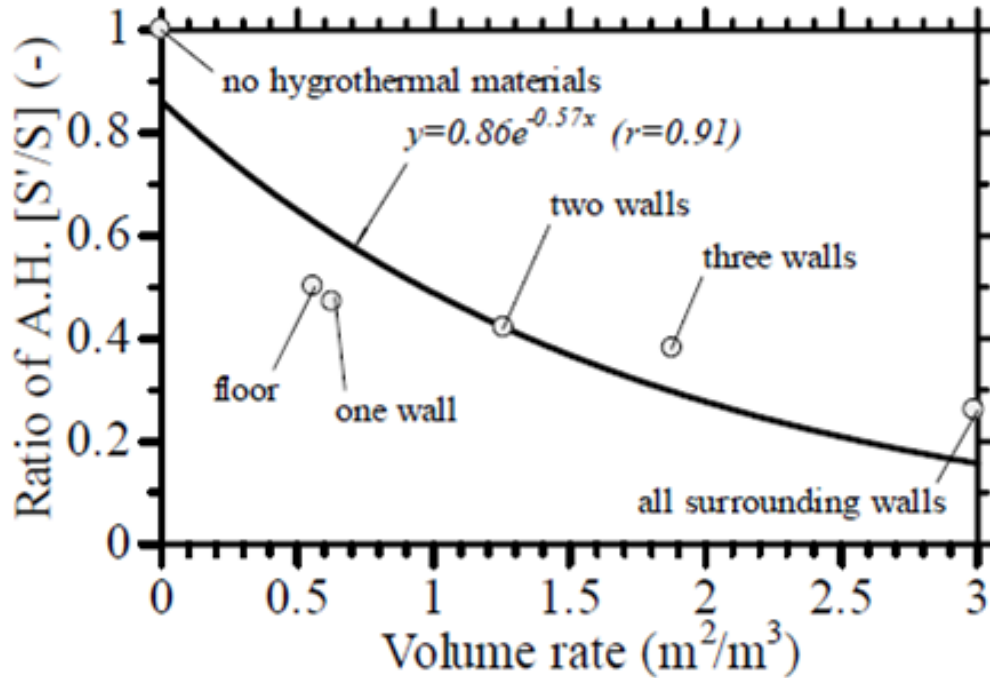


Figure 14. The diminishing effect of increase in moisture buffering material surface area, on overall moisture buffering performance at room level (Mitamura, et al. 2004)

Ventilation reduces overall indoor relative humidity, but also reduces the moisture buffering capacity of materials especially at high air change rates (Figure 15). This is likely due to humidity being exhausted by the ventilation system more quickly versus the absorption-desorption response by hygroscopic materials (Mitamura, et al. 2004).

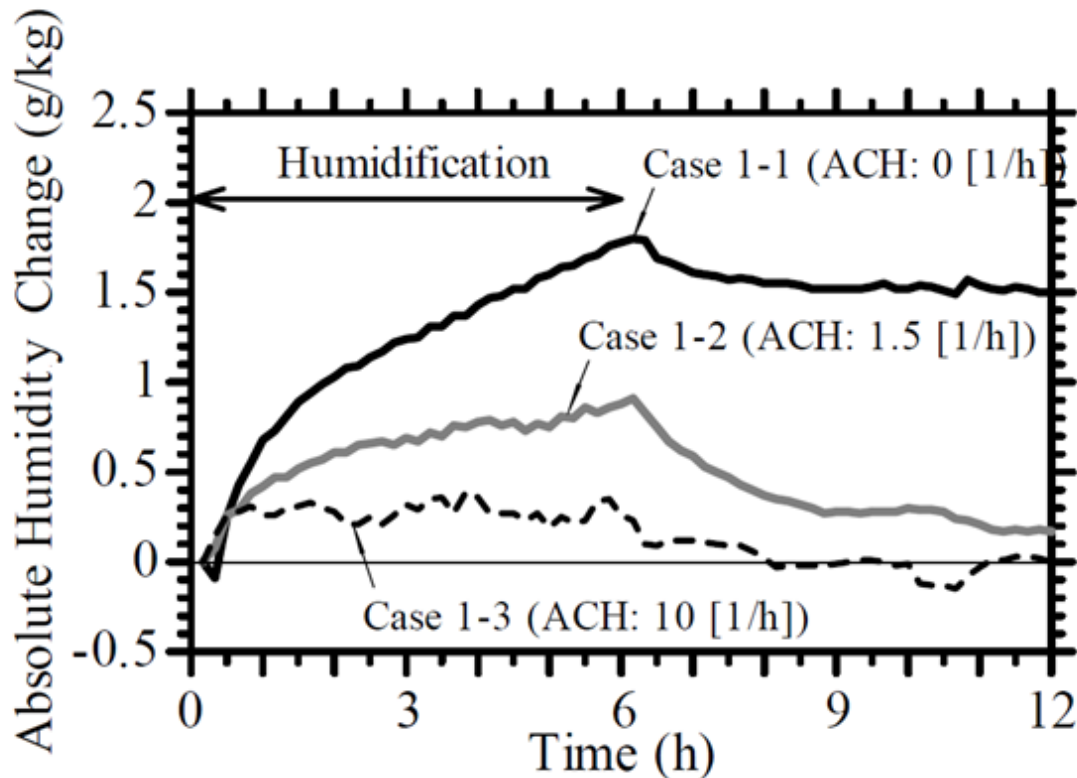


Figure 15. Increase in ventilation decreases the moisture buffering effect at room level as shown in Case 1-1 (0 air changes per hour), Case 1-2 (1.5 air changes per hour), and Case 1-3 (10 air changes per hour)

A large-scale field study in Germany compared the nature of interior moisture in a test hut with gypsum board versus a control hut with foil-covered interior surfaces. It was found that in the test hut 57% of interior moisture was buffered, 20% was ventilated, and 23% contributed to increase in relative humidity. In the control hut with no moisture buffering capability, 33% of interior moisture was ventilated while the remaining 67% was contained in the air and contributed to increase in relative humidity. This study has been extensively used for benchmarking simulation tools that account for moisture buffering of materials in their moisture balance model (Woloszyn & Rode, 2008).

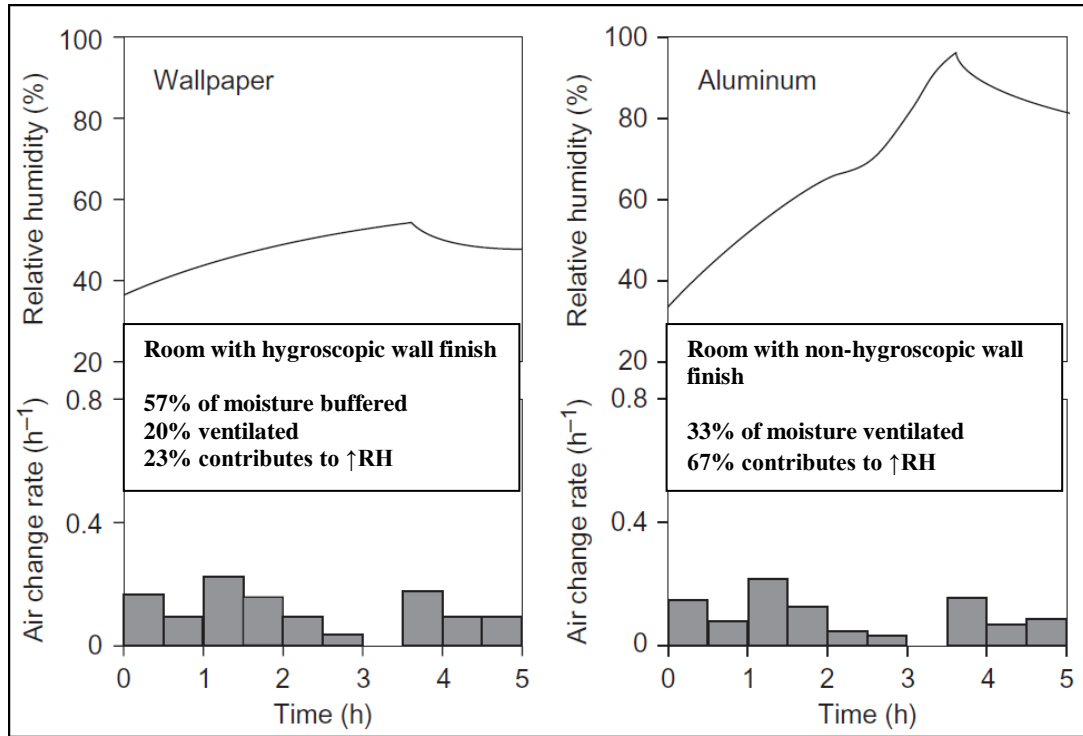


Figure 16. The effect of moisture buffering and non-moisture buffering building enclosure materials on interior humidity conditions at room level (Svennberg, Lengsfeld, Harderup, & Holm, 2007)

Moisture buffering is a term that should be included in moisture balance models to more accurately predict indoor humidity conditions. Those that have studied its effects have shown that ignoring moisture buffering effects results in poor indoor humidity predictions. One such study investigated the airflow behaviour of SF₆ tracer gas and airborne moisture in a multi-storey test building (Plathner & Woloszyn, 2002). Since SF₆ does not interact with furniture and finished surfaces as airborne moisture does, it simulated conditions with no moisture buffering effects. The results clearly show that increase in ambient SF₆ levels as a result of the gas release are much higher than air moisture levels. This was due to the moisture buffer capacity of furniture and finish surfaces in the kitchen and other areas in the test house, which also prevent moisture from getting to the other rooms. Results from two airflow models agree closely with the measured values. When sorption effect is taken out of the models, the predicted vapour pressures are greatly overestimated compared to measured values. This demonstrates that accounting for moisture

buffering is something that cannot be neglected in airflow, moisture balance, or whole building simulation models.

2.3.3 Moisture Buffering, Thermal Comfort, and Mould Growth Potential

The regulating effect of moisture buffering on indoor humidity can help to more passively maintain indoor air at acceptable humidity thresholds for thermal comfort, as well as halt the growth of mould.

A numerical study by Simonson, Salonvaara & Ojanen (2004) shows the effect of hygroscopic and non-hygroscopic materials on the comfort level of occupants at different ventilation rates. Their findings are summarized in Table 2. The criteria are based on acceptable relative humidity and temperature thresholds for thermal comfort as dictated by ASHRAE Standard 55 (between 25–60% and 18°–26° respectively), and percentage of occupants dissatisfied with warm respiratory comfort and perceived air quality (greater than 15%) being exceeded. The findings clearly show that overall, hygroscopic materials typically aid in improving the perceived indoor air quality and thermal comfort of occupants.

Table 2. Duration of Time (Equivalent Nights) That the Humidity, Temperature, Warm Respiratory Comfort, and Perceived Air Quality Are Unfavorable for Different Ventilation Rates (Simonson, et al. 2004)

Criteria		0.1 ach	0.25 ach	0.5 ach	1 ach
RH > 60%	Hygroscopic	44	5	56	133
	Non-hygroscopic	213	130	110	128
RH < 25%	Hygroscopic	0	0	10	27
	Non-hygroscopic	0	11	13	27
PD _{wrc} > 15%	Hygroscopic	206	108	55	25
	Non-hygroscopic	281	144	62	27
PD _{IAQ} > 15%	Hygroscopic	337	165	89	57
	Non-hygroscopic	321	233	130	61
T > 26°C	Hygroscopic	108	41	13	0
	Non-hygroscopic	92	41	16	1
T < 18°C	Hygroscopic	0	7	36	91
	Non-hygroscopic	0	9	45	96

Salonvaara, et al. (2004) completed a full-scale field test with two buildings (gypsum finish and aluminum covered) and benchmarked a model based on the data. Sensitivity analyses are then performed on the parameters for moisture buffering. They found that it is possible to design a hygroscopic building enclosure with good moisture performance. A hygroscopic building

enclosure is less susceptible to condensation and mould growth at the internal surface of thermal bridges such as corners. This is because peak indoor relative humidity would generally be lower with hygroscopic materials due to moisture buffering, and the percentage of time cold surfaces reach or surpass dew-point temperature would be decreased.

Straube & DeGraauw (2001) monitored 26 different walls and found that materials with both high permeability and hygroscopicity can create a “moderating effect” on indoor relative humidity peaks. Relative humidity peaks of an interior environment can support fungal growth even if average levels remain below threshold. In their study it was shown that walls with moisture buffering capabilities were able to maintain surface relative humidity at lower and more stable levels, as well as moderate short-term indoor relative humidity variations. The results showed that a regular steel stud wall with polyethylene vapour barrier and painted gypsum board finish underwent a peak and low relative humidity differential of 15%, versus 3% differential for a cement-bonded wood fiber wall with no vapour barrier over the heating season.

Ramos & de Freitas (2008) simulated the moisture buffering behaviour of different parameters for a hygroscopic and a non-hygroscopic interior finish clad test room. They classify daily moisture buffering potential of surface finishing materials based on a classification index developed by Ramos (2007), and conduct mould growth risk assessments based on “time of wetness” (i.e. percentage of time that surfaces exceed 80% relative humidity). Figure 17 shows the number of days time of wetness exceeded 50% in a day, or the number of days condensation was detected for each of the six test cases simulated. In all test cases, the hygroscopic clad test room with superior moisture buffering performance has significantly lower risk of mould growth potential.

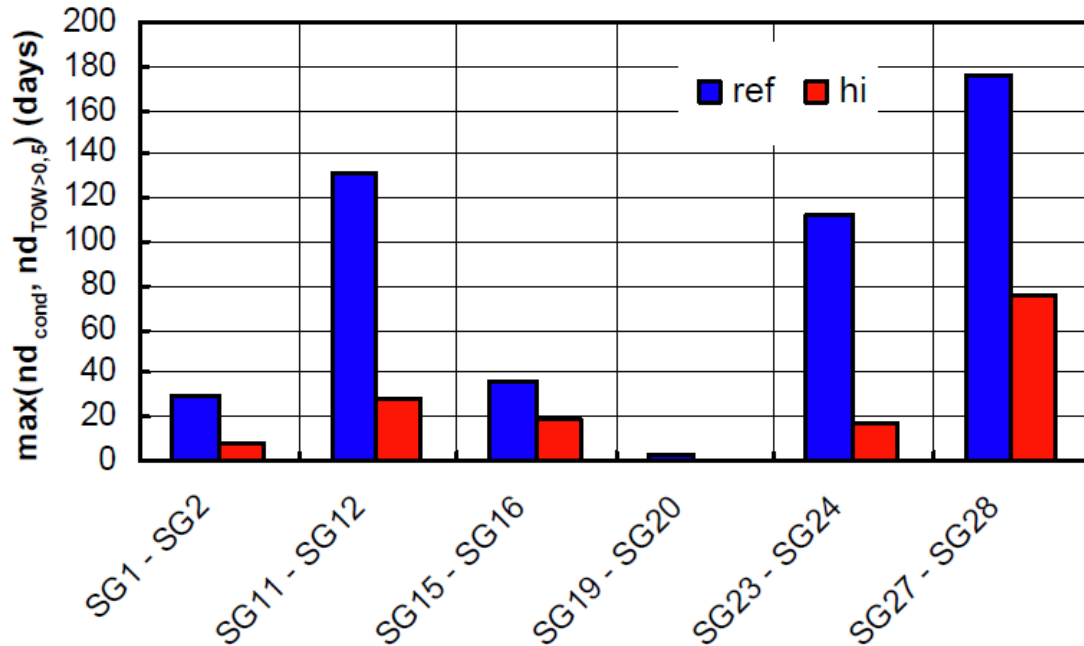


Figure 17. The mould growth risk assessment of a hygroscopic (hi) vs. non-hygroscopic (ref) interior finish clad test room for six different test cases (Ramos & de Freitas, 2008)

2.3.4 Moisture Buffering and Energy Efficiency

It may be possible to provide similar indoor climate conditions and perceived indoor air quality at lower ventilation rates with moisture buffering materials, although information regarding how to quantify the amount of reduction in ventilation with moisture buffering materials is still lacking.

Controlling moisture levels to remain stable and at target levels for occupant comfort has been shown to reduce energy consumption by means of reducing ventilation energy demand (Woloszyn & Rode, 2008). Annex 41 of the International Energy Agency's (IEA) Energy Conservation in Buildings and Community Systems program under "Subtask 1", a cooperative project on whole-building HAM response, involved modeling a set of common exercises to gauge consensus of the response of several different whole-building simulations on certain given parameters. One of these common exercises challenged the idea of optimizing ventilation rate and ventilation schedule combined with effective use of moisture buffering finishing materials to yield improved indoor humidity and reduced energy consumption. The consensus from this exercise across all six models' simulations is that the use of relative humidity controlled (RHC)

ventilation as opposed to constant ventilation coupled with the moisture buffering of materials reduces mean ventilation rate by 30 to 40% without compromising relative humidity levels and the risk of condensation. The reduction in ventilation rate corresponds to a reduction in energy consumption by 12 to 17% in cold exterior conditions. In addition, it was found that moisture buffering materials are very efficient in maintaining stability of indoor relative humidity, by reducing peak values, thereby reducing ventilation demand.

Using ventilation and moisture buffering to reduce relative humidity levels and energy consumption without deterring indoor air quality is a fine balancing act. Woloszyn, et al. (2009) found from modeling that in the winter with a RHC ventilation system, CO₂ levels exceeded 1000ppm, which is above the threshold for acceptable indoor air quality. This was not the case with constant ventilation. While RHC may be useful in regulating relative humidity without compromising energy demand, it may result in worsened indoor air quality, especially in the winter time. Moreover, hygroscopic materials have the ability to moderate airborne moisture levels, not other pollutants which can be removed by ventilation.

Ventilation power demand is not the only energy saving potential when it comes to moisture buffering. A numerical study of the affect of moisture buffering materials on changes in heating and cooling energy due to changes in latent heat loads and indoor enthalpy was done by Osanyintola & Simonson (2006). Figure 18 shows the energy savings potential of using hygroscopic materials in heating and cooling seasons for four different climate data. Energy savings are most effective when the HVAC control systems are optimized to take advantage of lower heating and cooling loads during occupancy.

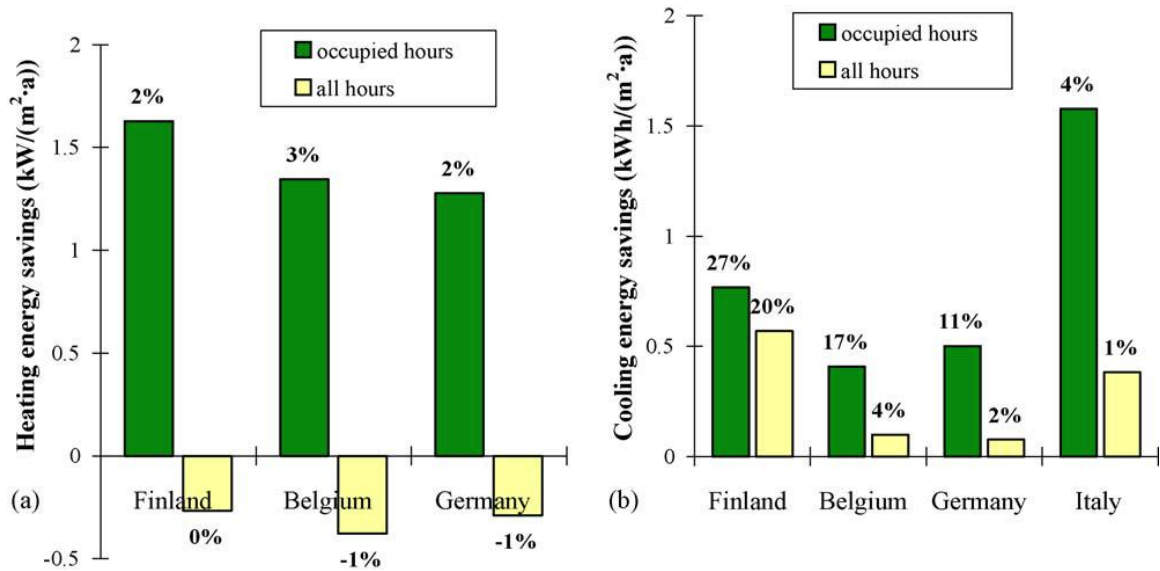


Figure 18. Total potential direct (a) heating and (b) cooling energy savings when applying hygroscopic materials (Osanyintola & Simonson, 2006)

Normally, moisture storage in materials is not accounted for in air-conditioning design, therefore systems may be oversized, and extra operating costs may be incurred. Isetti, Laurenti, & Ponticello (1988) account for moisture storage capacity by considering the mass transfer coefficient, permeability, and absorption capacity of plaster, wood, and an idealized absolute vapour barrier material (mass transfer coefficient set to zero). They observe a dampening effect in the relative humidity fluctuations of the cases with wood and plaster. By accounting for moisture storage capacity, the air-conditioning system's design inlet water vapour content can be increased without exceeding target 60% relative humidity levels inside the indoor space. This will result in a reduction in the cooling coil load of the equipment. Whereas if moisture storage is not accounted for, the inlet air would need to have lower water vapour content, putting more demand on the cooling coil load.

The effect of moisture buffering on cooling load is an area that has not been investigated in field testing. "2007 Survey of Household Energy Use" has reported increase in overall cooling degree-days and cooling energy use. More than 52% of Canadian households are now equipped with air-conditioning systems: 19% in British Columbia and 80% in Ontario, which has the highest

percentage. Harriman, et al. (1999) found that latent loads in cooling exceed sensible loads in most humid climates in North America, especially with ASHRAE's required ventilation rate requirements which reduce dehumidification effectiveness of conventional HVAC units. Ouazia, et al. (2008) noted that houses in hot and humid climates designed per ASHRAE's requirements for ventilation systems have longer periods of relative humidity exceeding 60%, than houses with no ventilation systems. Adequate ventilation is not only based on air intake from the outdoors, but also indoor humidity control. For example, in cooling seasons, occupants may lower thermostat setting when indoor humidity levels get too high. This can cause condensation in ducts, floors, and building surfaces and increase potential of health issues. Dehumidifiers can be a solution but are costly and use large amounts of energy. The effect of moisture buffering materials may be something that could be relied on to reduce latent cooling loads and resolve these issues. This is an area that needs to be further investigated.

3 PROBLEM STATEMENT

The review of past literature brings to light the motivation behind this research. In general, moisture buffering is not predominantly accounted for in design. It can be considered as a supplementary measure to ventilation strategy for management of indoor humidity, which can potentially provide energy saving benefits. Implementing moisture buffering in practice may help regulate diurnal relative humidity peaks, which can reduce the percentage of time interior cold surfaces are exposed to humidity levels above the threshold for microbial growth. Currently, there are no solid design methodologies for consideration of moisture buffering effect of materials on indoor humidity.

ASHRAE Standard 62.2 recommends interior relative humidity conditions of 60% or less. One way of maintaining this criterion is by way of continuously ventilating the indoor space. Continuous mechanical ventilation can reduce indoor humidity by replacing indoor moist air with dryer outdoor air. While this can improve air quality, it is an energy usage trade-off, since the system would continuously draw in cold air (or cold air and a percentage of re-circulated air) and exhaust warmer air, thereby increasing heating demand. Moreover, in mild climates with high outdoor humidity, continuous ventilation may not necessarily replace indoor air with intake air that is sufficiently dry for maintaining relative humidity below the threshold.

In the case of a low-income residential building, increasing ventilation rates and implementing active mechanical ventilation measures have not been successful in reducing high indoor humidity (Roppel, Lawton & Hubbs, 2007). Ricketts & Straube (2014) show that existing common ventilation systems in multi-unit residential buildings (MURBs) that use corridor pressurization in Vancouver are generally not effective in providing the ASHRAE required ventilation rates and adequate air changes into the units, and can be as low as 8% of the intended ventilation rate. In the case of some older MURBs, retrofitting of existing ventilation systems may not be feasible nor effective due to existing conditions of the building. For these reasons,

implementation of moisture buffering materials as a passive measure of reducing indoor moisture may be a viable solution.

The occupants' behaviour also contributes to the issue. While education may potentially aid in correcting behaviour, change in occupancy and nature of the occupants' life style may not necessarily make the problem of high indoor humidity disappear.

Studies on the effectiveness of moisture buffering materials in reducing and regulating indoor moisture have been conducted in a field experimental setting in cold climates such as Sweden (Hameury, 2004), Denmark (Woloszyn et al, 2005) and Germany (Kuenzel et al, 2004). However, the role of moisture buffering effect in reducing indoor humidity in a mild, marine climate such as Vancouver, BC under different ventilation strategies has not been previously explored.

4 RESEARCH APPROACH

4.1 Research Hypothesis & Objective

This research project seeks to investigate the effectiveness of moisture buffering in regulating indoor humidity in a marine climate under different ventilation strategies. At the same time, the effect of the ventilation strategies on ventilation heat loss and indoor air quality (based on CO₂ concentration) will be considered.

It is expected that demand-controlled ventilation will be a more efficient ventilation strategy than continuous ventilation. Coupled with the regulating effect of moisture buffering materials on indoor humidity, demand-control ventilation may allow the indoor environment parameters to remain at acceptable levels, even for high moisture loading scenarios such as high occupancy residences, while maintaining acceptable indoor air quality and minimizing ventilation heat loss.

4.2 Research Scope

Development of design criteria is not the intent, although it may provide future considerations for design in practice. The intent is to test a potential solution to a problem by way of field experimental testing. Data generated from this research is valuable, in that it can be used for validation of whole-building and hygrothermal models as well as other future research. These models can be integral engineering tools in optimizing energy consumption and indoor climate conditions in practice.

4.3 Research Methodology

To test the hypothesis covered in Section 4.1, a field experiment is designed to simulate the conditions of a residential suite and measure the response in indoor conditions under varying occupant loading, outdoor conditions, presence of hygroscopic and non-hygroscopic materials, and ventilation strategies. This research will primarily focus on moisture buffering at a smaller

time scale, considering the effect of occupants' daily activities and ventilation strategies, and its ability to manage indoor humidity.

Daily indoor moisture and CO₂ generation profiles are determined based on analysis of real occupants in a 'Reference Building' described in Section 4.4.

Indoor moisture and CO₂ is released in the field experiments based on the predetermined daily profiles using programmable occupant simulator units. Heating is provided with an electrical heater with an adjustable thermostat setting.

Algorithms are also defined for the ventilation system to operate as per pre-defined ventilation schemes for the field experiment test cases, and the moisture buffering performance of unpainted gypsum board is tested. Interior air and supply air conditions are continuously monitored, recorded and analyzed. For each test case, the performances of hygroscopic versus non-hygroscopic interior finished buildings are directly compared for the same outdoor conditions. Performance of the buildings across test cases is also compared.

4.4 Description of Reference Building

The motivation for this research stems from a research project that involved the monitoring of select suites in a low-income residential building, located in Vancouver, BC, Canada hereafter referenced in the thesis as the 'Reference Building'. Brief descriptions of the building and its problem are as follow.

The building is a six-storey low-income residential building, located in Vancouver, BC, Canada. Vancouver's climate is in ASHRAE climate zone 5, and is characterized as cold/ marine. The building is a concrete structure with steel stud infill walls and stucco cladding, constructed in the 1990's at the peak of Vancouver's leaky condo crisis. Approximately 10 years into its service life, the building was rehabilitated due to significant moisture damage from water ingress. The

building exterior walls were converted from a face-sealed stucco assembly to a rainscreen assembly, complete with two inches of exterior insulation added on the outside of the wall sheathing and water resistive barrier (Figure 19). The windows were also upgraded from non-thermally broken single pane aluminum frame windows to more thermally efficient double glazed aluminum frame windows.

Approximately 5 years following rehabilitation, it was discovered that moisture issues continued to persist. Although this time the moisture related issues were not related to water ingress from the exterior of the building enclosure, but from excessive indoor humidity. Further monitoring and investigations revealed that the indoor humidity was significantly high, and moisture was continually accumulating on the exterior wall sheathing. Moreover, mould had begun to grow on interior gypsum drywall in some suites.

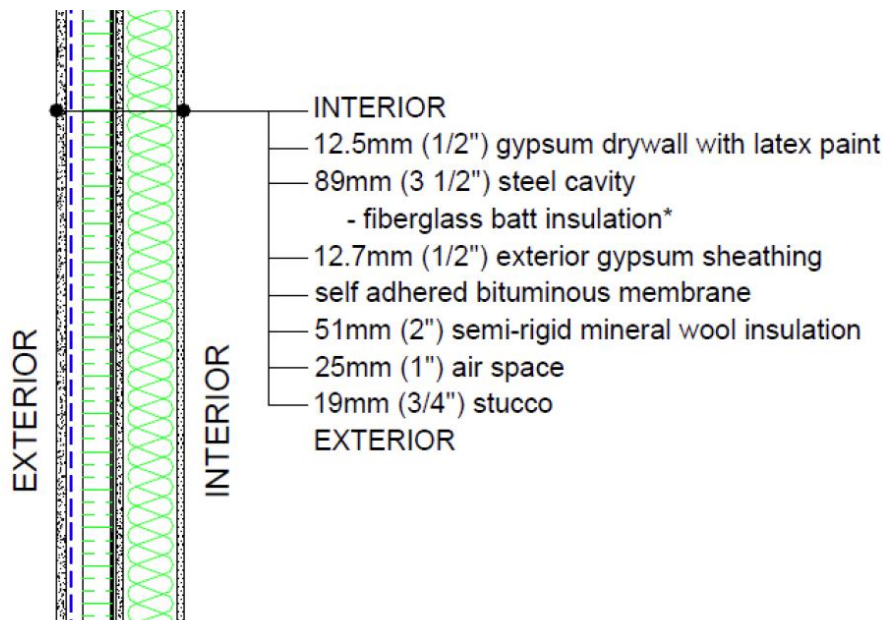


Figure 19. Rainscreen exterior wall assembly implemented during the building rehabilitation

The primary ventilation strategy at each of the suites in the building was user-operated spot venting in the bathroom and kitchen. Fresh air is passively supplied to the suites through opening windows, or the balcony doors, and the undercuts of suite entry doors. Further investigations revealed that adequate ventilation was not provided for the suites according to ASHRAE

recommendations, as well as the Vancouver Building Bylaw (VBBL). In order to address the excessive interior humidity, which was causing damage to the building enclosure, new bathroom exhaust fans were installed on a time-controlled schedule. The new higher volumetric airflow rate bathroom exhaust fans were programmed to run intermittently 4 hours twice per day, between the hours of 7am to 11am and 6pm and 10pm. The running times of the fans were chosen on the basis that the occupants would be most active during the set on-times, and highest daily moisture generation would correspond to the running time of the bathroom fans. Synchronization of the fans also allowed for inter-suite airflow to be minimized.

A monitoring program was implemented for a period of two years to assess the effectiveness of the new ventilation strategy on addressing indoor humidity issues in the building. The indoor conditions (including temperature and relative humidity) of four select suites were collected in 2-minute intervals. An on-site weather station also recorded exterior conditions.

The findings from the monitoring program are further discussed in Tariku & Simpson (2014). In general, the findings from the monitoring program reveal that high indoor humidity conditions continue to persist, despite implementation of the new higher volumetric airflow rate exhaust fans and time-controlled ventilation strategy. The possible reasons for this are listed below:

- The location of the bathrooms (and bathroom exhausts) is in close proximity to the suite entry doors. As a result, the air supply to the suites may be “short-circuited,” meaning any fresh air provided to the suites from door undercuts may immediately be exhausted prior to reaching the suite. This is especially the case in the winter season when doors and windows remain closed.
- The numbers of residents in the suites are higher than typical. As a result, ASHRAE and VBBL recommended ventilation rates may not be sufficient in addressing high indoor moisture generated by high occupancy suites from occupants’ daily activities.

- The occupants have habits that may contribute to the moisture related issues. For example, some suite occupants prefer low temperature thermostat settings in the winter time, which can increase the risk of interior surfaces such as window glazing and sites of thermal bridging having temperatures below dew-point. They also frequently cook food by boiling water, which can be a significant source of daily moisture generation.
- The gaps at the suite entry door undercuts may not be sufficiently wide to allow adequate airflow. In some cases they may also be unintentionally blocked by doormats and carpets, or intentionally blocked by occupants to prevent cold drafts.
- The new bathroom exhaust fans are rated as 110 CFM. However, measurement of the fan capacities revealed that they operate up to 50% less than the fans' rated capacity, between 51 to 72 CFM, depending on the suite. Bathroom exhaust fan flow measurements are provided in APPENDIX C.

In general, the behaviour of occupants and the nature of the ventilation system are the contributing factors to the high indoor humidity issues at this building.

5 OVERVIEW OF FIELD TESTING FACILITIES

This section will outline the field testing facilities, HVAC system, monitoring and instrumentation equipment. The Whole Building Performance Research Laboratory (WBPR) at the British Columbia Institute of Technology (BCIT) located in Burnaby, BC is used to conduct this research (Figure 20). The facilities are described here as they relate to the undertaking of the experiments designed to investigate the field experiment. The facilities consist of two small test buildings with identical construction and ventilation systems.

Two test building facilities with identical roof and floor assemblies, dimensions, orientation, and location were monitored to compare the effects of different surface moisture buffering materials on indoor humidity conditions. The buildings are located in Burnaby, British Columbia (latitude 49.2°N, longitude 123.0°W), an area characterized by mild climate, warm summers and cool rainy winters. All exterior boundary conditions during the monitoring period were recorded by a weather station on site (temperature, relative humidity, precipitation, wind speed and direction, and solar radiation).

Tariku, et al. (2013) outline the design, construction, systems, and equipment of the buildings in more detail. Additional photos are provided in APPENDIX A.

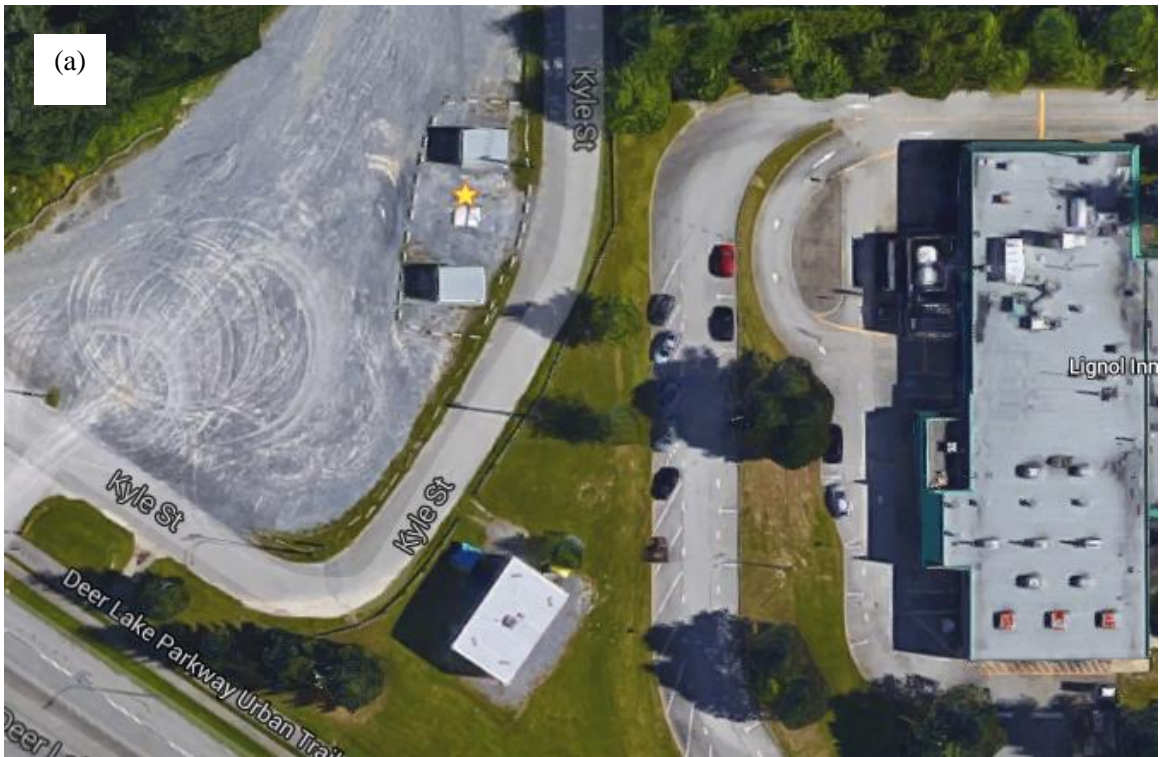


Figure 20. Aerial photograph (a) and field photograph (b) of the Whole Building Performance Research Laboratory (WBPRL) at the British Columbia Institute of Technology (BCIT)

5.1 Construction

The building dimensions are approximately 16 x 12 x 10 ft (4.9 x 3.7 x 3.0 m). Both buildings have HSS steel super-structure, insulated slab-on-grade foundation, and an insulated engineered truss roof. The modular test wall assemblies for both buildings are standard 2x6 wood frame with fiberglass batt insulation in the stud cavity. Each building has two 3 x 4 ft low-e coated and argon filled double-glazed vinyl frame sliding windows with a U-value of 0.32 (1.80 USI), solar heat gain coefficient of 0.35, and visible transmittance factor of 0.60, one on the north and one on the south wall. The buildings both have a 8.0 x 4.5 ft (2.4 x 1.4 m) mechanical room located on the north-west corner, which houses the air handling unit, the data acquisition system, a computer, control systems, a temperature bath, and a chiller. The exterior door is separated from the L-shaped test space in the buildings by the mechanical room. The partition walls separating the mechanical room from the test space are thermally insulated and air sealed, thus isolating the conditions inside the mechanical room from the test space. Figure 21 shows a typical floor plan of the buildings at the WBPRL.

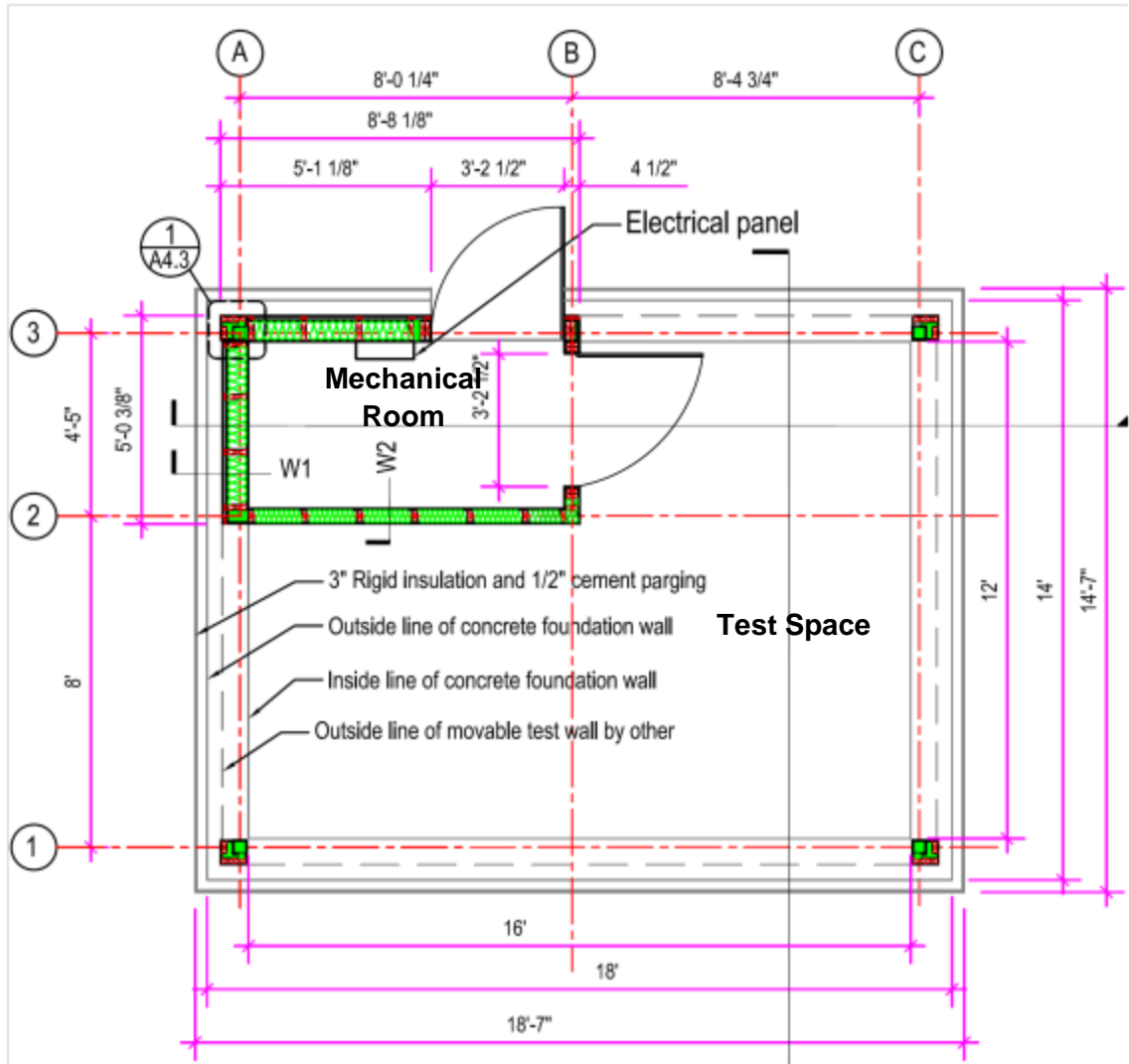


Figure 21. Typical floor plan of test buildings at the WBPR

In each building, the test space is 159 square feet (14.8 square meters) and has an approximate volume of 1430 cubic feet (40.5 cubic meters). The combined surface area of the test walls exposed to interior conditions is 395 square feet (36.7 square meters). All other interior surfaces of the buildings exposed to test conditions were isolated during testing; the concrete floor, footings, and ceiling were sealed with 6 mil polyethylene vapour retarder to prevent possible interactions between those materials and moisture inside the test space (Figure 22).



Figure 22. Concrete floor and footing (left) and gypsum board ceiling (right) were isolated from interaction with indoor air moisture by installing polyethylene sheet

5.2 Buildings' Airtightness

Both buildings were tested for airtightness to account for natural air infiltration and exfiltration across the envelope. The airtightness testing was done per ASTM Standard E1827-11 *Standard Test Methods for Determining Airtightness of Buildings Using an Orifice Blower Door* (ASTM, 2011). The effective leakage area of the test building and the control building are 25 cm² and 29 cm² at 4 Pa of pressure difference, respectively (Table 3). This equates to a normalized air leakage area of 0.43 cm²/m² and 0.49 cm²/m² for the buildings' exterior surface area above grade.

Table 3. Airtightness of the test building facilities at the WBPRL

Building	Air Change Rate at 50 Pa (hr ⁻¹)	Effective Leakage Area at 4 Pa (cm ²)	Normalized Air Leakage Area at 4 Pa (cm ² /m ²)
North (Test)	2.2	25	0.43
South (Control)	2.4	29	0.49

Based on the ASHRAE's *Handbook of Fundamental* (2013) building airtightness classification (Table 4), the test buildings can be considered very airtight.

Table 4. Classifications of buildings' airtightness (ASHRAE, 2013)

Building Airtightness Classification	Normalized Air Leakage Area at 4 Pa (cm²/m²)
Very leaky	>5.4
Typical	2.8
Good	1.4
Tight	<0.7

5.3 HVAC System

The WPRL buildings are each equipped with a customized heating, ventilation and air-conditioning system that are designed and built in the BCIT Building Science Centre of Excellence lab. Airflow rate, temperature, and relative humidity of the air supply from the outdoors, as well as the percentage of return air are all parameters that can be controlled and monitored during operation. The system also has an integrated feedback system that can ventilate the building and condition the supply air based on desired indoor test space conditions (e.g. through demand-control ventilation). The system's two major components are the forced airflow system, and the air handling unit.

5.3.1 Forced Airflow System

The forced airflow system allows the movement of air from the outdoor environment into the test space, re-circulation of the indoor air, or combinations of both. The system allows for controlling the amount of continuous airflow as well as the conditions of the air being supplied. Figure 23 shows a schematic diagram of the forced airflow system.

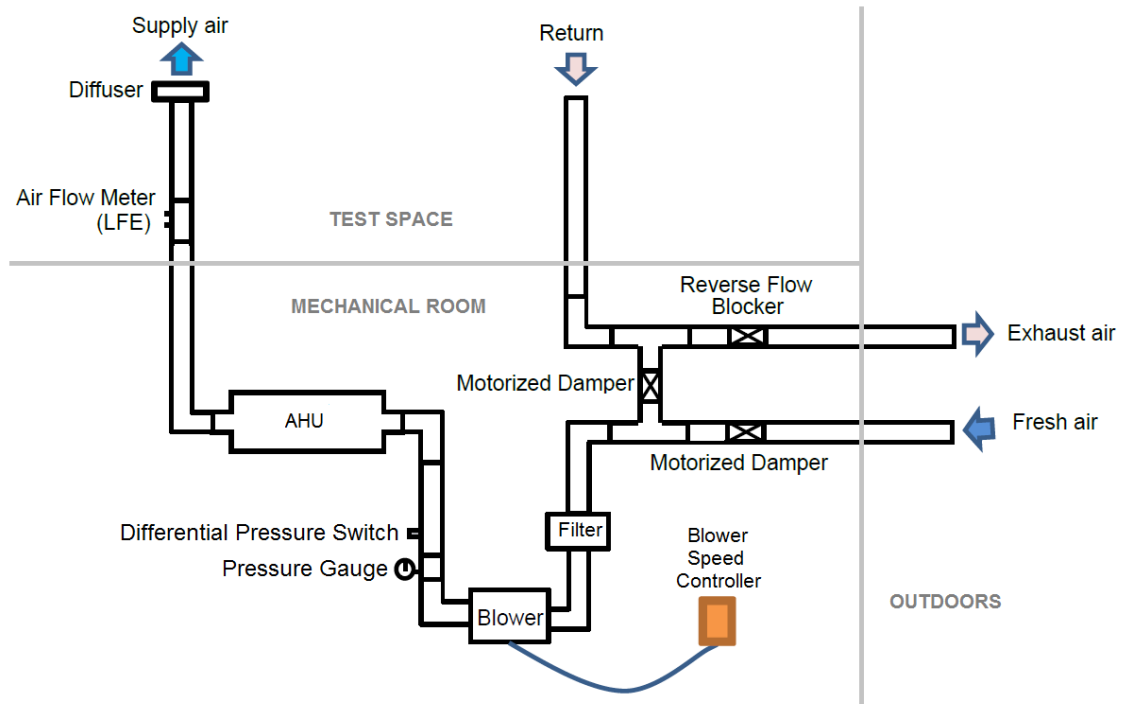


Figure 23. Schematic diagram of forced air system in the WPRL mechanical system design (adapted from Tariku, et al. 2013)

Starting from the right side of the diagram and going left, each component and its functions are listed as follows:

- **Motorized Dampers:** The percentage of re-circulated air is regulated. The air supply to the room can be controlled by closing or opening the automatic dampers via a computer program to provide 100% fresh air, 100% re-circulated air, or any ratio of mixed re-circulated and fresh air.
- **Reverse Flow Blocker:** When the system is running with fully re-circulated or mixed air supply, the reverse flow blocker prevents outdoor air from entering the system through the exhaust.
- **Air Filter:** The removable filter cleans incoming air of any dust or particles, before entering the blower.
- **Blower and Blower Speed Controller:** The blower is the mechanism that moves air from the outdoors into the buildings, similar to how a pump would move fluid through a pipe.

The volumetric air flow is controlled by setting the speed of the blower through the Speed Controller. It can be set at constant speed for continuous air flow ventilation, or programmed to vary depending on indoor conditions for demand-controlled ventilation.

- Pressure Gauge: A pressure gauge is located immediately downstream from the blower. It measures the air pressure in the system after passing through the blower.
- Differential Pressure Switch: The pressure switch is a safety mechanism incorporated in the air flow system, in case of blower failure. If air pressure exceeds a certain limit, the Differential Pressure Switch is activated and power to the entire system is shut down.
- Air Handling Unit (AHU): The AHU conditions the incoming air to reach the desired interior set-points of the test space.
- Laminar Flow Element (LFE): The LFE measures the system's volumetric air flow rate prior to entering the test space. The measurements can be used as feedback for the Blower Speed Controller to fine-tune building air intake at the desired rate.
- Diffuser and Return Vent: The diffuser is the inlet for supply air into the test space. It is located on the ceiling at the southeast corner of the test space. The return vent is the air outlet and is mounted on the bottom of the partition wall near the northwest corner of the test space (Figure 24).
- Ducts: The sheet metal and ABS ductwork allow air to travel from the outdoors, through the mechanical systems, into the test space, and exhaust.

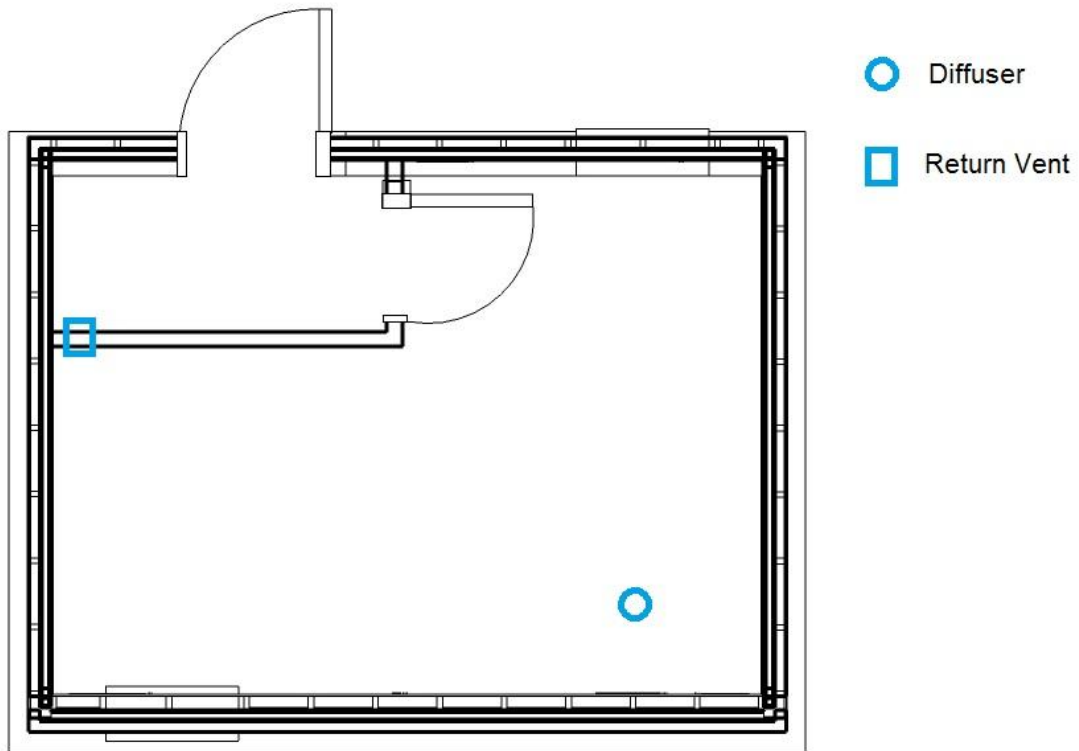


Figure 24. Locations of the diffuser on the ceiling (bottom left) and return vent on the partition wall (bottom right) and indicated on floor plan (top)

5.3.2 Air Handling Unit (AHU)

Each building's air supply conditions can be controlled by the automated AHU which can heat up, cool down, humidify, or dehumidify the air intake depending on desired interior conditions. A schematic diagram of the AHU is shown in Figure 25.

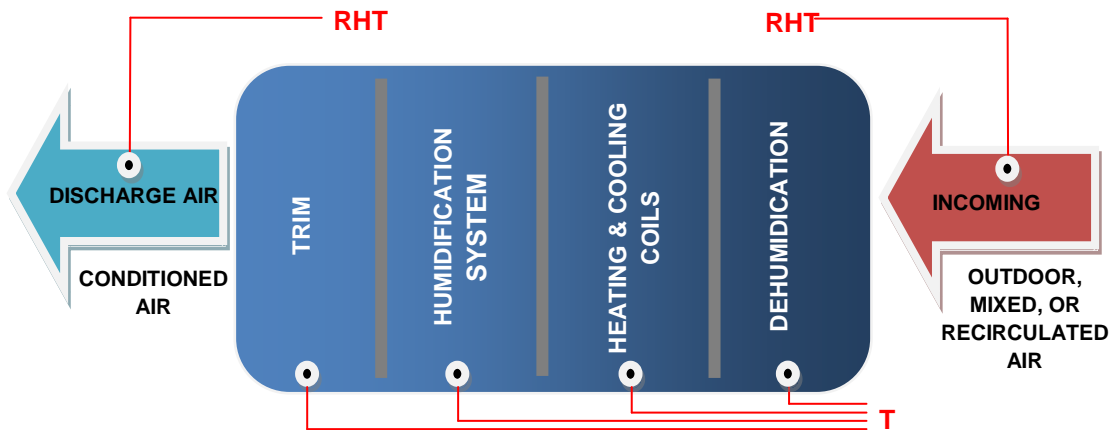


Figure 25. Schematic diagram of the Air Handling Unit

The AHU unit itself is made from sheet metal, and sealed and insulated with rigid foam insulation taped at the seams. Customized software developed for the operation of the AHU and airflow systems enable control and monitoring of the systems, to operate the buildings at desired conditions. The temperature and humidity conditions at each stage of the air conditioning and heating are measured for indoor climate control and data analysis purposes.

5.4 Occupant Simulators

In order to simulate people and their activities in the test room, each building is equipped with an occupant simulator unit that is designed to emit moisture, heat, and carbon dioxide (Figure 26). The rate and profile for humidity, heat, and carbon dioxide production of the occupant simulators can be programmed to mimic different occupant densities, as well their different activities.



Figure 26. Occupant simulator equipped with control box, humidifiers, water reservoirs, pumps, CO₂ release valve (not shown), and heat generating bulb (not shown)

5.4.1 Humidifiers

The humidifier units are Plexiglas® boxes, outfitted with a fan, two nebulizers, and two float sensors switches (Figure 27). The humidifier components are connected to a control box circuit, which is designed to supply power and control the humidification system. When water is present in the humidifiers, the nebulizers vibrate at a frequency of 2.4MHz, transforming surface water into micro particles that float in the air similar to water vapour. The fan directs the water particles out of the humidifier box and into the room. The two float switches are placed at different heights and act as a safety and a guide for a pump to refill the humidifier to a desired water level from a reservoir tank (Figure 28). The humidifiers can be used to add a known amount of water into the ambient air, without additional thermal energy that would be inherently added by way of evaporating water.

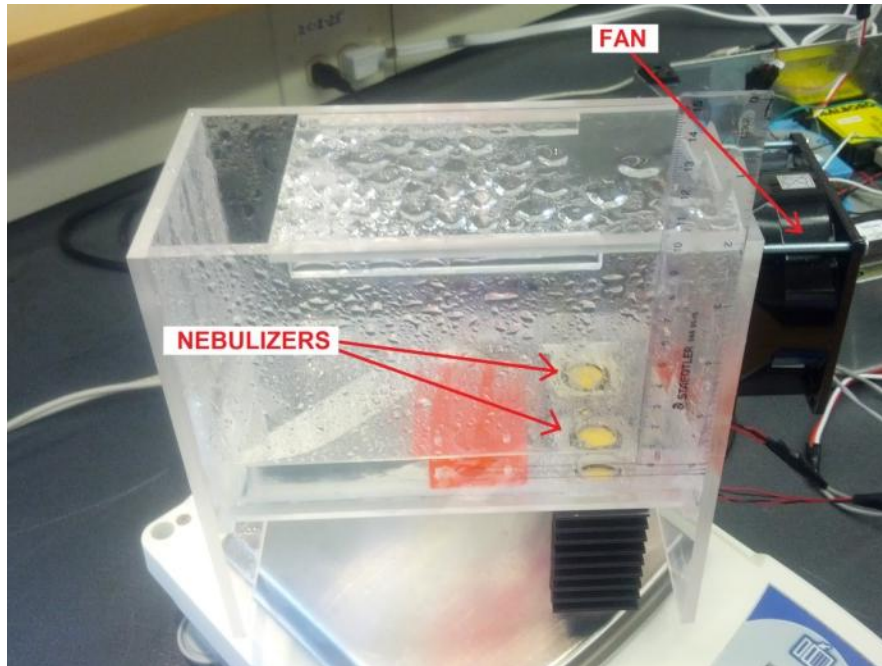


Figure 27. Plexiglas humidifier Box

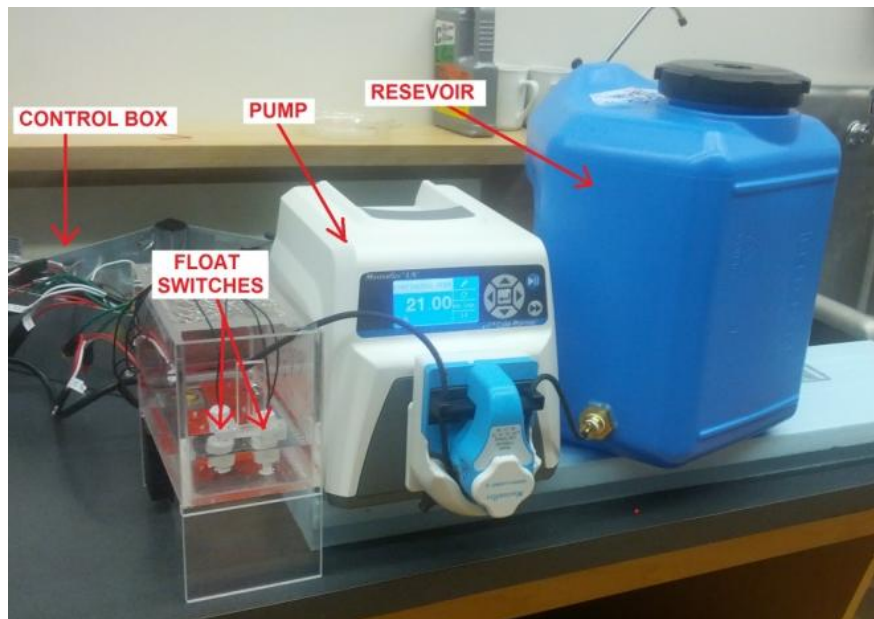


Figure 28. A humidifier connected to a control box, pump, and reservoir

For each unit, a humidifier can be programmed to simulate occupants' moisture production with a pre-set 24-hour moisture generation profile. The moisture generation profiles mimic activities such as cooking and bathing at predetermined hours of the day.

5.4.2 CO₂ Dispensing System

To simulate the metabolic CO₂ generation of occupants, a system that controls and measures the amount of the CO₂ dispensed into a space was developed as a component of the occupant simulator units (Figure 29).

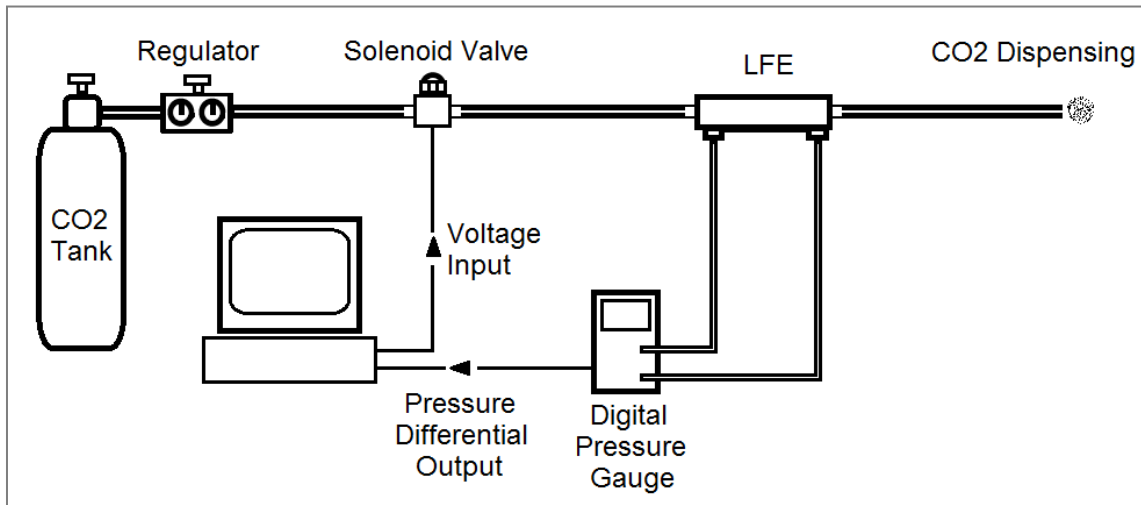


Figure 29. Schematic of Carbon Dioxide Dispersion System

The source of the CO₂ is a compressed gas tank, connected to a regulator, a solenoid valve and laminar flow element (LFE) via tubes for dispensing. The tap on top of the tank opens the tank valve and the gas then flows into the tubes. The regulator is used to adjust initial flow (Figure 30(a)). Once flow is established in the system, the regulator and tap are left untouched. A proportional solenoid valve then adjusts the desired flow rate into the system and into the room.

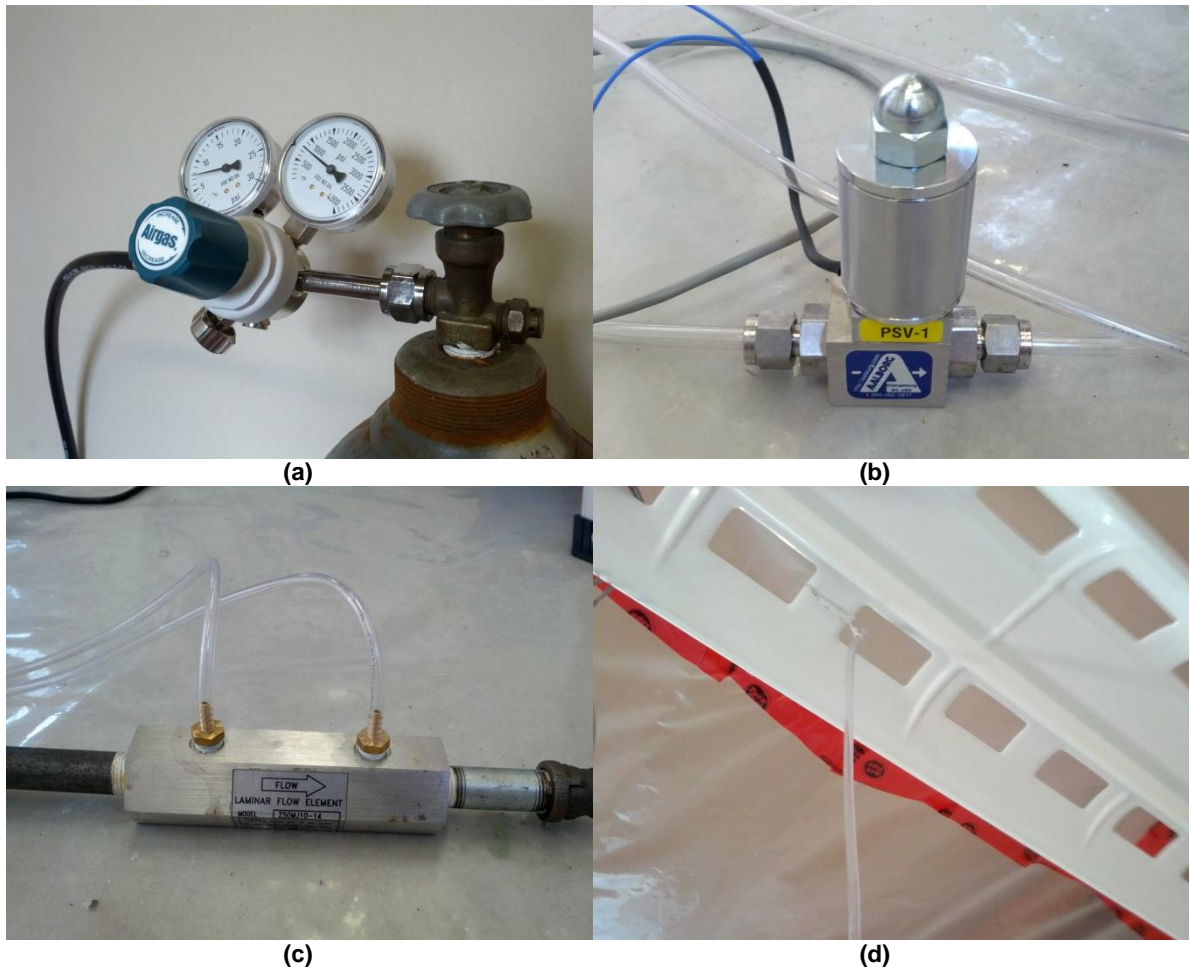


Figure 30. Photos of the components of CO₂ dispensing system: CO₂ tank and regulator (a), solenoid valve (b), laminar flow element with pressure tubes (c), and end of tube outlet suspended near ceiling (d)

The solenoid valve (Figure 30(b)) is the part of the system that controls the precise flow of gas through the tube. When power is supplied to it, an internal valve opens and closes depending on the voltage magnitude. No power supply or 0 volts corresponds to the valve closed (Figure 31). Varying the voltage proportionally varies the flow.

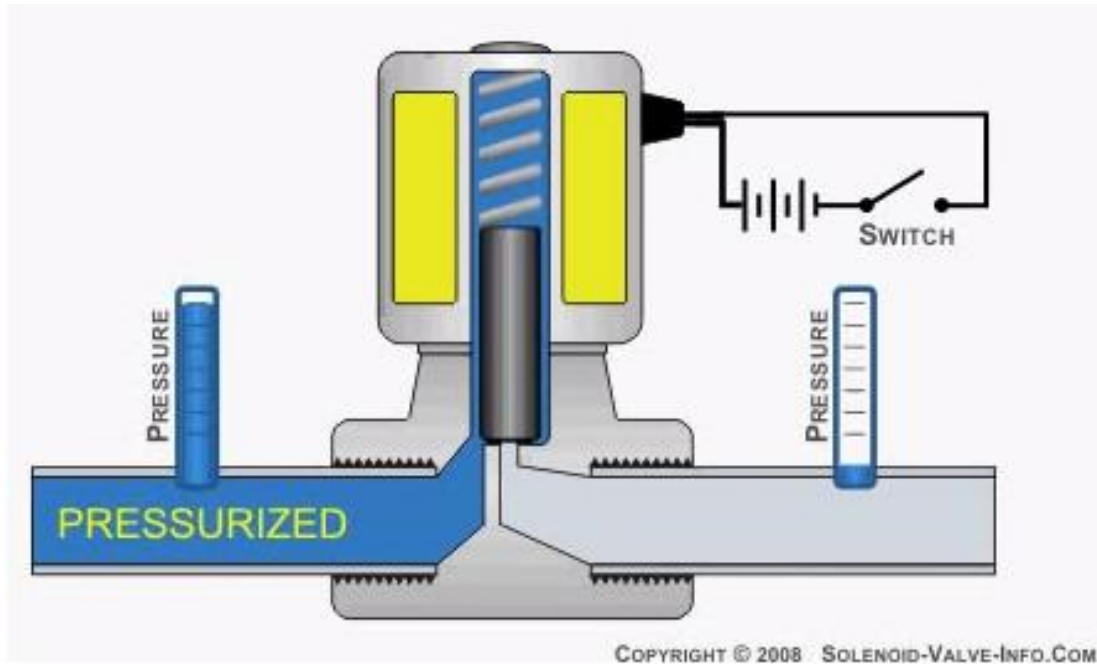


Figure 31. A solenoid valve in its fully closed state (source: solenoid-valve-info.com)

Once the desired flow rate is established by supplying a certain voltage to the solenoid valve, gas then passes through the LFE (Figure 30(c)) where the pressure drop is measured at this point in the system. As a result, the flow in the system can be measured before dispensing. The pressure drop is read using a digital pressure gauge and recorded in an electronic file. In this way, it is possible to keep track of exactly how much CO₂ is being dispensed at any given time. The amount of CO₂ being displaced from the tank into the room can be further fine-tuned using an on/off duty cycle for the voltage supplied to the solenoid valve. The solenoid valve closes and opens depending on the voltage it receives from the occupant simulator control box. Varying the voltage varies the flow of CO₂ and thus the amount of dispersion. The voltage is adjusted through trial and error to achieve the desired CO₂ generation profile.

The end of the tube is the location where CO₂ is dispensed into the room. Since the density of CO₂ is higher than that of air (1.98 kg/m³ vs. 1.23 kg/m³ respectively at 1 atm and 20°C), the tube outlet is placed at an elevated location near the air supply outlet diffuser of the HVAC system

(Figure 30(d)). This is done to allow for mixing and avoid possible stratification of the air. In addition, a fan in the middle of the test space further mixes the air in the room.

6 EXPERIMENTAL SET-UP

The two identical buildings in the WBPRL are exposed to real climatic conditions and monitored for change in indoor air conditions under changing parameters for a number of test cases. One building is clad with unpainted gypsum board on the interior of the building enclosure, which has hygroscopic properties and is designated as the test building. The non-hygroscopic building is covered with 6 mil polyethylene vapour retarder on all interior surfaces and is the designated control building. Both the test and control building are exposed to the same variables for a given test case, however, the test building has moisture buffering potential, while the control building has the moisture buffering effect eliminated. The experiment design variables and each test case are identified in Section 6.1.

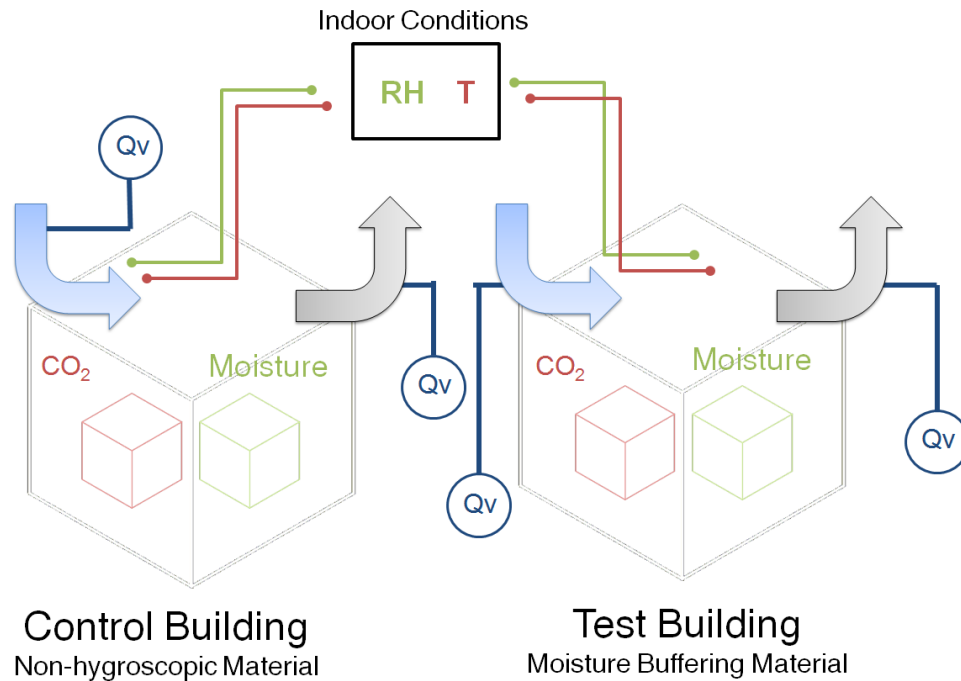


Figure 32. Schematic diagram of field experiment set-up

The instrumentation for the experiment, including those used to obtain data on changes in indoor conditions, are further explained in Section 6.2.

Different occupant densities are simulated by releasing predetermined rates of hourly moisture and CO₂ based on occupants' behaviour in the 'Reference Building,' using the automated occupant simulator units. Metabolic heat generation is not simulated for the purposes of this field experiment because with additional heat in the test space, the interior temperature would deviate from the desired set-points. Determination of daily moisture and CO₂ generation profiles from the 'Reference Building' is further described in Section 6.3. Their implementation using the occupant simulators in the field experimental set-up is described in Section 6.4.

The buildings are equipped with a supply ventilation system to provide outdoor air under continuous, time-controlled, relative humidity-controlled (RH-controlled), and CO₂-controlled ventilation schemes. For the purposes of the field experiments, 100% non-conditioned fresh air is supplied to the test space at various airflow rates depending on the test parameter. The air is not conditioned by the AHU prior to discharge, rather the outdoor air supply conditions are maintained. This is so that the typically wet and moist marine climate air of coastal British Columbia is used to ventilate the building, as is typical of residential housing in the region. The algorithms for each of the ventilation schemes are defined in Section 6.5.

6.1 Experiment Design Variables

The North building is the designated non-hygroscopic control building, and the South building is the hygroscopic test building (Figure 33).



Figure 33. Designation of the North (Control) and South (Test) buildings

The control building serves as a benchmark for indoor relative humidity and CO₂ readings. These readings are used to assess the moisture buffering effect of finishing materials on indoor moisture management. Unpainted gypsum board was chosen for the test building as the moisture buffering material due to its inherent common place in the construction industry, especially in North American construction. Unpainted gypsum board has maximum buffering potential, whereas painted gypsum board can lose some of its moisture buffering potential. Therefore, to assess the maximum moisture buffering potential of common gypsum board, the test building wall finishes were left uncoated, without any primer or paint.

Table 5 lists the test parameters for each of the buildings for eight test cases defined. The variables for each test case are the following:

- Interior wall finish: the determining factor on whether the building enclosure materials are hygroscopic gypsum wall board (GWB) or non-hygroscopic polyethylene.

- Occupant density: this variable determines the intensity of moisture generation and CO₂ loading. “Normal” occupant density represents typical moisture and CO₂ loading, while “Dense” represents higher than typical loading.
- Ventilation rate: the volumetric airflow rate of the air supply ventilation system. This is as per the ASHRAE recommended rate or less (under-ventilated).
- Ventilation scheme: the operating scheme of the ventilation system
 - Constant: the supply ventilation system is run continuously at a constant rate.
 - Time-controlled: the ventilation system supplies fresh air at a maximum ventilation rate during predetermined on-times (hours), and a minimum ventilation rate at all other times.
 - RH-controlled: the ventilation system supplies fresh air at a maximum ventilation rate when interior relative humidity exceeds a certain threshold, and a lower ventilation rate otherwise.
 - CO₂-controlled: the ventilation system supplies fresh air at a maximum ventilation rate when interior CO₂ level exceeds a certain threshold, and a lower ventilation rate otherwise.

Table 5. List of Test Parameters for Test Cases 1 – 8

Test Case (TC)	Dates Test Undertaken		NORTH (CONTROL) BUILDING	SOUTH (TEST) BUILDING
1	Nov. 4-7/13	Interior Finish	Polyethylene	Polyethylene
		Occupant Density	Normal	Normal
		Ventilation Rate	ASHRAE Recommended	ASHRAE Recommended
		Ventilation Scheme	Constant	Constant
2	Nov. 7-12/13	Material	Polyethylene	GWB
		Occupant Density	Normal	Normal
		Ventilation Rate	ASHRAE Recommended	ASHRAE Recommended
		Ventilation Scheme	Constant	Constant
3	Nov. 12-19/13	Material	Polyethylene	GWB
		Occupant Density	Normal	Normal
		Ventilation Rate	Under-ventilated	Under-ventilated
		Ventilation Scheme	Constant	Constant
4	Nov. 20-27/13	Material	Polyethylene	GWB
		Occupant Density	Dense	Dense
		Ventilation Rate	ASHRAE Recommended	ASHRAE Recommended
		Ventilation Scheme	Constant	Constant
5	Apr. 2-4/14	Material	Polyethylene	GWB
		Occupant Density	Normal	Normal
		Ventilation Rate	ASHRAE Recommended	ASHRAE Recommended
		Ventilation Scheme	Constant	Constant
6	Apr. 11-13/14	Material	Polyethylene	GWB
		Occupant Density	Normal	Normal
		Ventilation Rate	ASHRAE Recommended	ASHRAE Recommended
		Ventilation Scheme	Time-controlled	Time-controlled
7	Jun. 22-25/14	Material	Polyethylene	GWB
		Occupant Density	Normal	Normal
		Ventilation Rate	ASHRAE Recommended	ASHRAE Recommended
		Ventilation Scheme	RH-controlled	RH-controlled
8	Jul. 5-6/14	Material	Polyethylene	GWB
		Occupant Density	Normal	Normal
		Ventilation Rate	ASHRAE Recommended	ASHRAE Recommended
		Ventilation Scheme	CO2-controlled	CO2-controlled

Test case 1 (TC1) is the benchmarking test for determining whether under identical conditions the two test buildings perform identically. The interior finishes are both non-hygroscopic polyethylene, the occupant density is set to normal, and the ventilation scheme is constant under ASHRAE recommended rates.

TC2, TC3, and TC4 assess the effect of moisture buffering potential of gypsum board for the benchmark case, an under-ventilated space, and a densely occupied space respectively. For these test cases CO₂ generation of occupants was not simulated, and indoor air quality based on indoor CO₂ levels is not considered.

TC5 has the same parameters as TC2. However, to assess the impact of different ventilation schemes on indoor air quality, this test case along with TC6, TC7, and TC8 have CO₂ generation of occupants included.

Each test case is run for approximately one week. One or more days are dedicated to conditioning the materials for each test case, in order to reach quasi-equilibrium. Chapter 6 will present the results of each test case for duration of one to two days following conditioning.

A number of parameters between the control and test building were controlled for each test case.

These include the following:

- Volume of test space: the test buildings are the same dimensions.
- Outdoor conditions: by undertaking the test for the hygroscopic and non-hygroscopic buildings simultaneously, the buildings are exposed to identical weather conditions and supply air conditions. Some data processing is required to compare the performance of the buildings between different test cases with different outdoor weather conditions.
- Air leakage: the buildings are generally very airtight. The difference in air leakage rate is very minimal (refer to Section 5.2).
- Indoor temperature: portable electric radiator heaters with thermostat settings for temperature control are used to provide heating. The buildings have identical building enclosure assemblies, therefore conductive heat losses will be very similar.

With these parameters controlled, it will be possible to assess the effects of the variable test parameters: the effect of 1) ventilation strategy, 2) moisture buffering materials and 3) occupant density on indoor relative humidity, ventilation heat loss, and indoor air quality.

6.2 Instrumentation & Calibration

The interior test space of each test building is monitored by five RHT sensors and a CO₂ sensor. All sensor readings are collected at 5-minute intervals via a data acquisition system and stored on a hard drive on site. Specifications of the RHT and CO₂ sensors are included in APPENDIX B.

6.2.1 RHT Sensors

Zone air temperature and relative humidity readings are measured at three locations in the test room at mid-height (Figure 34). At the south-east location, two additional readings are taken approximately 2 feet above the floor and 2 feet below the ceiling. A fan is installed at the ceiling to ensure complete mixing of indoor air.

A separate RHT sensor at the center of the test space is used to control the HVAC system output. Additional RHT sensors are also located at the inlet and outlet of the AHU to monitor ventilation supply air conditions.

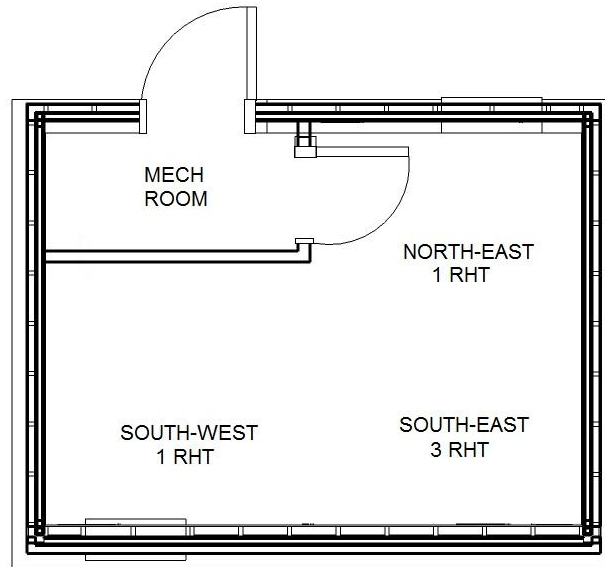


Figure 34. Locations of 5 RHT sensors inside the test space: 3 sensors are located at mid-height, 1 sensor is below mid-height and 1 is above mid-height at the south-east quadrant.

The RHT sensors were calibrated in a climate chamber by measuring the readings from each of the ten sensors (five in each test building) at pre-determined set-points for temperature and relative humidity. The calibration was completed for each sensor with readings taken every minute for duration of 180 minutes. Errors from readings from the RHT sensor were then calculated based on the chamber's internal sensor readings. The average error for the duration of the calibration process is then added if positive, or subtracted if negative, from the RHT sensor readings to achieve the calibrated reading for field testing.

Figure 35 to Figure 38 show the chamber set-point, chamber sensor reading data, and the ten RHT sensors' data.

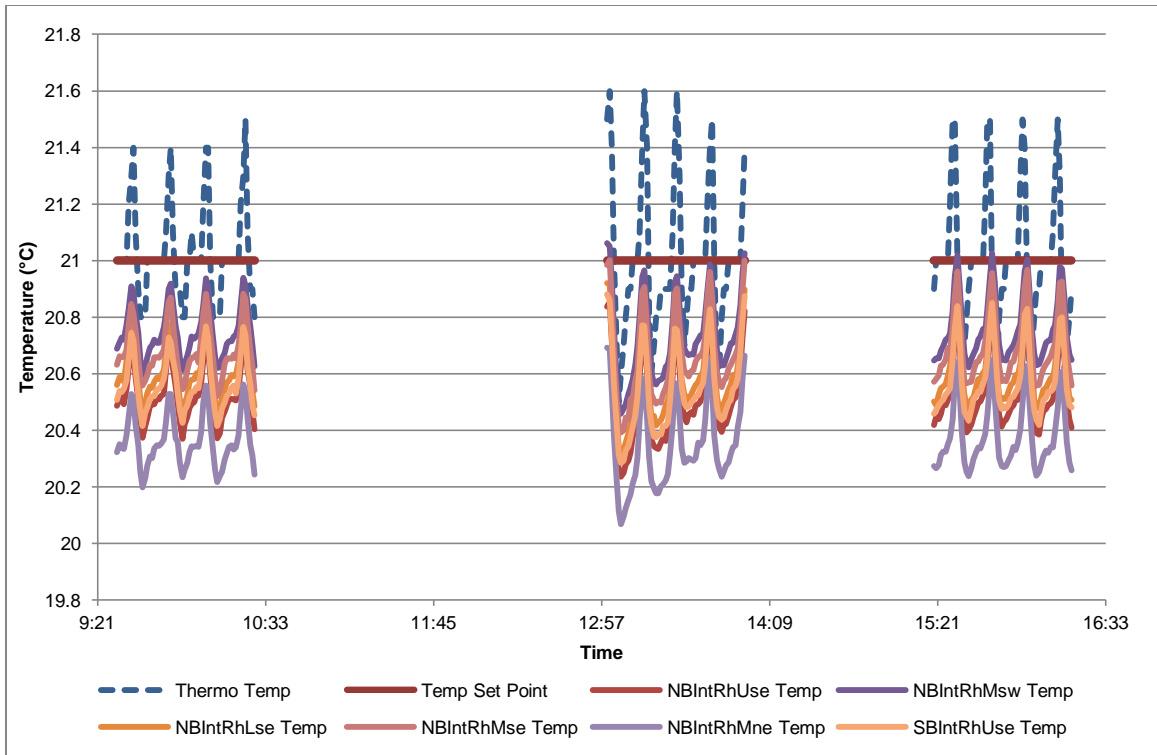


Figure 35. Temperature set-point, data from five RHT sensors in the north building, one RHT sensor in the south building, and climate chamber sensor used in calibration

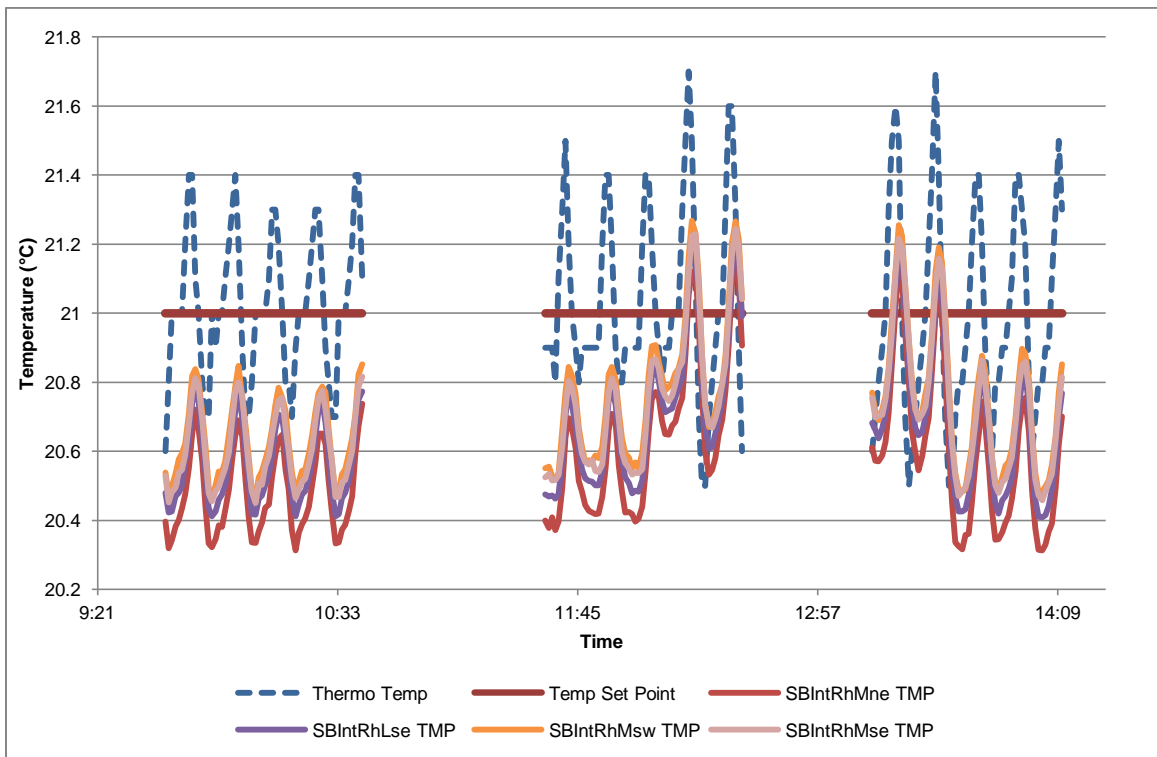


Figure 36. Temperature set-point, data from four RHT sensors in the south building, and climate chamber sensor used in calibration

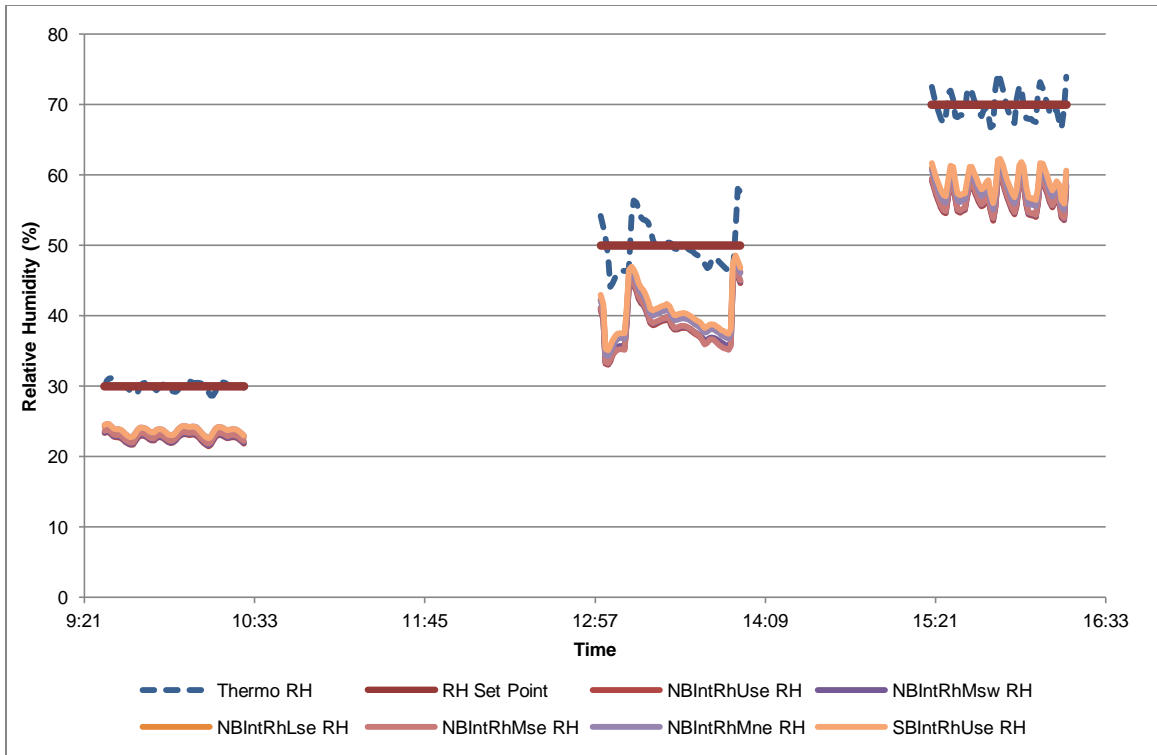


Figure 37. Relative humidity set-points, data from five RHT sensors in the north building, one RHT sensor in the south building, and climate chamber sensor used in calibration

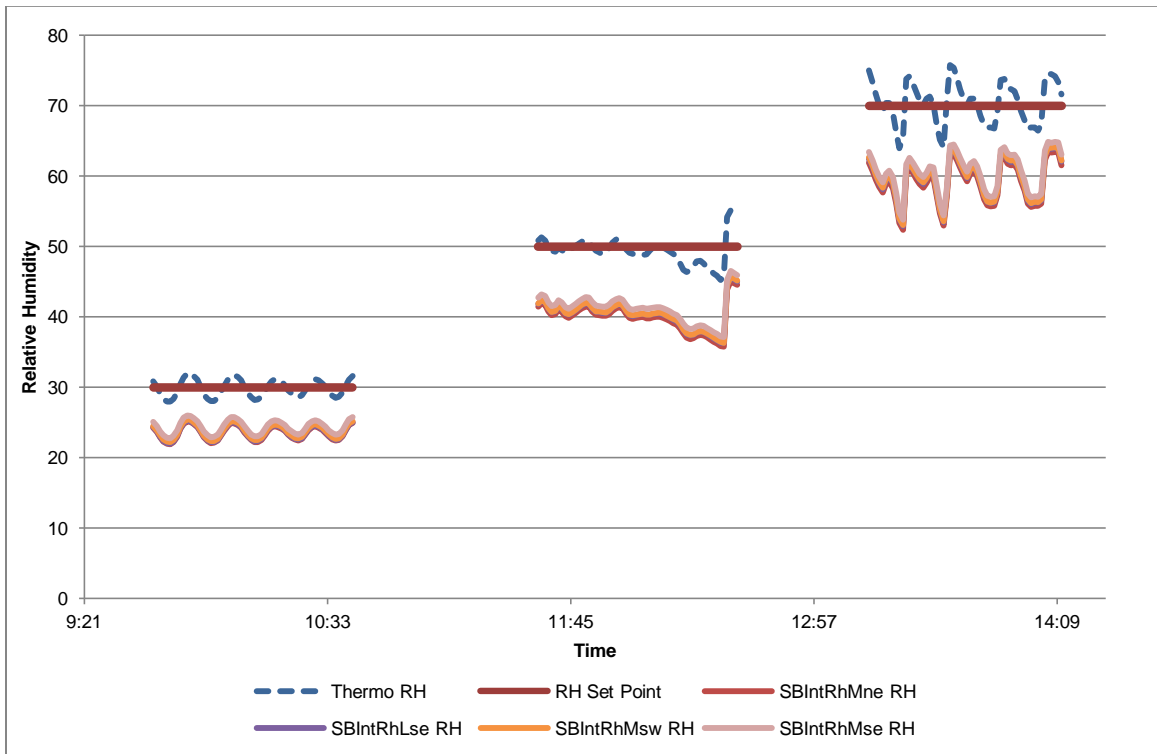


Figure 38. Relative set-points, data from four RHT sensors in the south building, and climate chamber sensor used in calibration

Table 6 shows the calculated errors from each round of calibration. Corrections obtained from calibration and tabulated below are then applied to sensor readings from field testing. Percentage errors are also provided for reference.

Table 6. Errors in readings from calibration of north and south building RHT sensors

Building	Sensor ID	Relative Humidity Error (%)	Temperature Error (°C)	Relative Humidity % Error	Temperature % Error
North	NBIntRhUse	+10.62	+0.49	22%	2%
	NBIntRhMse	+10.36	+0.33	21%	2%
	NBIntRhLse	+9.24	+0.41	19%	2%
	NBIntRhMne	+9.28	+0.65	19%	3%
	NBIntRhMsw	+10.43	+0.27	22%	1%
South	SBIntRhUse	+8.73	+0.45	18%	2%
	SBIntRhMse	+7.84	+0.32	16%	2%
	SBIntRhLse	+8.71	+0.36	18%	2%
	SBIntRhMne	+9.05	+0.44	19%	2%
	SBIntRhMsw	+8.57	+0.30	18%	2%

6.2.2 CO₂ Sensors

The concentration of CO₂ in the room is measured and recorded using a stand-alone CO₂ sensor for TC5 to TC8 (Figure 39). The non-dispersive infrared sensor can measure CO₂ concentration with an accuracy of $\pm 30\text{PPM} + 4.5\%$ of the measured reading. The same sensor can be used to control ventilation necessity in CO₂-demand ventilation.



Figure 39. CO₂ Sensor can measure and record CO₂ concentration

The sensor has a self-calibration function. However, prior to testing, monitoring of the sensor was completed to undertake further fine-tuning as required. One sensor was placed in each test building, and CO₂ levels were recorded. The high and low CO₂ readings are calculated and plotted based on the manufacturer's reported sensor accuracy. The percentage difference between the two sensors' readings is also determined. Figure 40 shows the monitoring data, and the self-calibration function increasing CO₂ level readings by approximately 50 PPM in the north building. Following the self-calibration function, the CO₂ reading ranges between the two building overlap, and the % difference between the sensors drop from approximately 40% to 20%.

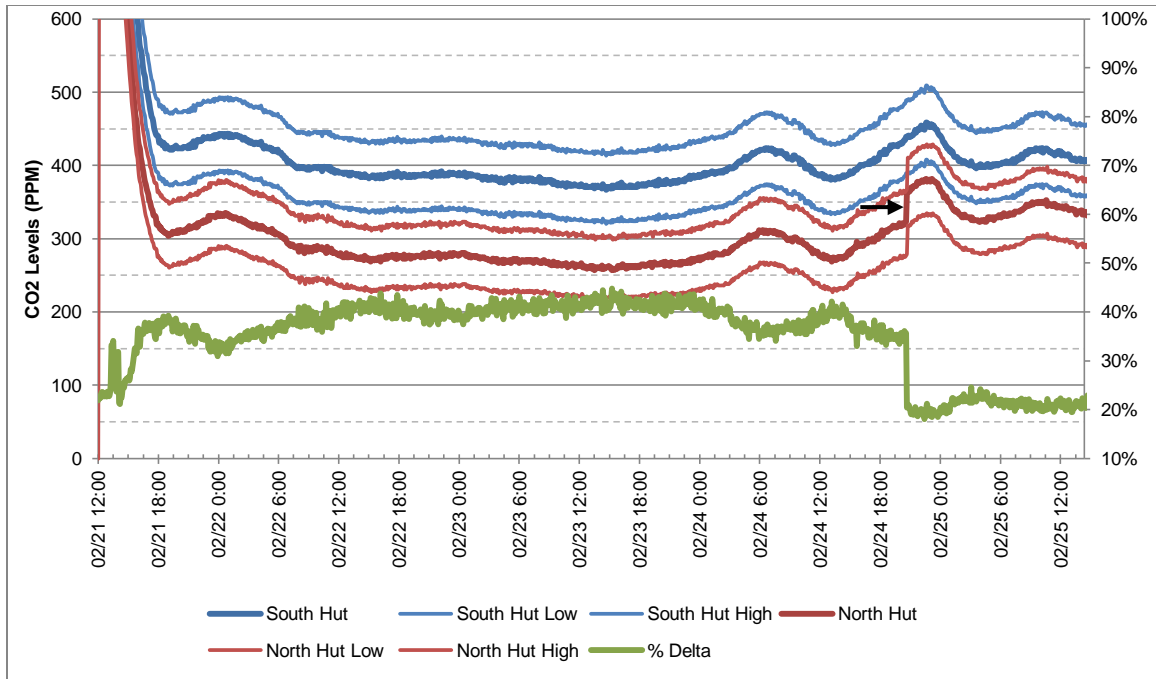


Figure 40. CO₂ data recorded over a duration of 4 days. The self-calibration function occurs on day 3 (denoted by arrow) to the north building's sensor, thereby reducing the % difference between the two CO₂ sensor readings.

The process is repeated as shown in Figure 41 for a shorter duration, in which time self-calibration of both sensors results in the % difference of readings of nearly 0%. The readings of CO₂ levels generally agree compared to a separate CO₂ sensor made by a different manufacturer, which was placed in the south building. As a result, CO₂ sensors are allotted time to self-calibrate, typically during the same time as building conditioning prior to the start of each test.

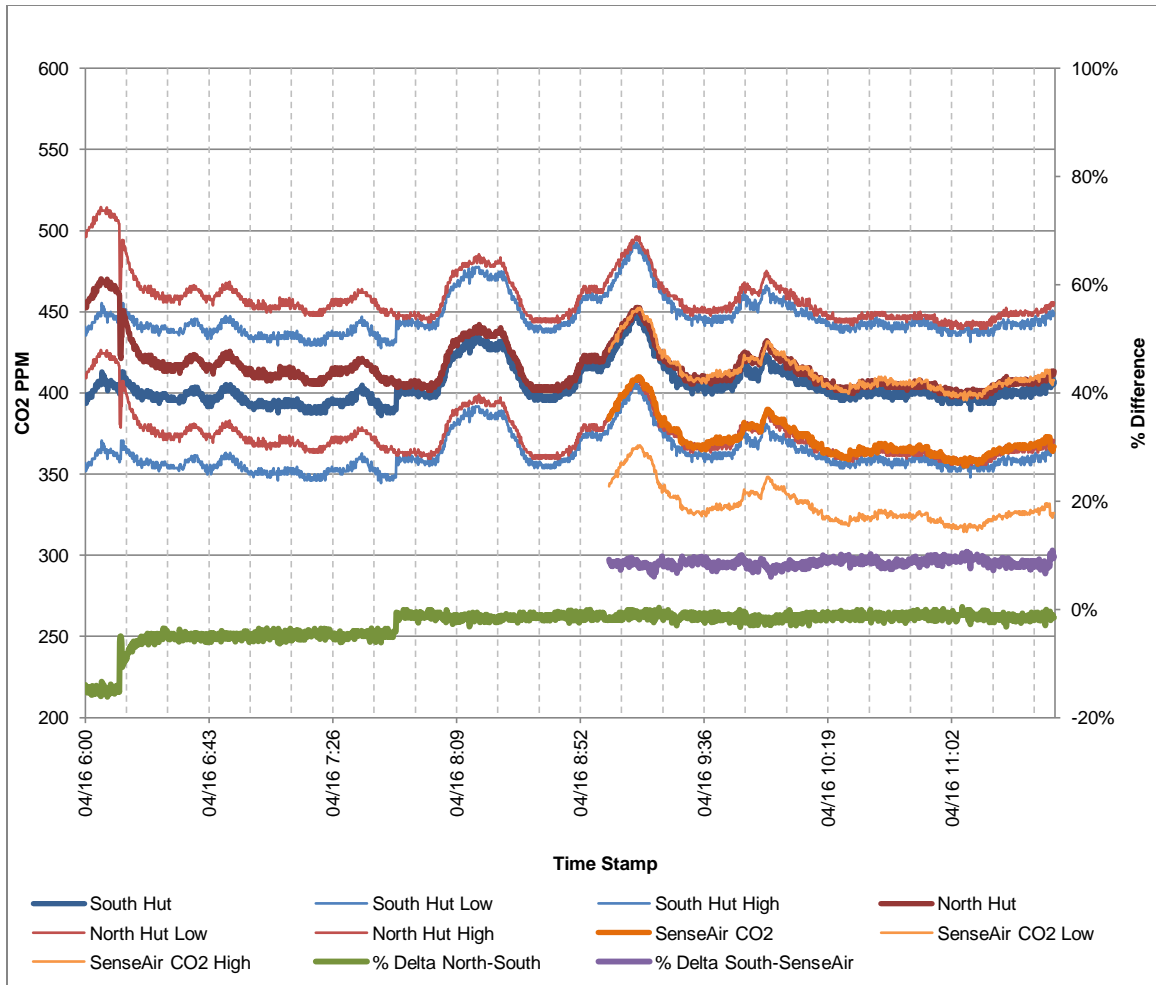


Figure 41. CO₂ data recorded in each building. The self-calibration function occurs in both buildings, resulting in % difference in CO₂ level readings of 0%. Readings for a separate CO₂ sensor by a different manufacturer are also plotted for comparison.

6.3 Determination of Interior Moisture and Carbon Dioxide Generation Profiles

This section describes the methodology for obtaining a realistic moisture production profile for the testing, based on data collected from a real apartment suite in the ‘Reference Building.’ The motivation behind doing this was the discrepancies in moisture production rate of different occupants’ activities in literature (refer to Section 2.1). It is followed by the methodology for obtaining CO₂ production profile of occupants, which is based on the relationship between occupants’ level of activity and CO₂ production as given by ASHRAE Standard 62.1.

6.3.1 Moisture Production Profiles

Based on literature review on indoor humidity, there are many ways occupants and their behaviours contribute to indoor moisture loading. The moisture production rates of these activities (breathing, cooking, cleaning, etc.) are derived empirically and may not be representative of the lifestyle of all occupants. For example, food preparation and cleaning styles of different communities may vary culturally and socially, which can contribute to different moisture generation profiles.

To isolate the moisture production of occupants and their activities, indoor conditions of a two-bedroom apartment suite in the ‘Reference Building’ (see Section 4.4) were analyzed (Pedram & Tariku, 2015). The suite, which will be referred to as ‘Suite A’ is occupied by a family of four, two adults and two children. The square footage of ‘Suite A’ is 643 square feet (59.7 square meters), and with a clear height of 8 ft encompasses 5144 cubic feet (149 cubic meters) of volume. The north-facing wall is the only exterior wall of the suite. This wall has one window in each bedroom, and a balcony adjacent to the living room. All other walls are adjacent to other suites or the building corridor. The kitchen is enclosed by interior walls on three sides and open to the living room on one side. The bathroom is located near the entrance door of the suite (Figure 42).

As described in Section 4.4, the suite has a bathroom exhaust fan, which is intermittently on at 7 to 11 am and 6 to 10 pm. The kitchen is equipped with a range hood fan that is turned on manually. Fresh air is supplied to the suite through open windows, the balcony door, or the entrance door undercut.

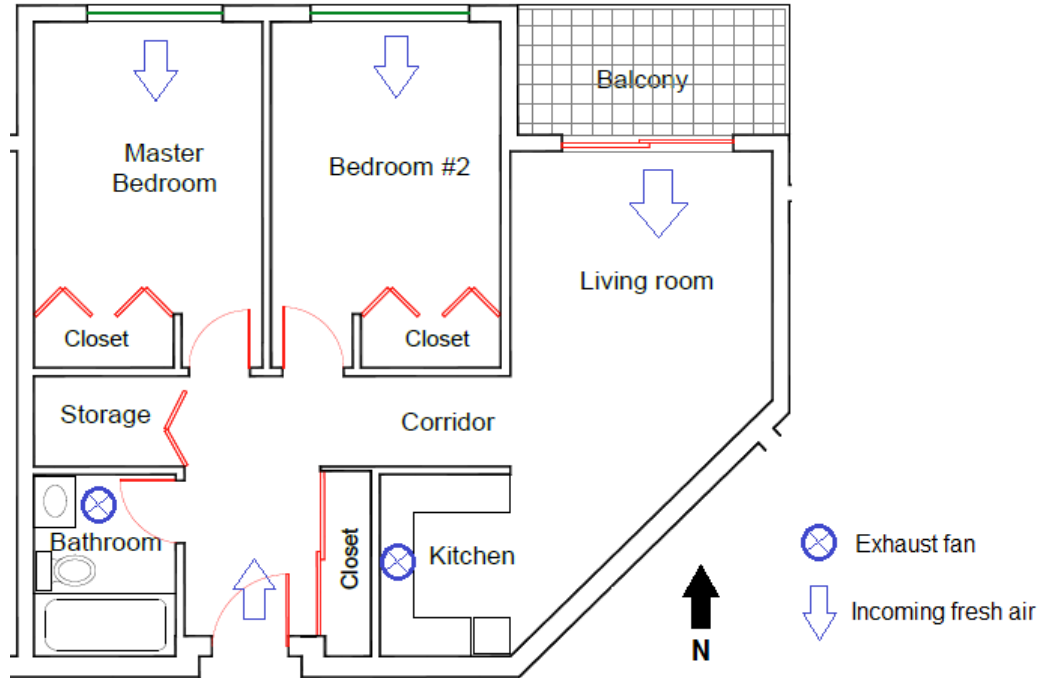


Figure 42. Floor plan of Suite A

For a period of one year between 2010 and 2011, the indoor and outdoor conditions (including temperature and relative humidity) of ‘Suite A’ were collected in 2-minute and 1-minute intervals respectively. Data between December 1st and February 28th were isolated from the data files to look at worst-case-scenario moisture loading conditions, typical of winter months in Vancouver. Hourly averages for the data sets were calculated. Figure 43 shows the daily RH profiles in the suite. Intermittent ventilation provided between 7 to 11 am and 6 to 10 pm is highlighted and indicated as “Ventilation On,” which typically coincide with decreasing RH in the daily RH profiles.

Absolute humidity for the indoors and the outdoors are calculated using psychrometrics as per Equation 4.

Equation 4. Determination of absolute humidity

$$W = 0.6219 \frac{P_v}{P_a}$$

$$\text{where } P_v = RH(P_{sat})$$

$$\text{where } P_{sat} = 611 \times 10^{\frac{7.5T}{237.3+T}}$$

W = absolute humidity [g_{moisture} / kg_{dry air}]

P_v = Vapour pressure [Pa]

P_a = Atmospheric pressure [Pa], taken as 101325 Pa

P_{sat} = Saturation vapour pressure [Pa]

T = Temperature [°C]

RH = Relative humidity [%]

Excess moisture (ΔW) is determined as the difference between indoor and outdoor absolute humidity. Then based on the mass flow rate (\dot{w}) of ‘Suite A’, the moisture production (m) of the suite’s occupants is determined for each hour of the 90 days selected (Equation 5).

Equation 5. Determination of moisture production rate

$$m = \dot{w}(\Delta W)$$

$$\text{where } \Delta W = W_{indoor} - W_{outdoor}$$

m = moisture production rate [g_{moisture} / hr]

\dot{w} = mass flow rate [kg_{dry air} / hr]

ΔW = excess moisture [g_{moisture} / kg_{dry air}]

W_{indoor} & $W_{outdoor}$ = indoor and outdoor absolute humidity [g_{moisture} / kg_{dry air}]

Because of intermittent ventilation in the suite, two different mass flow rates were used depending on the hour of the day. Between 7 to 11 am and 6 to 10 pm., the mass flow rate was based on the measured flow rate of the bathroom exhaust fan. APPENDIX C outlines the procedure for measurement of the volumetric flow rate of the bathroom exhaust fan. Although it is rated for 110 CFM (52 L/s), it has a measured flow rate of 66 CFM (31 L/s). For all other times of the day, the mass flow rate was based on an assumed infiltration rate of 0.2 air changes per hour. This assumption is based on ASHRAE Standard 160’s default air exchange rate for standard construction. For the purposes of the analysis, it was assumed the occupants did not use the range hood, or leave doors and windows open in winter months.

In Figure 44, each curve represents the moisture production profile of the family of four in 'Suite A' for each of the 90 days analyzed. The question remains how it is possible to obtain a typical moisture production profile based on this information. Can any one of these curves be used in the WBPR for the experiments using the occupant simulators to replicate a representative daily moisture production profile of real people?

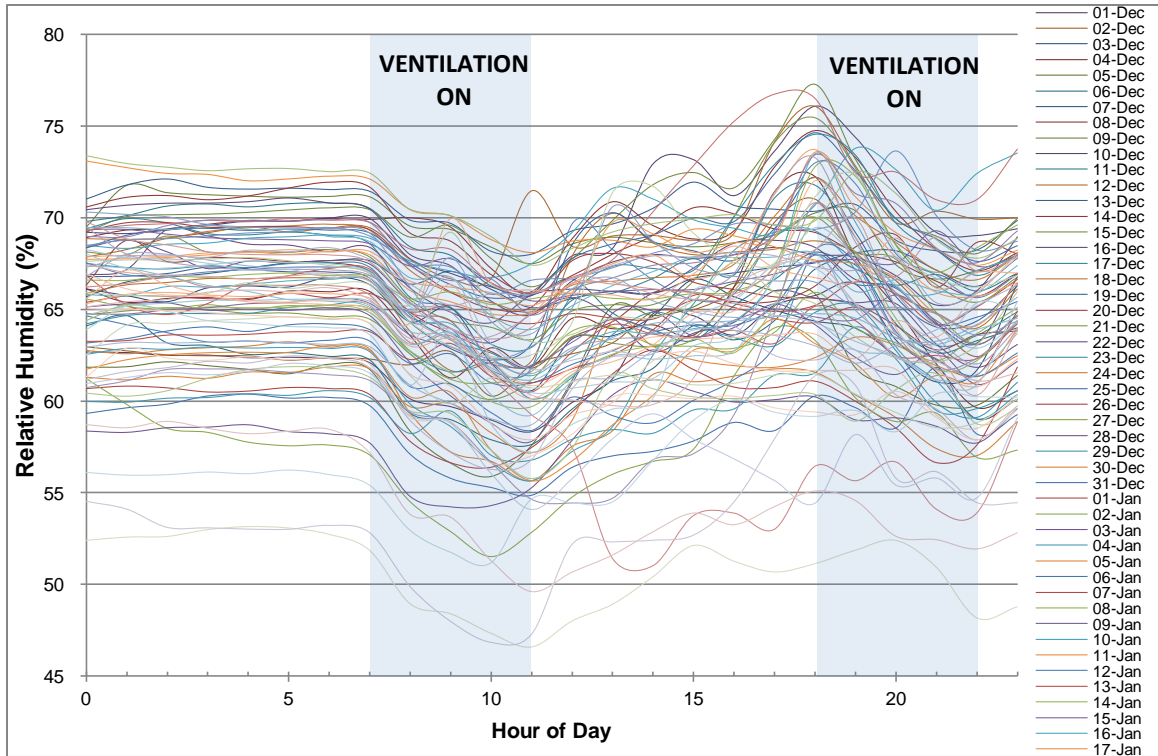


Figure 43. Daily indoor relative humidity profiles of 'Suite A' for December 1st to February 28th

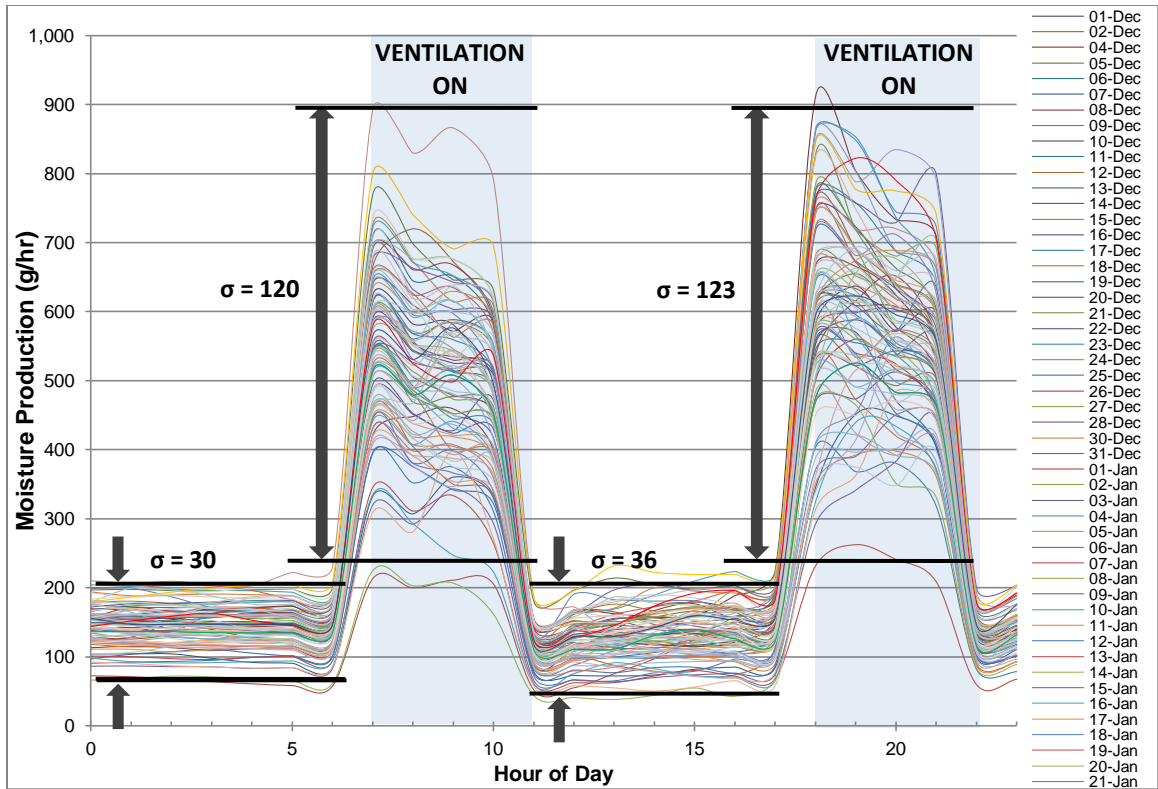


Figure 44. Daily indoor moisture production profiles (m) of Suite A for December 1st to February 28th. Standard deviation or “spread” (σ) of data sets is indicated for ventilation “on” and “off” periods.

To answer this question, statistical analysis was used. It is clear that moisture production peaks coincide with the ventilation-on periods. During on periods, moisture production rates have a higher spread than during off periods. For closer analysis, 9 am (hour-9) and 8 pm (hour-20) data, which fall approximately in the middle of the ventilation-on periods, were selected for further investigation.

The normal distribution curve, cumulative distribution function, and linear probability correlation of m for hour-9 and hour-20 were determined from the sample space of 90 days (Figure 45). The fits indicate that it is reasonable to assume both data sets are normally distributed. In order to come up with a typical moisture production profile for ‘Suite A’, the 50th-percentile values that coincided with moisture loading at hour-9 and hour-20 for a given day were identified, and thus two days out of the 90-day data set were isolated.

Similarly, in order to identify a curve that would represent worst-case scenario moisture loading, that is, high moisture production or high occupant density, 95th-percentile values for hour-9 and hour-20 were also identified and linked to another corresponding two days. In this way, a total of four curves from Figure 44 were isolated amongst the data set, two representing typical, and two representing high moisture production profiles (Table 7). The four curves are highlighted in Figure 46.

Table 7. Selection of four *m*-profiles based on 50th and 95th percentile values for hour-9 and hour-20

Cumulative Probability	0%	5%	10%	15%	20%	25%	30%	35%	40%	45%	50%
											Dec. 13
<i>m</i> , hour-9	-∞	314	356.8	385.6	408.5	428.1	445.8	462.1	477.7	492.7	507.5
											Dec. 3
<i>m</i> , hour-20	-∞	389.4	434.4	464.8	488.9	509.6	528.2	545.5	561.8	577.7	593.2
Cumulative Probability	55%	60%	65%	70%	75%	80%	85%	90%	95%	100%	
											Jan. 30
<i>m</i> , hour-9	522.2	537.2	552.8	569.1	586.8	606.4	629.3	658.2	700.9	∞	
											Dec. 29
<i>m</i> , hour-20	608.8	624.6	641	658.2	676.8	697.6	721.7	752.1	797.1	∞	

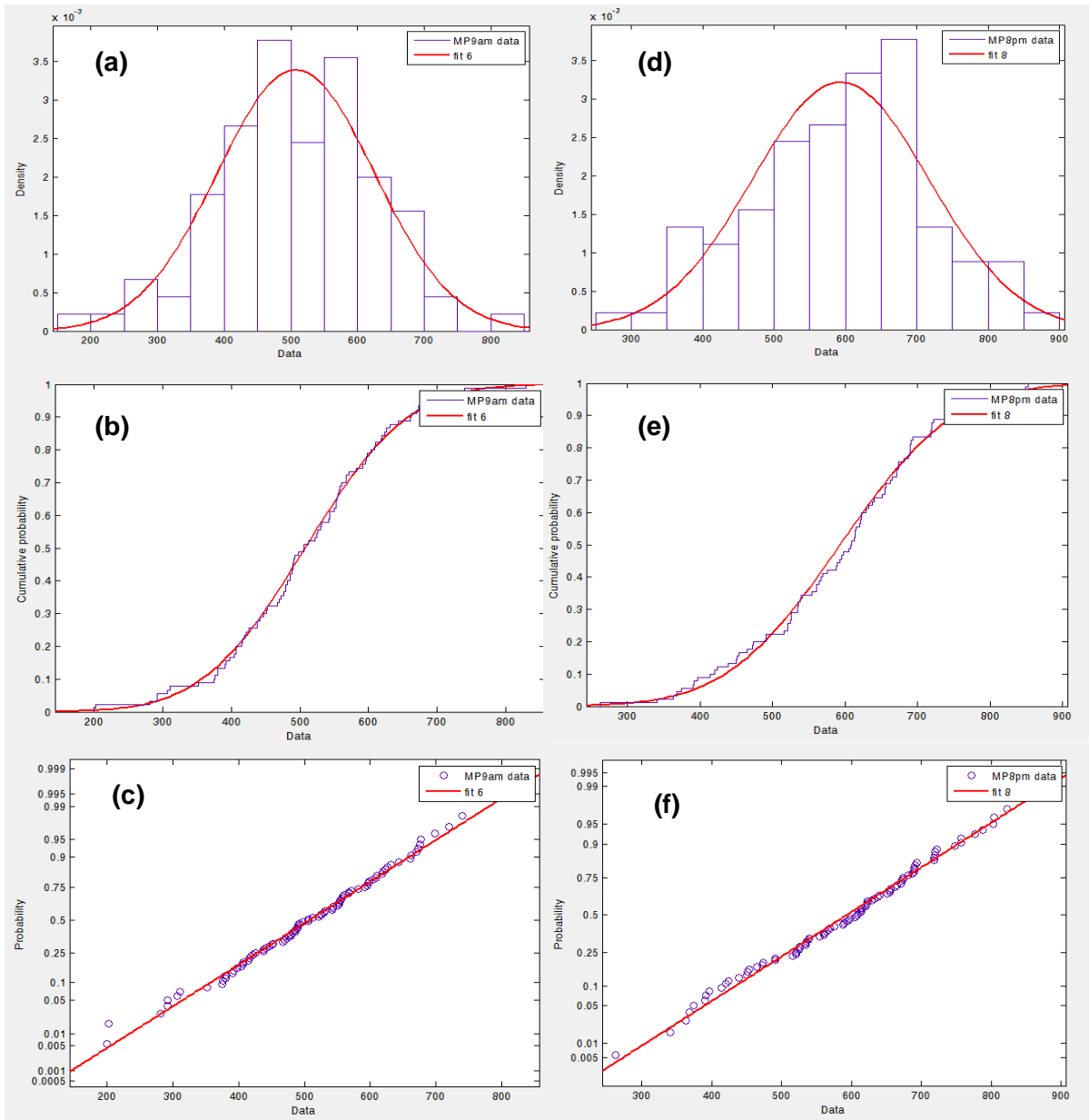


Figure 45. Normal distribution curve, cumulative distribution function, and linear probability correlation of m for hour-9 (a–c) and hour-20 (d–f) from 90 days of Suite A monitoring data

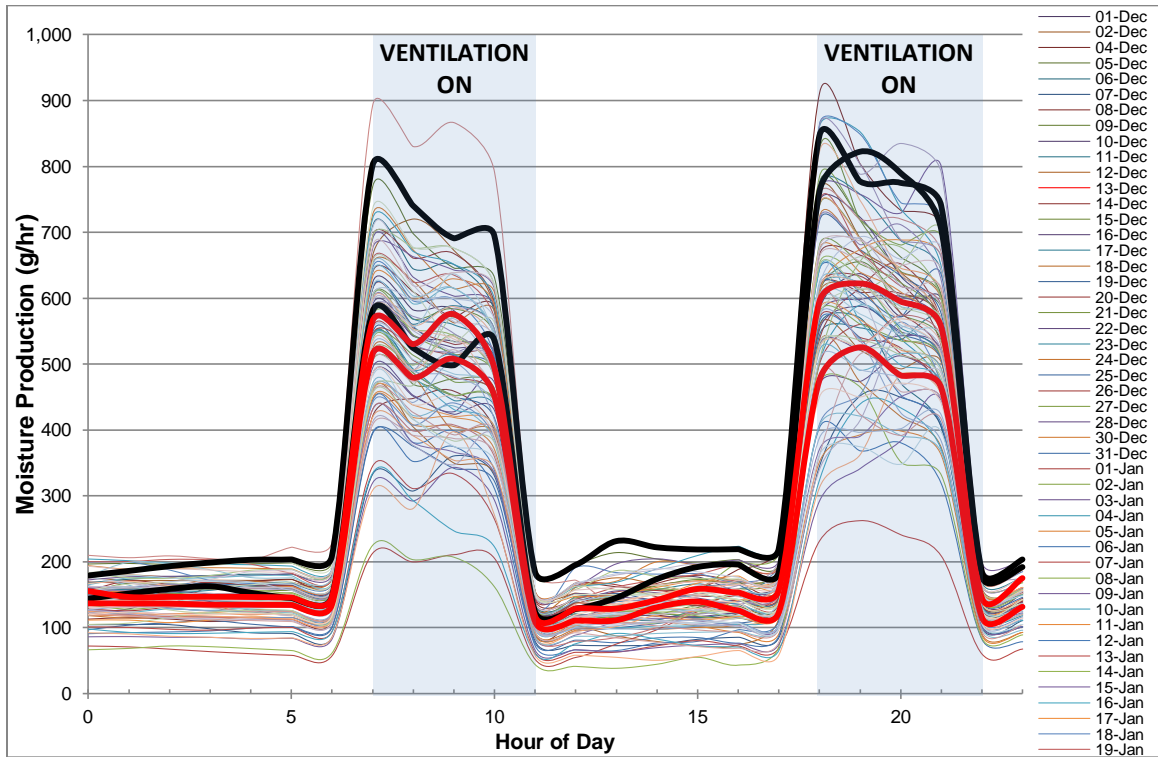


Figure 46. Four curves isolated amongst the data set in Figure 44, two representing typical or 50th percentile (red), and two representing high or 95th percentile (black) moisture production profiles

The selection was further narrowed down to two moisture production profiles. According to Kunzel, et al. (2004), 48 g/m³ per day is a typical moisture generation rate of occupants based on a study on German homes. This corresponds to 7.8 kg per day for a 3-person, 65 m² family home. To see how the selected profiles compare to this value, the area under all four curves, which represent moisture production per day, were calculated (Table 8). Based on the findings, December 3rd *m*-profile yields a value of 7.6 kg per day, which is within 3% of the value given by Kunzel, et al (2004). January 30th *m*-profile yields 10.4 kg per day, a higher value than the other three “short-listed” daily profiles, which indicates it as a suitable choice for simulating a high moisture loading scenario. As a result, *m*-profiles for December 3rd and January 30th were chosen as typical and high moisture production profiles respectively.

Table 8. Four short-listed moisture production curves, and their total production per day

	hour-20, 50p	hour-9, 50p	hour-20, 95p	hour-9, 95p
Date	Dec. 3	Dec. 13	Dec. 29	Jan. 30
Area under <i>m</i> -profile curve (Total Moisture Production [kg/day])	7.6	6.6	8.7	10.4

To apply the determined typical and high moisture loading curves to the moisture buffering experiments in the field, first the curves were proportionally scaled down 75%, based on the ratio of the volume of ‘Suite A’ to the test buildings in the WBPRL (Figure 47, (a)). Then they were smoothed to a step function based on average moisture production rate for each ventilation on and off periods (Figure 47, (b)). This was done to ensure consistency in moisture produced by the occupancy simulator units, and deciphering data based on the moisture production profiles. The final moisture generation profiles were then programmed into the occupant simulators to mimic the moisture production of occupants and their activities in the field experiment.

As previously mentioned, typical moisture loading identified by Kunzel, et al. (2004) in studies of German homes is about 48g/m^3 per day. This corresponds to 1.9 kg of moisture per day for a building with a volume of 40.5 cubic meters, the size of the ones at the WBPRL. The total moisture production per day of each curve from Figure 47 (b) calculated from the area under the curves, are 1.9 kg per day for typical and 2.6 kg per day for high moisture loading. Thus, the moisture generation curves can be applied to the field experiment with confidence that they are fairly representative of real occupants.

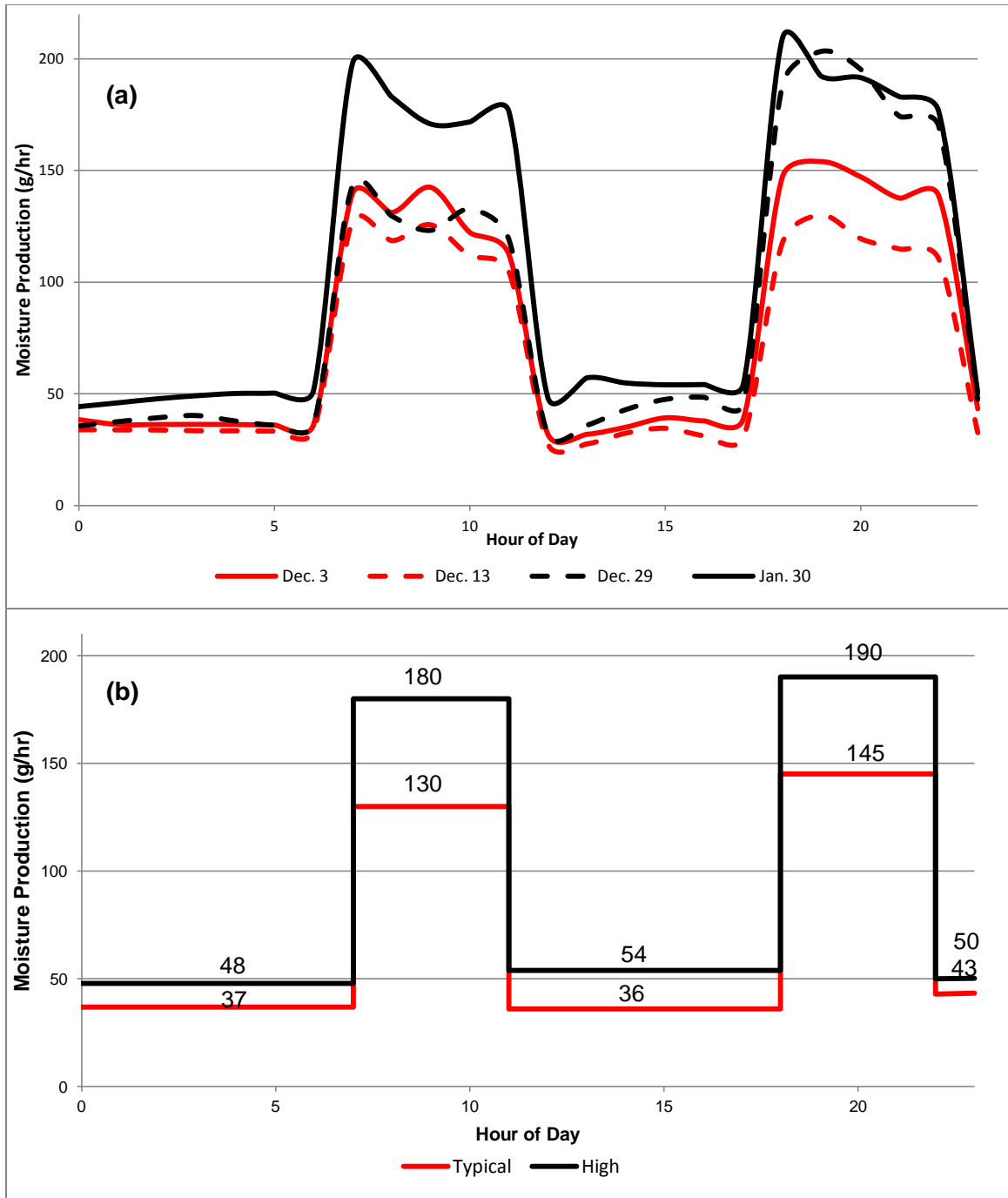


Figure 47. *m*-profiles obtained from Suite A scaled down 75% (a), and typical (based on Dec. 3) and high (based on Jan. 30) smoothed curves used as moisture production profiles in the field experiments to simulate the moisture generation of occupants and their activities (b)

6.3.2 Carbon Dioxide Generation Profile

CO₂ is a natural byproduct of human and animal respiration. CO₂ is not a harmful gas on its own, except at very high concentrations (e.g. 350,000 ppm) it can be an asphyxiant due to oxygen displacement (ASHRAE, 2013). Because it is difficult to measure odour intensity in a space, CO₂ concentration is typically used as a surrogate indicator to evaluate the indoor air quality and ventilation adequacy of a space. CO₂ concentration in a building is dictated by the occupants, as well as the CO₂ levels in the ambient outdoor air.

CO₂ production rate depends on the occupants' level of activity and diet. CO₂ generation per person can be estimated using the oxygen consumption rate, from Equation 6 given in ASTM Standard D6245 (2012).

Equation 6. Oxygen Consumption of Occupants (ASTM D6245, 2012)

$$V_{O_2} = \frac{0.00276 A_D M}{0.23 RQ + 0.77}$$

V_{O_2} = Oxygen consumption rate (L/s),

A_D = DuBois body surface area (m²),

M = Metabolic rate per unit of surface area (1 met = 58.2 W/m²)

RQ = Respiratory quotient, volumetric ratio of CO₂ produced to oxygen consumed (unitless)

The body surface area is dependent on a person's height and mass, but can be estimated as 1.8 m² for adults and 1.0 m² for children. Metabolic rate of occupants depends on the physical intensity of their activity, and can range from 1.0 when sedentary to 5.0 when exercising. Respiratory quotient is estimated as 0.83 for an average-sized adult at sedentary state (ASHRAE 62.1, 2013). Thus, oxygen consumption rate, V_{O_2} , multiplied by RQ is equal to the CO₂ generation rate, G . Figure 48 shows this relationship for an average-sized adult at various activity levels.

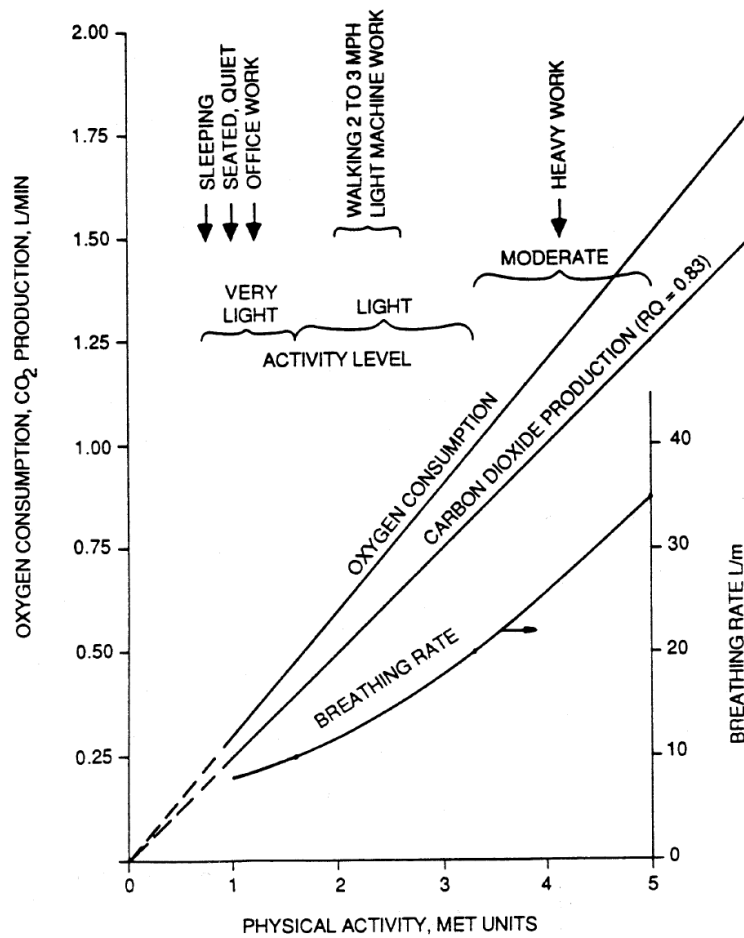


Figure 48. Dependence of CO₂ Production per Person on the Level of Activity (ASHRAE 62.1, 2013)

To determine the rate of CO₂ emission of the occupant simulators for the testing based on Equation 6 and Figure 48, first the level of occupants' activity had to be assumed for a typical day. Figure 49 shows the assumed level of activity for a family of four throughout the day, assuming there are two adults who work from home with two children. The metabolic activity rates were estimated from each occupant's level of activity from Figure 48, and corresponding CO₂ generation rates were determined based on oxygen consumption rate (Equation 6) and RQ . Body surface area was assumed to be 1.8 and 1.0 m² for adults and children respectively. RQ was assumed to be 0.83. The resulting total CO₂ generation rates are summarized in Table 9. When scaled down by the volumetric ratio of 'Suite A' to the test buildings, the occupants' normal and

peak activity CO₂ generation rates are 0.20 and 0.33 L/min respectively. Section 6.4.2 will cover how the determined CO₂ generation rates of occupants will be used to emit the correct amount of CO₂ by occupant simulator units in the field experiments.

Table 9. Estimated CO₂ generation rates of family of four

		Metabolic Rate (met)	CO ₂ Generation (L/min/person)
Normal Activity Hours	2 adults	1.0	0.26
	2 children	1.0	0.14
	Total		0.80 L/min
Peak Activity Hours	1 adult	1.2	0.31
	2 children	1.2	0.17
	1 adult	2.5	0.64
	Total		1.30 L/min

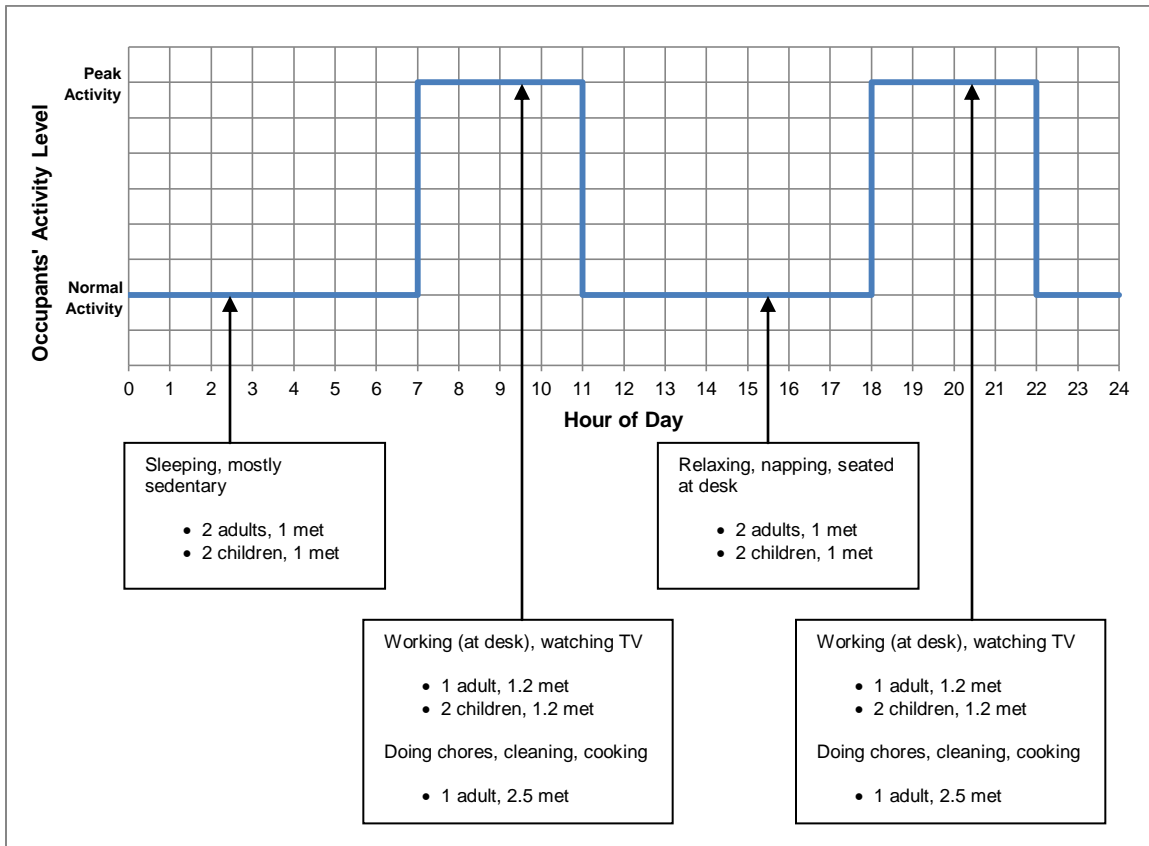


Figure 49. Typical activities of a family of four throughout the day and their corresponding metabolic activity

6.4 Implementation of Daily Profiles in Occupant Simulators

Figure 47 and Figure 49 respectively show the daily moisture and CO₂ generation profiles that are implemented to simulate the activities of occupants in the control and test buildings for the field experiment. The following sections describe the implementation of these profiles.

6.4.1 Implementation of Moisture Generation Profiles

Since each nebulizer in the occupant simulators' humidifiers behaves differently, calibration was done to determine the rate of water lost as mist per hour. To calibrate each nebulizer, 10V of input voltage was provided to the nebulizer to create misting. The mass of the humidifier box was measured and recorded quasi-continuously in 10 second intervals over one hour, using a digital scale with a USB port connected to a computer. Each nebulizer was then characterized by its loss of water mass over time.

Loss of water mass over time was plotted over time, and rate of mass change over time was determined based on the slope of the mass change over time. The calibration process was done multiple times for each nebulizer for repeatability. In this way, the characteristic misting rate (rate of mass change over time) for each nebulizer was determined.

The calibration was repeated for pairs of nebulizers running simultaneously outfitted to each of four humidifier units. This is because the net effect of two nebulizers vibrating in tandem at ultrasonic rates does not linearly increase the rate of water misting. This is indeed the case when characteristic misting rates for pairs of nebulizers are compared to the sum of each individual nebulizer. Misting rates of pairs are generally lower than sum of two individual nebulizers' rates.

Figure 50 shows the plots of all the calibrations that were run on the humidifier units, both individual and pairs of nebulizers. The nebulizers are numbered 1 through 7. In general, for the water levels tested, the regression of cumulative water loss over time was strongly linear. The

slope of each plot represents the characteristic misting rate of each nebulizer or pair set in units of grams of water per hour (g_w/hr).

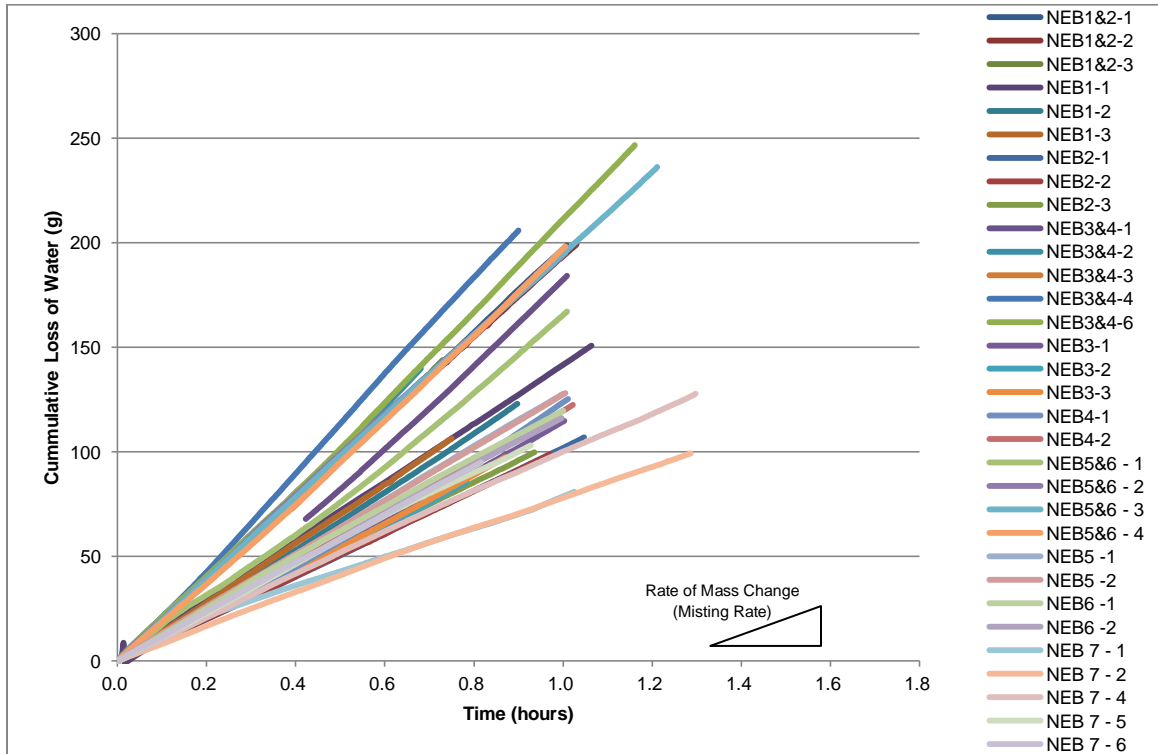


Figure 50. Plot of cumulative loss of mass of water from humidifier box over time for each pair or individual nebulizer

During the calibration process, some calibration plots underwent a slight increase in slope after a certain period. This is attributed to the fact that in a dry humidifier box, a certain mass of water particles forms on the interior surfaces in the form of water droplets (Figure 51). Once a limit is reached when no more water droplets can form, all the mist created by the nebulizers is directed out of the humidifier by the fan.

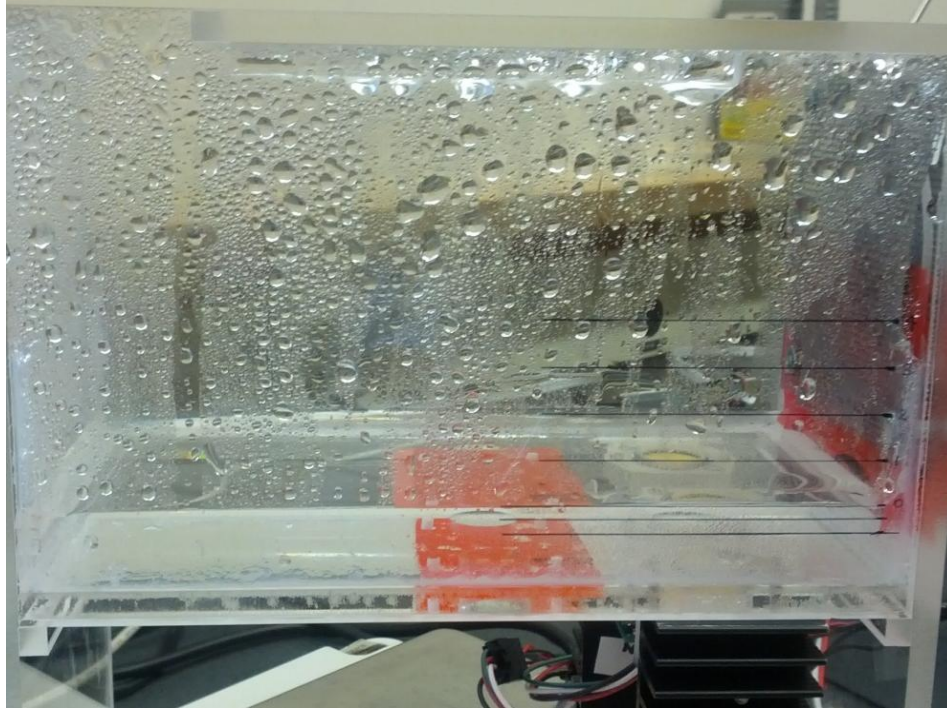


Figure 51. Water Droplets Forming on the Interior Surfaces of Humidifier Box

As a result, calibration tests were done after water droplets were fully formed on the humidifier. The results of the calibration are presented in Table 10. Nebulizer 7 was excluded from testing because it did not have consistent misting rates for each round of calibration. Nebulizers 3 and 4 had reliable misting rates individually, but as a pair, they had a high variation in misting rates each time the calibration was repeated. Based on the calibration results, nebulizers 3 and 4 were separated and installed in two separate humidifier units. With a total of six calibrated nebulizers in four humidifier units, it is possible to program the moisture generations profiles determined from Figure 47 to simulate occupants' moisture generation.

Table 10. Linear correlation fits from the nebulizer calibration tests and corresponding mean and standard deviation of characteristic misting rates

Nebulizer(s)	1&2	1	2	3&4	3	4	5&6	5	6	7
Equation 1	y = 198.95x - 2.3557	y = 140.97x + 0.8475	y = 102.38x - 0.5232	y = 199.04x - 17.692	y = 114.22x - 1.146	y = 122.73x - 2.8149	y = 194.28x + 1.0489	y = 128.47x - 0.1617	y = 118.34x - 0.8182	y = 98.189x + 1.7349
Correlation 1	R ² = 0.9996	R ² = 0.9994	R ² = 1	R ² = 0.9996	R ² = 0.9997	R ² = 0.998	R ² = 0.9999	R ² = 1	R ² = 0.9998	R ² = 0.9992
Equation 2	y = 194.47x - 0.4863	y = 136.4x - 0.7169	y = 101.66x - 0.2314	y = 229.75x - 16.224	y = 108.84x - 0.8452	y = 119.86x - 0.6834	y = 194.53x + 0.3648	y = 127.02x + 0.4481	y = 120.11x + 1.2476	y = 76.748x + 1.7097
Correlation 2	R ² = 1	R ² = 0.9997	R ² = 1	R ² = 0.9999	R ² = 0.9998	R ² = 0.9999	R ² = 1	R ² = 1	R ² = 0.9994	R ² = 0.9991
Equation 3	y = 196.77x - 0.6124	y = 141.59x - 0.3426	y = 106.43x + 0.2412	y = 219.47x - 13.617	y = 111.93x - 1.0122		y = 197.63x - 2.6951			y = 112.51x + 0.6795
Correlation 3	R ² = 0.9999	R ² = 0.9999	R ² = 1	R ² = 0.9999	R ² = 0.9996		R ² = 0.9995			R ² = 0.999
Equation 4				y = 232.44x - 2.6793						y = 116.23x + 0.1895
Correlation 4				R ² = 0.9997						R ² = 0.9981
Equation 5				y = 233.01x - 61.91						y = 73.762x + 5.1623
Correlation 5				R ² = 0.9999						R ² = 0.9953
Equation 6				y = 212.57x - 2.5682						
Correlation 6				R ² = 0.9995						
Rate (g_w/hr)	199	141	102	199	114	123	194	128	118	98
	194	136	102	229	109	120	195	127	120	77
	197	142	106	219	112		198			113
				232						
				233						
				212						
Mean (g_w/hr)	197	140	103	221	112	121	196	128	119	96
Stdev/2 (±g_w/hr)	1.12	1.42	1.29	6.70	1.35	1.01	1.04	0.51	0.63	9.00

The moisture generation profiles provide a known rate of moisture to be added to the room for each hour of the day. The moisture generation rate for the hour divided by humidification units' maximum moisture generation capacity, that is, the characteristic misting rate determined from calibrations, provides the duty cycle required for the humidification unit for the hour. A duty cycle is the percentage of time the humidification system will be on and misting moisture at a constant rate for a given time period. For example, for a 33% duty cycle at 60 second periods, the unit will be on for 20 seconds and off for 40 seconds per cycle.

Table 11 provides duty cycles of each humidifier for each hour based on the moisture generation profiles. During moisture peaks, the dual-nebulizer units will run because of their higher moisture generation capacity. For the remaining hours of the day, the single-nebulizer units are sufficient to provide the correct moisture generation rates.

Table 11. Duty cycles of humidifiers based on pre-determined moisture generation profiles

Building One	Mean (gw/hr)	Stdev/2 (±gw/hr)		Building Two	Mean (gw/hr)	Stdev/2 (±gw/hr)	
Unit 1 = Nebulizers 1&2 (high capacity)	197	1.12		Unit 1 = Nebulizers 5&6 (high capacity)	196	1.04	
Unit 2 = Nebulizer 3 (low capacity)	112	1.35		Unit 2 = Nebulizer 4 (low capacity)	121	1.01	
Full Capacity	308			Full Capacity	317		
Average Moisture Production	Period = 60s			Average Moisture Production	Period = 60s		
Hour	Duty Cycle	1&2	3	Hour	Duty Cycle	5&6	4
0	33%	OFF	ON	0	31%	OFF	ON
1	33%	OFF	ON	1	31%	OFF	ON
2	33%	OFF	ON	2	31%	OFF	ON
3	33%	OFF	ON	3	31%	OFF	ON
4	33%	OFF	ON	4	31%	OFF	ON
5	33%	OFF	ON	5	31%	OFF	ON
6	33%	OFF	ON	6	31%	OFF	ON
7	66%	ON	OFF	7	66%	ON	OFF
8	66%	ON	OFF	8	66%	ON	OFF
9	66%	ON	OFF	9	66%	ON	OFF
10	66%	ON	OFF	10	66%	ON	OFF
11	66%	ON	OFF	11	66%	ON	OFF
12	32%	OFF	ON	12	30%	OFF	ON
13	32%	OFF	ON	13	30%	OFF	ON
14	32%	OFF	ON	14	30%	OFF	ON
15	32%	OFF	ON	15	30%	OFF	ON
16	32%	OFF	ON	16	30%	OFF	ON
17	32%	OFF	ON	17	30%	OFF	ON
18	74%	ON	OFF	18	74%	ON	OFF
19	74%	ON	OFF	19	74%	ON	OFF
20	74%	ON	OFF	20	74%	ON	OFF
21	74%	ON	OFF	21	74%	ON	OFF
22	74%	ON	OFF	22	74%	ON	OFF
23	33%	OFF	ON	23	31%	OFF	ON
High Moisture Production	Period = 60s			High Moisture Production	Period = 60s		
Hour	Duty Cycle	1&2	3	Hour	Duty Cycle	5&6	4
0	45%	OFF	ON	0	41%	OFF	ON
1	45%	OFF	ON	1	41%	OFF	ON
2	45%	OFF	ON	2	41%	OFF	ON
3	45%	OFF	ON	3	41%	OFF	ON
4	45%	OFF	ON	4	41%	OFF	ON
5	45%	OFF	ON	5	41%	OFF	ON
6	45%	OFF	ON	6	41%	OFF	ON
7	91%	ON	OFF	7	92%	ON	OFF
8	91%	ON	OFF	8	92%	ON	OFF
9	91%	ON	OFF	9	92%	ON	OFF
10	91%	ON	OFF	10	92%	ON	OFF
11	91%	ON	OFF	11	92%	ON	OFF
12	48%	OFF	ON	12	45%	OFF	ON
13	48%	OFF	ON	13	45%	OFF	ON
14	48%	OFF	ON	14	45%	OFF	ON
15	48%	OFF	ON	15	45%	OFF	ON
16	48%	OFF	ON	16	45%	OFF	ON
17	48%	OFF	ON	17	45%	OFF	ON
18	97%	ON	OFF	18	97%	ON	OFF
19	97%	ON	OFF	19	97%	ON	OFF
20	97%	ON	OFF	20	97%	ON	OFF
21	97%	ON	OFF	21	97%	ON	OFF
22	97%	ON	OFF	22	97%	ON	OFF
23	45%	OFF	ON	23	42%	OFF	ON

Water level in the humidifier affects the rate of misting. At greater depths, vibrations from the nebulizers are further dampened before they reach the water surface. The calibrations were done for water level between 0 and 1 cm, measured 2.5 cm above the nebulizers (Figure 52). 2.5 cm is the minimum water level required to prevent damaging the nebulizers. At 0 to 1 cm, the maximum rate of misting can be achieved before the misting rate dampens slightly above 1 cm. As a result, the float switches were adjusted to achieve the same water level range as the calibration by way of the pump refilling in operation.

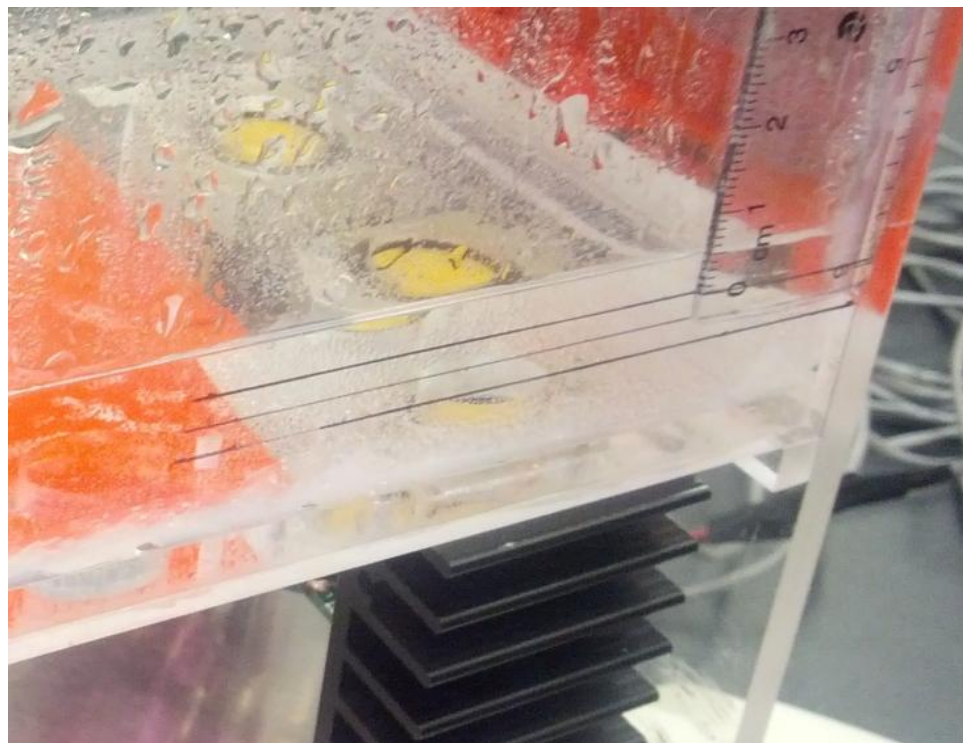


Figure 52. Water level measured 2.5 cm above nebulizers

The moisture production schedule from Table 11 is used as the input for the occupant simulators' control system. The values are input into a spreadsheet, which then dictates when and how long the controller provides voltage to the humidification system, via communication through a computer.

In this way, the humidification system is able to simulate the desired occupant behavior in terms of moisture production. The design of the system allows for the flexibility to program different

moisture generation intensities and schedules. This enables for simulation of different activities throughout the day, as well as variation in occupant density.

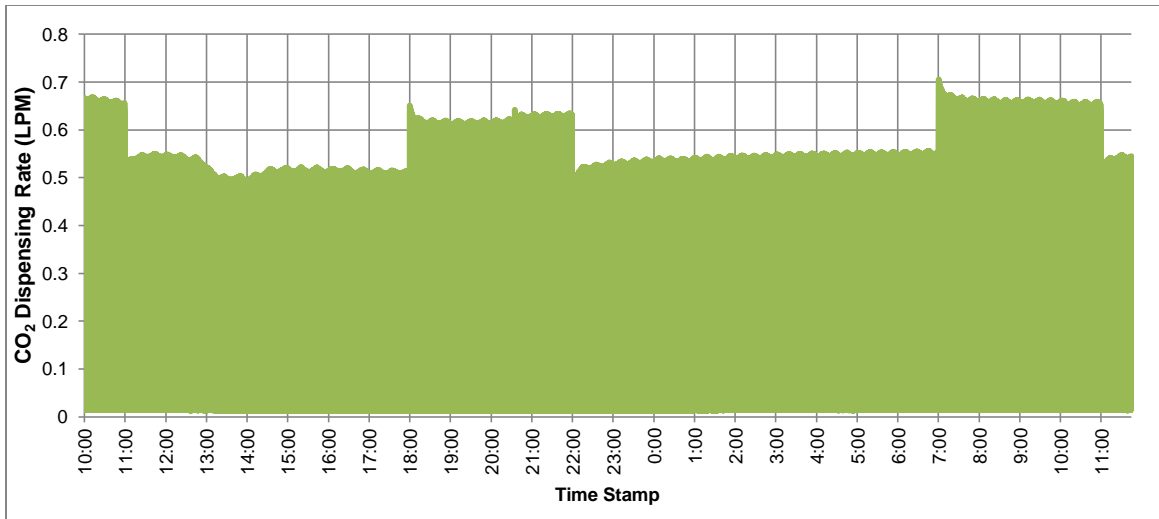
6.4.2 Implementation of Carbon Dioxide Generation Profiles

Similar to the operation of the nebulizers, the solenoid valve on the CO₂ dispensing system requires voltage input for release of pre-determined rate of CO₂ into the room. This mechanism is further described in Section 5.4.2. The rate of CO₂ release varies linearly with the voltage.

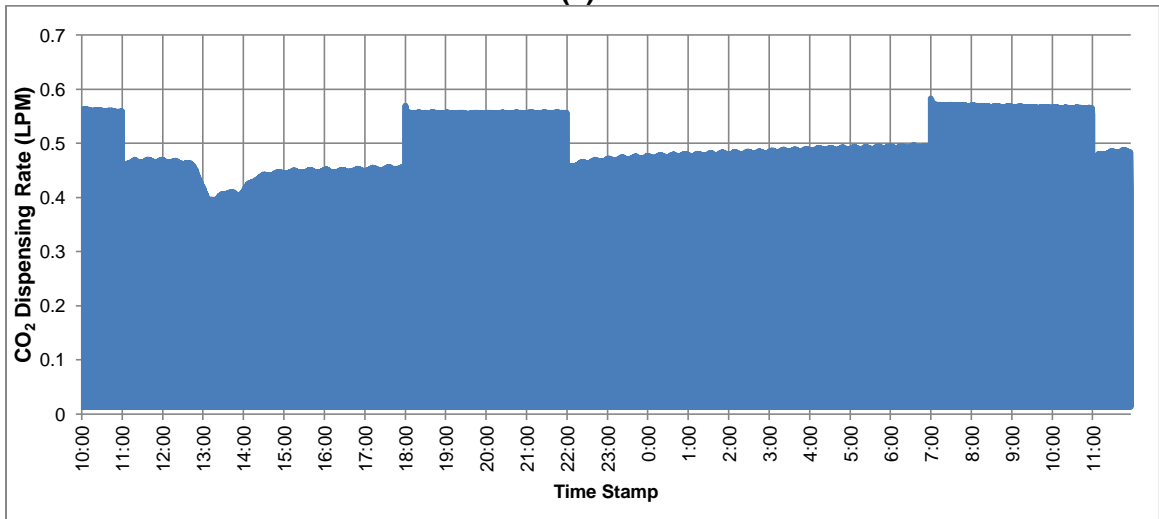
Typically, prior to the beginning of a test, the voltage is adjusted through trial and error to achieve the desired generation rates using the human simulator input program from a computer. CO₂ generation profile from Figure 49 was achieved in this way, by providing the resulting voltage for each hour of the day in occupant simulator control system program.

Figure 53 shows the CO₂ dispensing rate in the L/min achieved by tweaking the voltage provided to the solenoid for each building. Over time, the CO₂ dispensing rate equilibrates and normalizes, and becomes more consistent.

Duty cycles are used to further fine-tune the rate of CO₂ dispensing into the room. For example, to achieve 0.3 L/min during peak activity, and 0.2 L/min during normal activity, 50% on and 50% off duty cycles are applied to the peak period when the dispensing rate is approximately 0.6 L/min. Similarly, 40% on and 60% off duty cycles are applied to periods when the dispensing rate is approximately 0.5 L/min.



(a)



(b)

Figure 53. CO₂ dispensing rate for the north building (a) and south building (b) based on 100% continuously on duty cycle, adjusted

6.5 Ventilation Scheme Algorithms

Different ventilation strategies identified in test cases TC5 to TC8, are implemented in the field experiment to evaluate the effectiveness of each on managing indoor moisture that can affect indoor air quality. The algorithms for the ventilation strategies defined in the HVAC control systems for each test case are outlined.

6.5.1 Constant Ventilation

Constant ventilation is the simplest ventilation strategy. Fresh air is supplied to the test room at a constant rate. A rule of thumb is to supply fresh air to a residential space at a rate of 15 CFM (7.5 L/s) per person to dilute odours and bioeffluents to a level to satisfy 80% of occupants (ASHRAE, 2013).

Based on a simple a steady-state, single-zone mass balance of CO₂ called Equilibrium Analysis, the flow rate of the outdoor air supplied to a building can be estimated (Equation 7).

Equation 7. Equilibrium Analysis (ASTM D6245, 2012)

$$Q_o = \frac{G}{C_s - C_o}$$

Q_o = Outdoor flow rate into zone (L/s),

G = Total CO₂ generation of occupants (L/s) of all occupants

C_s = CO₂ concentration in the space (%),

C_o = CO₂ concentration of the outdoor air (%),
typically 300 – 400 ppm

For example, given the indoor CO₂ concentration of a zone is measured to be 0.10% (1000ppm) and the outdoors 0.035% (350ppm), at a metabolic activity rate of 1.0 met (CO₂ production rate of 0.0043 L/s (0.26 L/min)) per person, the outdoor flow rate required is

$$Q_o = (0.0043 \text{ L/s}) / (0.0010 - 0.00035)$$

$$= 6.6 \text{ L/s (14 CFM) per person}$$

For acceptable indoor air quality, ASHRAE 62.1 (2013) recommends maximum CO₂ levels of 1000 to 1200 ppm. This threshold is derived from Equilibrium Analysis as is shown in the above example, but for a slightly higher metabolic rate of 1.2 met units. This is representative of providing approximately 7.5 L/s (15 CFM) of fresh air from the outdoors per person in a space to

achieve at least 80% of occupants' satisfaction, which agrees with the findings of Berg-Munch, et al. (1986) among others.

For 'Suite A' from the 'Reference Building' this equates to 60 CFM of continuous fresh air supply. The required ventilation rate is proportionally reduced by volume on the basis that the test buildings are 25% of the volume of 'Suite A'. As a result, 15 CFM represents the ASHRAE recommended rate for constant ventilation in the test buildings. This ventilation strategy is used in TC1, TC2, TC4, and TC5 (Figure 54).

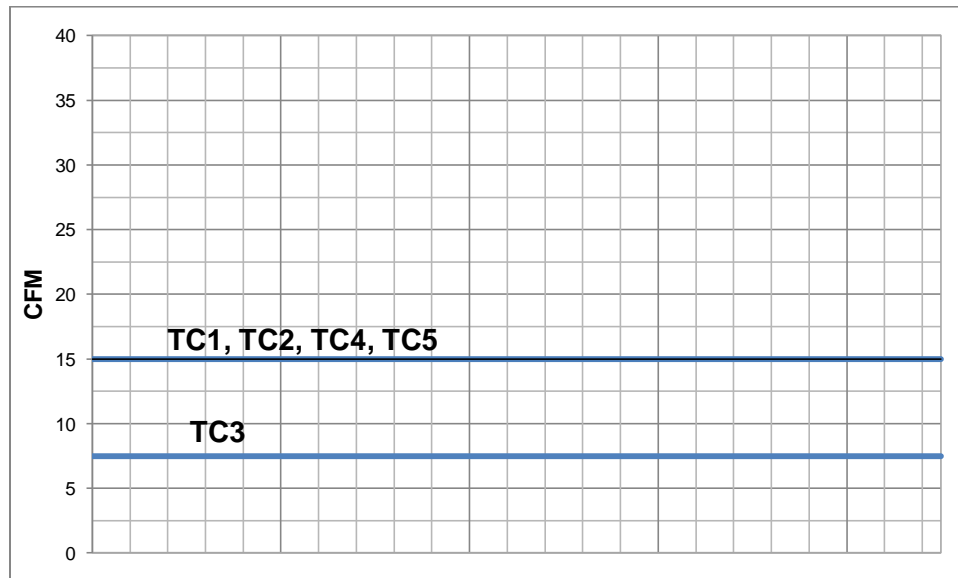


Figure 54. Representation of ventilation algorithm for constant ventilation, test cases T1 to TC5

For TC3, the “under-ventilated” ventilation rate is run at 7.5 CFM, or 50% of the required ventilation rate.

6.5.2 Time-controlled Ventilation

Due to variation in occupants' activities and moisture loading, the ASHRAE recommended rate of ventilation may not be required for 24 hours of the day, especially when a space is not occupied. For energy saving reasons, time-controlled ventilation is a suitable ventilation strategy when the activities of occupants are predictable (note that the same ventilation strategy was implemented in the 'Reference Building' to address excess indoor humidity issues following the

rehabilitation of the building enclosure).The HVAC system is set to turn on when occupants are most active and producing the most moisture or odour levels (e.g. from showering, cooking, etc.).

For TC6, time-controlled ventilation is run according to the algorithm represented in Figure 55. The ventilation system runs at maximum rate at moisture peak hours, offset by one hour (i.e. 8am-12pm and 7pm-11pm). The minimum ventilation is set to 7.5 CFM, while the maximum ventilation rate is set to 30 CFM. The daily weighted average ventilation rate under this scheme is 15 CFM, (8 hours at 30 CFM and 15 hours at 7.5 CFM), the same rate as the ASHRAE recommended rate.

The maximum ventilation rate times are offset from the moisture peak times by one hour due to the gradual rise in humidity levels within the first hour of peak moisture loading. Within the first hour of peak moisture loading, the rise in humidity is not instantaneous, and may not necessarily reach high threshold levels. Therefore, energy expended on maximum ventilation rate within the first hour of peak loading may be “wasted.” Similarly, when peak moisture loading ends, the drop in humidity levels is gradual and indoor moisture may not be displaced rapidly enough to drop to acceptable levels. Therefore, the maximum ventilation rate is maintained for an hour following the end of peak loading.

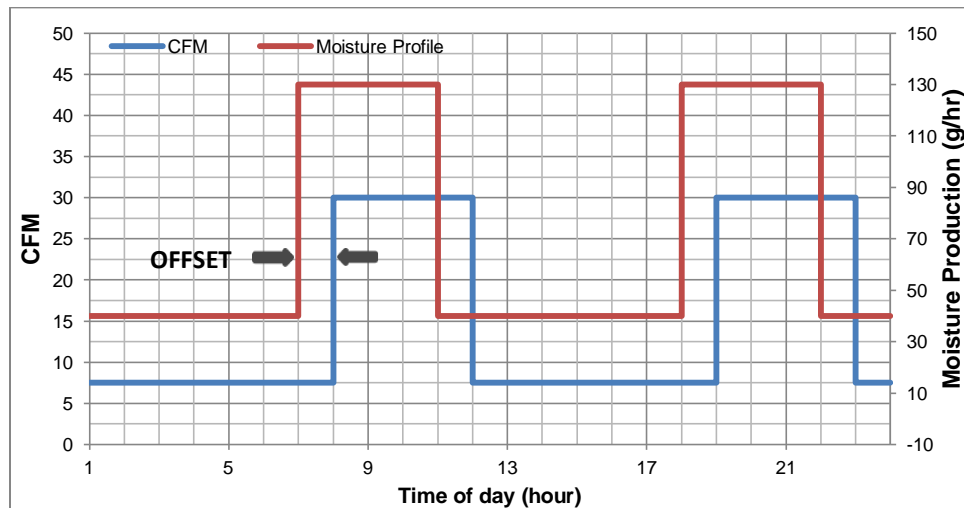


Figure 55. Representation of ventilation algorithm for time-controlled ventilation

6.5.3 RH-controlled Ventilation

When the behaviour of occupants is not predictable, “smart” ventilation systems may be required to aid in keeping indoor air conditions at acceptable levels. RH-controlled ventilation adjusts the required ventilation rate depending on indoor relative humidity levels. Humidistats are essentially a means of ventilation based on relative humidity levels.

Figure 56 shows a representation of the RH-controlled ventilation algorithm used in TC7. The minimum and maximum ventilation rates were set to 7.5 and 30 CFM respectively. The system runs at minimum ventilation rate at relative humidity levels below 50%, and maximum ventilation rate at levels above 60%. Between 50% and 60%, the ventilation rate varies linearly with increase or decrease in relative humidity.

As discussed in Section 2.2.3, ideal upper and lower indoor RH levels are generally between 50 to 60%. Generally at this level, cold surfaces in a space are maintained below levels that may result in germination and growth of mould, and condensation may be avoided depending on operating and outdoor temperatures. The RH-controlled ventilation scheme is designed to maintain the indoor humidity within this range, by ramping up ventilation rate when RH levels begin to increase, and reduce ventilation rate when RH levels decrease.

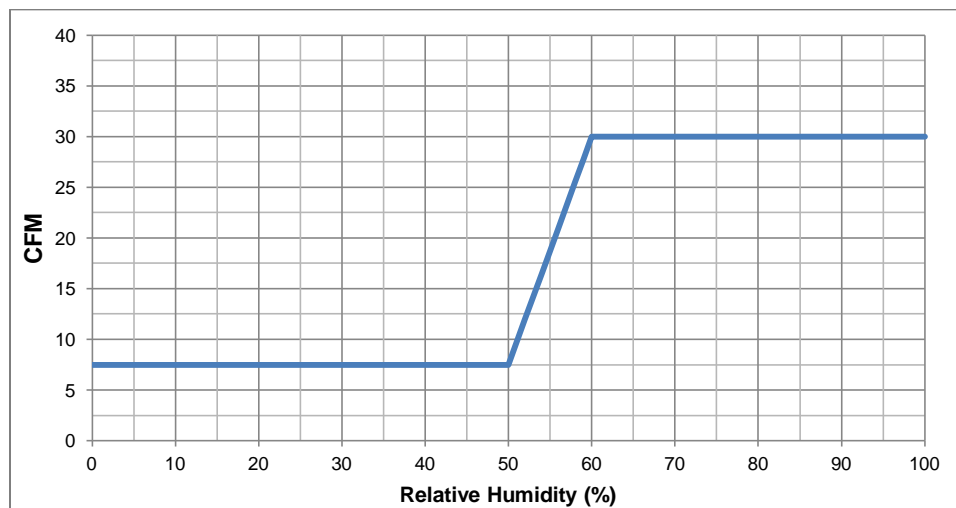


Figure 56. Representation of ventilation algorithm for RH-controlled ventilation

6.5.4 CO₂-controlled Ventilation

Ventilation based on CO₂ levels can provide fresh air supply based a direct correlation on the number of occupants and/ or their level of metabolic activity. Figure 57 shows a representation of the CO₂-controlled ventilation algorithm used in TC8. Similar to RH-controlled ventilation, this ventilation scheme has a lower threshold and an upper threshold, between which the ventilation rate varies linearly based on CO₂ levels. The system operates at a minimum ventilation rate of 7.5 CFM below the lower threshold, and a maximum rate of 30 CFM runs above the upper threshold. The high and low CO₂ concentrations are chosen as 1000 and 800 ppm respectively.

The upper CO₂ threshold is based on ASHRAE 62.1 (2013) recommended maximum CO₂ levels of 1000 to 1200 ppm. The lower limit is arbitrary, and is based on realistic indoor CO₂ levels that can be achieved with outdoor CO₂ levels of 350 to 400 ppm, and the simulated occupant densities in the room.

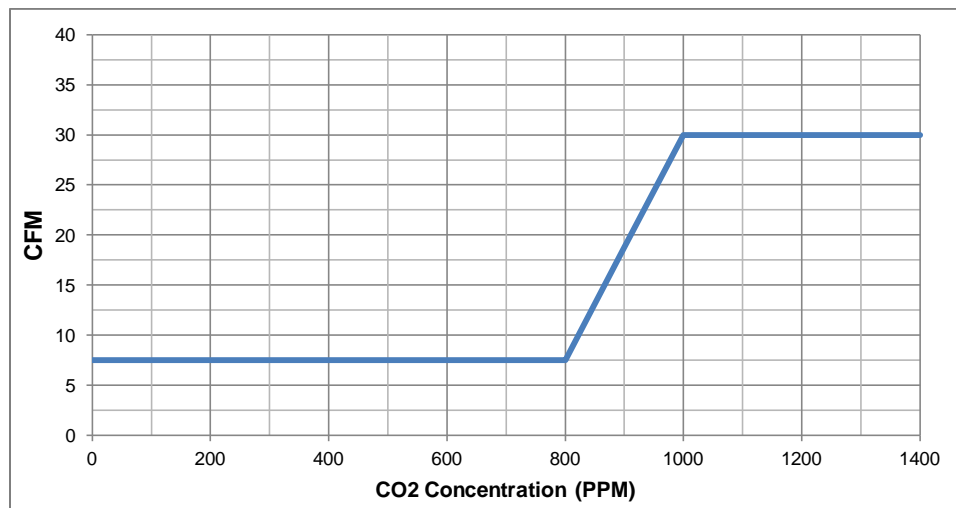


Figure 57. Representation of ventilation algorithm for CO₂-controlled ventilation

7 EXPERIMENTAL RESULTS AND ANALYSIS

In the field experiments the management of indoor moisture is investigated by two means: passive and active measures. Passive measures are means of utilizing the benefit of moisture buffering ability of materials to regulate indoor moisture. Active measures are use of mechanical systems, namely ventilation to exhaust excess moisture from the building. The effectiveness of the passive measures in TC1 to TC4 and active measures in TC5 to TC8 are discussed in the proceeding sections. The implications of active measures on ventilation heat loss and indoor air quality are also discussed. Plots of indoor temperature and relative humidity for the control building are denoted by “north” or “n”, and the test building are denoted by “south” or “s”. A full-day indoor temperature and humidity data after the buildings reach quasi-equilibrium condition are presented and analyzed for each test case.

7.1 Data Processing

All measurements of indoor, outdoor, and AHU supply and exhaust air conditions (relative humidity and temperature), as well as indoor CO₂ were measured and recorded at 5-minute intervals.

The measurement data from the five RHT sensors indicate that the temperature and relative humidity in the test rooms were consistent (Figure 58 & Figure 59). For each building, the percentage deviation was determined based on the maximum and minimum measurements from each of the calibrated sensors taken at each time interval for the duration of test case TC1. On average, the deviation between the maximum and minimum relative humidity measurements was 3% for the duration of monitoring. The reported accuracy of the sensors at 20°C are as follows:

±3% RH (0 – 90% relative humidity)

±5% RH (90 – 98% relative humidity)

The deviation between the five sensors is within the reported accuracy of the sensor. Therefore, results shown based on the average readings of all five sensors for each 5-minute reading are reliable, and used for presenting the results in this section.

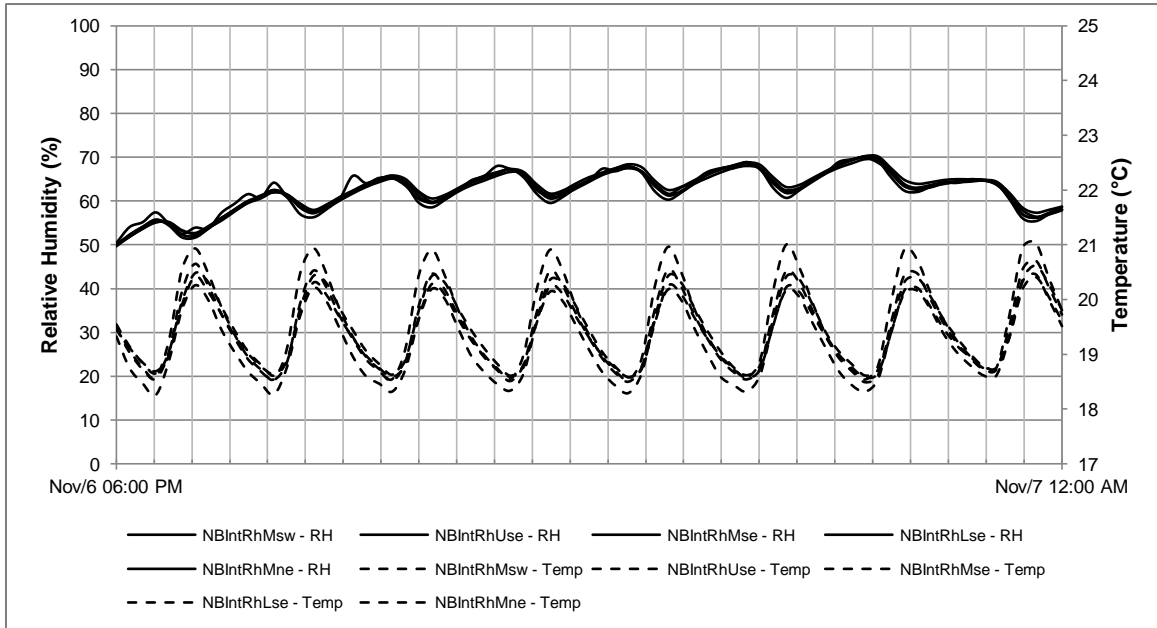


Figure 58. RHT sensor readings from the control building (north) show relative humidity and temperature readings in each test room deviate within the % error of the sensor

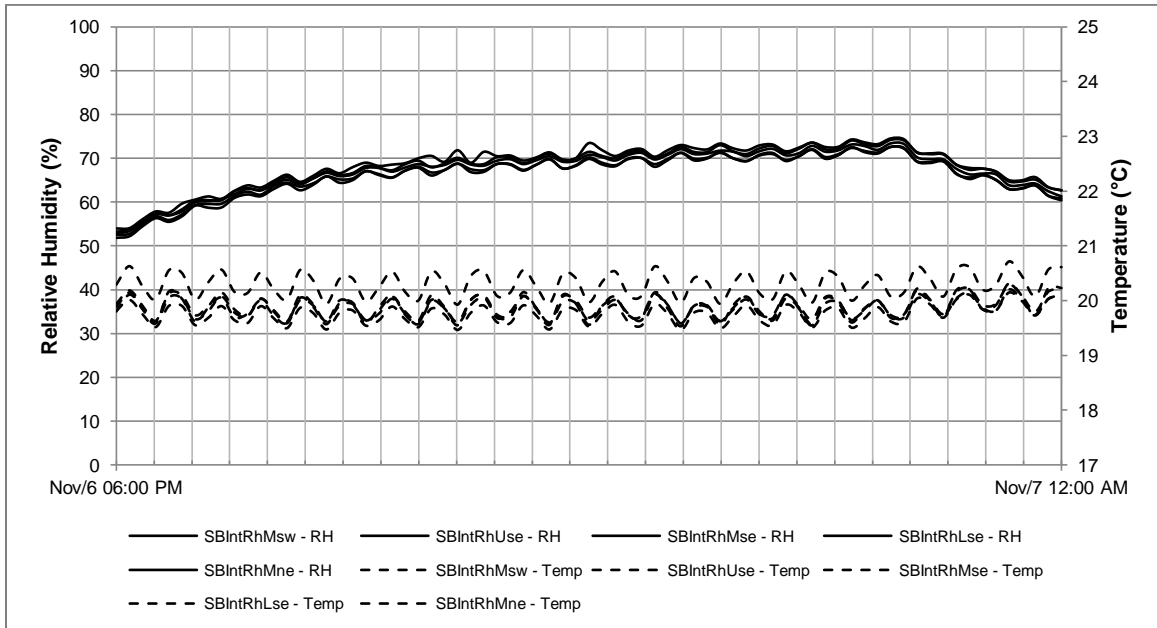


Figure 59. RHT sensor readings from the test building (south) show relative humidity and temperature readings in each test room deviate within the % error of the sensor

For test cases TC1 to TC4, an oscillating noise pattern is seen in the indoor temperature, which is consistently more attenuated in the test building (Figure 60). The noise pattern is also seen in the relative humidity readings, due to the temperature dependency of relative humidity measurements taken by the sensors. This is attributed to the way the heaters operate to reach the thermostat set-point temperature. The heater measures the room temperature, and overshoots in raising the room temperature when it falls below the set-point. Then it ceases heating and drops below the set-point. In the control building, the heater repeats this cycle approximately every 45 minutes with temperatures ranging between 18.7 to 20.4°C for the duration shown below. In the test building, the cycles are shorter and the overshooting is less drastic, resulting in indoor temperature swings between 19.6 to 19.8°C. The heaters for TC1 to TC4 are different models in each test building due to availability around the time of testing. For TC5 to TC8 the same heater model is incorporated in both buildings.

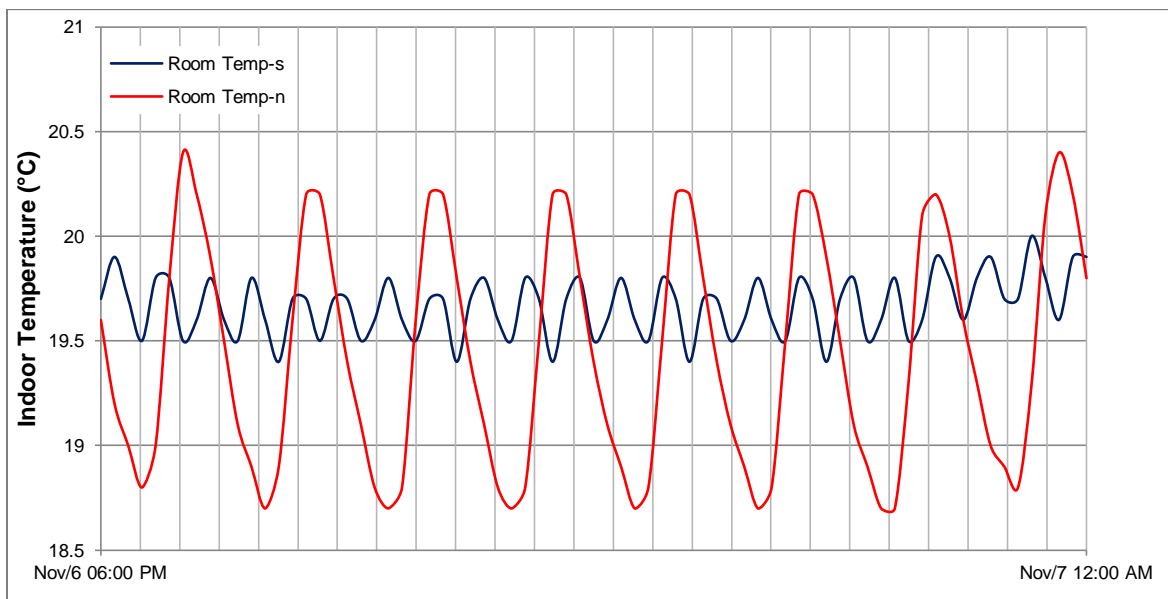


Figure 60. Oscillation pattern seen in interior conditions of WBPRL buildings during field testing TC1 to TC4

The noise observed in the data does not deter from drawing conclusions on the diurnal indoor temperature and relative humidity patterns in the buildings. To account for the patterns seen in

indoor temperature in Figure 60, temperature-corrected relative humidity is back-calculated for the control building (Equation 8).

Equation 8. Determination of relative humidity in control building (north) for test building (south) equivalent temperature

$$RH_{north} = \frac{W_{north} \cdot P_a}{0.6219 \cdot P_{sat_south}}$$

$$\text{where } P_{sat_south} = 611 \times 10^{\frac{7.5T_{south}}{237.3 + T_{south}}}$$

W_{north} = Absolute humidity [g_{moisture} / kg_{dry air}], in the north building

P_a = Atmospheric pressure [Pa], taken as 101325 Pa

P_{sat_south} = Saturation vapour pressure [Pa], calculated based on interior temperature in the south building

RH_{north} = Relative humidity [%], calculated based on interior temperature in the south building

The absolute humidity in the control building is determined, and converted to equivalent relative humidity for the temperatures measured in the test building. Without this step, there would be too much noise in the plots as demonstrated in Figure 61.

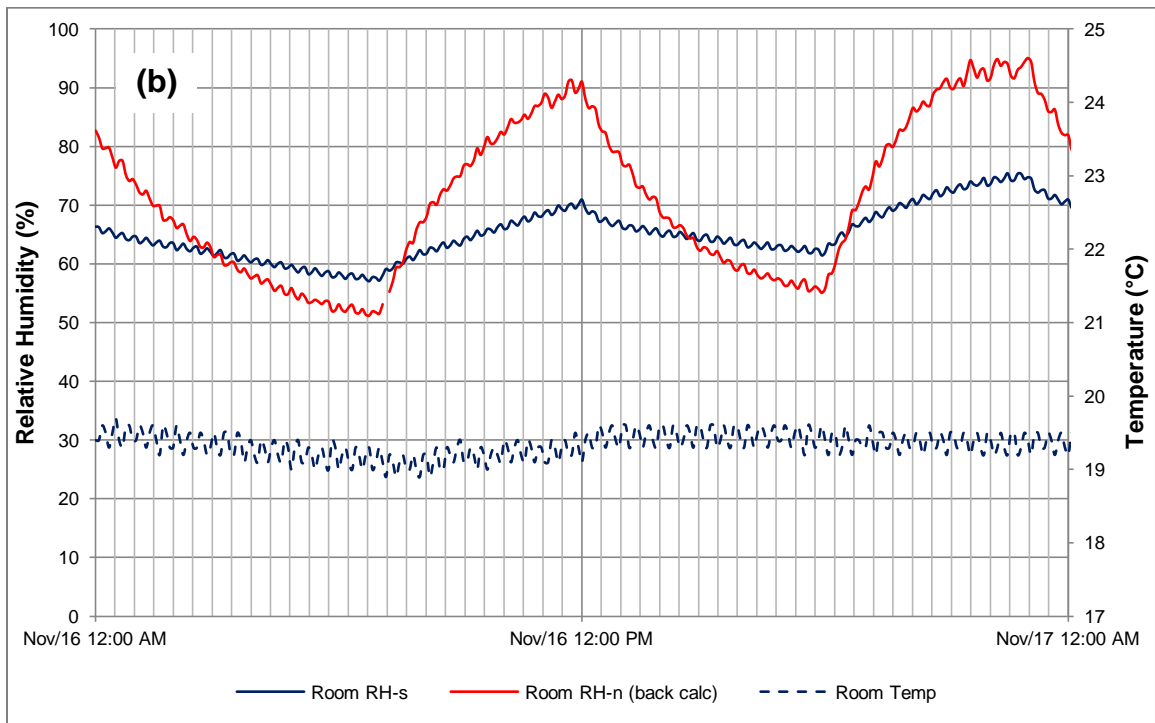
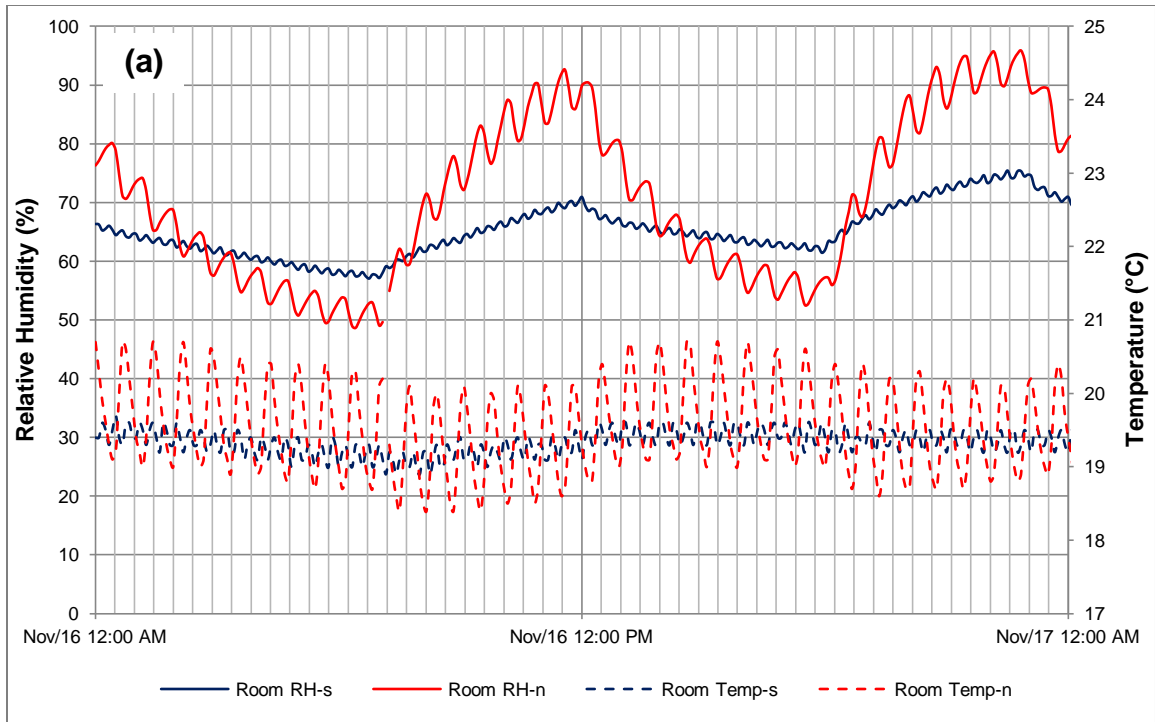


Figure 61. (a) 5-minute indoor conditions, (b) after temperature correction for control building

As a result, TC1 to TC4 data are presented with relative humidity of the control building back-calculated based on the test building interior temperatures.

7.2 Passive Moisture Management Methods

The parameters for test cases TC1, TC2, TC3, and TC4 are repeated in Table 12 below. These test cases represent passive moisture management methods, that is, test cases which moisture buffering effect of gypsum board in the test building can be directly compared to the non-hygroscopic polyethylene in the control building in managing moisture for an under-ventilated space (TC3) or a high occupancy space with extra moisture loading (TC4).

Table 12. List of Test Parameters for Test Cases 1 – 4

Test Case (TC)	Dates		NORTH (CONTROL) BUILDING	SOUTH (TEST) BUILDING
1	Nov. 4-7/13	Interior Finish	Polyethylene	Polyethylene
		Occupant Density	Normal	Normal
		Ventilation Rate	ASHRAE Recommended	ASHRAE Recommended
		Ventilation Scheme	Constant	Constant
2	Nov. 7-12/13	Material	Polyethylene	GWB
		Occupant Density	Normal	Normal
		Ventilation Rate	ASHRAE Recommended	ASHRAE Recommended
		Ventilation Scheme	Constant	Constant
3	Nov. 12-19/13	Material	Polyethylene	GWB
		Occupant Density	Normal	Normal
		Ventilation Rate	Under-ventilated	Under-ventilated
		Ventilation Scheme	Constant	Constant
4	Nov. 20-27	Material	Polyethylene	GWB
		Occupant Density	Dense	Dense
		Ventilation Rate	ASHRAE Recommended	ASHRAE Recommended
		Ventilation Scheme	Constant	Constant

7.2.1 Test Case 1 (Benchmark Test)

Test case TC1 is intended to confirm the consistency of the performance of the two field experiment buildings under identical conditions.

Figure 62 shows that the temperature and relative humidity profiles in the test and control buildings, with the interior moisture loading cycle superimposed on the figure. The results of this benchmark test show a very close agreement between the two buildings' responses as expected and desired. The decreasing sections of the relative humidity curves coincide with low

background moisture production and as ventilation removes moisture, while the upward curving sections coincide with peak moisture production (humidity levels gradually increase as excess moisture is put in the air). Thus the upward and downward cycles follow the moisture production cycles of Figure 47(b) for “typical” moisture loading. In TC1, relative humidity cycles of both buildings undergo similar amplitude variations. Two cycles are shown following conditioning of the test buildings. Over time, the indoor air, interior finishing materials, and ventilation air equilibrate. This is evident from the converging of the relative humidity levels of both buildings under the same conditions.

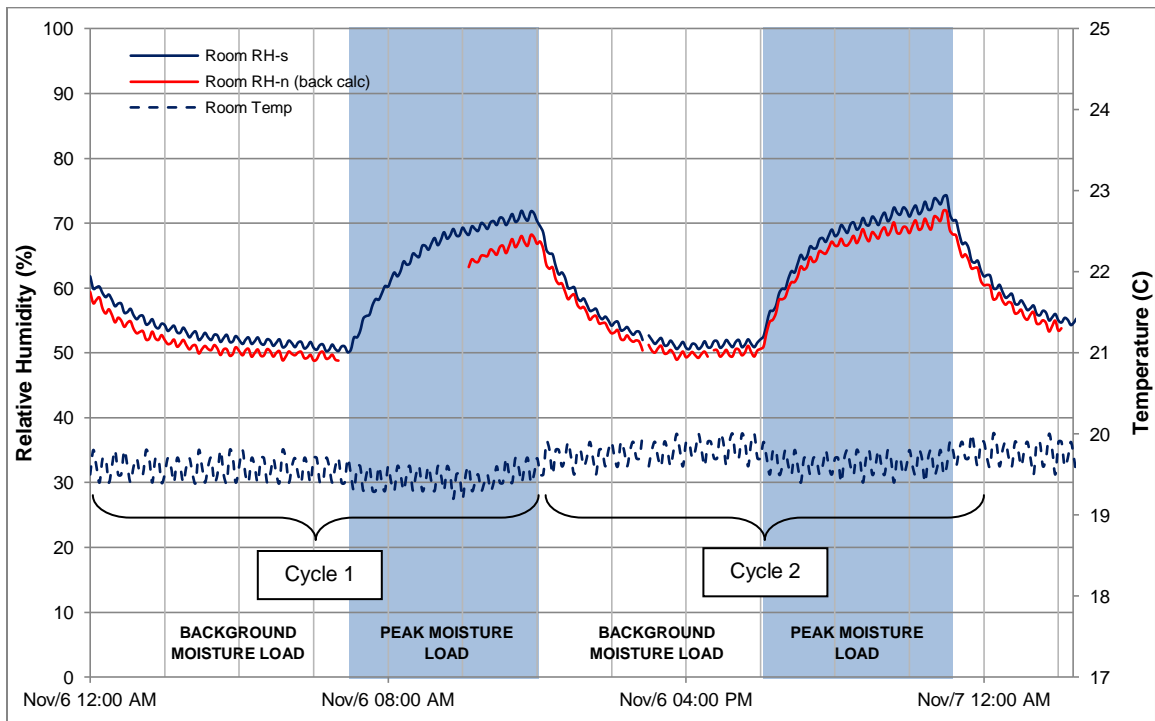


Figure 62. The indoor temperature and relative humidity of the control building (red) and test building (blue) under TC1 – benchmarking case. Relative humidity peaks coincide with moisture loading peaks.

Table 13 shows the maximum and minimum RH values for each of the moisture loading cycles shown, as well as the RH amplitude (calculated as the difference between maximum RH and minimum RH), and mean RH (calculated as the mean of the maximum and minimum RH). The “% Difference” column denotes the % deviation for each RH value – minimum, maximum, and amplitude, and mean – between the two buildings, calculated as:

Equation 9. Determination of “% Difference” between RH values

$$\% \text{ Difference} = \frac{|RH_{north} - RH_{south}|}{\text{minimum}\{RH_{north}, RH_{south}\}}$$

Figure 63 shows each corresponding value obtained from Figure 62 during Cycle 2. Similar tables are presented for all test cases.

Table 13. Comparison of indoor relative humidity (RH) between the control & test building for TC1

	Cycle 1			Cycle 2		
	Control	Test	% Difference	Control	Test	% Difference
Min RH	49	50	2%	50	52	4%
Max RH	67	71	6%	71	74	4%
RH Amp	18	21	17%	21	22	5%
Mean RH	58	60.5	4%	60.5	63	4%

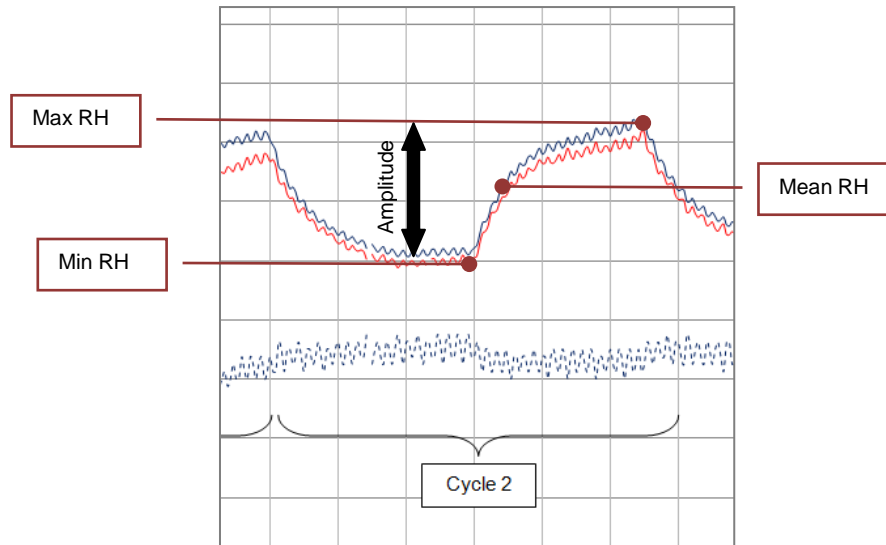


Figure 63. Maximum RH, minimum RH, RH amplitude and mean RH for Cycle 2

The RH amplitude dictates the sensitivity of indoor relative humidity to changing conditions. In TC1, the RH amplitudes of the test building is comparable to the control building, within 17% during the first cycle, and 5% during the second cycle as indoor conditions reach quasi steady-state. This means that the relative humidity levels vary at the same order of magnitude with changing moisture production rates.

Mean RH values are presented to compare the overall humidity level in each building. In TC1, the mean RH values are comparable between the test and control buildings, the values being within 4%.

The results of the bench-marking test confirm that the two buildings perform similarly under the same operation conditions.

7.2.2 Test Case 2

Test case TC2 is intended to confirm the moisture buffering potential of the test building in the field experimental setting.

For TC2 (Figure 64), the test building finish material is changed to hygroscopic unfinished gypsum board, therefore giving the test building moisture buffering potential, while the control building remains non-hygroscopic. In this case, the amplitude of the control building relative humidity cycles are greater than those in the test building; that is, the RH peaks are higher and the RH minimums are lower in the control building. This can be attributed to the excess moisture being buffered by the test building's gypsum board finish.

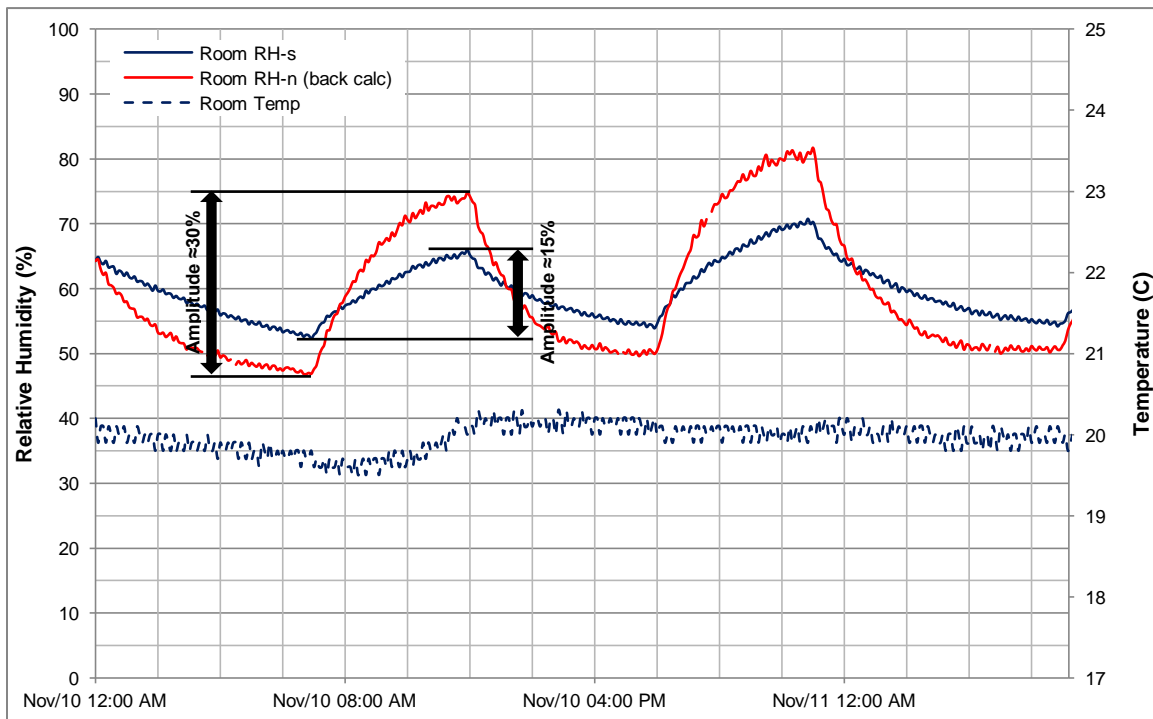


Figure 64. The indoor temperature and relative humidity of the control building (red) and test building (blue) under TC2 – normal occupancy and ventilation

Table 14. Comparison of indoor relative humidity (RH) between the control & test building for TC2

	Cycle 1			Cycle 2		
	Control	Test	% Difference	Control	Test	% Difference
Min RH	46	53	15%	50	54	8%
Max RH	75	67	12%	81	70	16%
RH Amp	29	14	107%	31	16	94%
Mean RH	60.5	60	1%	65.5	62	6%

As expected, the regulating effect of moisture buffering results in excess moisture being absorbed by gypsum board when RH levels rise and the desorbed back into the air RH level fall. In TC2, the RH level variations (amplitudes) are double that of those in the test building. The overall RH levels (mean) are comparable, at approximately 60-65%. This test case confirms the expected field experimental moisture buffering performance of the test building. The results generally agree with findings from literature (see Section 2.3).

7.2.3 Test Case 3

Test case TC3 demonstrates the effect of under-ventilating a space under typical moisture loading conditions, for both hygroscopic and non-hygroscopic buildings.

Figure 65 shows that the moisture buffering effect still prevails on the indoor humidity levels of the test building.

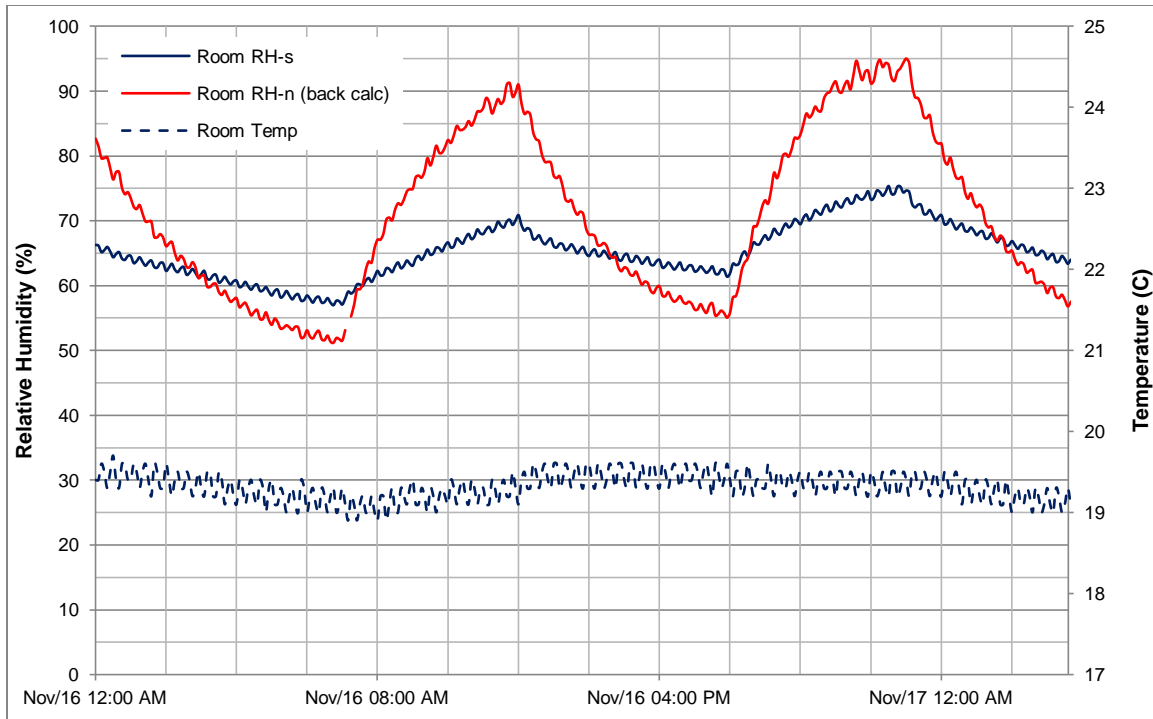


Figure 65. The indoor temperature and relative humidity of the control building (red) and test building (blue) under TC3 – normal occupancy, under-ventilation

Table 15. Comparison of indoor relative humidity (RH) between the control & test building for TC3

	Cycle 1			Cycle 2		
	Control	Test	% Difference	Control	Test	% Difference
Min RH	51	58	14%	55	62	13%
Max RH	91	71	28%	95	75	27%
RH Amp	40	13	208%	40	13	208%
Mean RH	71	64.5	10%	75	68.5	9%

The RH amplitudes in the test buildings are 13% for both cycles, comparable to those observed in TC2, at 14 and 16%. The overall humidity levels are slightly higher, at 64.5 and 68.5% compared to 60 and 62% for TC2.

Similar to TC2, the RH amplitudes in the control building are higher than those in the test building. However, the RH amplitudes in TC3 are more pronounced, 40% compared to 29 and 31% in TC2. The overall RH levels have increased by more than 10%, at 71 and 75% compared to 60.5 and 62% for TC2.

These results indicate that the indoor humidity response of a non-hygroscopic building is more sensitive to ventilation rate, than a hygroscopic building, once again confirming the regulating

effect of moisture buffering on indoor humidity levels. In TC3, the difference in amplitudes between the two buildings are 208% for both cycles, compared to 107% and 94% differences in the cycles of TC2.

Another point to note is the rise in maximum RH levels in both buildings when the buildings are exposed to the same moisture loading, but under-ventilated, with only 50% of the ASHRAE recommended rate provided for air change. The maximum RH exceeds 90% for both cycles in the control building, and 70% in the test building. This has implications on dew point temperatures in the buildings, and increased likelihood of condensation and microbial growth. More information regarding the dew point temperatures and the buildings' performance is discussed in Section 7.2.5.2.

7.2.4 Test Case 4

Test case TC4 demonstrates the effect of providing adequate ventilation as per ASHRAE recommended rates to a space, under high moisture loading conditions, for both hygroscopic and non-hygroscopic buildings.

Figure 66 shows the results of providing continuous ventilation at the ASHRAE recommended rate, under high moisture production profile from the field experiment. Unfortunately, this test coincided with a cold snap (a sudden drop in outdoor temperatures), therefore the heaters in both buildings did not have the capacity to maintain the building interior temperatures consistent throughout. The interior temperatures fluctuated at approximately 18°C, slightly less than the intended 20°C. As a result, the RH levels cannot be directly compared to those in the previous three test cases that have different operating temperatures, due to the temperature dependence of RH. Nonetheless it is possible to compare the performance of the test building conditions to the control building at a given point in time for this test case.

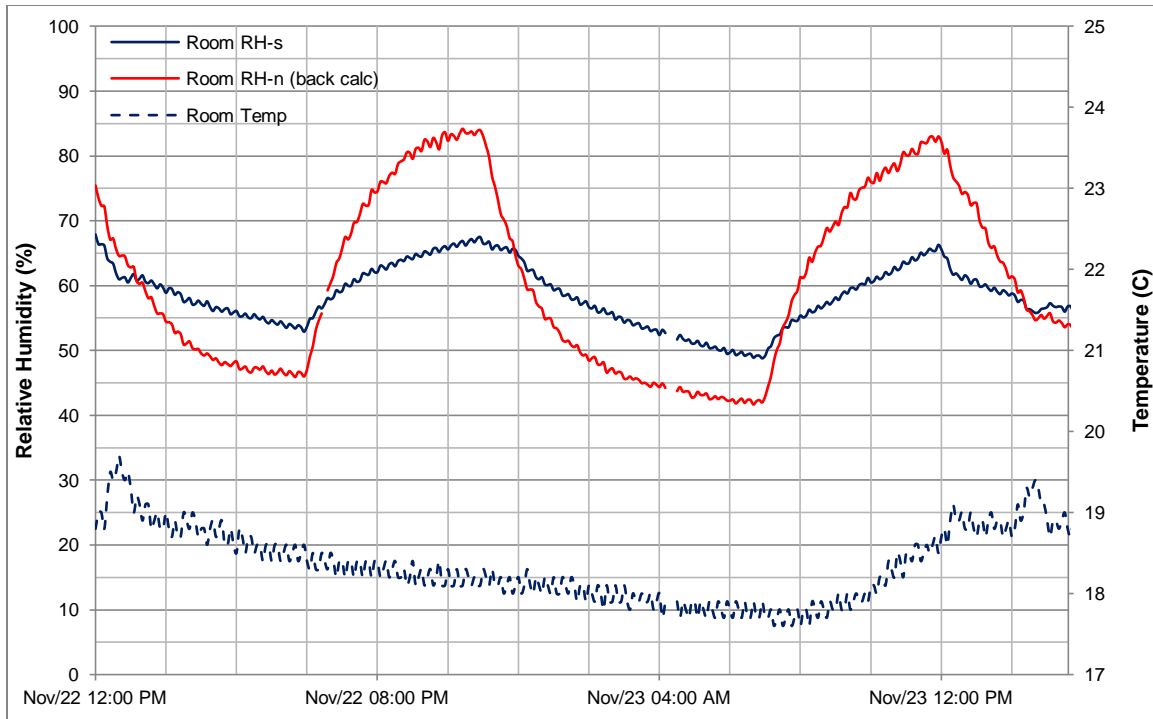


Figure 66. The indoor temperature and relative humidity of the control building (red) and test building (blue) under TC4 – high occupancy

Table 16. Comparison of indoor relative humidity (RH) between the control & test building for TC4

	Cycle 1			Cycle 2		
	Control	Test	% Difference	Control	Test	% Difference
Min RH	46	53	15%	42	49	17%
Max RH	84	67	25%	83	66	26%
RH Amp	38	14	171%	41	17	141%
Mean RH	65	60	8%	62.5	57.5	9%

The effect of high moisture loading on RH variations is similar to the under-ventilation case in TC3. The RH swings are more drastic, with amplitudes 171 and 141% greater in the control building in comparison to the test building for cycles 1 and 2 respectively. The mean RH levels are nearly 10% higher in the control building.

The results from this test case indicate that the control building’s interior environment is more sensitive to changes in moisture loading than the test building.

7.2.5 Analysis

The phenomenon observed in the first four test cases can be attributed to the moisture buffering properties of unfinished gypsum board. When indoor humidity rises, the moisture present in the

air is absorbed by the surface, and when humidity falls, it is desorbed back into the air, creating the regulating affect of relative humidity fluctuations (Pedram & Tariku, 2015). The effect of moisture buffering virtually is non-existent in the control building, given moisture buffering is defined by vapour permeability, sorption capacity, and surface mass transfer of materials (see Section 2.3.2.1), which are all minuscule in non-hygroscopic materials such as polyethylene.

7.2.5.1 Regulating Effect of Moisture Buffering

Figure 67 & Figure 68 below provide a visual summary of RH amplitudes and the respective % Difference in RH amplitude between the two buildings from Table 13 to Table 16.

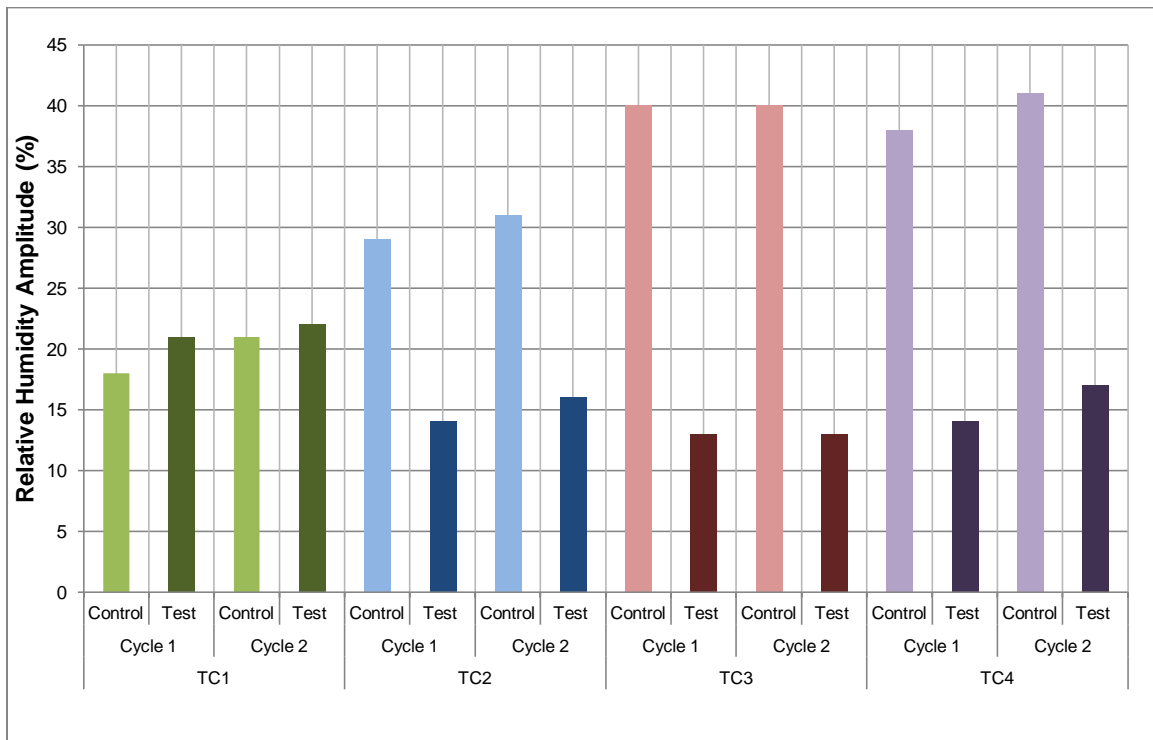


Figure 67. RH amplitude (Max RH – Min RH) for Cycle 1 & 2 from test cases TC1, TC2, TC3, and TC4

RH amplitude dictates the magnitude of relative humidity variation swings throughout the day under the moisture production loading cycles. With the exception of the bench marking test (TC1), RH amplitudes are consistently higher in the control building in all other three test cases. This is expected, as the majority of the moisture emitted in the test building is stored in gypsum board rather than in the air.

There is an inverse relationship between moisture buffering and RH amplitude, i.e. lower value of RH amplitudes are attributed to higher magnitude of the regulating effect of moisture buffering. According to Figure 67, the RH amplitudes in the test building are lowest during TC3, the under-ventilation case. Conversely, the RH amplitudes in the control building are highest when the space is under-ventilated, as rate of excess moisture being input into the space is higher than the rate of moisture being removed by ventilation. As a result, under-ventilation yields the highest % differential between the control and test building RH amplitudes, as seen in Figure 68 for TC3.

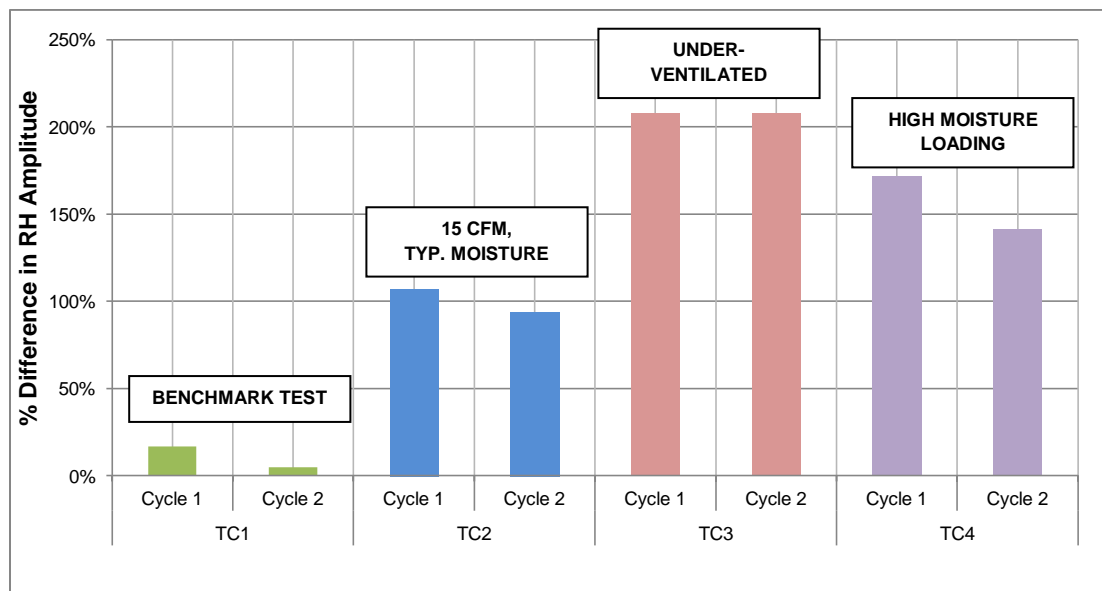


Figure 68. % Difference in RH amplitudes between the control and test building from test cases TC1, TC2, TC3, and TC4

The % differential between the control and test building RH amplitudes is negligible in the benchmark test, when both operate under the same conditions. Given that the % differential between the control and test building RH amplitudes is at approximately 100% when moisture buffering is present, the effect of under-ventilation yields 200% differential, while high moisture loading yields 150% differential.

It is possible that in TC3 lower ventilation rate has resulted in higher vapour pressure in the room, and increased the mass transfer at the surface of gypsum board, thereby increasing the moisture

buffering potential of the test building. Similarly, high moisture loading increases excess moisture in the space, which increases surface mass transfer and moisture buffering potential – through to a lesser degree than low ventilation rate.

This implies that moisture buffering is most effective under low space ventilation and air velocities. However, there is a caveat to this: while moisture buffering potential can be maximized with lower ventilation rate and zonal air velocities, other negative consequences such as increased condensation potential on window glazing surfaces can be exacerbated. In fact, the Homeowner Protection Office of British Columbia recommends increasing air movement and space ventilation to avoid condensation (HPO, 2006).

Figure 69 & Figure 70 below provide a visual summary of RH minimum, maximum, mean and their respective % difference from Table 13 to Table 16.

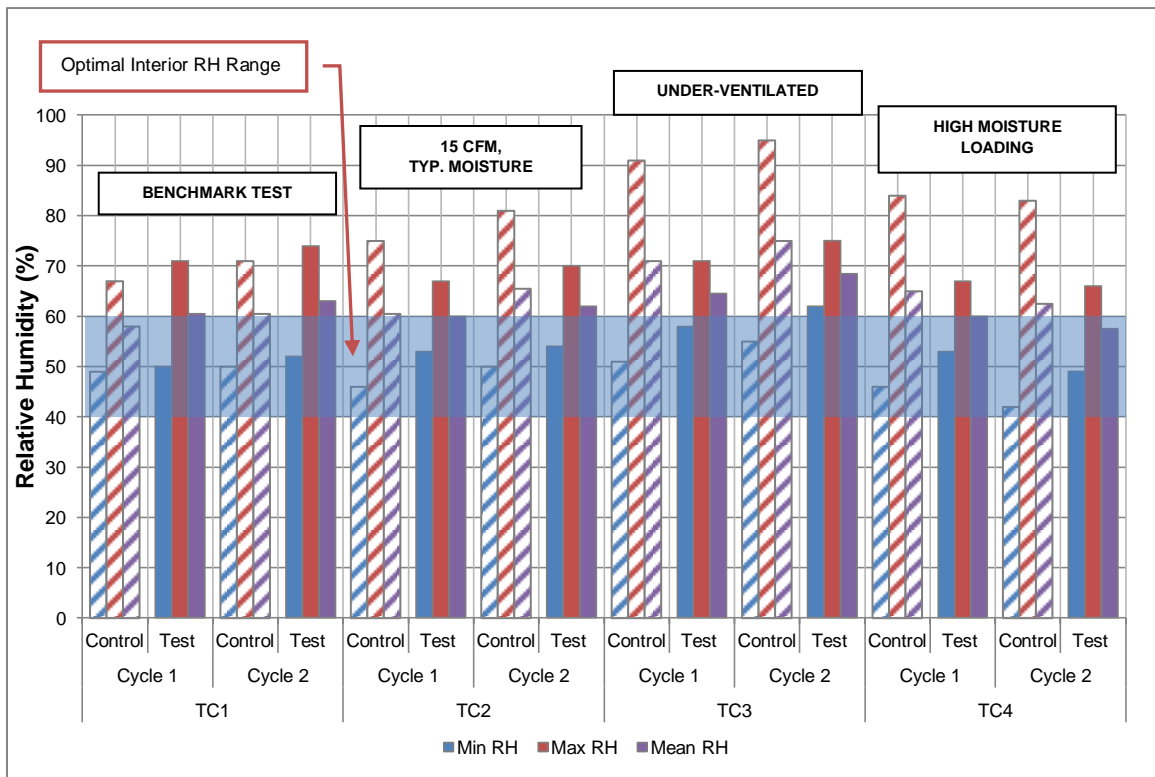


Figure 69. Minimum, maximum, and mean RH for Cycle 1 & 2 from test cases TC1, TC2, TC3, and TC4. The test building is shown in solid and the control building is shown in hatched. Optimal interior RH range is highlighted in blue.

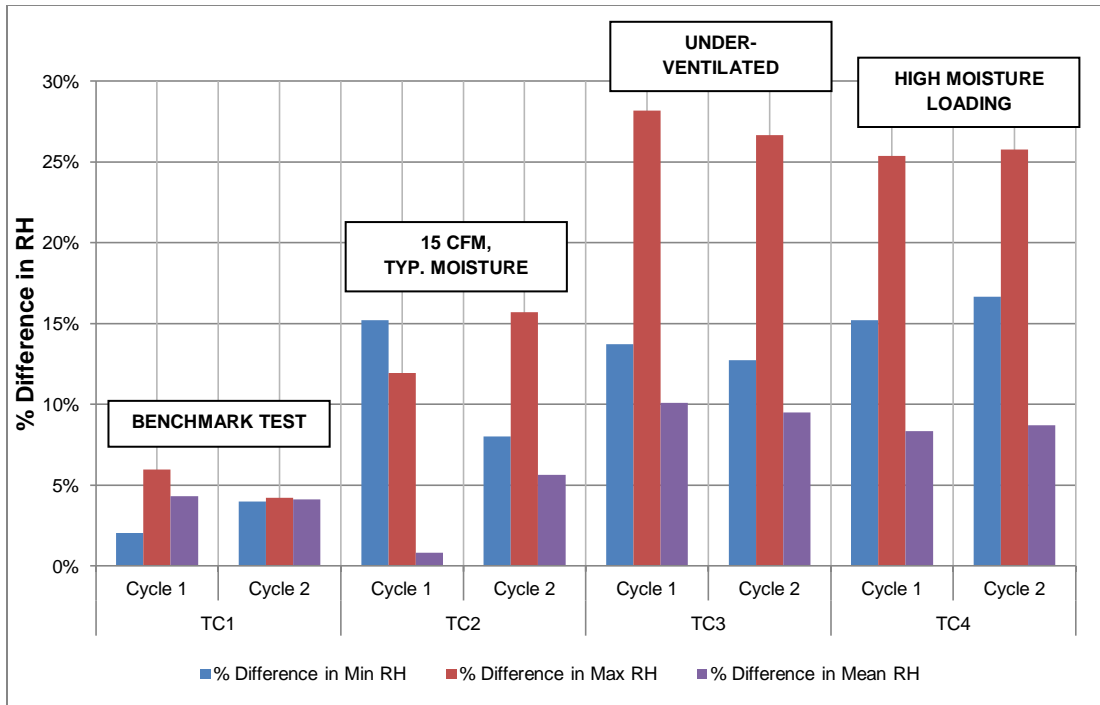


Figure 70. Difference in minimum, maximum, and mean RH between the control and test building from test cases TC1, TC2, TC3, and TC4

Ideally, interior operating conditions must allow indoor humidity levels to fluctuate between 40 to 60% to avoid condensation on cold surfaces, microbial growth, and thermal comfort issues. In general, the overall relative humidity levels (mean RH) in the test building are better maintained in this range than the control building. Once again, this can be attributed to the regulating effect of moisture buffering potential of hygroscopic, unfinished gypsum board. The only test case during which mean RH exceeds this range in the test building is TC3, when under-ventilated (Figure 69). On the other hand, the control building consistently exceeds this range for almost all cases.

Looking at % difference in RH levels between the test and control building compared across test cases TC2 to TC4, mean RH levels are within 5 to 10%, minimum RH levels are within 10 to 15%, and maximum RH levels are within 25% or above. Maximum RH levels are most variable between the test and control building, when all other operating conditions are otherwise similar. This has implications on dew point temperatures in each building.

7.2.5.2 Dew Point Temperatures

Higher relative humidity peaks in the control building under TC2 to TC4 correspond to higher dew point temperatures. High dew point temperatures result in higher likelihood of mould and microbial growth.

Figure 71 to Figure 74 show the dew point temperatures inside each test building under TC1 to TC4, that is, the temperature at which condensation would occur. In other words, condensation can form on any cold surface in either building (e.g. window glazing, sites of thermal bridging, etc.) with the temperature at or below the building's respective dew point temperature. When the dew point temperature approaches the interior temperature, it signals increasing/ high indoor humidity levels. When this occurs for a long period of time, germination and growth of microbial agents can occur.

Among all test cases, the indoor conditions in the control building under TC3 are most favourable for formation of condensation, as the peak dew point temperatures nearly reach the room temperature.

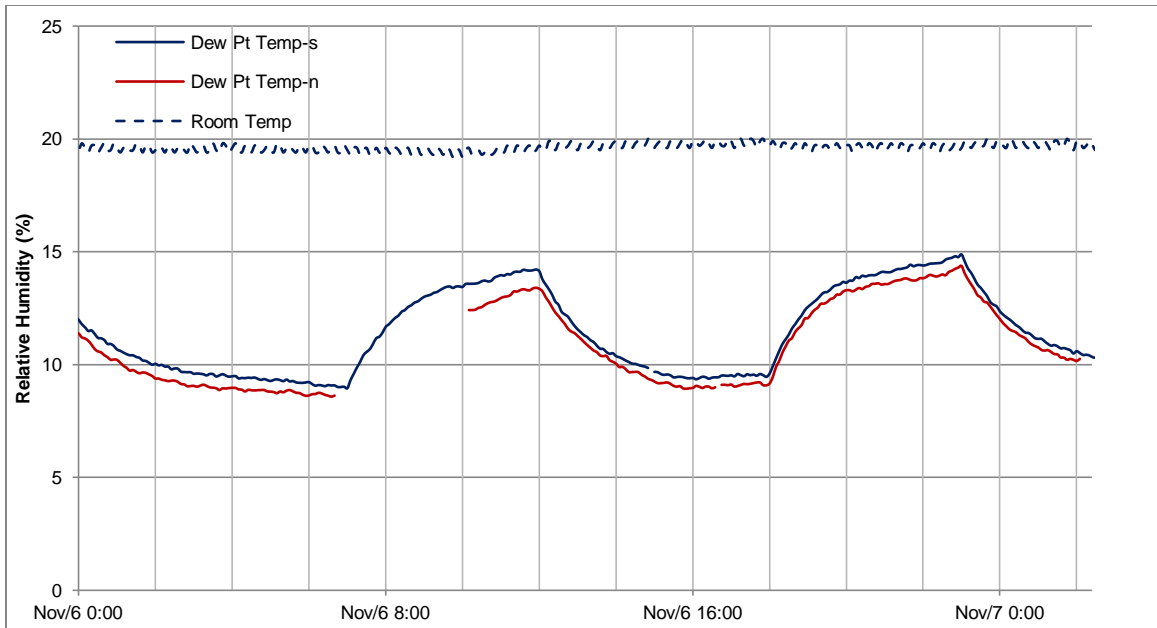


Figure 71. The indoor and dew point temperatures of the control building (red) and test building (blue) under TC1 – bench marking test

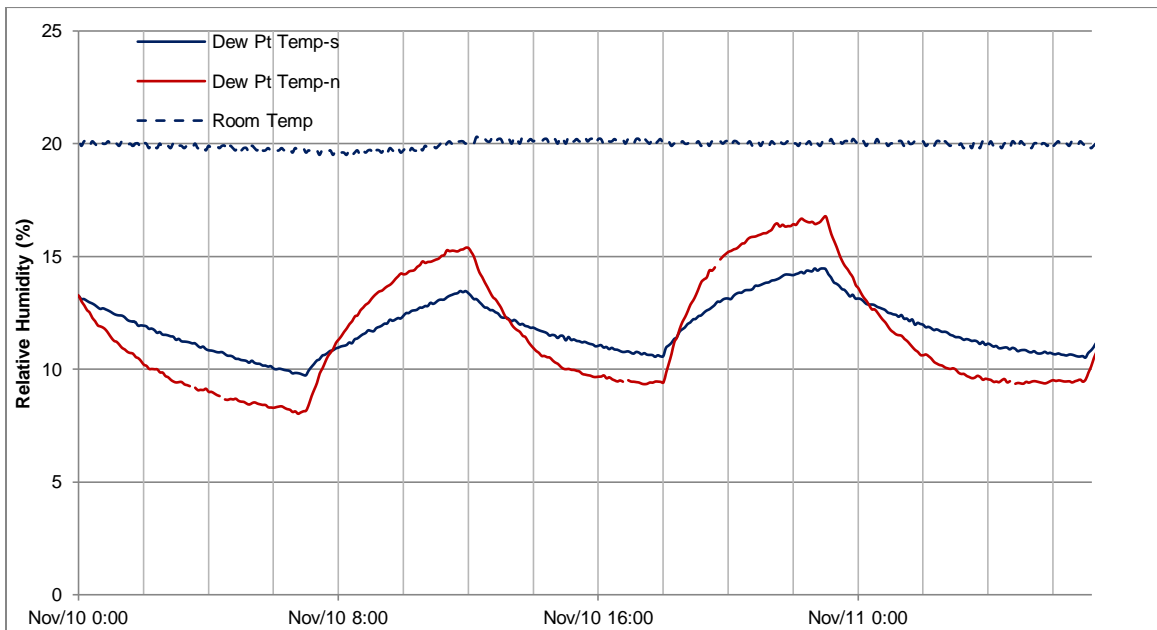


Figure 72. The indoor and dew point temperatures of the control building (red) and test building (blue) under TC2

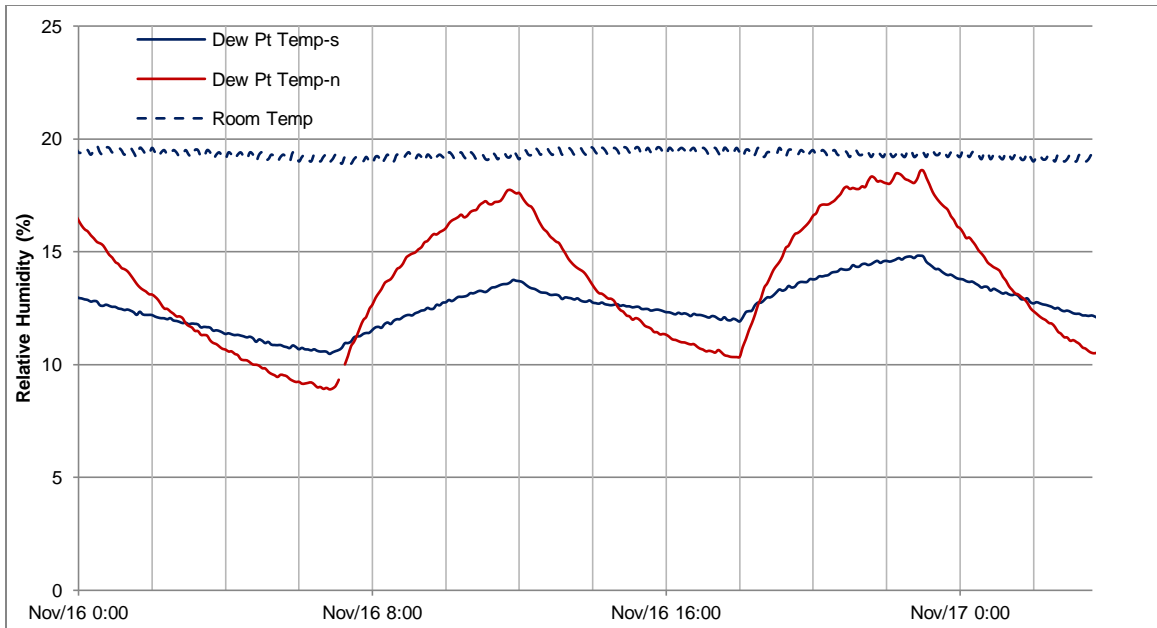


Figure 73. The indoor and dew point temperatures of the control building (red) and test building (blue) under TC3 – under-ventilation

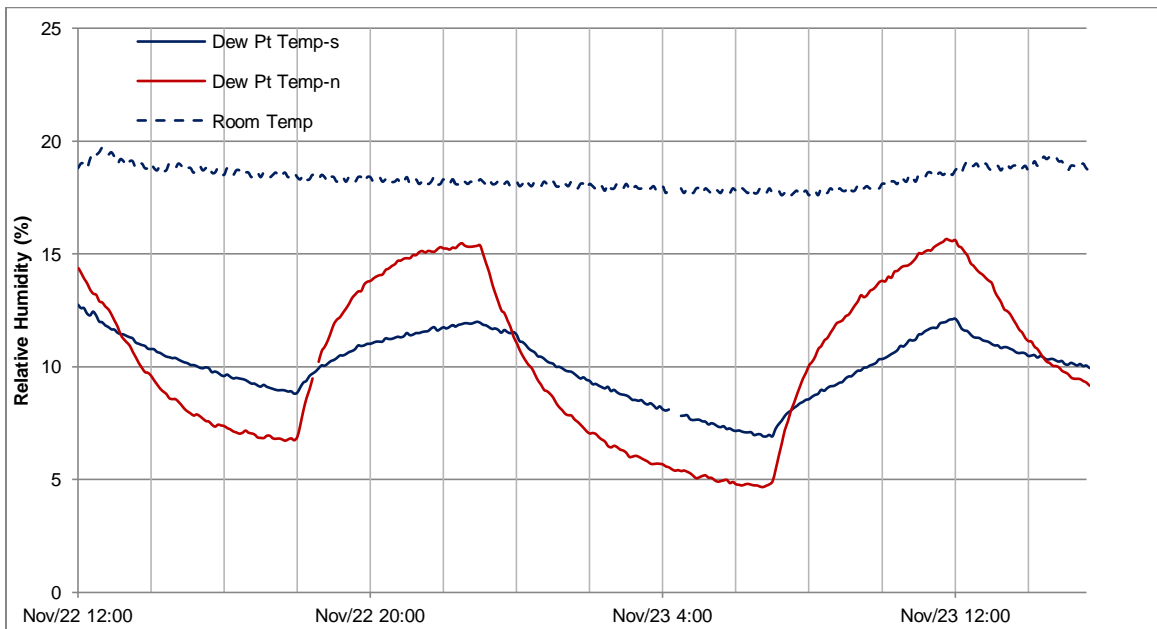


Figure 74. The indoor and dew point temperatures of the control building (red) and test building (blue) under TC4 – high occupancy

7.2.5.3 Excess Humidity Levels

In order to analyze the effect of exterior humidity on interior humidity, the excess humidity levels in the buildings are presented for readings taken at the same time of day between test cases. Excess humidity allows direct comparison of interior conditions across test cases. It is intended to

eliminate temperature variations that would otherwise be present with presenting relative humidity data. Excess humidity levels in the test building are compared for the following pairs of test cases:

- TC1 vs. TC2 – variable parameter: presence of moisture buffering phenomenon
- TC2 vs. TC3 – variable parameter: ventilation rate
- TC2 vs. TC4 – variable parameter: moisture loading

Excess humidity is calculated as the difference between the interior absolute humidity levels and the corresponding exterior absolute humidity levels. Absolute humidity is calculated in accordance with Equation 4 from Section 6.3.1. Figure 75 shows the outdoor absolute humidity levels and indoor absolute humidity levels in the control building during TC1 and TC2. Figure 76 shows excess humidity in the control building during TC1 and TC2.

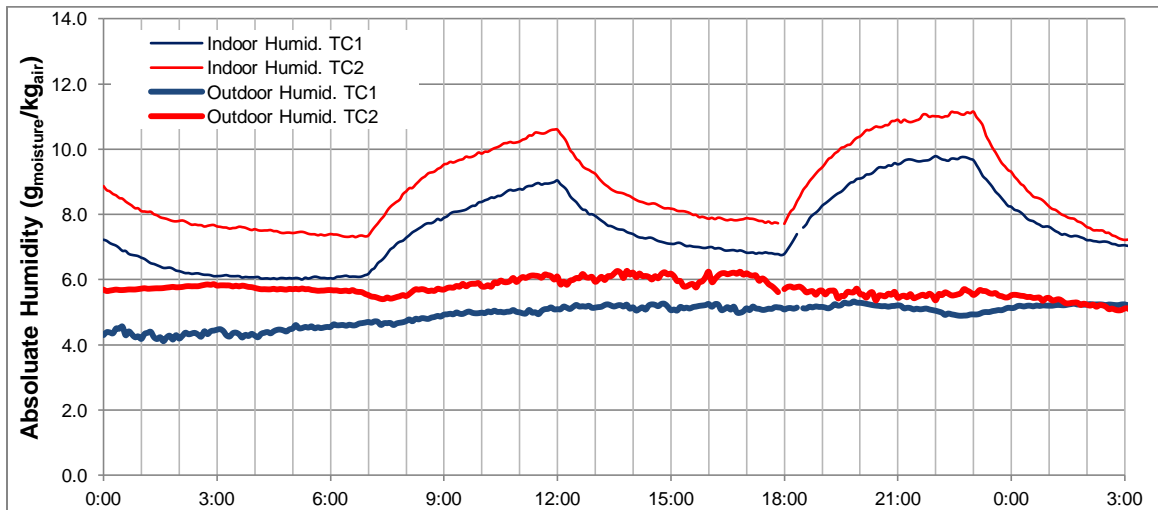


Figure 75. Interior and exterior absolute humidity in the control building during test cases TC1 and TC2

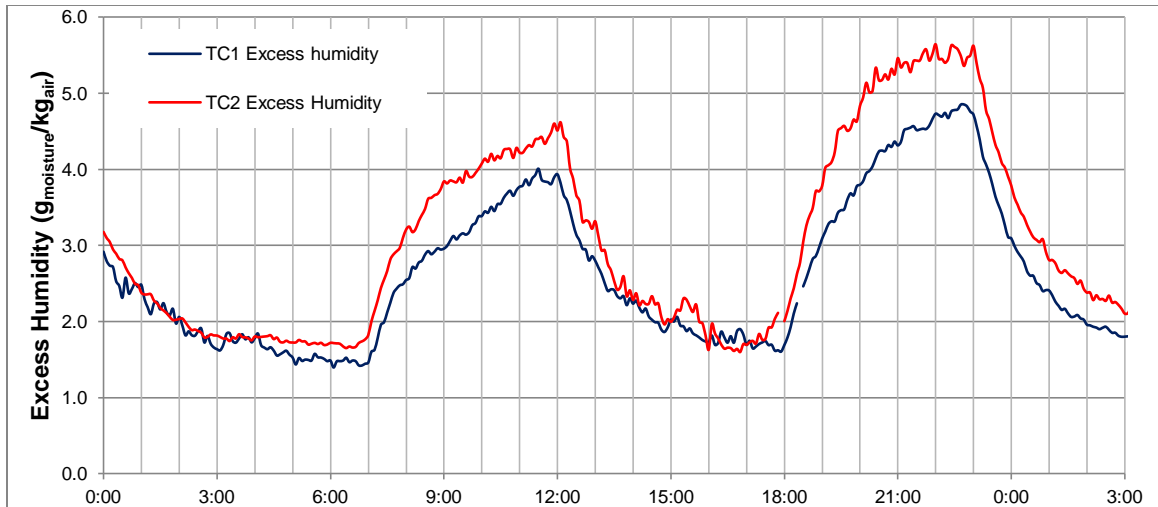


Figure 76. Excess humidity (interior absolute humidity – exterior absolute humidity) in the control building during test cases TC1 and TC2

The test parameters, namely ventilation rate, occupant density (moisture generation rate), and presence of no moisture buffering materials in the test space, were identical for the control building between TC1 and TC2. As a result, the interior environments are expected to be similar except when they are affected by outdoor humidity levels. Due to higher outdoor humidity levels during TC2, the indoor humidity levels under TC2 consequently exceed levels during TC1.

Similar to the previous figure, Figure 77 shows excess humidity in the test building during test cases TC1 and TC2. The variable parameter between the two test cases is the presence of moisture buffering materials in the test space – the test building wall surfaces are clad with gypsum board and are hygroscopic during TC2. The regulating effect of moisture buffering can be observed in excess moisture levels during TC2, as excess humidity peaks are lower, and lows are higher. In this case, the effect of elevated outdoor humidity levels during TC2 is outweighed by the moisture buffering effect of the building. This demonstrates the ability of the moisture buffering phenomenon in controlling indoor humidity peaks, even under high outdoor humidity conditions. This has positive implications on the performance of moisture buffering on indoor moisture management in the marine climate of the Lower Mainland of BC.

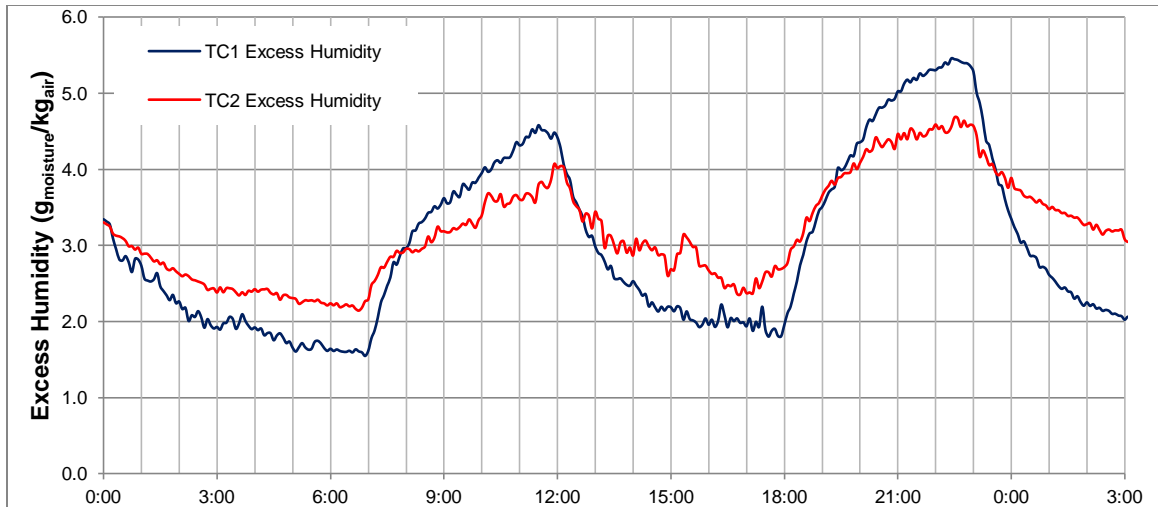


Figure 77. Excess humidity in the test building during test cases TC1 and TC2

Similarly, cross-test comparisons can be made for other combinations of tests. Figure 78 shows excess humidity during test cases TC2 and TC3 in the test building.

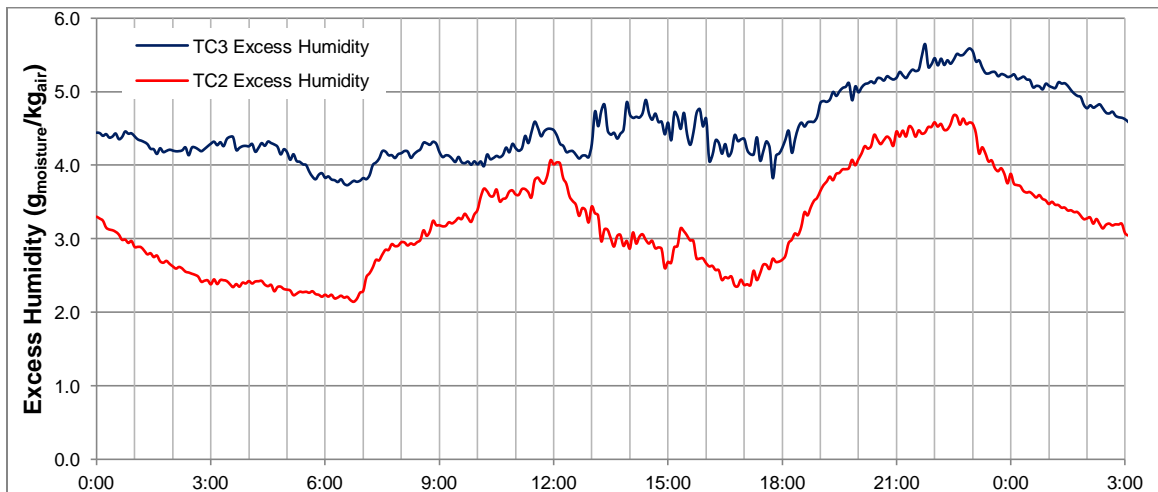


Figure 78. Excess humidity in the test building during test cases TC2 and TC3

The variable parameter between the two test cases is the ventilation rate – under TC2, the test space is ventilated at 15 CFM, the ASHRAE recommended rate, however, under TC3 the space is ventilated at 7.5 CFM, only half of the ASHRAE recommended rate. The test building is clad with hygroscopic gypsum board for both of these test cases; therefore the moisture buffering effect is present in either case. The variable parameter (under-ventilation) once again outweighs the effect of outdoor humidity levels on indoor conditions, however, the effect has negative

implications for indoor humidity. The indoor humidity levels are significantly elevated when the space is ventilated less than the ASHRAE recommended level.

Excess humidity levels in the control building are similarly compared between TC2 and TC4 in Figure 79. The variable parameter between these test cases is moisture loading – under TC2, typical moisture production profile is emitted, while under TC4, high moisture production profile is emitted. In this case, high moisture loading emitted from the occupant simulators once again outweighs the effect of outdoor conditions on indoor humidity. The excess humidity levels are consistently higher under TC4.

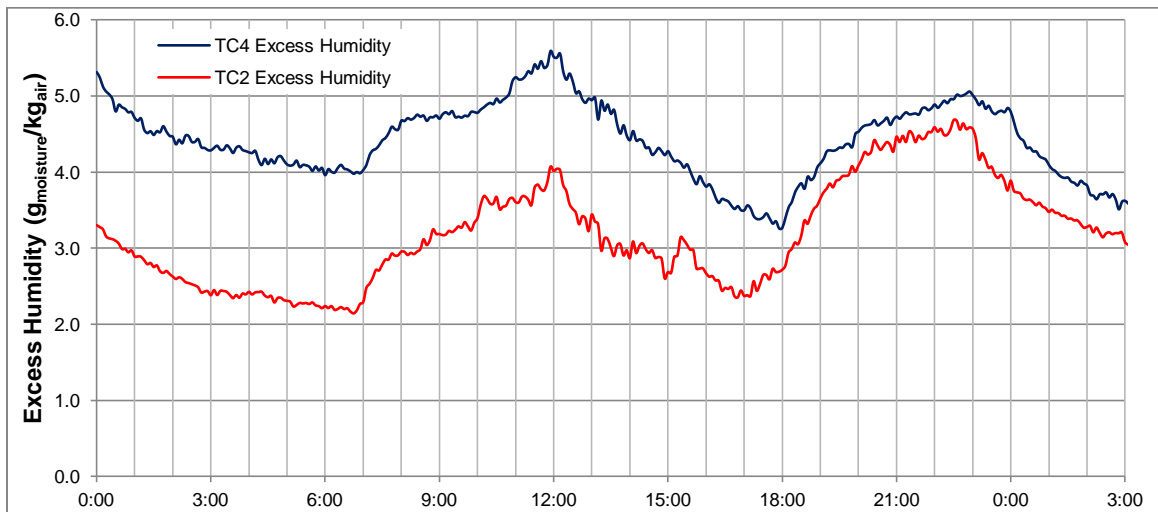


Figure 79. Excess humidity in the test building during test cases TC2 and TC4

7.2.5.4 Frequency of High RH Levels

TC3 dictates the fact that under-ventilating a space can nevertheless increase the relative humidity of a space above acceptable levels for thermal comfort and microbial growth, despite presence of moisture buffering finishes. Figure 80 shows the percentage of time the relative humidity levels in the buildings exceed a high threshold – 60%, 65%, and 70% – for the duration of the monitoring period presented.

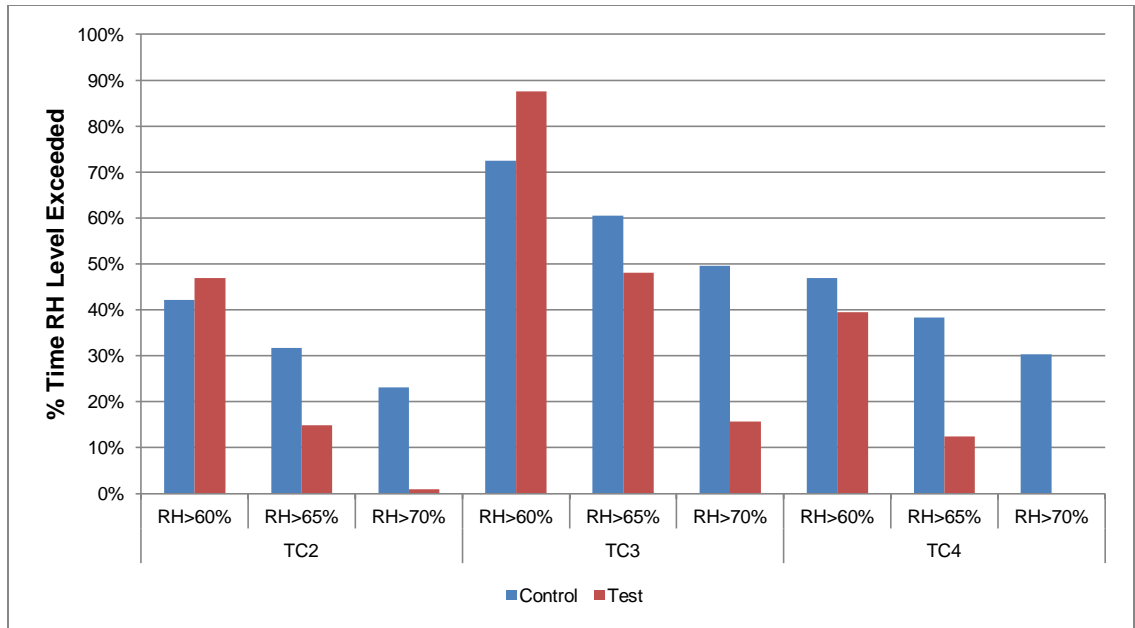


Figure 80. % of time interior relative humidity levels exceed high thresholds for TC2, TC3, and TC4

Compared to TC2, the RH levels in the test building exceed 70% relative humidity 7 extra hours than when the space is under-ventilated under TC3; similarly, compared to TC4, the RH levels exceed 70% relative humidity 5 extra hours, over a period of approximately 28 hours, thereby increasing the likelihood of condensation and microbial growth.

The field experiment testing results reveal that moisture buffering cannot be a viable substitute for adequate ventilation, and should be designed in tandem with proper ventilation design to help regulate changes in relative humidity levels. The results also indicate that presence of moisture buffering can be effective in regulating indoor humidity under high moisture loading, with ASHRAE recommended ventilation rates.

7.3 Active Moisture Management Methods

TC5 to TC8 are designed to evaluate the effectiveness of different ventilation strategies in managing indoor moisture as well as indoor air quality. The parameters from Table 5 are repeated in Table 17. In all test cases, the interior temperatures were similar for a given period in time, therefore interior temperature data has been omitted from graphs for better clarity and

presentation of data. Data collected from testing results presented are relative humidity of the indoor air and the flow rate of the ventilation system for each given ventilation scheme in CFM.

Table 17. List of Test Parameters for Test Cases 5 – 8

Test Case (TC)	Dates		NORTH (CONTROL) BUILDING	SOUTH (TEST) BUILDING
5	Apr. 2-4/14	Material	Polyethylene	GWB
		Occupant Density	Normal	Normal
		Ventilation Rate	ASHRAE Recommended	ASHRAE Recommended
		Ventilation Scheme	Constant	Constant
6	Apr. 11-13/14	Material	Polyethylene	GWB
		Occupant Density	Normal	Normal
		Ventilation Rate	ASHRAE Recommended	ASHRAE Recommended
		Ventilation Scheme	Time-controlled	Time-controlled
7	Jun. 22-25/14	Material	Polyethylene	GWB
		Occupant Density	Normal	Normal
		Ventilation Rate	ASHRAE Recommended	ASHRAE Recommended
		Ventilation Scheme	RH-controlled	RH-controlled
8	Jul. 5-6/14	Material	Polyethylene	GWB
		Occupant Density	Normal	Normal
		Ventilation Rate	ASHRAE Recommended	ASHRAE Recommended
		Ventilation Scheme	CO2-controlled	CO2-controlled

Under these test cases, CO₂ production was also simulated as described in the experimental set-up, in order to evaluate the effect of each ventilation scheme on indoor air quality. Data for indoor CO₂ levels are also presented. Analysis on the impact of the ventilation schemes on indoor conditions (namely indoor humidity and air quality), as well as building energy due to ventilation heat loss is also evaluated.

7.3.1 Test Case 5

Test case TC5 is intended to confirm the operating conditions of the control and test buildings under a constant ventilation scheme. The parameters are identical to TC2, however, the test is repeated with CO₂ production.

Figure 81 shows the relative humidity for the test and control buildings, and their respective ventilation flow rate over time. This test case is undertaken under constant ventilation at 15 CFM. The effect of the moisture buffering of gypsum board in regulating relative humidity amplitudes is apparent between the test building and the control building, as demonstrated in Table 18.

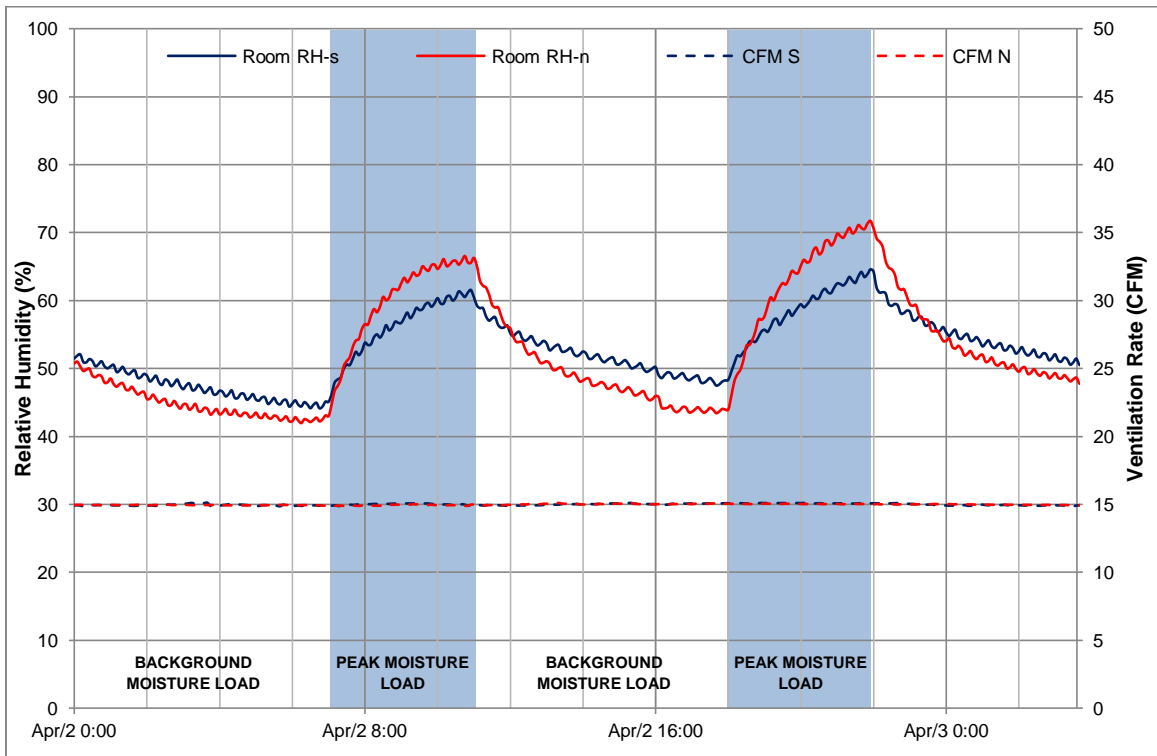


Figure 81. The indoor relative humidity and ventilation rate of the control building (red) and test building (blue) under TC5 – constant ventilation

Table 18 provides RH levels from TC5 as well as TC2 for comparison purposes. The performance of moisture buffering in managing indoor moisture in the test building is similar to the results obtained from TC2.

In TC5 the % difference in RH amplitudes between the control and test building are lower than those in TC2, 56% and 69% compared to 107% and 94%. This may be a result of the time of year the two tests take place, TC2 in November and TC5 in April.

Table 18. Comparison of indoor relative humidity, RH (%) and CO₂ (ppm) between the control & test building for TC5 (TC2 shown in parentheses for comparison)

	Cycle 1			Cycle 2		
	Control	Test	% Difference	Control	Test	% Difference
Min RH	41 (46)	45 (53)	10% (15%)	44 (50)	48 (54)	9% (8%)
Max RH	66 (75)	61 (67)	8% (12%)	71 (81)	64 (70)	11% (16%)
RH Amp	25 (29)	16 (14)	56% (107%)	20 (31)	23 (16)	69% (94%)
Mean RH	53.5 (60.5)	53 (60)	1% (1%)	54 (65.5)	59.5 (62)	10% (6%)
Min CO₂	868	875	1%	868	875	1%
Max CO₂	1126	1121	0%	1125	1150	2%
CO₂ Amp	258	246	5%	257	275	7%
Mean CO₂	997	998	0%	996.5	1012.5	2%

In April, during TC5 the outdoor vapour pressure is generally lower than in November, during TC2 (Figure 82). Due to lower vapour pressures, ventilation is more effective at removing excess moisture from the test buildings, as humid indoor air is replaced with drier outdoor air. As a result the moisture buffering effect is dampened under the same moisture loading.

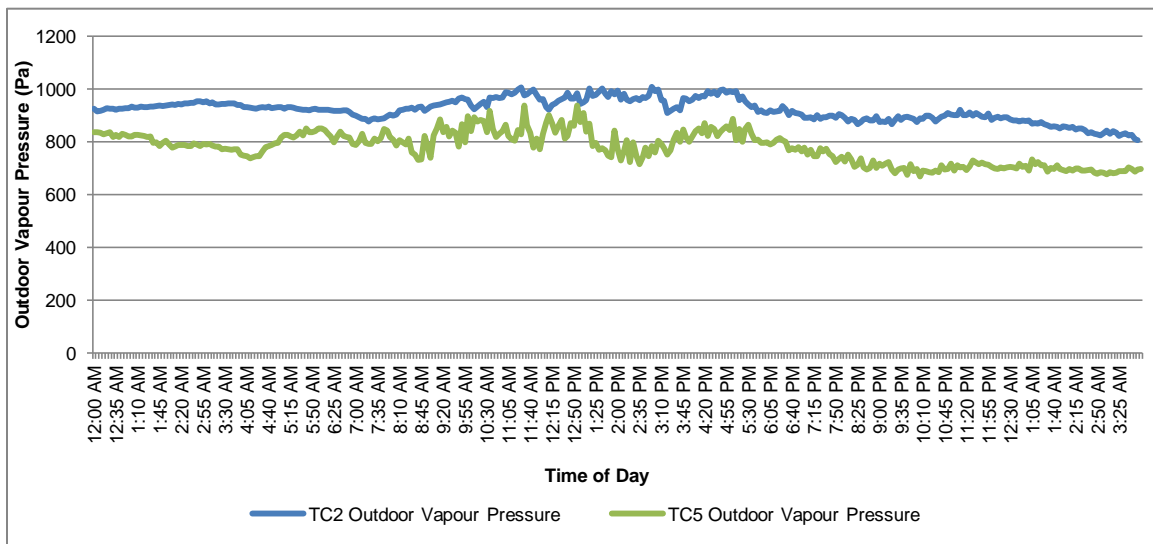


Figure 82. Outdoor vapour pressures for duration of 28 hours during TC2 and TC5

Figure 83 shows the CO₂ levels under constant ventilation in the buildings. The CO₂ loading peaks are designed to coincide with relative humidity peaks in all test cases, to emulate increased occupants' CO₂ generation with increased metabolic activity (e.g. from doing chores, etc.).

Similar to moisture levels, increasing CO₂ levels coincide with peak CO₂ emission, and decreasing levels coincide with background CO₂ emission. The CO₂ input into the air and ventilation rates are designed to be identical in both buildings, therefore the CO₂ levels are similar

and within the reported accuracy of the CO₂ sensors, which is $\pm (30\text{ppm} + 3\% \text{ of reading})$ from 15°C to 30°C (reference APPENDIX B for CO₂ sensor’s manufacturer’s datasheet).

ASHRAE recommends CO₂ levels be maintained under 1000 to 1200 ppm (ASHRAE, 2013). Under constant ventilation at the ASHRAE recommended ventilation rate, the overall CO₂ levels are maintained under 1200 ppm in both building, and are generally maintained under 1000 ppm except during peak loading. Given that the CO₂ loading and ventilation rates are similar in both buildings, the CO₂ levels are also similar, within 7% or less.

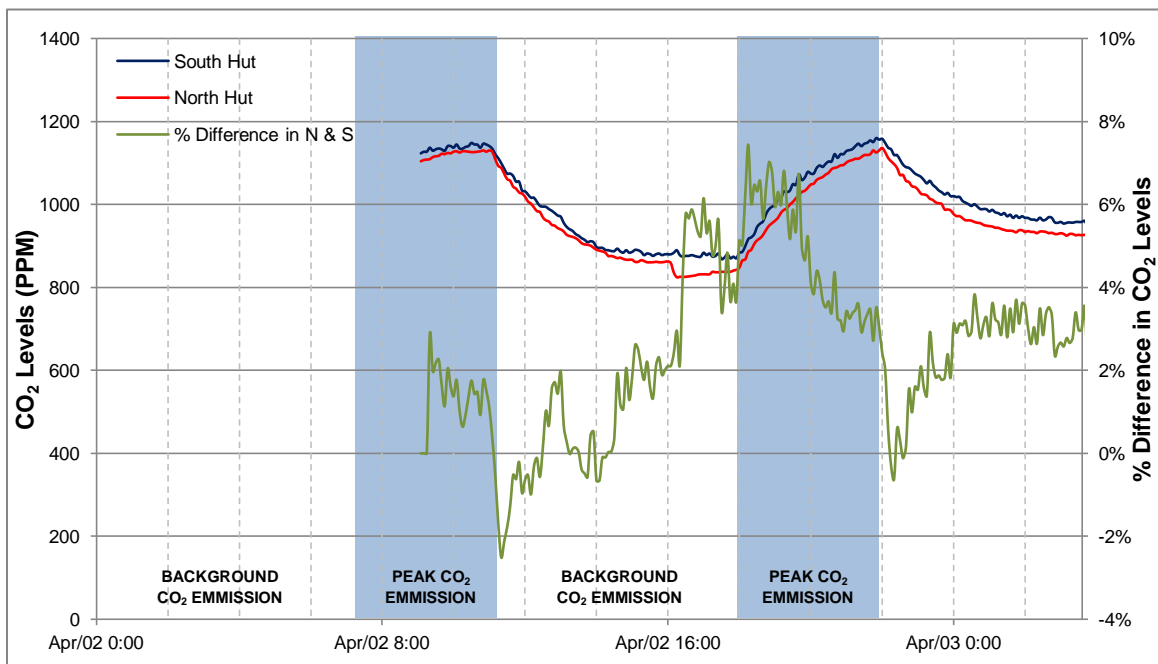


Figure 83. Indoor CO₂ levels of the control building (red) and test building (blue) under TC5 – constant ventilation

7.3.2 Test Case 6

Test case TC6 is intended to show the effect of time-controlled ventilation based on the algorithm defined in Section 6.5.2 on indoor conditions.

Figure 84 shows the relative humidity levels and ventilation rates of both buildings under the time-controlled ventilation scheme. The relative humidity rise and drop curve patterns seen here are different from all previous test cases. This is due to the nature of the ventilation scheme. The

ventilation system operates at the maximum rate of 30 CFM one hour after the beginning of the moisture loading peak periods. It then resumes back to 7.5 CFM one hour after the moisture peak loading period ends. As explained in Section 6.5.2, since high humidity levels are not reached instantaneously at the beginning of peak moisture loading cycles, maximum ventilation rate is offset from peak moisture loading by one hour so that ventilation energy expended on the first hour of peak moisture loading may not be “wasted.”

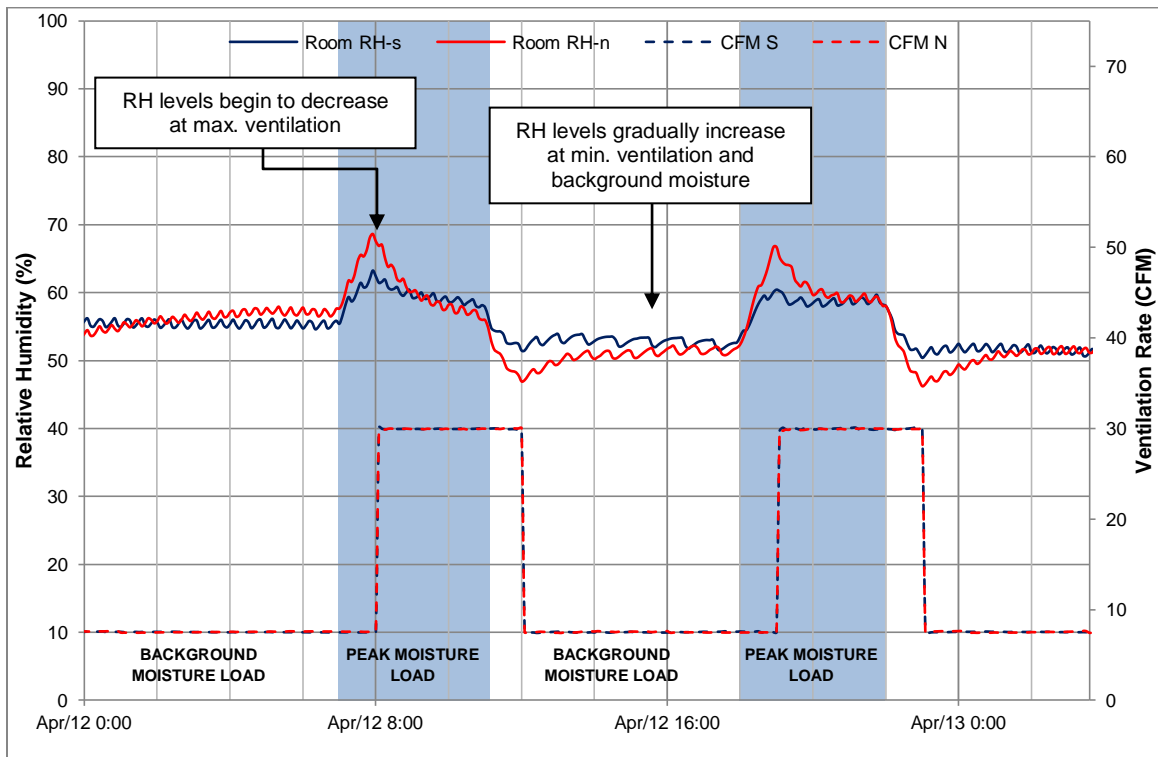


Figure 84. The indoor relative humidity and ventilation rate of the control building (red) and test building (blue) under TC6 – time-controlled ventilation

Table 19 shows the values for minimum, maximum, mean RH, and RH amplitude, and the % difference for each between the control and test building. The values for this test case were obtained as shown in Figure 85.

Table 19. Comparison of indoor relative humidity (RH) between the control & test building for TC6

	Cycle 1			Cycle 2		
	Control	Test	% Difference	Control	Test	% Difference
Min RH	47	53	13%	48	51	6%
Max RH	69	62	11%	65	60	8%
RH Amp	22	9	144%	17	9	89%
Mean RH	58	57.5	1%	56.5	55.5	2%
Min CO₂	653	687	5%	683	719	5%
Max CO₂	1500	1500	0%	1271	1303	3%
CO₂ Amp	847	813	4%	588	584	1%
Mean CO₂	1076.5	1093.5	2%	977	1011	3%

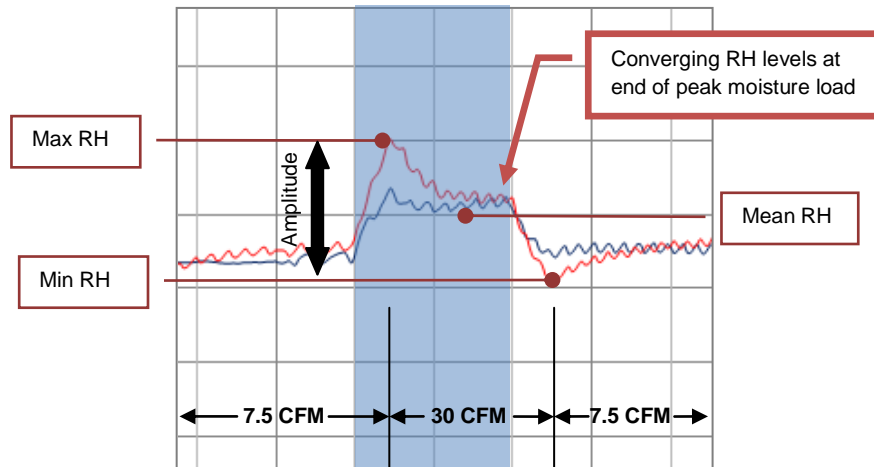


Figure 85. Maximum RH, minimum RH, RH amplitude and mean RH in control building for Cycle 2

Under the time-controlled ventilation scheme, the regulating effect of moisture buffering on relative humidity can still be observed in the test building. The RH amplitudes in the test building are less than half of those in the control building, only 7 and 9%, compared to 18 and 19%.

However, a point worth noting is that under 30 CFM ventilation rate, the regulating effect of moisture buffering seems to diminish. That is, the relative humidity levels begin to converge at maximum ventilation. This is most evident at the end of peak moisture loading during Cycle 2 (Figure 85).

TC3 revealed that the effect of moisture buffering was more pronounced under constant ventilation rate of 7.5 CFM compared to 15 CFM. TC6 reveals that the moisture buffering effect diminishes by increasing ventilation rate to 30 CFM. This is attributed to decreased vapour

pressure and surface mass transfer under higher ventilation rates. These results agree with findings on the inverse relationship of ventilation rate and moisture buffering effect in Mitamura, et al. (2004).

Figure 86 shows the effect of time-controlled ventilation on indoor CO₂ levels.

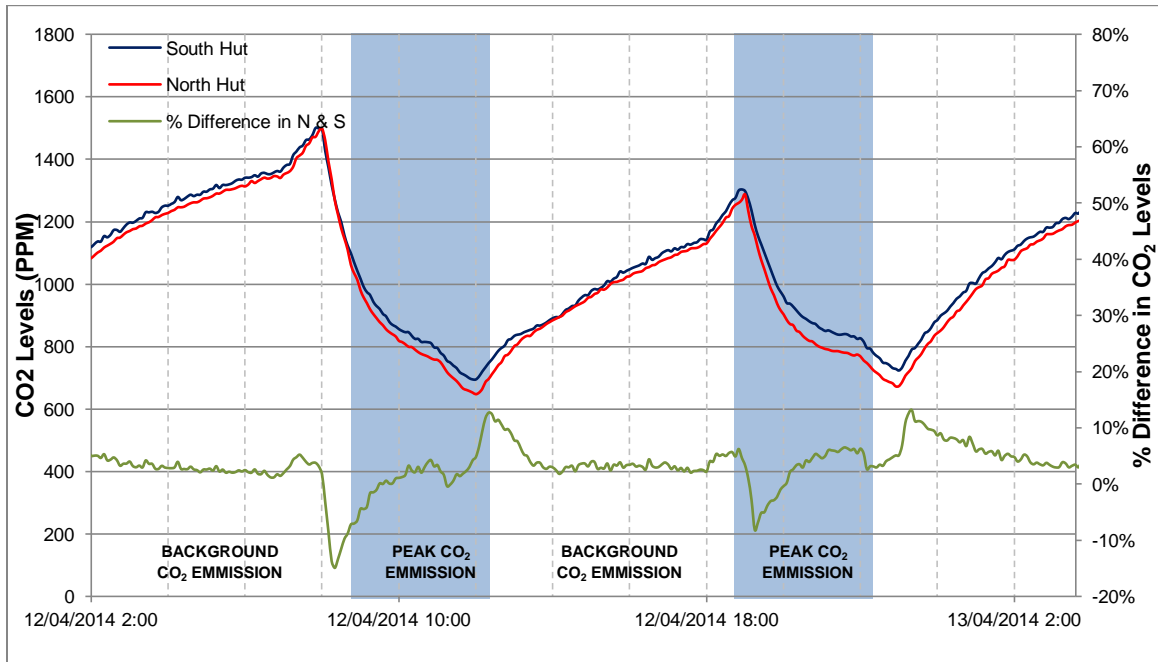


Figure 86. Indoor CO₂ levels of the control building (red) and test building (blue) under TC6 – time-controlled ventilation

Under time-controlled ventilation, CO₂ levels exceed acceptable thresholds during peak loading. Offsetting peak moisture generation and maximum ventilation rate is effective for maintaining relative humidity. However, due to faster response of CO₂ levels to change in ventilation rate, offsetting the maximum ventilation rate and peak loading is not effective in maintaining CO₂ levels below ASHRAE recommended levels.

In the both buildings, CO₂ levels rise rapidly and quickly exceed 1200 ppm at the beginning of peak loading when ventilation is at the minimum rate. At the end of the peak loading when ventilation is still at the maximum rate, CO₂ levels drop rapidly, lowering to below 800 PPM.

This ventilation strategy is not ideal for maintaining good indoor air quality. Acceptable RH levels were generally maintained within the test building with the aid of moisture buffering (the same cannot be said about the control building). While this approach may save energy in terms of ventilation heat loss, it has negative consequences on the indoor air quality.

It may be possible to tweak the ventilation rates, and maximum ventilation durations under this strategy to achieve both acceptable indoor humidity and CO₂ levels. In this regard, more testing should be done.

7.3.3 Test Case 7

Test case TC7 is intended to show the effect of RH-controlled ventilation based on the algorithm defined in Section 6.5.3 on indoor conditions.

TC7 is a complex case. The ventilation rate is dependent on the relative humidity levels, while the behaviour of the change in relative humidity levels is also dependent on ventilation rates.

Figure 87 shows the fluctuations in relative humidity levels in both buildings under RH-controlled ventilation. When the relative humidity threshold is exceeded, maximum ventilation rate causes relative humidity levels to drop more quickly in the control building while the test building responds to changes in ventilation rate slowly due to the effect of moisture buffering. This phenomenon can also be seen in other test cases during decreasing relative humidity in the variation cycles. This is due to residual moisture in unfinished gypsum board gradually undergoing desorption back into the air as the relative humidity levels in the test space decrease.

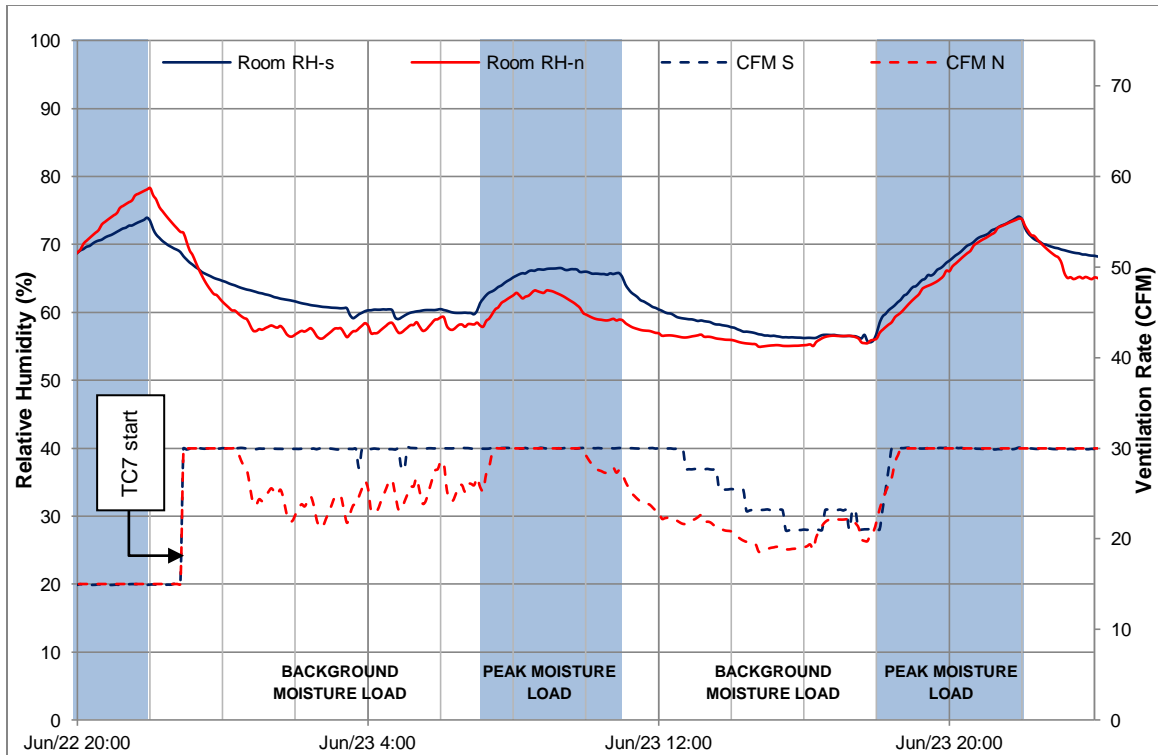


Figure 87. The indoor relative humidity and ventilation rate of the control building (red) and test building (blue) under TC7 – RH-controlled ventilation

Table 20. Comparison of indoor relative humidity (RH) between the control & test building for TC7

	Cycle 1			Cycle 2		
	Control	Test	% Difference	Control	Test	% Difference
Min RH	58	60	3%	55	55	0%
Max RH	63	66	5%	73	73	0%
RH Amp	5	6	20%	18	18	0%
Mean RH	60.5	63	4%	64	64	0%
Min CO ₂	760	740	3%	710	730	3%
Max CO ₂	850	810	5%	790	830	5%
CO ₂ Amp	90	70	29%	80	100	25%
Mean CO ₂	805	775	4%	750	780	4%

The moisture buffering effect greatly weakens at high ventilation rates, as noted in TC6. At the start of test case TC7, both buildings' relative humidity levels are above 60%, the level at which the maximum threshold is set in this ventilation scheme's algorithm (reference Figure 56 in Section 6.5.3). As a result, the demand ventilation system operates at its maximum rate in both buildings, and is the only mechanism that can effectively reduce indoor humidity. Results may vary with different initial conditions, however, the effect of varying initial conditions are beyond of the scope of this field experiment.

In general, the moisture levels in the test building are not synergistic with RH-controlled ventilation due to slow change in relative humidity response to changing ventilation rates. Maximum ventilation rate is run for a longer duration in the test building, which can in fact increase ventilation heat loss, and have negative impacts on the building energy demand. This is further explored in Section 7.3.5.3.

As indicated in Table 20, at the end of the test case period the buildings are performing similarly in managing moisture as ventilation rate remains at 30 CFM during Cycle 2 (% differences between RH levels are all 0%).

Overall, this ventilation scheme is not very well synchronized with the moisture buffering effect. While it is generally effective in controlling interior relative humidity levels, it is difficult to couple the benefits of moisture buffering with this ventilation scheme.

Figure 88 shows indoor CO₂ under RH-controlled ventilation. Due to irreversible malfunction in the CO₂ dispensing system in the control building, the CO₂ data obtained from field testing is incomplete. To obtain data for the remainder of the testing duration, HAMFitPlus whole building simulation model was utilized to obtain the indoor CO₂ conditions for the remainder of the test case. More information regarding the model and verification can be found in Tariku (2008) and Tariku et al (2011). The model has been previously verified, and the results are consistent with the first half of the test data from the control building. Therefore, simulated data is reliable and can be analyzed with confidence.

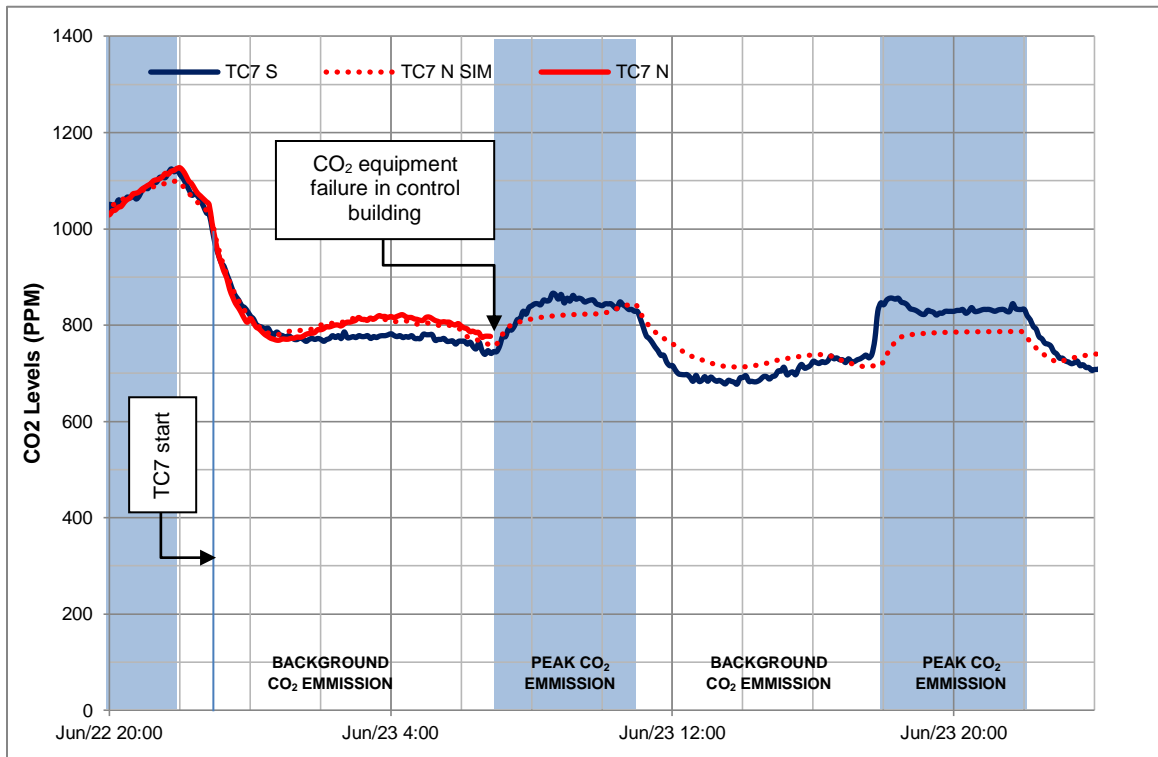


Figure 88. Indoor CO₂ levels of the control building measured (red) and simulated using HAMFitPlus model (dotted red), and test building (blue) under TC7 – RH-controlled ventilation

Figure 87 shows that at maximum ventilation rate, the relative humidity levels are reduced only by way of ventilation, and moisture buffering is not effective. For the duration that ventilation rate is maintained at its maximum rate, CO₂ levels rapidly decrease and reach levels below 900 ppm. High sensitivity of indoor CO₂ to ventilation rate, as well as the nature of the ventilation scheme algorithm which maintains the ventilation rate at the maximum for the majority of the duration of the test case, result in CO₂ levels well below the ASHRAE recommended level.

7.3.4 Test Case 8

Test case TC8 is intended to show the effect of CO₂-controlled ventilation based on the algorithm defined in Section 6.5.4 on indoor conditions.

For this test case, only the test building was operational due to equipment malfunctions of the occupant simulators (both the CO₂ dispensing system and nebulizers failed). Relative humidity

and ventilation rate data for the control building are obtained from HAMFitPlus whole building simulation model. In this ventilation scheme, the CO₂ levels in the control building are expected to be the same as the test building. Ventilation rate data from the test building is utilized to simulate the indoor conditions of the control building.

Ventilation rates under CO₂-controlled ventilation are determinant based on the level of indoor CO₂ and are independent of the interior relative humidity levels. Consequently, for the same CO₂ loadings similar ventilation rates are expected in the two buildings. Figure 89 demonstrates the effect of this ventilation scheme on interior relative humidity levels of both buildings.

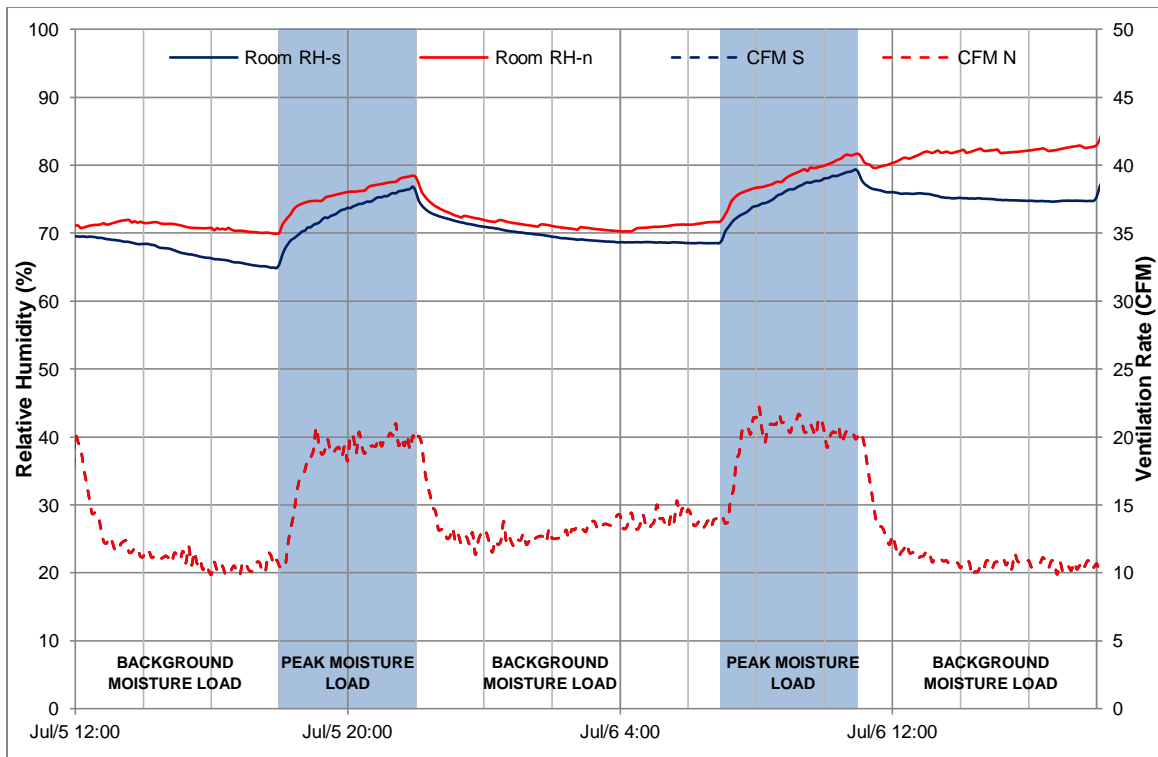


Figure 89. The indoor relative humidity and ventilation rate of the control building (red) and test building (blue) under TC8 – CO₂-controlled ventilation. Control building data is simulated using HAMFitPlus.

Table 21. Comparison of indoor relative humidity (RH) between the control & test building for TC8

	Cycle 1			Cycle 2		
	Control	Test	% Difference	Control	Test	% Difference
Min RH	70	65	8%	72	69	4%
Max RH	79	77	3%	82	79	4%
RH Amp	9	12	33%	10	10	0%
Mean RH	74.5	71	5%	77	74	4%
Min CO₂	820	820	0%	850	850	0%
Max CO₂	910	910	0%	910	910	0%
CO₂ Amp	90	90	0%	60	60	0%
Mean CO₂	865	865	0%	880	880	0%

The relative humidity levels continue to increase with each moisture peak loading cycle. This is because CO₂ levels are more sensitive to changes in ventilation rate, and a slight increase in ventilation rate results in a greater decrease in CO₂ levels than in relative humidity levels. Therefore, relative humidity levels continue to gradually rise, while CO₂ levels are maintained at acceptable levels (Figure 90).

Similar to the results from TC7, it can be said that based on TC8 results, CO₂-controlled ventilation is not synergistic with moisture buffering potential. The performance of the test and control buildings in regulating indoor humidity is comparable. The % difference values for RH levels between the two buildings are less than 5%, indicating that the two buildings perform similarly (Table 21). Although, the relative humidity levels in the control building continue to increase more rapidly than in the test building at the end of TC8 as seen in Figure 89.

Under this ventilation scheme CO₂ levels are maintained at acceptable levels, below 1000ppm, while relative humidity levels continue to gradually rise.

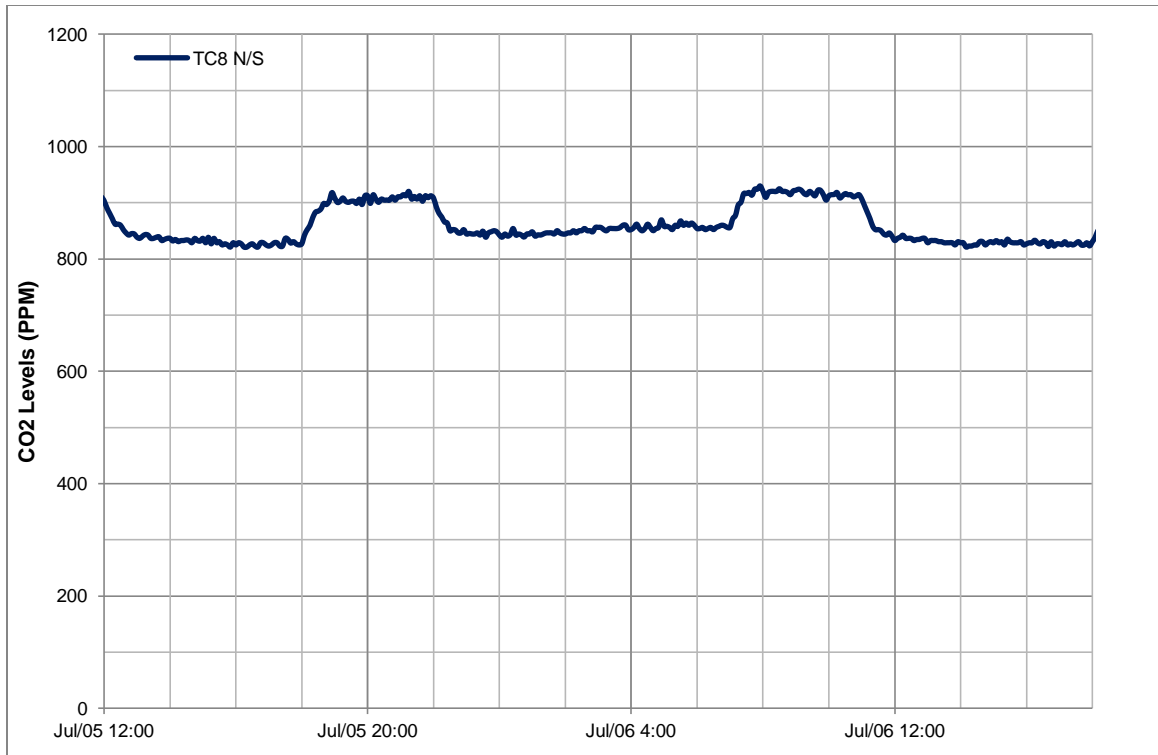


Figure 90. Indoor CO₂ levels of the test building under TC8 – CO₂-controlled ventilation

7.3.5 Analysis

Test cases TC1 to TC4 reveal that moisture buffering properties in the test building are generally effective in regulating the interior relative humidity levels, especially peaks, to varying degrees depending on ventilation rate and moisture loading.

Test cases TC5 to TC8 seek to couple the benefits of passive moisture management from moisture buffering, with active moisture management of various ventilation schemes. The effect of constant, time-controlled, RH-controlled, and CO₂-controlled ventilation in accordance with the predefined algorithms on indoor humidity, energy, and indoor air quality are further analysed.

7.3.5.1 Indoor Humidity

Figure 91 shows the RH amplitude, and Figure 93 shows RH minimum, maximum, and mean of Cycles 1 and 2 for each test case. Under TC6, the % difference in RH amplitudes between the control and test building are more than double, 157% and 111% for Cycles 1 and 2 respectively

(Figure 91). This indicates that time-controlled ventilation is the only ventilation scheme that successfully works with the relative humidity regulating benefit of moisture buffering. In test cases TC7 and TC8, the % difference in RH amplitude is much lower between the two buildings, equal to or less than 20%. This indicates that the regulating effect of moisture buffering is not effective under these ventilation schemes. Under the constant ventilation scheme, the % difference in RH amplitude between the two buildings is greater than 50% for each cycle. Thus, relative humidity is regulated under this scheme, but comparatively to a lesser degree than under time-controlled ventilation.

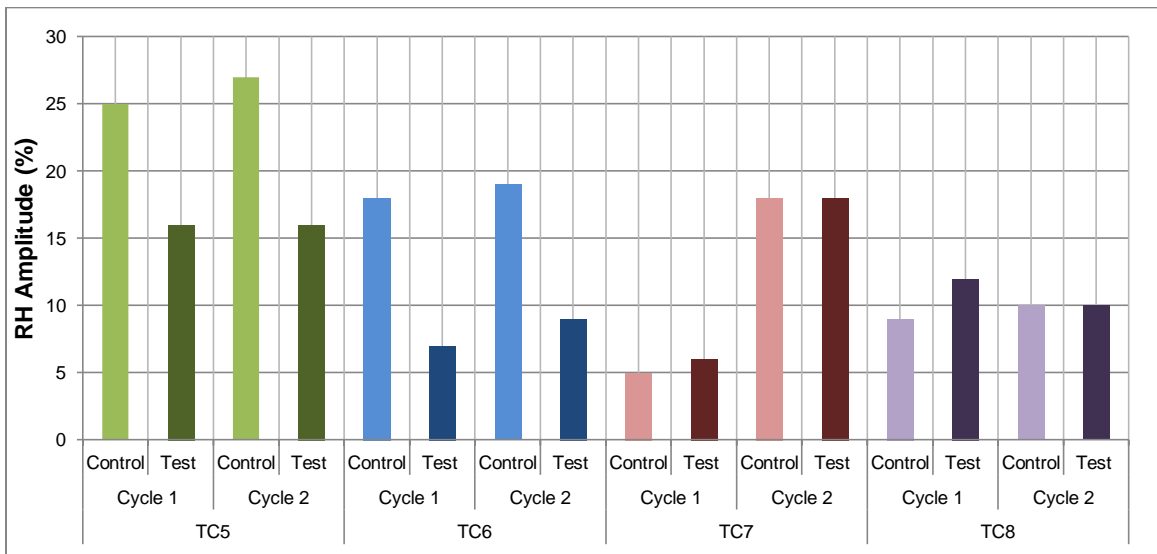


Figure 91. RH amplitude (Max RH – Min RH) for Cycle 1 & 2 from test cases TC5, TC6, TC7, and TC8

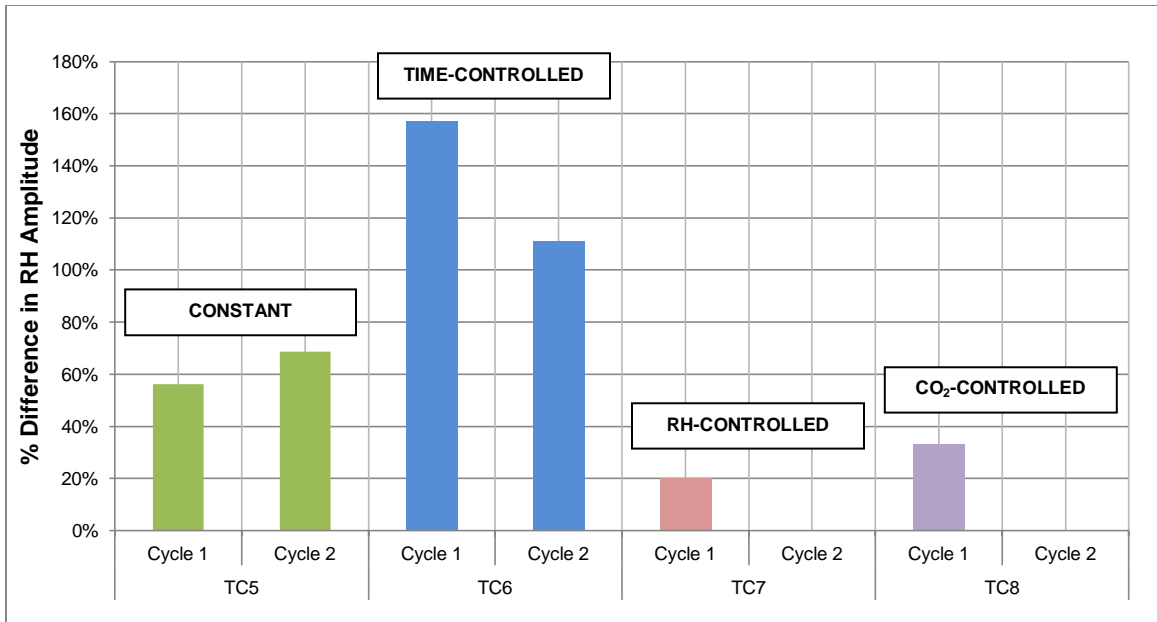


Figure 92. % Difference in RH amplitudes between the control and test building from test cases TC1, TC2, TC3, and TC4

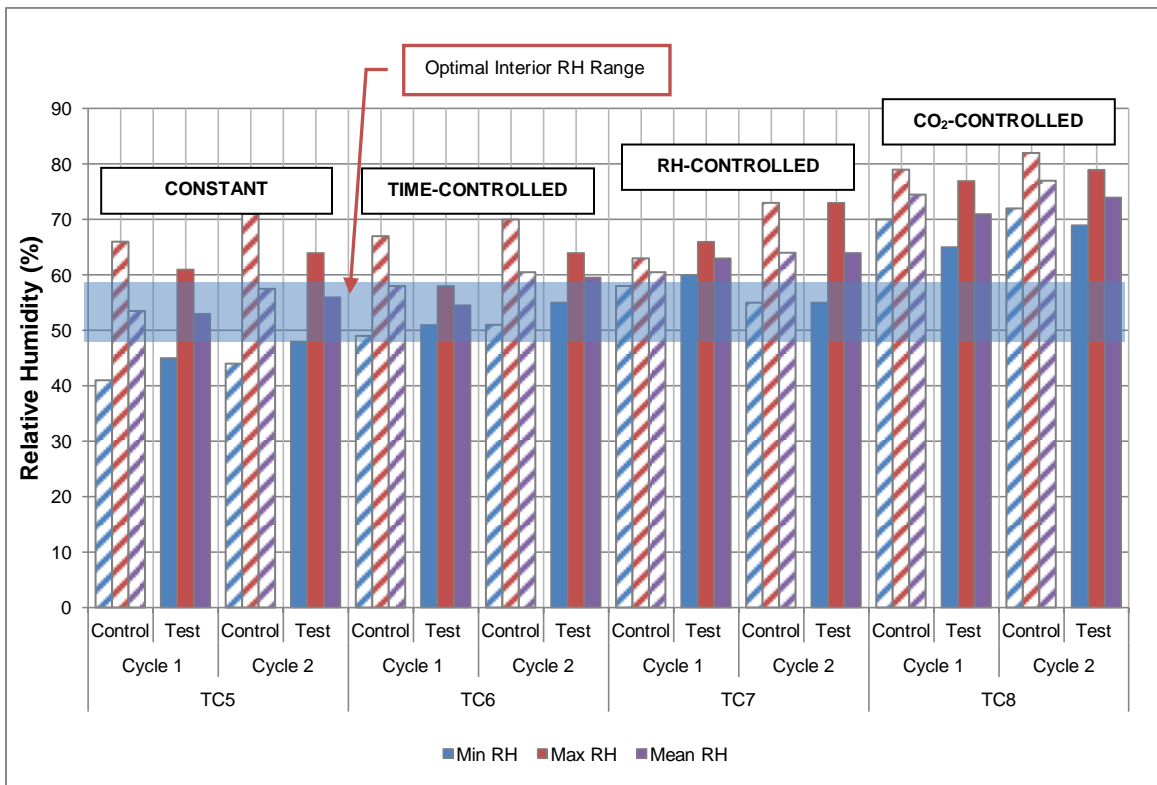


Figure 93. Minimum, maximum, and mean RH for Cycle 1 & 2 from test cases TC5, TC6, TC7, and TC8. The test building is shown in solid and the control building is shown in hatched. Optimal interior RH range is highlighted in blue.

In general, under test cases TC5, TC6, TC7 and TC8 indoor humidity levels in the control building are consistently similar to those in the test building. The mean RH levels are indicative of overall relative humidity levels in each building. The % differences between the buildings' mean RH levels are 6% or less (Figure 94). Under TC5 and TC6, the mean RH levels are generally within the ASHRAE recommended range of 50 to 60%. However, under TC7 and TC8, the mean RH levels exceed the acceptable range.

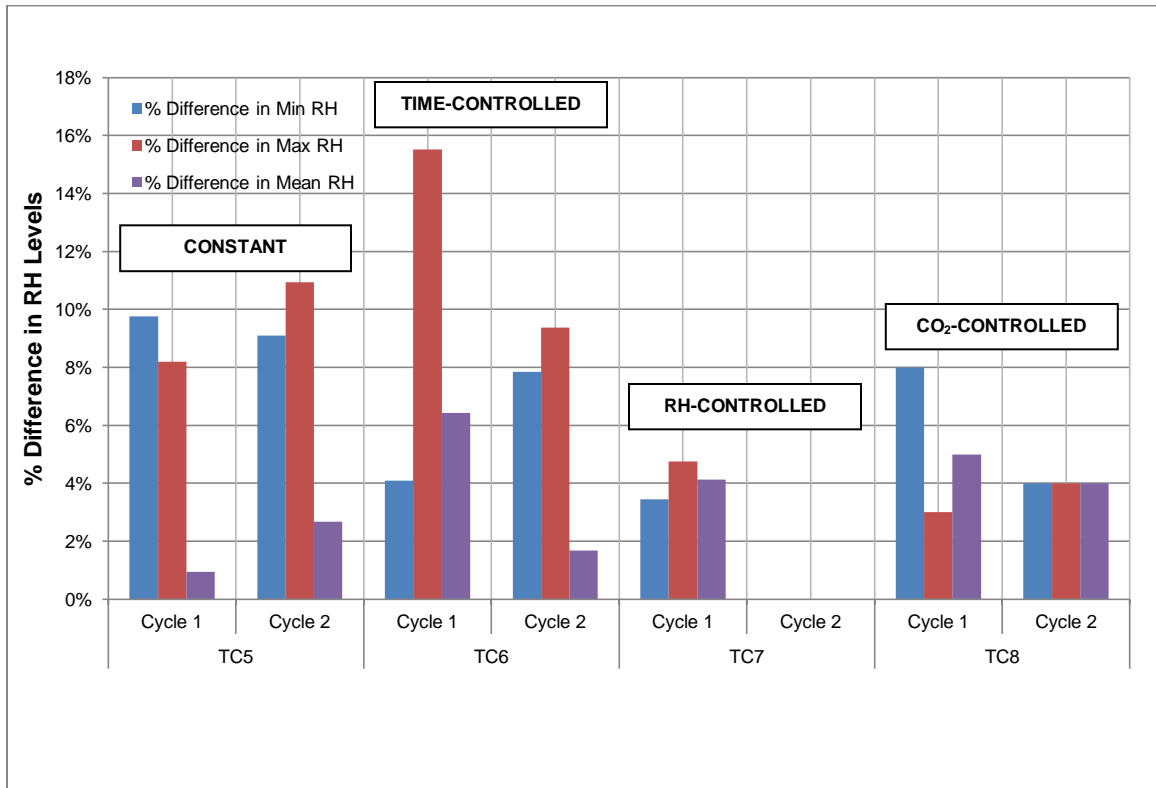


Figure 94. Difference in minimum, maximum, and mean RH between the control and test building from test cases TC5, TC6, TC7, and TC8

Amongst the active moisture management measures, time-controlled ventilation is most effective in maintaining both buildings' relative humidity levels below the 65%, close to the acceptable range. However, in practice, time-controlled ventilation may not be as successful as in field testing due to uncertainty in the duration and frequency of peak moisture loading of occupants.

Time-controlled ventilation may be a viable solution in spaces where peak moisture loading can be accurately predicted, such as a commercial kitchen, gymnasium, theatre, or spa. In a residential setting where moisture loading is a function of the occupants' density, daily habits, presence, and other factors that cannot be accurately predicted in design, it may not successfully address moisture issues. This is the case in the Reference Building.

An alternative to time-controlled ventilation in application can be motion detector sensing ventilation systems. These systems may can detect the presence of occupants and boost when occupants are active and present. They also provide savings benefits in that the ventilation demand can be lowered when occupants are not home.

TC8 is effective at maintaining CO₂ levels at acceptable levels for indoor air quality, but fails to maintain relative humidity levels below acceptable levels.

The effectiveness of ventilation methods used in TC5 to TC8 as active measures to manage moisture are further discussed as related to ventilation heating energy and indoor air quality.

7.3.5.2 Indoor Air Quality: CO₂ levels

CO₂ levels are emitted and monitored to evaluate the effectiveness of each ventilation scheme on indoor air quality. In part, CO₂ levels are dependent on outdoor CO₂ levels which generally range between 350 to 450 PPM (Dlugokencky & Pieter, 2016). Locally, the outdoor CO₂ levels at the WBPRP are within this range (Figure 95).

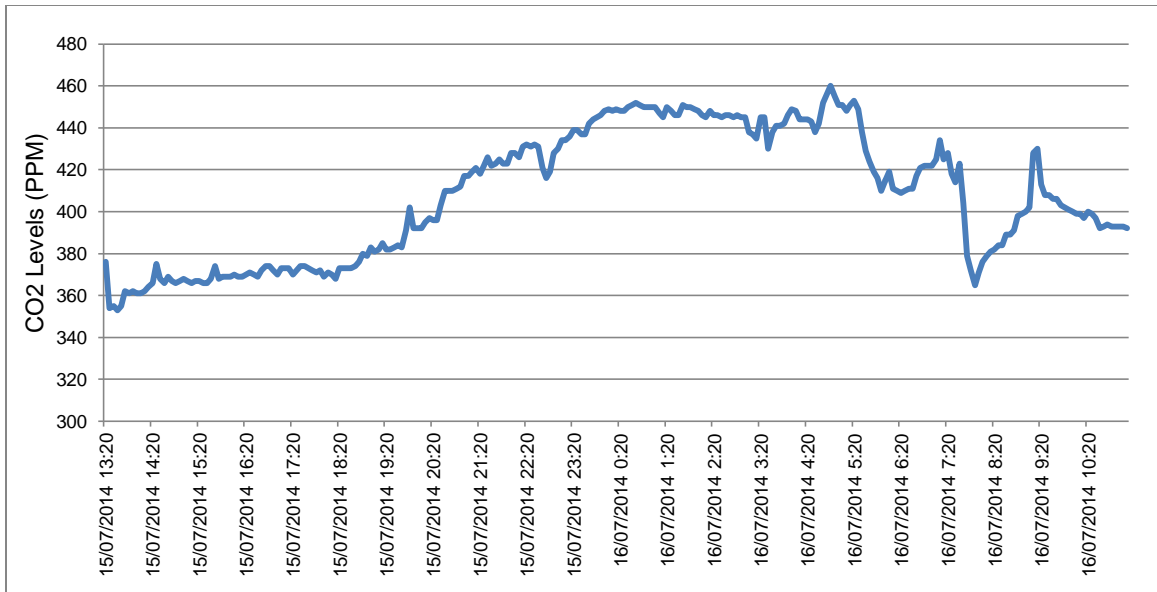


Figure 95. Outdoor CO₂ Levels

Figure 96 shows the maximum, minimum and mean CO₂ levels for each cycle in TC5 to TC8. In test cases TC5 and TC6, the mean CO₂ levels are above or within 1000 PPM, and maximum CO₂ levels consistently exceed this level. Under TC7 and TC8, the CO₂ levels are consistently below 1000 PPM.

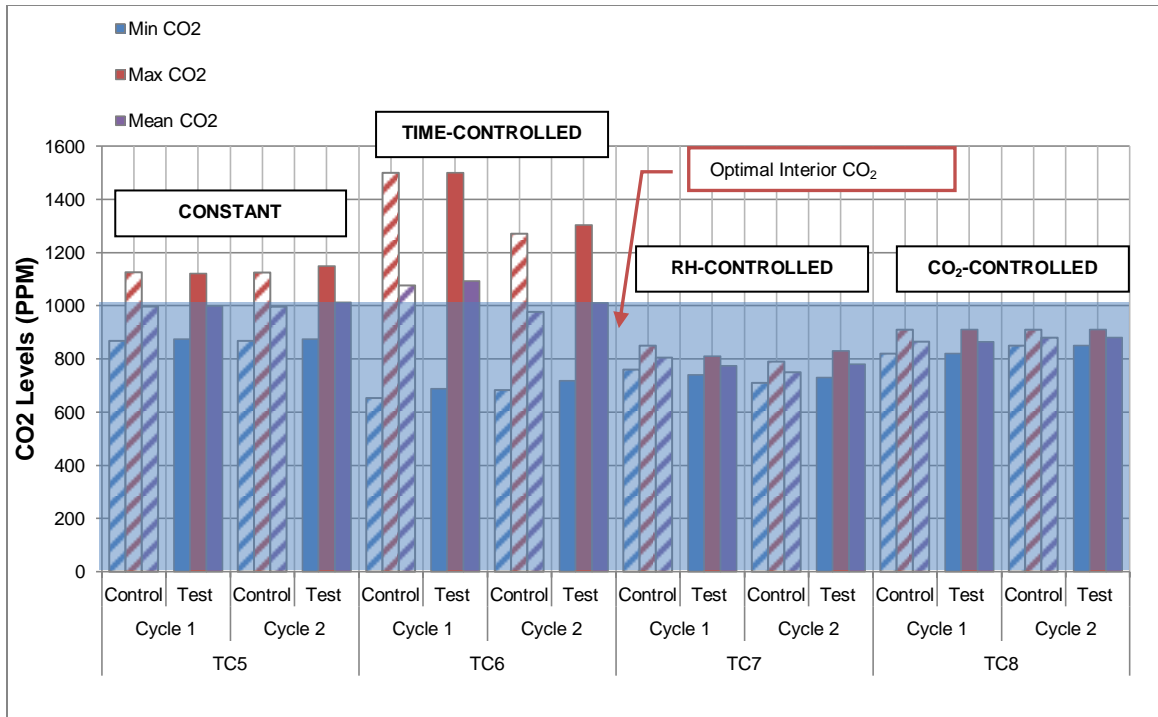


Figure 96. Minimum, maximum, and mean CO₂ for Cycle 1 & 2 from test cases TC5, TC6, TC7, and TC8. The test building is shown in solid and the control building is shown in hatched. Optimal interior RH range is highlighted in blue.

The CO₂ levels between the test and control buildings are comparable, the mean within 5% for all test cases, and minimum and maximum levels within 6% (Figure 97).

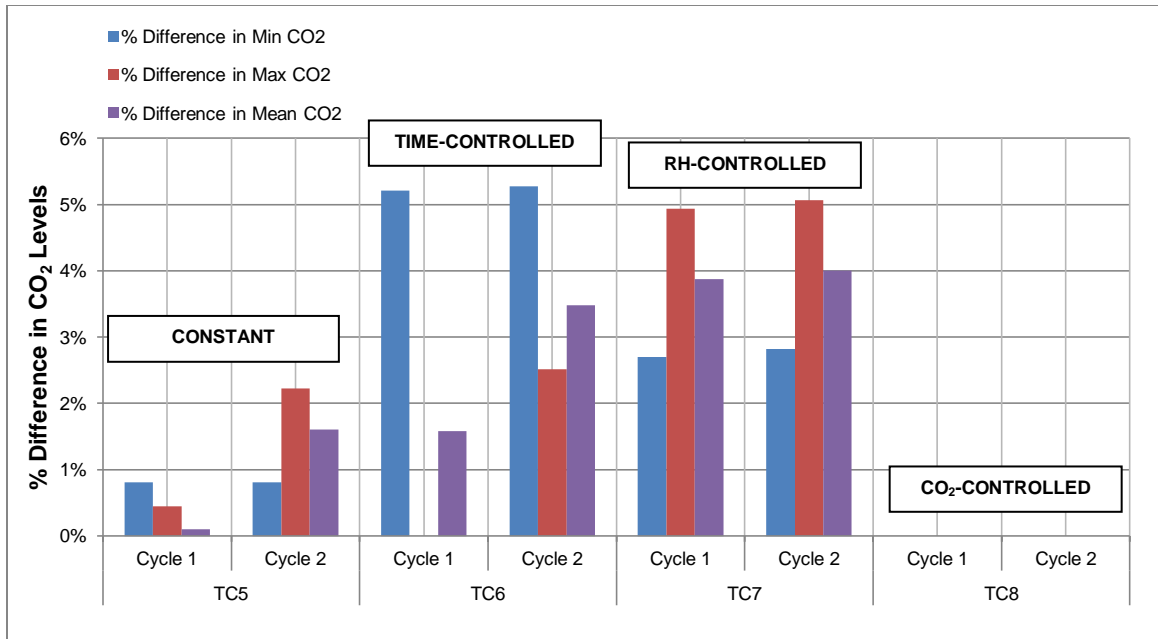


Figure 97. % Difference in minimum, maximum, and mean CO₂ between the control and test building from test cases TC5, TC6, TC7, and TC8

Table 22 shows the total percentage of time CO₂ levels exceed 1000 PPM in each building for the total duration of the data presented for each test case. According to analysis of CO₂ levels, indoor air quality exceeds acceptable levels under constant and time-controlled ventilation for nearly half of the testing period.

Table 22. % of time CO₂ levels exceed 1000 PPM threshold

	Control Building	Test Building
TC5	40%	48%
TC6	51%	55%
TC7	0%	0%
TC8	0%	0%

While TC7 and TC8 result in CO₂ being maintained at desirable levels, there are implications for heating energy of the buildings. When the space is over-ventilated, good indoor air quality is maintained, but energy consumption may be compromised. Therefore, there may be a tolerance for CO₂ levels exceeding the threshold for a short period of time, if RH levels and heating energy is optimized. Ventilation heat loss energy for each test case is further discussed in the next section.

7.3.5.3 Energy: Ventilation Heat Loss

Heat loss of the buildings can occur through the following ways:

1. Transmission losses to the exterior through the building envelope,
2. Radiation heat losses,
3. Ventilation heat losses.

Given that the building envelope characteristics, indoor, and outdoor temperatures are similar for each building during each test case, the radiation and transmission heat losses can be considered equal. For a given ventilation scheme, if the ventilation rates are the same in both buildings, the ventilation heat losses are also considered equal.

However, ventilation heat loss varies between the buildings where demand-controlled ventilation results in different ventilation rates over time. The ventilation heat loss for TC5 to TC8 is calculated as per Equation 10:

Equation 10. Ventilation heat loss (J/s)

$$Q = \dot{m} \cdot c_p \cdot \Delta T$$

Q = ventilation heat loss [J/s]

\dot{m} = airflow (ventilation) rate [m^3/s]

c_p = specific heat of dry air, [1007 J/kg·°C]

ΔT = indoor-outdoor temperature differential [°C]

Greater temperature differentials between the indoors and the outdoors corresponds to greater heating demand. Similarly, greater mass flow rate \dot{m} also corresponds to greater heat loss.

Figure 98 and Figure 99 show the ventilation heat loss of the test and control buildings under TC5 as calculated by Equation 10, in comparison to the indoor and outdoor temperature, and ventilation rate respectively. Under TC5, the ventilation rate is constant and nearly equal in both buildings; therefore the heating energy demand is consistent between both buildings.

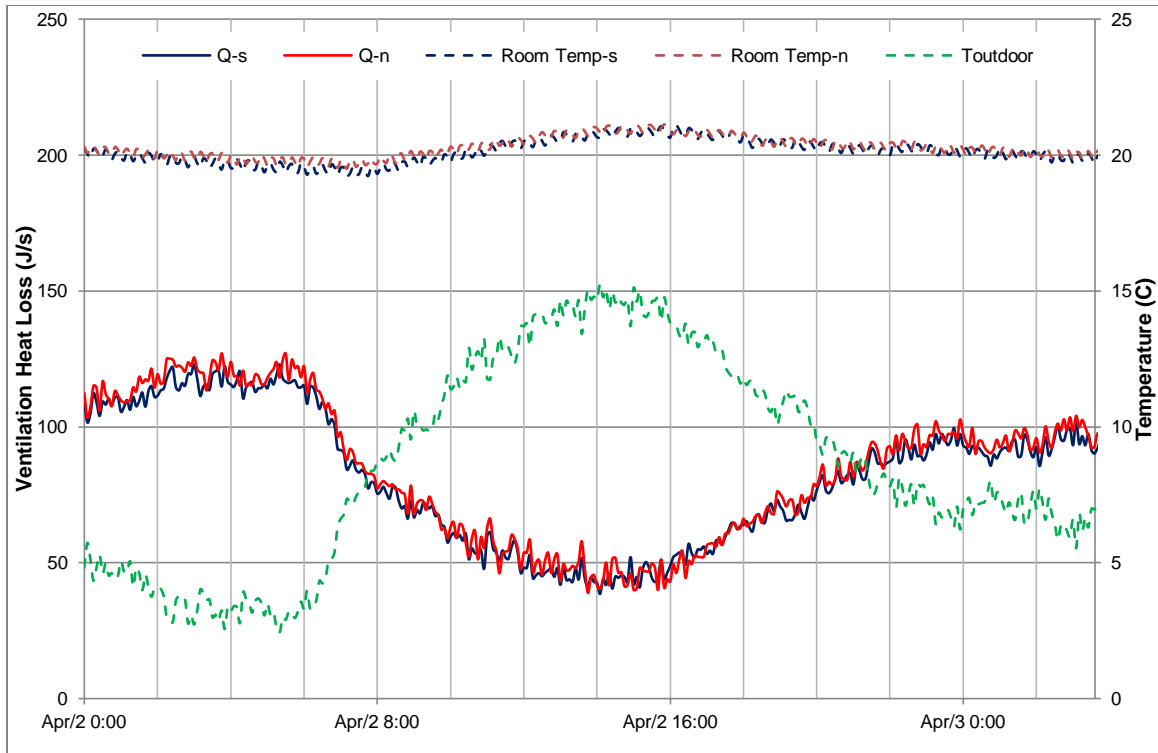


Figure 98. Ventilation heat loss, indoor and outdoor temperatures for the control building (red) and test building (blue), and outdoor temperatures under TC5 – constant ventilation

As the difference in indoor and outdoor temperatures increase, so do ventilation heat losses. For example, at night time between midnight and 6am on April 2nd, the outdoor temperatures hover around 3°C, which means conditioned air that is exhausted from the buildings is replaced with colder air. This results in increased heating demand on the buildings’ heating system to maintain the interior temperature at 20°C. The ventilation heat loss during this period is approximately 100 to 125 J/s. On the same day in the afternoon, the outdoor temperature peaks at 15°C and ventilation heat loss ranges between 40 to 60 J/s, approximately half the heat loss rate of the night time.

In TC5, since the ventilation rate, \dot{m} , is constant, variations in heat loss due to ventilation air displacement vary purely on temperature differential between the interior and the exterior.

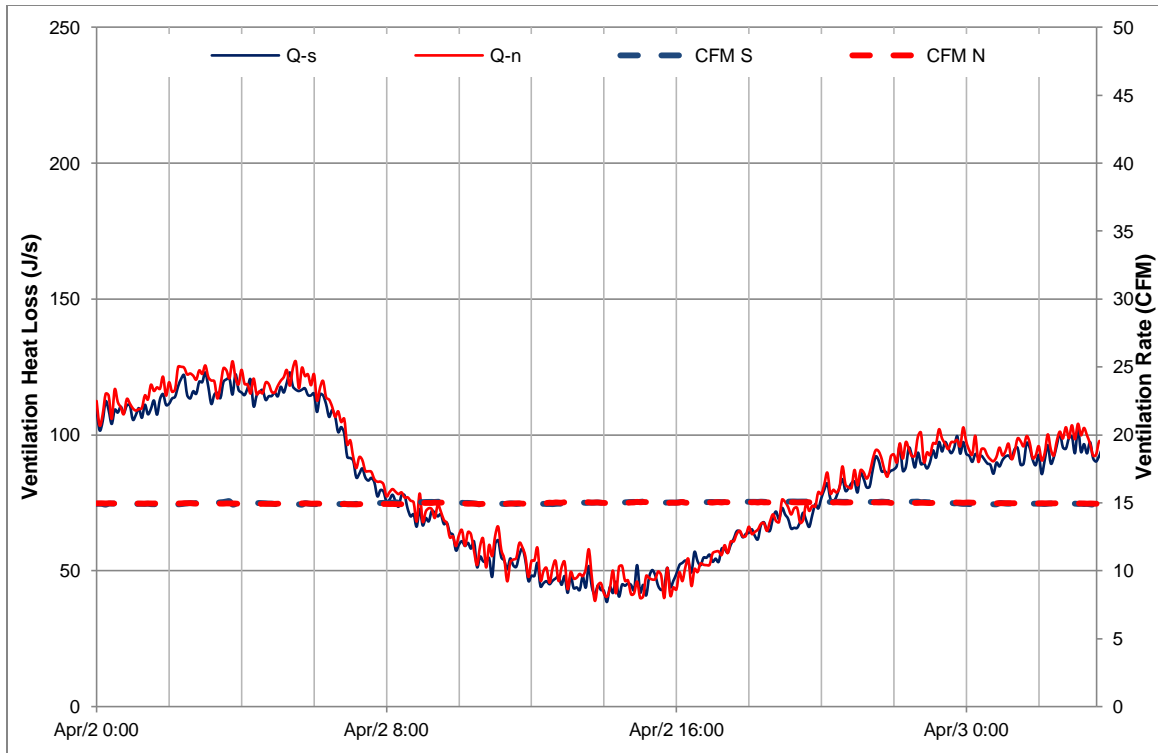


Figure 99. Ventilation heat loss, and ventilation rate for the control building (red) and test building (blue) under TC5 – constant ventilation

Figure 100 and Figure 101 similarly show the ventilation heat losses, indoor and outdoor temperatures, and ventilation flow rate, for time-controlled ventilation under TC6. Periods of maximum ventilation correspond to high ventilation heat loss, and minimum ventilation with low ventilation heat loss. For this test case, the ventilation heat loss is consistent between both buildings as the two parameters \dot{m} and ΔT are the same at a given time for the two buildings.

Change in \dot{m} proportionally increases the ventilation heat loss rate. As a result, the ventilation heat loss has the potential to increase four-fold as the ventilation scheme steps between 7.5 CFM and 30 CFM. Changes in outdoor temperatures also dictate the magnitude of heat loss at a given time. For example, ΔT between the exterior and the interior ranges from a maximum of 17°C during night time to 3°C in the afternoon for the period shown. The combined variations between both \dot{m} and ΔT result in the ventilation heat loss patterns seen in the figures.

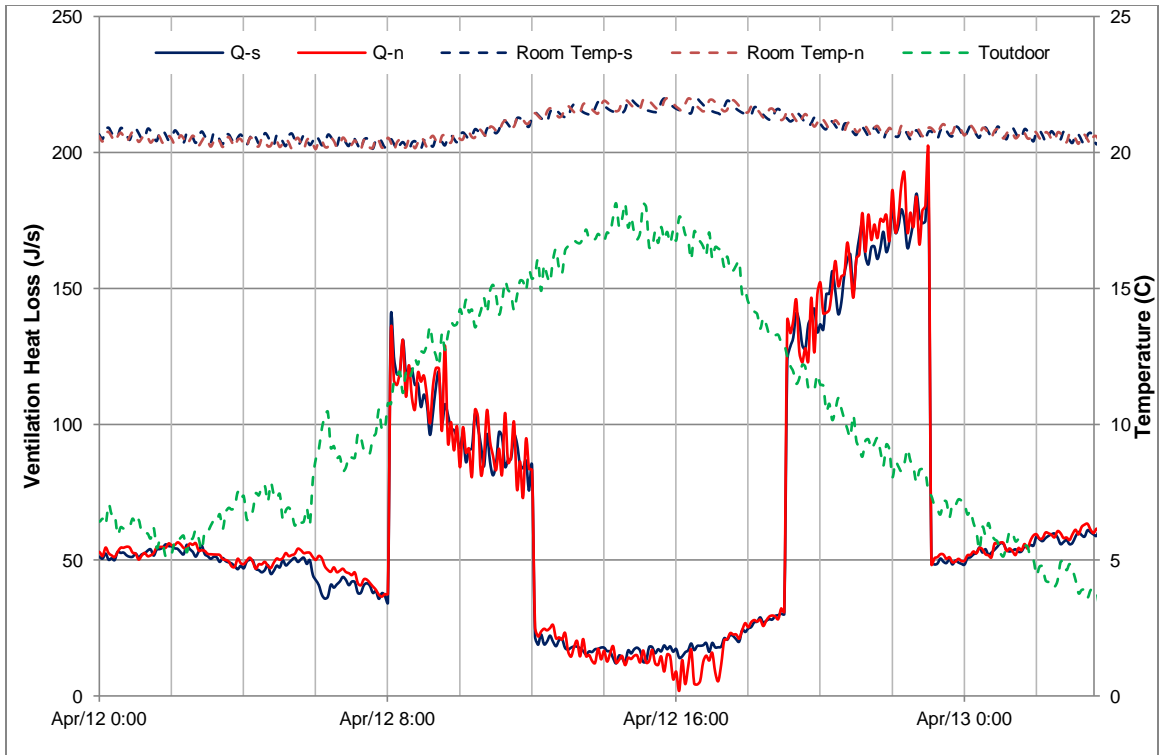


Figure 100. Ventilation heat loss, indoor and outdoor temperatures for the control building (red) and test building (blue), and outdoor temperatures under TC6 – time-controlled ventilation

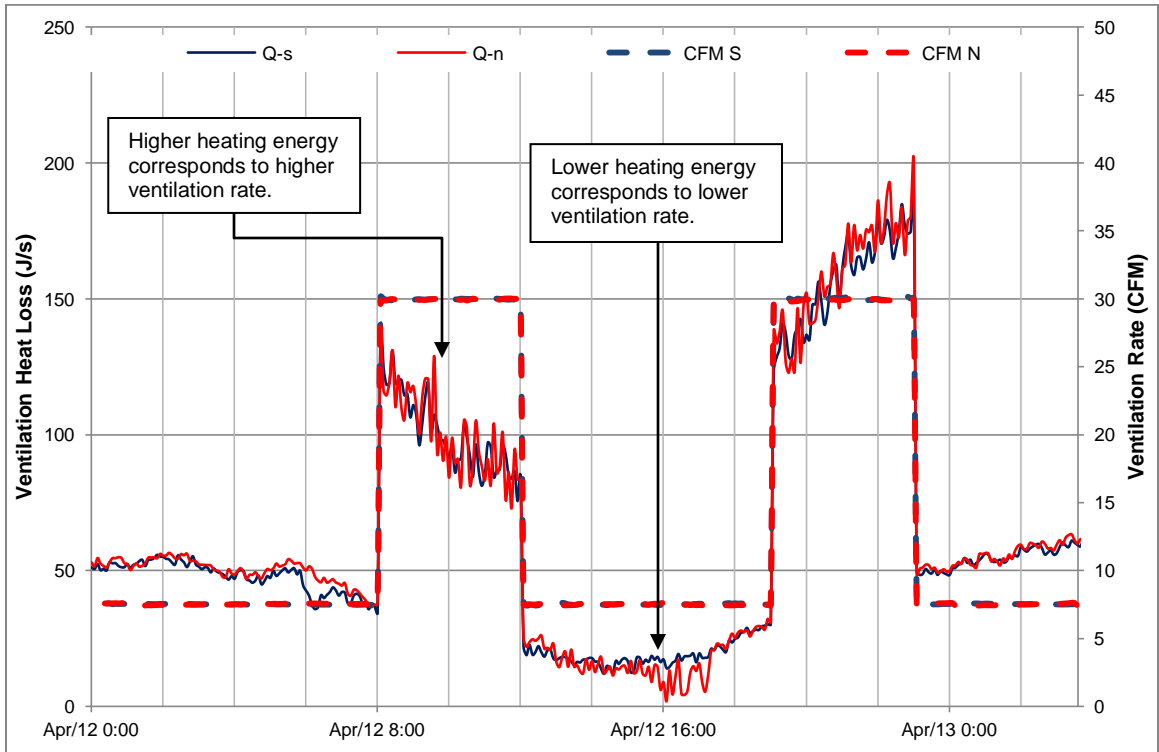


Figure 101. Ventilation heat loss, ventilation rate for the control building (red) and test building (blue) under TC6 – time-controlled ventilation

Figure 102 and Figure 103 show the ventilation heat loss under RH-controlled ventilation. This is the only test case where the parameter \dot{m} may be different between the two buildings at a given point. Nonetheless, the ventilation heat losses do not deviate much between the two buildings, except for a period during peak moisture loading and maximum ventilation rate. During this period, the quick response of the relative humidity in the control building cause the relative humidity levels and the ventilation rate to dip below the test building. For this brief period, \dot{m} in the control building is lower than \dot{m} in the test building, and thus heat loss in the test building exceeds those in the control building. This depicts the mechanisms under which slow response of moisture buffering materials to changes in relative humidity levels can actually be detrimental to energy performance.

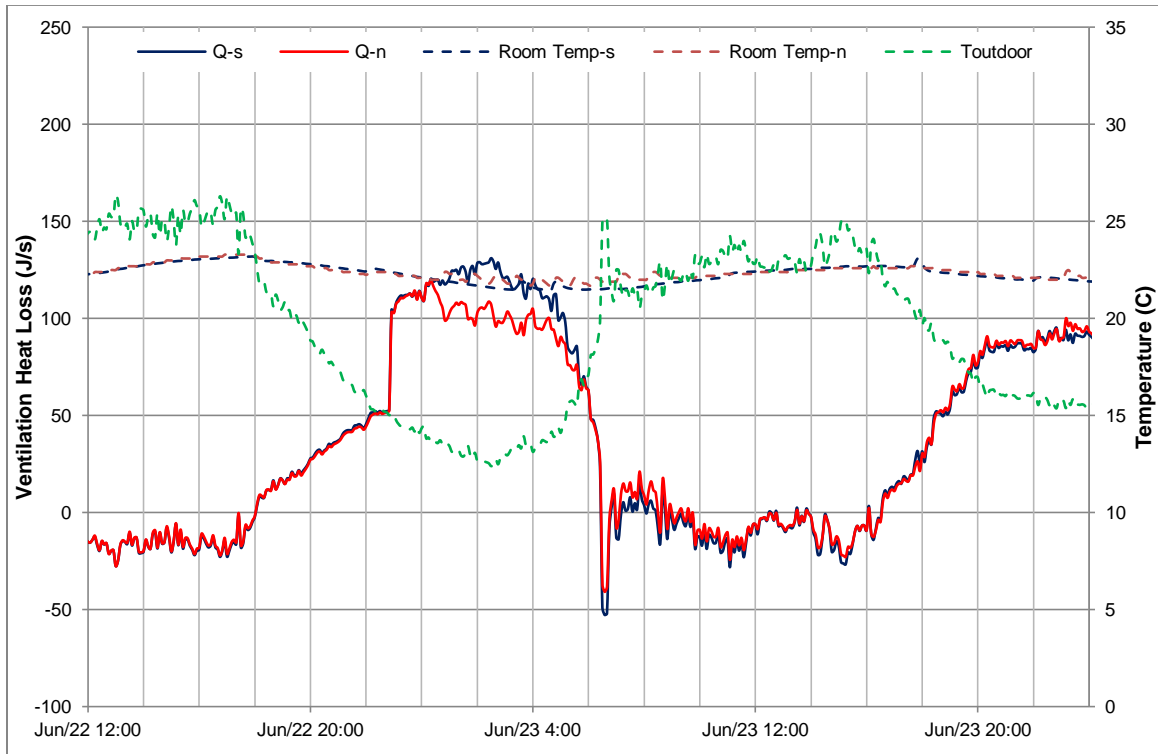


Figure 102. Ventilation heat loss, indoor and outdoor temperatures for the control building (red) and test building (blue), and outdoor temperature under TC7 – RH-controlled ventilation

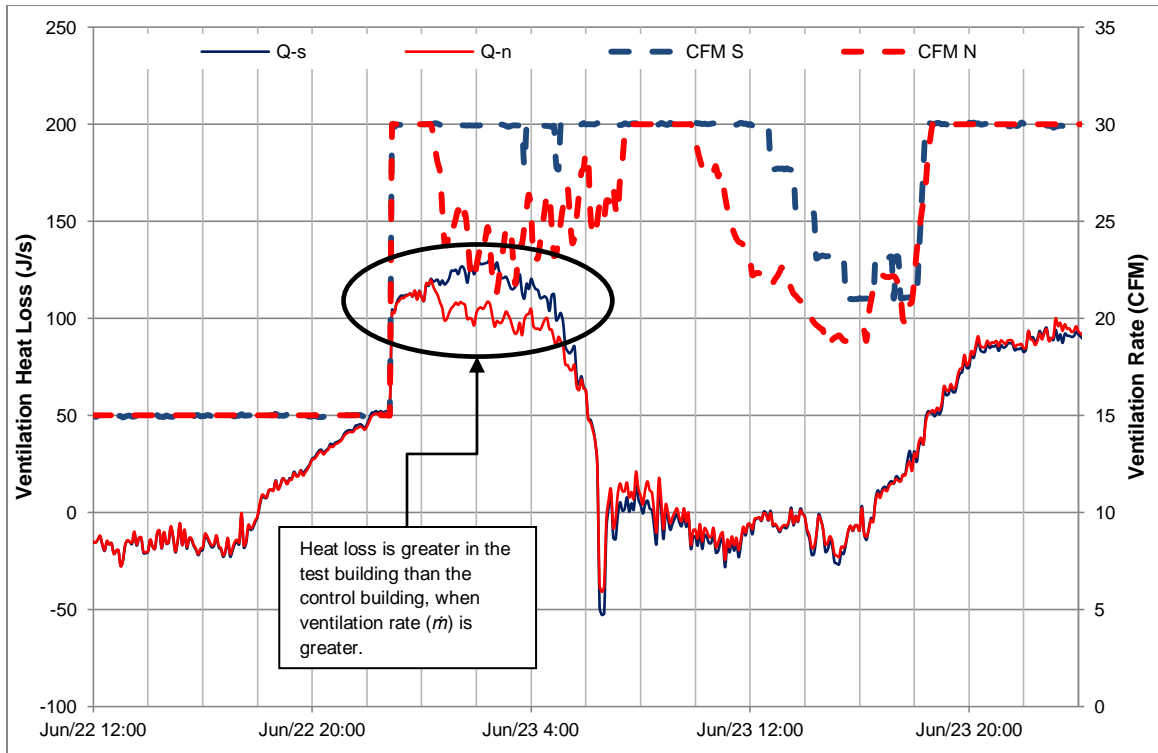


Figure 103. Ventilation Heat Loss and ventilation rate for the control building (red) and test building (blue) under TC7 – RH-controlled ventilation

It should be noted that when ventilation heat loss is negative, this corresponds to cooling in the buildings. Since TC7 and TC8 were undertaken in the summer months, air conditioning was required to maintain indoor temperatures near 20°C. Cooling was provided by way of a stand-alone air-conditioning unit.

Figure 104 and Figure 105 show ventilation heat loss, indoor and outdoor temperatures, and ventilation flow rate, for CO₂-controlled ventilation. The heat loss is also consistent under TC8 between both buildings as the two parameters \dot{m} and ΔT are the same at a given time in the two buildings.

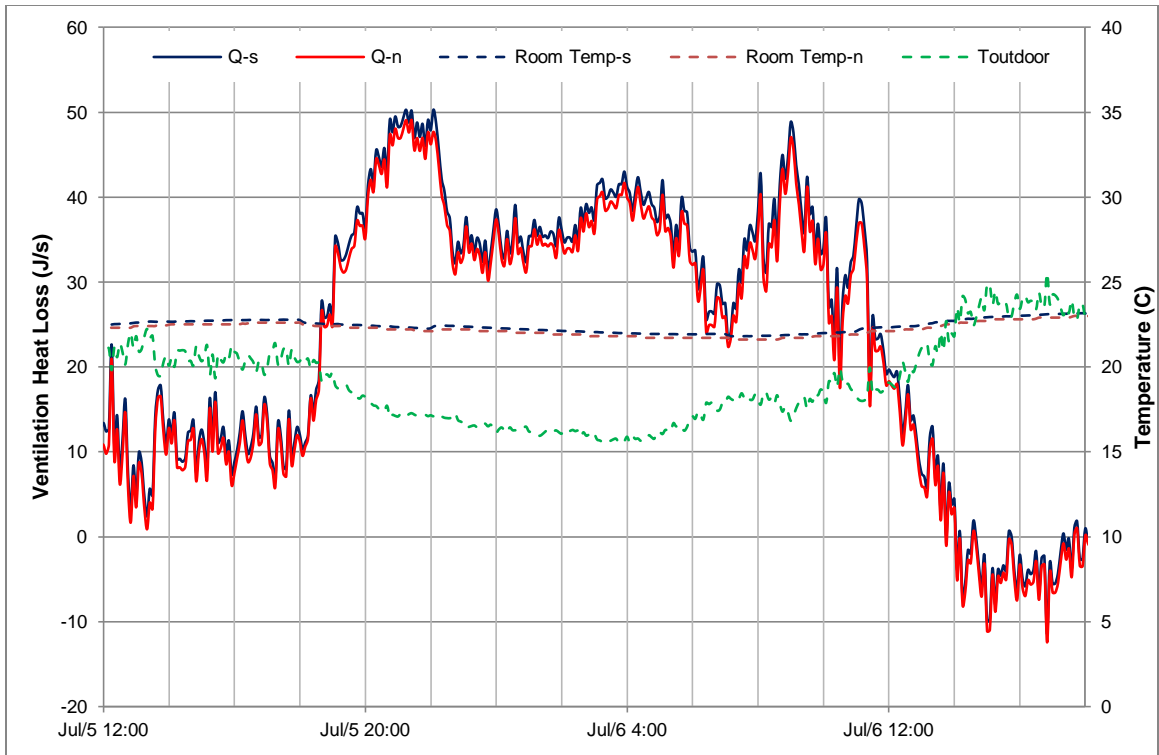


Figure 104. Ventilation heat loss, indoor and outdoor temperatures for the control building (red) and test building (blue), and outdoor temperature under TC8 – CO₂-controlled ventilation

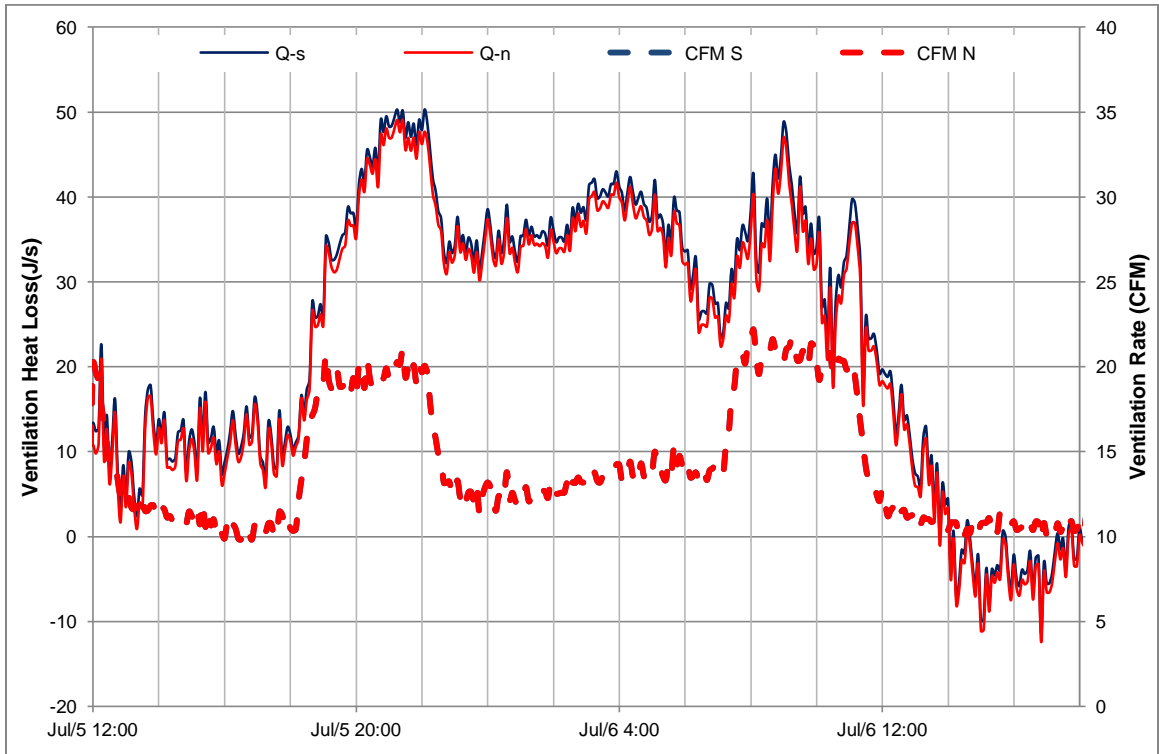


Figure 105. Ventilation heat loss and ventilation rate for the control building (red) and test building (blue) under TC8 – CO₂-controlled ventilation

In order to compare the ventilation heat loss as a result of the each ventilation scheme directly, the energy required to maintain the interior temperature set points at around 20°C is obtained. The ventilation heat loss energy is determined by calculating the estimated area under each Q curve.

The area estimation calculation is done as per Equation 11.

Equation 11. Ventilation heat loss energy (J)

$$E = \sum \frac{(Q_2 + Q_1)}{2} \cdot (t_2 - t_1)$$

Q_1, Q_2 = ventilation heat loss [J/s] at time $t=t_1$ and $t=t_2$ respectively

$t_2 - t_1$ = change in time between values Q_1 and Q_2 , taken at 5 minutes for each reading for the field testing

For consistency, the ventilation heat loss energy for each building is calculated over a 28 hour period as shown in Figure 106. Note that cooling energy (area between negative Q values and 0 J/s) was included as an absolute value in the summation to include both heating and cooling energy.

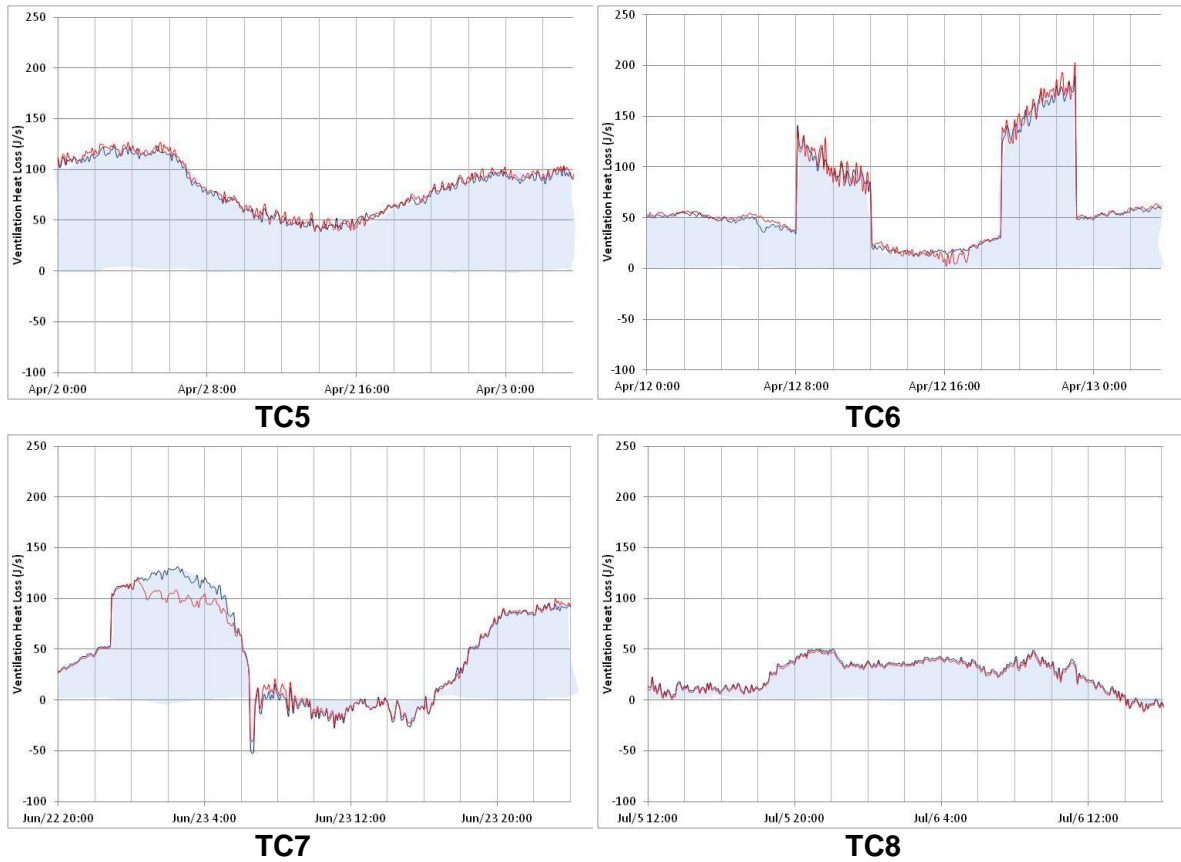


Figure 106. Area under each ventilation heat loss curve used for calculation of heat loss energy under TC5 to TC8

Figure 107 shows a summary of the total energy due to ventilation heat loss for each building under each test case. Energy is calculated in kilojoules, however, values are also converted to and indicated in kilowatt-hours above each bar for comparison.

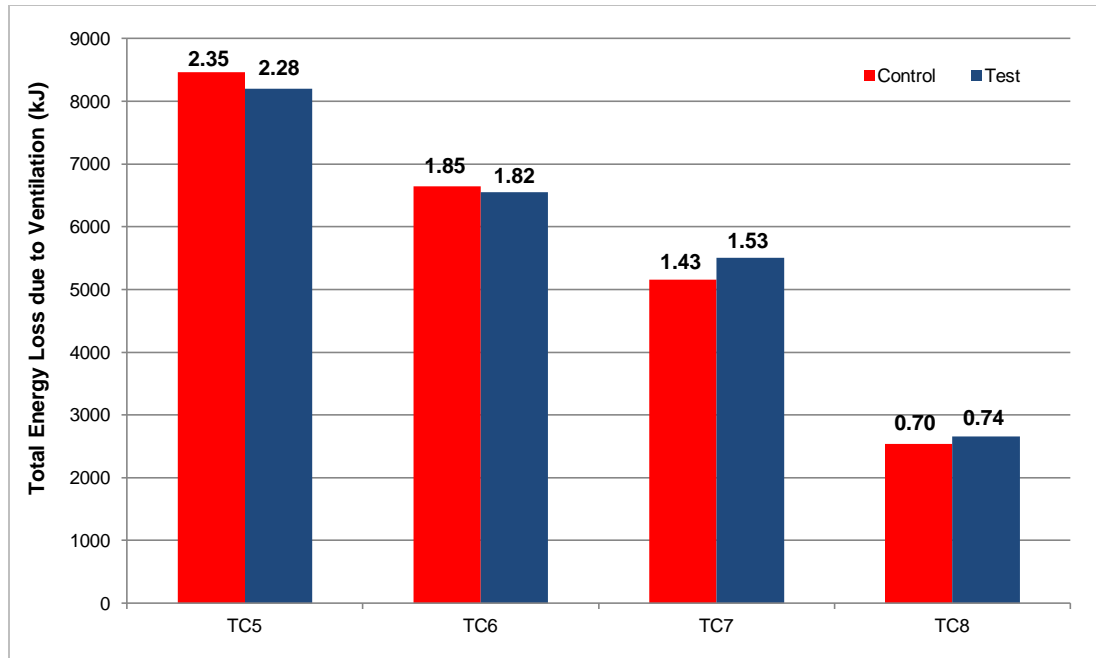


Figure 107. Total energy loss (heating and cooling) due to ventilation for a duration of 28 hours under test cases TC5 to TC8. Values indicated above each bar are energy loss in kilowatt-hours.

In general, the following conclusions can be drawn from the results above:

1. A direct comparison between TC5 and TC6 can be made given that these test cases took place within the same time of year (April) and same time of day for the 28-hour duration (from day-1 at midnight to day-2 at 4AM). Based Figure 107, the time-controlled ventilation scheme results in 20% energy savings in both buildings. This energy saving is achieved without compromising indoor humidity levels, especially in the test building where moisture buffering potential allows regulation of humidity peaks. Conversely, indoor air quality in terms of indoor CO₂ levels are most adversely affected under time-controlled ventilation, remaining above 1000 PPM for approximately 50% of the monitoring period.
2. Test cases TC7 and TC8 show improved ventilation energy savings in comparison to the latter two test cases. TC7 results in approximately 35% ventilation heating and cooling energy savings, and TC8 results in approximately 70% savings compared to TC5 for both buildings. However, since these test cases took place in the months of June and July

respectively, their comparison to TC5 and TC6 can be misleading, given the outdoor temperature dependence of ventilation heat loss. Moreover, the 28-hour duration window for energy calculation was taken at different times of day than TC5 and TC6 due to availability of data. Refer to Figure 106 for the time durations for energy calculation of each test case. RH-demand and CO₂-demand ventilation schemes produced the best indoor air quality, with CO₂ levels never exceeding 1000 PPM during the monitoring period. However, indoor humidity levels were generally above acceptable levels for thermal comfort.

8 CONCLUSION

This chapter concludes this research with final remarks, limitations and areas for improvements, and potential future or follow-up research.

8.1 Concluding Remarks

This research is based on developing an optimal solution to indoor moisture, energy efficiency and building durability, in a high occupant density residential setting. The importance of energy efficiency was highlighted in the introductory chapter. The issues related to high indoor moisture and uncertainty in moisture loading were discussed. The potential of moisture buffering materials as a means to optimize energy efficiency and indoor moisture were explored from different literature. All of this was put into perspective by highlighting findings from a reference building of a low-income housing building in Vancouver with durability and high indoor humidity issues.

What is the most viable way of utilizing moisture buffering potential of gypsum board in the marine climate of the Lower Mainland of BC to manage indoor humidity in a residential setting?

To answer this question, field experimentation was done to evaluate the effectiveness of both passive measures and active measures of managing indoor moisture, while also monitoring the indoor air quality in terms CO₂ concentration, and ventilation heat loss.

Based on TC1 to TC4, it is evident that moisture buffering of gypsum board is effective in regulating relative humidity levels at the acceptable range as a passive measure, when adequate ventilation is provided. Adequate ventilation here is defined as the ASHRAE recommended rate based on occupancy and area of ventilated space. This is true for both normal occupancy and high occupancy cases. In an under-ventilated space, high indoor moisture cannot be resolved with moisture buffering of materials alone. Therefore adequate ventilation is required as the bare minimum. When designed in tandem with proper ventilation design, moisture buffering can help

to regulate changes in relative humidity levels due to moisture loading peaks. The results from TC4 showed that moisture buffering can also be effective in regulating indoor humidity, even under high moisture loading, when ASHRAE recommended ventilation rates are provided. This has positive implications on the use of moisture buffering materials in residential settings with higher than normal moisture loading, which meet minimum ventilation requirements set out by codes and standards, which may require a passive measure of controlling indoor humidity.

Based on existing knowledge on the moisture buffering of materials, it may be possible to create a suitable indoor environment by using alternative finishing materials that may have different material properties than conventional gypsum board, which may maximize the moisture buffering ability. On this notion, there could be an opportunity to reduce ventilation energy demand in certain cases. This is an area that needs more exploratory studies on emerging new materials in the market, many of which are marketed as “green” or sustainable alternatives to painted gypsum board for various reasons.

TC5 to TC8 seem to provide competing benefits when it comes to managing moisture or managing indoor air quality. For example, under time-controlled ventilation, relative humidity levels are best regulated, whereas CO₂ levels are exceeded. Conversely, under CO₂-demand ventilation, indoor air quality is best maintained, whereas relative humidity levels are exceeded. In this regard, more investigation is required to determine the best option for optimizing both indoor humidity and indoor air quality. Time-controlled ventilation is the only ventilation scheme that works best in tandem with moisture buffering potential of the test building in regulating indoor humidity peaks in the field testing.

When it comes to ventilation heat loss, it is difficult to compare TC5 to TC8 directly, however, a direct comparison between TC5 and TC6 reveals that with time-controlled ventilation energy 20% heating energy saving is achieved without compromising indoor humidity levels, especially

in the test building where moisture buffering potential allows regulation of humidity peaks. Indoor air quality performance under constant ventilation is comparable, but slightly better compared to time-controlled ventilation, with indoor CO₂ levels exceeding 1000 PPM for approximately 40 to 48% of the monitoring period compared to 51 to 55%.

Under RH- and CO₂-controlled ventilation schemes, more significant ventilation energy savings are realized for both cooling and heating. Direct comparison to the former two test cases is difficult given the variable time of year the tests were undertaken and the dependency of outdoor temperature on the magnitude of ventilation heat loss.

Moisture buffering effect of unpainted gypsum board in the test building generally helped the building performance in regulating interior humidity levels under low ventilation rates. Conversely, under demand-controlled ventilation schemes, especially when the rate of ventilation is generally higher, the moisture buffering phenomenon is negligible.

8.2 Limitations and Improvements

This research does not provide guidelines for practicing engineers on how to incorporate moisture buffering materials in design. The basis of this research is exploratory, and a starting point for more research projects to come.

There are areas upon which this research can be improved upon. These are listed below:

- Field testing season: Due to time required for commissioning of the test facilities, some test cases were completed in the summer months and are not representative of winter conditions outlined in the reference study building. Field testing should be conducted in winter months during high precipitation and outdoor relative humidity levels to present worst case moisture loading scenarios.

- Optimized ventilation algorithms: It was found that different ventilation schemes have competing benefits on indoor air quality and indoor moisture management. It may be possible to develop more optimized ventilation schemes and algorithms first by way of computer modeling. Modeling results can then be validated with field testing.
- Field testing versus laboratory testing: Field testing has many benefits. It provides insight on the behaviour of buildings, their materials, systems, and performance when exposed to real climatic conditions. Unfortunately, climatic conditions are unique at a given time, and testing undertaken at different time periods cannot be reasonably compared. Laboratory testing allows for climatic conditions to be controlled, and comparisons can be more easily made. However, laboratory testing may not be reflective of actual conditions. For this research, test cases undertaken at different times can be compared on a higher level; however, in-depth data processing cannot be undertaken without taking outdoor conditions out of the equation.

8.3 Areas for Future Research

There are areas upon which this research can be expanded upon. These are listed below:

- More investigation is required to determine the most optimal moisture management method in the marine climate of Lower Mainland. This can be in the form of additional test cases, or utilizing established whole building models to perform sensitivity analyses on parameters such as ventilation rates and schemes, moisture loading rates and durations, and outdoor climate conditions.
- There are also alternative hygroscopic materials to gypsum board for interior finishing, which can be used to maximize the moisture buffering potential of a space. Although testing has been done in the past in laboratory settings, more field testing is needed to determine the room level performance of various finishing materials, and their benefits to applications in the field. Similarly, the evaluation of coatings such as paint or primer

systems can aid determine the limitations of moisture buffering potential of gypsum board at a room level with common finishes.

- Quantification of moisture absorbed from the air in gypsum board and desorbed back into the air under different conditions can aid in determination of the best way to optimize active moisture management methods, and aid in determining the best approach to regulating indoor humidity, while minimizing ventilation heat loss and maintaining good indoor air quality. It can also help designers understand the extent of moisture buffering potential at the room level.
- The field testing was undertaken under winter ventilation and moisture loading conditions. More investigation with regards to changes in occupants' behaviour and moisture loading during different seasons, as well as the effect of opening windows in heating seasons on ventilation or air change rate can aid in best utilizing the phenomenon under various seasonal conditions.
- Sensitivity analysis on ventilation algorithms with the aid of building models can help to determine the optimum scheme that will ensure acceptable indoor humidity levels, indoor air quality, while minimizing ventilation heat loss. The parameters that can be evaluated for sensitivity include the maximum and minimum ventilation rates, demand control ventilation upper and lower thresholds, on-times for time-controlled ventilation, and percentage of re-circulated air. Further testing can then be pursued in smart ventilation systems, and more robust ventilation algorithms.

9 REFERENCES

- Arlian, L.G. (1992). Water balance and humidity requirements of house dust mites. *Experimental and Applied Acarology*, 16:15–35.
- ASHRAE. (2009). *Standard 160-2009, Criteria for Moisture-Control Design Analysis in Buildings*. Atlanta, GA: American Society of Heating, Refrigerating and Air-Conditioning Engineers, Inc.
- ASHRAE. (2010). *Standard 55-2010, Thermal Environmental Conditions for Human Occupancy*. Atlanta, GA: American Society of Heating, Refrigerating and Air-Conditioning Engineers, Inc.
- ASHRAE. (2010). *Standard 90.1, Energy Standard for Buildings Except Low-Rise Residential Buildings*. Atlanta, GA: American Society of Heating, Refrigerating and Air-Conditioning Engineers, Inc.
- ASHRAE. (2013). *Handbook of Fundamentals*. Atlanta, GA: American Society of Heating, Refrigerating and Air Conditioning Engineers.
- ASHRAE. (2013). *Standard 62.1-2013, Ventilation for Acceptable Indoor Air Quality*. Atlanta, GA: American Society of Heating, Refrigerating and Air-Conditioning Engineers, Inc.
- ASHRAE. (2013). *Standard 62.2-2013, Ventilation and Acceptable Indoor Air Quality in Low-Rise Residential Buildings*. Atlanta, GA: American Society of Heating, Refrigerating and Air-Conditioning Engineers, Inc.
- ASTM (2012). *ATSM Standard D6245, Standard Guide for Using Indoor Carbon Dioxide Concentrations to Evaluate Indoor Air Quality and Ventilation*. Philadelphia: American Society for Testing and Materials, D6245-12.
- ASTM. (2011). *Standard E1827-11 Standard Test Methods for Determining Airtightness of Buildings Using an Orifice Blower Door*. Philadelphia: American Society for Testing and Materials, E1827-11.
- Atwal, L., & Mora, R. (2014). *Ventilation for a House as a System*. Presented at the 13th International Conference on Indoor Air Quality and Climate, Hong Kong.
- Berg-Munch, B., Clausen, G., & Fanger, P. O. (1986). Ventilation requirements for the control of body odor in spaces occupied by women. *Environment International*, 12(1-4), 195–199. doi:10.1016/0160-4120(86)90030-9
- Christian, J. E. (2009). *Moisture Sources*. In H. R. Trechsel & M. Bomberg (Eds.), *Moisture control in buildings: the key factor in mold prevention* (2nd ed., pp. 103–109). West Conshohocken, PA: ASTM International.
- Cunningham, M.J. (2003) *The Building Volume with Hygroscopic Materials – An Analytic Study of a Classical Building Physics Problem*. *Building and Environment* 38: 329–337.

- Dlugokencky, E., & Pieter, T. (2016, February). Trends in Atmospheric Carbon Dioxide. Retrieved from <http://www.esrl.noaa.gov/gmd/ccgg/trends/global.html>
- El Diasty, R., Fazio, P., & Budaiwi, I. (1992). Modelling of indoor air humidity: the dynamic behaviour within an enclosure. *Energy and Buildings*, 19(1), 61–73.
- Fanger, P. O. and Berg-Munch, B. (1983) Ventilation requirements for the control of body odor. Proc. of Engineering Foundation Conference on Management of Atmospheres in Tightly Enclosed Spaces, ASHRAE, Atlanta, GA.
- Hameury, S. (2006). The hygrothermal inertia of massive timber constructions. Ph.D. Thesis. KTH, Royal Institute of Technology, Stockholm, Sweden.
- Hameury, S. (2007). Influence of coating systems on moisture buffering capacity of panels of *pinus sylvestris* L. *Wood Material Science and Engineering*, 2(3-4), 97–105.
- Harriman, L. G., Czachorski, M., Witte, M. J., Kosar, D. R. (1999). "Evaluating active desiccant systems for ventilating commercial buildings." *ASHRAE Journal* 41 (10): 28-37.
- HPO. (2006). Building Envelope Maintenance Matters Bulletin No. 3: Avoiding Condensation Problems. Home Owner Protection Office Branch of BC Housing. Retrieved from <http://www.hpo.bc.ca/files/download/MMR/MM3.pdf>
- Isetti, C., Laurenti, L., & Ponticiello, A. (1988). Predicting vapour content of the indoor air and latent loads for air-conditioned environments: Effect of moisture storage capacity of the walls. *Energy and Buildings*, 12(2), 141–148.
- Jone, R., (1993). Modelling water vapour conditions in buildings. *Building Services Engineering Research and Technology*. 14(3): 99-106.
- Kalamees, T., Korpi, M., Vinha, J., & Kurnitski, J. (2009). The effects of ventilation systems and building fabric on the stability of indoor temperature and humidity in Finnish detached houses. *Building and Environment*, 44, 1643–1650.
- Kalamees, T., Vinha, J., & Kurnitski, J. (2006). Indoor Humidity Loads and Moisture Production in Lightweight Timber-frame Detached Houses. *Journal of Building Physics*, 29(3), 219–246. doi:10.1177/1744259106060439
- Kuenzel, H., Holm, A., Sedlbauer, K., Antretter, F., & Ellinger, M. (2004). Moisture buffering effect of interior linings made from wood or wood based products (No. HTB-04/2004/e). Fraunhofer Institut Bauphysik.
- Kuenzel, H., Holm, A., Sedlbauer, K., Antretter, F., & Ellinger, M. (2004). Moisture buffering effect of interior linings made from wood or wood based products (No. HTB-04/2004/e). Fraunhofer Institut Bauphysik. Retrieved from http://www.ibp.fraunhofer.de/content/dam/ibp/en/documents/oeVB_eng_3_tcm1021-30995.pdf

- Kunzel, H. (1965). Die Feuchtigkeitsabsorption von Innenoberflächen und Inneneinrichtungen, Report of Building Research, 42: 102–116.
- Kunzel, H. (1968). Die Feuchtigkeitsabsorption der Innenoberflächen von Beton- und Kunststoffwänden, 51: 79–97.
- Li, Y., Fazio, P., & Rao, J. (2010). An investigation of moisture buffering performance of wood paneling at room level and its buffering effect on a test room. *Building and Environment*, 42, 205–216.
- Loudon, A.G., (1971). The effects of ventilation and building design factors on the risk of condensation and mould growth in dwellings. Current Paper 31/71. United Kingdom: Building Research Station, Department of the Environment.
- Lstiburek, J. (2002). Relative Humidity (No. Research Report - 0203). Retrieved from <http://www.buildingscience.com/documents/reports/rr-0203-relative-humidity>.
- Lu, X. (2003). Estimation of indoor moisture generation rate from measurement in buildings. *Building and Environment*, 38(5), 665–675.
- Mitamuta, T.; Hasegawa, K.; Yoshino, H.; Matsumoto, S. & Takahashi, N. (2004). Experiment for moisture buffering and effects of ventilation rate, volume rate of hygrothermal materials. 5th International Conference of Indoor Air Quality, Ventilation and Energy Conservation, Toronto.
- National Council on Welfare. (2007). First Nation, Métis and Inuit children of youth: Time to act. Catalogue No. HS54-1/2007E.
- Osanyintola, O. F., & Simonson, C. J. (2006). Moisture buffering capacity of hygroscopic building materials: Experimental facilities and energy impact. *Energy and Buildings*, 38(10), 1270–1282.
- Ouazia, B., Manning, M., Swinton, M., & Barhoun, H. (2008). Improving moisture management and cooling energy use in residential buildings. Presented at the 5th Windsor Conference: Air Conditioning and the Low Carbon Cooling Challenge, Windsor, UK.
- Padfield, T., & Jensen, L. A. (2011). Humidity buffering of building interiors by absorbent materials (Vol. 1). Presented at the 9th Nordic Symposium on Building Physics - NSB 2011.
- Pedram, S., & Tariku, F. (2014). Moisture Buffering Effect of Gypsum Board in a Marine Climate: A Field Experimental Study. *Advanced Materials Research* (Vol. 1051, pp. 763–773). Trans Tech Publ.
- Pedram, S., Tariku, F. (2015). Determination of Representative Daily Moisture Production Profile of Occupants in a Residential Setting. Proceedings of the International Conference on Energy and Environmental Systems Engineering (EESE2015), May 17-18, 2015, Beijing, China.

- Plathner, P., & Woloszyn, M. (2002). Interzonal air and moisture transport in a test house: experiment and modelling. *Building and Environment*, 37, 189–199.
- Ramos, N. (2007) The importance of hygroscopic inertia in the hygrothermal behaviour of buildings (in Portuguese). Ph.D. Thesis. Department of Civil Engineering, FEUP, Porto, Portugal.
- Ramos, N. M. M., & de Freitas, V. P. (2008). Daily Hygroscopic Inertia Classes: Application in a Design Method for the Prevention of Mould Growth in Buildings. Presented at the 11DBMC International Conference on Durability of Building Materials and Components, Istanbul, Turkey.
- Ricketts, L., & Straube, J. (2014). A Field Study of Airflow in Mid to High-Rise Multi-Unit Residential Buildings. In 14th Canadian Conference on Building Science and Technology Toronto, Ontario. Retrieved from <http://obec.on.ca/sites/default/uploads/files/members/CCBST-Oct-2014/A3-2-a.pdf>
- Rode, C. (2005). Moisture Buffering of Building Materials (No. BYG·DTU R-126). Department of Civil Engineering Technical University of Denmark.
- Roppel, P., Brown, W. C., & Lawton, M. (2007). Modeling of Uncontrolled Indoor Humidity for HAM Simulation of Residential Bldgs.pdf. In Buildings X Conference.
- Roppel, P., Lawton, M., & Brown, W. C. (2009). Setting Realistic Design Indoor Conditions for Residential Buildings by Vapor Pressure Difference. *Journal of ASTM International*, 6(9).
- Roppel, P., Lawton, M., & Hubbs, B. (2007). Balancing the Control of Heat, Air, Moisture, and Competing Interests. In Proceedings of the 11th Canadian Building Science and Technology Conference.
- Salonvaara, M., Ojanen, T., Holm, A., Künzeli, H. M., & Karagiozis, A. N. (2004). Moisture buffering effects on indoor air quality-experimental and simulation results. In Proceedings of Buildings IX, Clearwater, Florida.
- Sedlbauer, K. (2002). Prediction of mould growth by hygrothermal calculation. *Journal of Building Physics*, 25(4), 321–336.
- Simonson, C., Salonvaara, M., & Ojanen, T. (2004). Moderating indoor conditions with hygroscopic building materials and outdoor ventilation. *ASHRAE TRANSACTIONS*, 110(2), 804–819.
- Straube, J. (2006). Moisture and Materials (No. Building Science Digest 138). Building Science Corporation. Retrieved from <http://www.buildingscience.com/documents/digests/bsd-138-moisture-and-materials>
- Straube, J., & DeGraauw, J. (2001). Indoor air quality and hygroscopically active materials. *ASHRAE TRANSACTIONS*, 107, 444–450.

- Svennberg, K. (2006). *Moisture Buffering in the Indoor Environment*. Ph.D. Thesis. Lund University, Lund, Sweden.
- Svennberg, K., Lengsfeld, K., Harderup, L.-E., & Holm, A. (2007). Previous Experimental Studies and Field Measurements on Moisture Buffering by Indoor Surface Materials. *Journal of Building Physics*, 30(3), 261–274.
- Tariku, F. (2008). *Whole Building Heat and Moisture Analysis*. Ph.D. Thesis. Concordia University, Montreal, Canada.
- Tariku, F., & Simpson, Y. (2014). Temperature and Humidity Distributions in Mid-rise Residential Building Suites. Presented at the 14th CCBST Conference, Toronto, Canada.
- Tariku, F., Kumaran, M. K., & Fazio, P. (2009). The need for an accurate indoor humidity model for building envelope performance analysis.
- Tariku, F., Kumaran, M.K., Fazio, P. (2011). Determination of Indoor Humidity Profile Using a Whole-Building Hygrothermal Model. *Building Simulations*. Vol. 4, No.1. pp. 61-78.
- Tariku, F., Simpson, Y., Pedram, S., Horn, D. (2013). Development of a Whole-Building Performance Research Laboratory for Energy: Indoor Environment and Building Envelope Durability Study. *Proceedings from ZEMCH 2013 International Conference*. Miami, FL.
- TenWolde, A., & Glass, S. V. (2009). Review of Moisture Balance models for residential indoor humidity. Presented at the 12th Canadian Conference on Building Science and Technology, Montreal, QC.
- TenWolde, A., & Walker, I. S. (2001). Interior Moisture Design Loads for Residences. *ASHRAE Buildings VIII Conference*.
- UNEP, Sustainable Buildings & Climate Initiative. (2009). *Buildings and Climate Change: Summary for Decision-Makers*. Retrieved from <http://www.unep.org/sbci/pdfs/SBCI-BCCSummary.pdf>
- Vereecken, E., Roels, S., & Janssen, H. (2011). In situ determination of the moisture buffer potential of room enclosures. *Journal of Building Physics*, 34(3), 223–246.
- Viitanen, H., Vinha, J., Salminen, K., Ojanen, T., Peuhkuri, R., Paajanen, L., & Lähdesmäki, K. (2010). Moisture and bio-deterioration risk of building materials and structures. *Journal of Building Physics*, 33(3), 201–224.
- Washington State Energy Code (2012). Title 51, Chapter 51-11, Section 51-11-1314 “Air Leakage.” Retrieved from <http://apps.leg.wa.gov/wac/default.aspx?cite=51-11-1314>
- Woloszyn, M. & Rode, C. (2008). *Annex 41 Whole Building Heat, Air and Moisture Response: Modeling and Principles and Common Exercises*, pp. 170-179 (ISBN 978-90-334-7057-8).
- Woloszyn, M., & Rode, C. (2008). *Modeling Principles and Common Exercises: Annex 41 Whole Building Heat, Air, Moisture Response*. France: International Energy Agency.

- Woloszyn, M., Kalamees, T., Olivier Abadie, M., Steeman, M., & Sasic Kalagasidis, A. (2009). The effect of combining a relative-humidity-sensitive ventilation system with the moisture-buffering capacity of materials on indoor climate and energy efficiency of buildings. *Building and Environment*, 44(3), 515–524.
- Wu, Y., Fazio, P., & Kumaran, M. K. (2007). Moisture buffering capacities of 5 north american building materials.
- Yaglou, C., Riley, E., & Coggins, D. (1936). Ventilation requirements. *ASHVE Transactions*, 42, 133–162.
- Yang, X. (2010). Investigation on moisture buffering of hygroscopic mats using full-scale experiment and HAM simulations. Ph.D. Thesis. Concordia University, Montreal, Canada.

10 PUBLICATIONS

Pedram, S., & Tariku, F. (2014). Moisture Buffering Effect of Gypsum Board in a Marine Climate: A Field Experimental Study. *Advanced Materials Research* (Vol. 1051, pp. 763–773). Trans Tech Publ.

Pedram, S., Tariku, F. (2015). Determination of Representative Daily Moisture Production Profile of Occupants in a Residential Setting. *Proceedings of the International Conference on Energy and Environmental Systems Engineering (EESSE2015)*, May 17-18, 2015, Beijing, China.

11 APPENDICES

11.1 APPENDIX A

PHOTOGRAPHS OF WBPRL TEST FACILITIES

PHOTOGRAPHS



WBPRL Test Buildings



WBPRL Test Buildings

PHOTOGRAPHS



Test Space in the Test (South) Building



Components of the Occupant Simulator Unit in the Control (North) Building

PHOTOGRAPHS



Components of the Occupant Simulator Unit in the Control (South) Building



RHT Sensors Suspended From Ceiling used for Measurement of Interior Conditions

PHOTOGRAPHS



RHT Sensors Suspended From Ceiling used for Measurement of Interior Conditions

11.2 APPENDIX B

RHT & CO₂ SENSOR DATA SHEETS

Vaisala INTERCAP® Humidity and Temperature Probe HMP60



The HMP60 for extreme conditions.

Features/Benefits

- Miniature-size humidity probe
- Low power consumption
- Measurement range:
0 ... 100 %RH; -40 ... +60°C
- Cable detachable with
standard M8 connector
- Rugged metal housing
- Interchangeable Vaisala
INTERCAP® Sensor
- Optional RS485 digital output
- Optional dew point output
- Applications: volume
applications, integration
into other manufacturers'
equipment, glove boxes,
greenhouses, fermentation
chambers, data loggers

HMP60

The HMP60 is a simple, durable and cost-effective humidity probe. It is suitable for volume applications, integration into other manufacturers' equipment, incubators, glove boxes, greenhouses, fermentation chambers, and data loggers.

Easy Installation

The probe cable has a screw-on quick connector for easy installation. Different cable lengths are available. Also other compatible M8 series cables can be used. Accessories are available for different installation needs.

Low Current Consumption

The HMP60 is suitable for battery-powered applications because of its very low current consumption.

Several Outputs

There are two configurable voltage outputs with relative humidity, temperature or dew point scaling. Four voltage output ranges are available.

Rugged Design

The HMP60 is designed for extreme conditions. The stainless steel body of the HMP60 is classified as IP65. The probe has a sealed structure and the sensor is protected by a membrane filter and a plastic grid, or optionally by a stainless steel filter.

Recalibration Not Needed

The Vaisala INTERCAP® Sensor is interchangeable. No recalibration is required; the sensor can simply be replaced, also in the field.

Technical Data

Performance

RELATIVE HUMIDITY	
Measurement range	0 ... 100 %RH
Typical accuracy	
temperature range	0 ... +40 °C
0 ... 90 %RH	±3 %RH
90 ... 100 %RH	±5 %RH
temperature range	-40 ... 0 °C, +40 ... +60 °C
0 ... 90 %RH	±5 %RH
90 ... 100 %RH	±7 %RH
Humidity sensor	Vaisala INTERCAP®
TEMPERATURE	
Measurement range	-40 ... +60 °C
Accuracy over temperature range	
+10 ... +30 °C	±0.5 °C
-40 ... +10, +30 ... +60 °C	±0.6 °C
DEW POINT	
Measurement range	-40 ... +60 °C
Typical accuracy	
temperature range	0 ... +40 °C
when dew point depression < 15 °C	±2 °C
temperature range	-40 ... 0 °C, +40 ... +60 °C
when dew point depression < 10 °C	±3 °C
dew point depression = ambient temperature - dew point	
ANALOG OUTPUTS	
Accuracy at 20 °C	±0.2 % of FS
Temperature dependence	±0.01 % of FS/°C

Inputs and Outputs

Operating voltage	5 ... 28 VDC / 8 ... 28 VDC with
(Use lowest available operating	5 V output
voltage to minimize heating.)	8 ... 28VDC with loop power
	converter
Current consumption	1 mA average, max. peak 5 mA
Start-up time	
probes with analog output	4 s at operating voltage
	13.5 ... 16.5 VDC
	2 s at other valid operating voltages
probes with digital output	1 s
Outputs	
2 channels	0 ... 1 VDC / 0 ... 2.5 VDC / 0 ... 5 VDC / 1 ... 5 VDC
1-channel loop-power converter (separate	
module, compatible with humidity accuracy only)	4 ... 20 mA
digital output (optional)	RS485 2-wire half duplex
External loads	
0 ... 1 V	R _L min 10 kΩ
0 ... 2.5 V / 0 ... 5 V	R _L min 50 kΩ

Operating Environment

Operating temperature	-40 ... +60 °C
Electromagnetic compatibility	EN 61326-1: Electrical equipment for measurement, control and laboratory use – EMC requirements – for use in industrial locations.

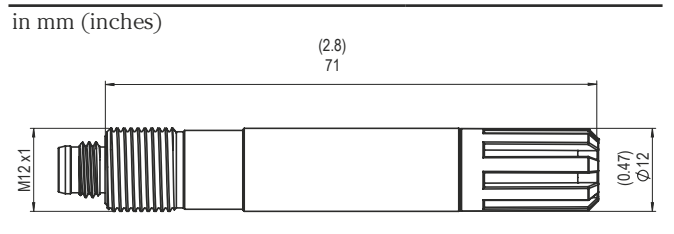
Mechanics

Materials	
body	stainless steel (AISI 316)
grid filter	chrome coated ABS plastic
cable	polyurethane or FEP
Housing classification	IP65
Body thread	M12x1 / 10 mm
Cable connector	4-pin M8 (IEC 60947-5-2)
Weight	
probe	17 g
probe with 0.3 m cable	28 g

Options and Accessories

Vaisala INTERCAP® Sensor, 1 piece	15778HM
Vaisala INTERCAP® Sensor, 10 pcs	INTERCAPSET-10PCS
Sensor protection	
plastic grid	DRW010522
membrane filter	DRW010525
stainless steel sintered filter	HM46670SP
4 ... 20mA loop power converter	UI-CONVERTER-1CB
Mounting bracket for converter	225979
Plastic M12 installation nuts, pair	18350SP
USB cable for PC connection	219690
Probe mounting clamp set, 10 pcs	226067
Probe mounting flange	226061
Connection cables	
0.3 m PU	HMP50Z032SP
3 m PU	HMP50Z300SP
180 °C 3 m FEP	226902SP

Dimensions



VAISALA

www.vaisala.com

Please contact us at
www.vaisala.com/requestinfo



Scan the code for
more information

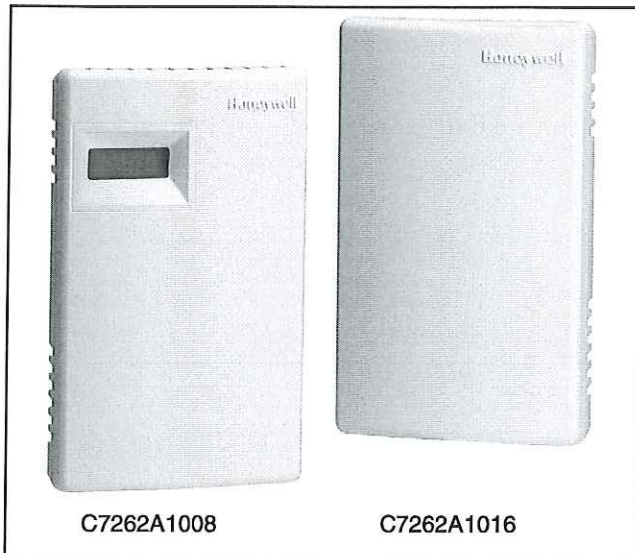
Ref. B210851EN-D ©Vaisala 2014

This material is subject to copyright protection, with all copyrights retained by Vaisala and its individual partners. All rights reserved. Any logos and/or product names are trademarks of Vaisala or its individual partners. The reproduction, transfer, distribution or storage of information contained in this brochure in any form without the prior written consent of Vaisala is strictly prohibited. All specifications — technical included — are subject to change without notice.

C7262A Sensor and Controller

CARBON DIOXIDE/TEMPERATURE SENSOR

PRODUCT DATA



APPLICATION

The C7262 Sensor is a stand-alone carbon dioxide (CO₂) and temperature sensor for use in determining ventilation necessity with HVAC controllers. The C7262 measures the CO₂ concentration and temperature in the ventilated space. The C7262 is used in ventilation and air conditioning systems to control the amount of fresh outdoor air supplied to maintain acceptable levels of CO₂ in the space and to sense the temperature of the space.

FEATURES

- Used for CO₂ based ventilation control.
- Integral 20K ohm NTC temperature output.
- Models available with LCD that provides CO₂ ppm level.
- Non-Dispersion-Infrared (NDIR) technology used to measure carbon dioxide gas.
- Device provides voltage or current output based on CO₂ levels.
- Models available with SPST relay output.

- Automatic Background Calibration (ABC) algorithm based on long-term evaluation reduces required typical zero-drift check maintenance.

SPECIFICATIONS

Models: C7262 Sensor. A stand-alone carbon dioxide (CO₂) and temperature sensor with two jumper-adjustable CO₂ outputs (one analog and one SPST relay).

C7262A1008: Wall module with display.

C7262A1016: Wall module without display.

Dimensions: See Fig. 1.

Sensor Performance Ratings:

Response Time: Less than 3 min.

Carbon Dioxide Sensor:

Operation: Non-dispersive infrared (NDIR).

Sampling: Diffusion.

CO₂ Range: 0 to 2000 ppm

Accuracy: ± (30 ppm + 3% of reading) from 59°F to 85°F (15°C to 30°C).*

Temperature Sensor:

Thermistor: 20K ohms NTC.

Operating temperature range: 22°F to 122°F

(-6°C to +50°C).

- * This product complies with Title 24 Part 6, CEC Standard for Residential and Non-Residential Buildings—2005, when installed according to instructions.

Electrical Ratings:

Power Supply: 24 Vac/dc ±20%, 50/60 Hz (Class 2).

Maximum Power Consumption: 1W.

Peak Current (20 ms duration): At rated voltages it is 120mA or less.

Relay:

Configuration: Shipped N.O.

Contact Rating: 1A at 50 Vac/24 Vdc.

Minimum Permissible Load: 1 mA at 5 Vdc.

Linear Analog Output:

Voltage: 0/2-10 Vdc (resistive load greater than 5000 ohms).

Current: 0/4-20 mA (resistive load less than 500 ohms).

Outputs (Jumper Adjustable, see Table 2):

CO₂ outputs



62-0353-03

Analogue: 0-10 Vdc (Default: 0-10 Vdc, 0 to 2000 ppm),
2-10 Vdc, 4-20mA.
Relay: Normally Open SPST (Default: Close at 800 ppm).

Ambient Ratings:

Temperature:
Operating: +32°F to +122°F (0°C to +50°C).
Storage: -4°F to +158°F (-20°C to +70°C).
Relative Humidity (non-condensing): 0 to 95 percent.

CO₂ Pressure Dependence: 1.6% change in reading per
1 kPa deviation from 100 kPa.

Wiring Connections: Terminals (16 gauge maximum)

Mounting:

Vertical surface with standard single-gang junction box.

Automatic Background Calibration (ABC) default: On.

Calibration: This product is factory calibrated. No field calibration is necessary for the life of this product.

Approvals: CE

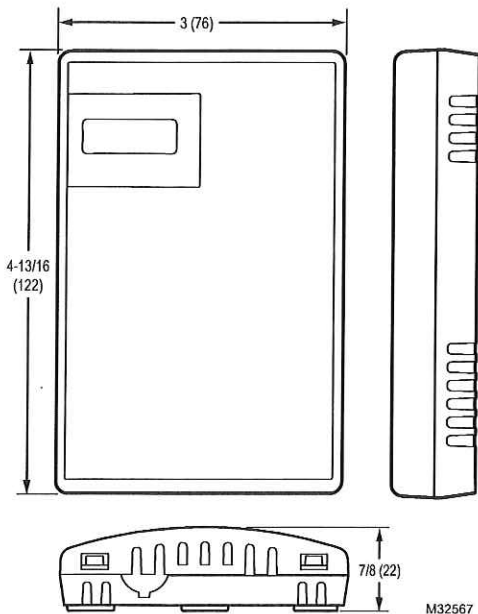


Fig. 1. C7262A dimensions in inches (mm).

INSTALLATION

When Installing this Product...

1. Read these instructions carefully. Failure to follow them could damage the product or cause a hazardous condition.
2. Check the ratings given in the instructions and on the product to make sure the product is suitable for your application.
3. Installer must be a trained, experienced service technician.
4. After installation is complete, check out product operation as provided in these instructions.

IMPORTANT

All wiring must agree with applicable codes, ordinances and regulations.



CAUTION

Health Hazard.
Improper use can create dangerous situations. Use in application for sensing carbon dioxide and temperature only. For life-safety applications, this device can function only as a secondary or lesser device.



CAUTION

Electrical Shock or Equipment Damage Hazard.
Can shock individuals or short equipment circuitry. Disconnect power supply before installation.



CAUTION

Equipment Damage Hazard.
Electrostatic discharge can short equipment circuitry. Ensure that you are properly grounded before handling the unit.

C7262A Cover Removal/Replacement

A snap-fit locking mechanism is used to attach the cover of the wall module to its subbase. To disassemble the cover from the subbase:

ORDERING INFORMATION

When purchasing replacement and modernization products from your TRADELINE® wholesaler or distributor, refer to the TRADELINE® Catalog or price sheets for complete ordering number. If you have additional questions, need further information, or would like to comment on our products or services, please write or phone:

1. Your local Honeywell Environmental and Combustion Controls Sales Office (check white pages of your phone directory).
2. Honeywell Customer Care
1885 Douglas Drive North
Minneapolis, Minnesota 55422-4386
3. <http://customer.honeywell.com> or <http://customer.honeywell.ca>

International Sales and Service Offices in all principal cities of the world. Manufacturing in Belgium, Canada, China, Czech Republic, Germany, Hungary, Italy, Mexico, Netherlands, United Kingdom, and United States.

1. Insert a thin, flat blade screwdriver into each of the two slots at the bottom of the module to release the two locking tabs.
2. Tilt the cover out and away from the subbase to release the top two locking tabs.

Location and Mounting

C7262 Sensors mount directly on the wall, sheet metal duct, or a panel. When planning the installation, allow enough clearance for maintenance and service. Mount the sensor in a well-ventilated area.

NOTES:

Do not install the sensor where it can be affected by:
 — drafts or dead spots behind doors and in corners.
 — air from ducts.

Sensor must be mounted in a location which sees at least one 4-hour unoccupied period per week so that the CO₂ level drops to outdoor levels. Automatic Background Calibration will not work properly in locations without four hours of unoccupied time per week, or where there are sources of CO₂ other than people (breweries, mushroom farms, etc).

IMPORTANT

This sensor is not for use in highly corrosive environments.

Wall Mounting

The C7262 Wall Mount models can be mounted using two or four screws:

1. Remove C7262 cover.
2. Mount the subbase to the wall using washers and two or four screws (not supplied) appropriate for the wall material.

NOTE: When mounting on a junction box, see Fig. 2.

3. Replace the cover.

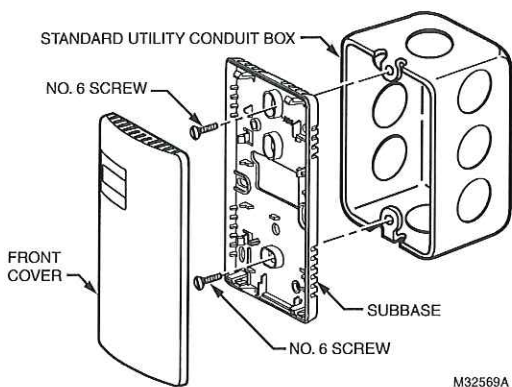


Fig. 2. Junction box mounting (C7262A).

WIRING

The factory ships the device with the output default settings shown in Tables 2 and 3. Set the jumpers and wire the device (see Table 1 and Fig. 3).



CAUTION

Electrical Shock or Equipment Damage Hazard.
 Can shock individuals or short equipment circuitry.
 Disconnect power supply before installation.



CAUTION

Equipment Damage Hazard.
 Electrostatic Discharge Can Short Equipment Circuitry.
 Ensure that you are properly grounded before handling the unit.

IMPORTANT

1. All low voltage connections to this device must be 24 Vac Class 2.
2. All wiring must comply with applicable local codes, ordinances and regulations.

Table 1. C7262 Terminal Connections (see Fig. 3).

Designation	Function
V+	24V Hot
Com AC/DC	24V Common for OUT1 and OUT2
TEMP	20k ohm NTC temperature output
TEMP	
OUT1: CO2	Analog Output, CO2
OUT2: CO2	Analog Output, CO2
RELAY NO	Normally Open potential free relay contacts
RELAY NO	

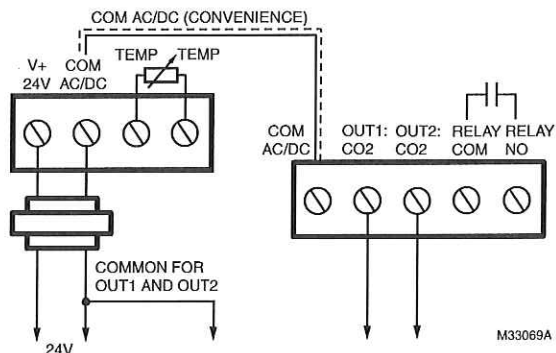


Fig. 3. Wiring the C7262.

Input Signal

The C7262 Sensors have an adjustable range. These ranges are determined by the SW1 and SW2 jumper settings (see Table 2).

Table 2. CO₂ Range Jumper Settings

SW1 ^a	SW2 ^a	OUT1 & OUT2 (ppm)	Relay ^b (ppm)
On	On	500 to 1500	1200
On	Off	500 to 2000	1200
Off	On	0 to 1000	1000
Off ^c	Off ^c	0 to 2000	800

- ^a SW1 ON and SW2 ON state means jumper is set in upper position and OFF state means jumper is set in lower position.
- ^b When the level reaches this value, the contacts close; when the level drops 100 ppm below this value, the contacts open.
- ^c Setting when shipped from the factory.

Output Signal

The output signal can be adjusted for 0/2-10 Vdc or 0/4-20 mA (see Table 3).

Table 3. Output Signal Jumper Settings

AN OUT1 & OUT2	OUT 1 & OUT 2	
	0-100%	20-100%
Voltage	0-10Vdc	2-10Vdc
Current	0-20 mA	4-20 mA

NOTES:

- Jumpers are shown on the sticker on the inside of the cover.
- Use needle nose pliers to carefully reposition jumpers.
- The CO₂ settings and the output signal settings are independent of each other. 0-100% and 20-100% are simply markings for the OUT jumper settings on the sensor (to differentiate between the two voltage and the two current ranges) and do not refer to or alter the ppm range chosen.

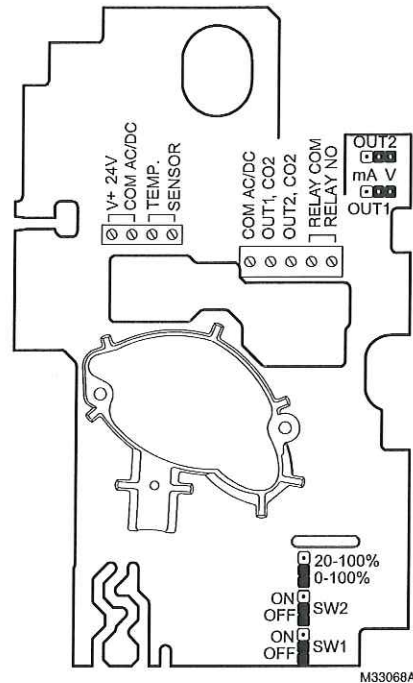


Fig. 4. C7262 default jumper settings.

Example

For a CO₂ setting of 0-2000 ppm and a voltage output of 0-10 Vdc, the output would be as shown in Table 4 (arbitrary points along the analog curve).

Table 4. 0-10 Vdc Output Example.

CO ₂ Level (ppm)	0	200	400	600	800	1000	1200	1400	1600	1800	2000
Voltage Output (Vdc)	0	1	2	3	4	5	6	7	8	9	10

For a CO₂ setting of 0-2000 ppm and a voltage output of 2-10 Vdc, the output would be as shown in Table 5 (arbitrary points along the analog curve).

Table 5. 2-10 Vdc Output Example.

CO ₂ Level (ppm)	0	250	500	750	1000	1250	1500	1750	2000
Voltage Output (Vdc)	2	3	4	5	6	7	8	9	10

CHECKOUT

Perform a quick test of the unit with the unit powered:

1. Stand close to the unit and breathe air into the sensor.
2. Check the CO₂ level registered by the controller to ensure a strong rise.
3. When connected to a damper in a ventilation system, the controller typically signals an increase in air flow.

Automation and Control Solutions

Honeywell International Inc.
 1985 Douglas Drive North
 Golden Valley, MN 55422
 customer.honeywell.com



11.3 APPENDIX C

BATHROOM EXHAUST FAN FLOW MEASUREMENTS

Flow rate measurements for the bathroom fan at Suite A were taken using a SwemaFlow 233 Air Flow Meter (Figure 1). The steps for obtaining representative air flow measurements of the bathroom fan are outlined in Table 1.

The instrument was calibrated with no window or doors open, and no fans turned on. Then to simulate different airflow scenarios throughout the suite, a combination of doors/ windows opened or closed, and the bathroom and kitchen exhausts fans turned on or off scenarios were used to take airflow measurements. The measurements were taken three times for each scenario to ensure repeatability.

The average airflow measurement of the bathroom fan for all scenarios and each of the three readings is 31.2 L/s with a standard deviation of 0.91 L/s. Therefore, flow rate of 31 L/s is used for the mass flow rate in moisture production calculations.



Figure 1. Photograph of the SwemaFlow 233 unit during measurements in Suite A

Table 1. Bathroom exhaust fan flow measurements

17-Jul-13

10:50 - 11:10 AM

Air flow measurement of bathroom fan in Suite A, using SwemaFlow 233 and hood

Duct diameter is 3". The air flow rate measurements are in L/s.

Measurement Scenarios	Fans		Windows		Doors	Air flow measurement (l/s) Bathroom fan		
	Bathroom	Kitchen	Master bedroom	2 nd bedroom	Balcony door	Reading 1	Reading 2	Reading 3
1. calibration	off	off	closed	closed	closed	0	0	0
2. bathroom fan on only	on	off	closed	closed	closed	30.7	31.0	31.6
3. balcony door open	on	off	closed	closed	open	31.2	31.0	31.4
4. window open (1)	on	off	open	closed	open	31.0	32.0	31.5
5. window open (2)	on	off	open	open	open	32.0	31.7	32.2
6. window open (3)	on	off	open	open	closed	31.8	32.0	31.9
7. window open (4)	on	off	open	closed	closed	31.2	31.2	31.6
8. kitchen fan turned on (1)	on	on	open	closed	closed	31.5	31.4	31.2
9. kitchen fan turned on (2)	on	on	open	closed	open	31.5	31.0	31.1
10. kitchen fan turned on only	on	on	closed	closed	closed	28.4	29.2	29.1